THE UNIVERSITY
of EDINBURGH

Evading the anti-tumour immune response – a novel role for Focal Adhesion Kinase

Thomas Anthony Lund

Doctor of Philosophy – The University of Edinburgh – 2015

I declare;

(a) that this thesis has been composed by me, **Thomas Anthony Lund** and
(b) either that the work is the my own, or that the I have made a substantial contribution to the work, such contribution being clearly indicated, and
(c) that this work has not been submitted for any other degree or professional qualification

Signed

Abstract

Here I describe a new function of Focal Adhesion Kinase (FAK) in driving anti-tumour immune evasion. The kinase activity of FAK in squamous cancer cells drives the recruitment of regulatory T-cells (Tregs) by transcriptionally regulating chemokine/cytokine and ligand-receptor networks, including the transcription of CCL5 and TGFβ, which are required for enhanced Treg recruitment. In turn, these changes inhibit antigen-primed cytotoxic $CD8^+$ T-cell activity in the tumour microenvironment, permitting survival and growth of FAK-expressing tumours. I show that immune evasion requires FAK's catalytic activity, and a small molecule FAK kinase inhibitor, VS-4718, which is currently in clinical development, drives depletion of Tregs and permits $CD8^+$ T-cell-mediated tumour clearance. It is therefore likely that FAK inhibitors may trigger immune-mediated tumour regression, providing previously unrecognized therapeutic benefit.

Lay Summery

Cancer is a disease where cells of the body become damaged, grow uncontrollably and form tumours. Like many diseases, the body's immune system has evolved to recognise and destroy infected or damaged cells. After a cell becomes damaged, the immune system is turned on and destroys the damaged cell, allowing healthy cells to take its place. However, after the immune system has done this, it must be turned off to stop healthy cell coming under attack. Specialized regulatory cells called Tregs help to turn off the active immune system, allowing the damaged cells to be quickly recognised and destroyed without this 'autoimmune response' damaging healthy tissues. So why does this not happen in cancer? Tumours can hijack Tregs in order to turn off the immune response prematurely, before it can destroy the whole tumour. This allows the tumour to escape the immune response, and the tumour continues to grow without attack from the immune system.

Recent work has begun to try and 're-activate' the immune system in cancer. Here, drugs aimed at the immune cells themselves, turn the immune response 'back on', causing the tumour to become under attack from the immune cells once more. This approach can have some drastic side effects however, as activating the immune response in this way can lead to autoimmune disease, and so treatment with these drugs becomes a balancing act; by activating the immune system to kill the cancer by stopping the ability to turn itself off, treatment with these drugs hopes to destroy the tumour before the autoimmune response damages healthy tissue. Not only this, but the tumour still has the ability to hijack the regulatory Tregs, and so these types of treatments can be ineffective at destroying the tumour but still carry the risk of seriously damaging healthy tissue.

I have discovered a way to target the tumours ability to hijack the regulatory Tregs, making the tumour visible to the immune system. Using drugs to target a protein that is found in tumour cells called Focal Adhesion Kinase (FAK), these compound stop the tumour from using Tregs to hide from the immune response, allowing the immune cells to destroy the tumour. Drugs aimed at FAK have very few side effects and are much safer to use. I have also shown that this not only leads to the destruction of tumours by the immune system in a number of different types of

cancer, but that this could make other drugs aimed at the immune cells safer and more effective at treating cancer.

Table of Figures

Published Figures

The following figures have been published in (See **Published Work**);

Nuclear FAK Controls Chemokine Transcription, Tregs, and Evasion of Anti-tumor Immunity

Alan Serrels,[*] Tom Lund[*], Bryan Serrels, Adam Byron, Rhoanne C. McPherson, Alexander von Kriegsheim, Laura Gomez-Cuadrado, Marta Canel, Morwenna Muir, Jennifer E. Ring, Eleni Maniati, Andrew H. Sims, Jonathan A. Pachter, Valerie G. Brunton, Nick Gilbert, Stephen M. Anderton, Robert J.B. Nibbs, and Margaret C. Frame [*]Authors contributed equally

Cell *163, 160–173*, September 24, 2015

Figure	Title	Page No.
5.2	SCC FAK-/- tumours show host-dependent growth characteristics	89
5.7	Validation of $CD8^+$ and $CD4^+$ antibodies antibody-mediated T-cell depletion in FVB/N mice from both commercially available antibodies and in-house purified antibodies	96
5.9	Validation of sustained CD8 and CD4 T-cell depleting antibodies in tumour bearing FVB/N mice	98
5.10	SCC tumour growth +/- $CD8^+$ and $CD4^+$ T-cell depletion	99
5.12	Tumour rechallenge implies common antigen between SCC FAK-wt and SCC FAK-/- cells	101
5.13	FAK kinase activity is required for SCC tumour growth and survival	103
6.4	Gating strategy and FMO controls for FACS analysis of myeloid cells and their polarization status	117
6.5	Gating strategy and FMO controls for FACS analysis to identify T-cells and their activation status	118
7.1	FAK-depleted tumours exhibit a heightened $CD8^+$ T-cell response	128
7.2	Intra-tumoural macrophages in SCC FAK-wt, SCC FAK-/- and SCC FAK-kd tumours	131
7.4	MDSC FACS gating strategy	134
7.5	FACS analysis of MDSC populations did not correlate with tumour clearance characteristics	135
7.6	Treg FACS gating strategy	136
7.7	Increase in the number of intra-tumoural Tregs in SCC FAK-wt tumours	137
7.8	SCC FAK-wt tumour clearance after antibody depletion of $CD25^+$ cells	138
8.1	Transcriptional profiling of SCC FAK-wt and SCC FAK-/- cells reveled a number of upregulated chemokine ligands in SCC FAK-wt tumours	145

1 Introduction

Cancer is a multifactorial disease in which cells uncontrollably proliferate, invade and destroy surrounding tissue. It is one of the leading causes of morbidity and mortality worldwide, with approximately 14 million new cases and 8.2 million cancer related deaths in 2012[1]. DNA damage-induced mutations can give rise to cancer initiating oncogenes that drive the transformation of a single normal cell into a cancer cell, which in turn proliferate and grow into a tumour. A number of factors contribute to the onset of transformation, the most prevalent being exposure to carcinogens including: 1) chemical carcinogens such as tobacco and asbestos, 2) physical carcinogens such as exposure to UV and ionizing radiation and 3) biological carcinogens including infection from parasites, bacteria or viruses such as HPV-16. The majority of cells damaged in this way undergo programmed cell death, however, a very small contingent of cells may progress to form a tumour. These initiating factors may interact with predisposing genetic, age-related, environmental, dietary, and exercise-related factors to determine a person's susceptibility to cancer development. For example, a number of high-risk heritable mutations are linked to increased genetic susceptibility. Mutations in the *BRCA1/2* genes are known to predispose women to an 80% and 55% chance of developing breast and ovarian cancer respectively by the time they are 90 years old. Mutations in the *APC* gene lead to the autosomal dominant familial adenomatous polyposis (FAP) syndrome, greatly increasing the risk of bowel cancer. This complex relationship between genetic predisposition and exposure to a vast array of carcinogens is one of the reasons why cancer is such a heterogeneous disease and remains difficult to treat.

Following the initiating event, cancer cells must acquire a number of distinct capabilities necessary to promote tumour growth, progression and survival as proposed in the seminal review by Hanahan and Weinberg[2,3] (**Figure 1.1**). These include genome instability and mutation, sustaining proliferative signals, avoiding immune destruction and activating invasion and metastatic progression, all of which a tumour must acquire to survive. The progression and development of a tumour compares to and even exceeds the complexity of that of a developing healthy organ.

The archetypal view of cancer development and tumour progression is focussed on a mass of transformed cells proliferating unhindered to produce a solid primary tumour. This mass contains a heterogeneous population of transformed cells from different clonal origins, each potentially harbouring distinct mutational differences. However, cancer is not merely an autonomous mass of mutant cells. Rather, a large body of work has identified that tumours contain a complex milieu of immune and stromal cells, sequestered by the tumour to help promote survival and progression. The requirements of a tumour are not sustainable by the surrounding tissue alone, and thus developing tumours establish a new, more permissive niche in order to survive, known as the tumour microenvironment. Which cells are recruited to the tumour microenvironment and whether they aid or hinder the development and progression of a tumour is the primary focus of this chapter. I will also discuss how the tumour influences, subverts or evades these responses.

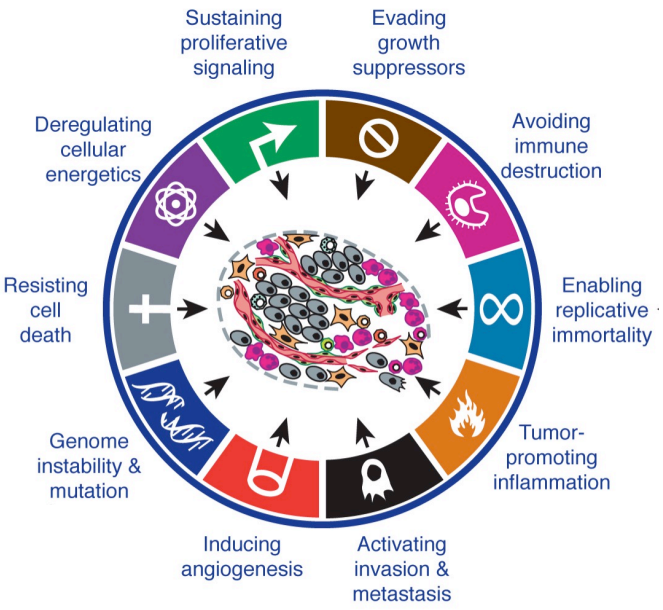

Figure 1.1 | The Hallmarks of Cancer. Outline of the ten Hallmarks of cancer (the original six (Hanahan and Weinberg, 2000) and four emerging hallmarks (Hanahan & Weinberg 2011)). Hanahan and Weinberg propose that cancers must acquire most if not all of these capabilities in order to grow, survive and progress. Adapted from *Hallmarks of cancer: the next generation.* Hanahan, D. & Weinberg, R.A, Cell, 2011

2 The tumour and its surrounding microenvironment

In response to the unrestrained proliferation of transformed cells, and in an attempt to re-establish tissue homeostasis, the surrounding stroma generates an acute inflammatory response leading to an imbalance of immune and stromal cells[4,5]. Manipulation of this microenvironment therefore becomes imperative to tumour survival. Pioneering studies, in part lead by the Dvorak lab, have made the collective conclusion that stromal involvement in tumorigenesis resembles that of acute inflammatory responses such as wound healing[6-9]. Classical players in wound healing (immune cells, endothelial cells and fibroblasts) that typically coordinate to resolve damage after a wound, instead react paradoxically and promote tumour survival[5], identifying cancer as 'a wound that never heals'[10]. Further work has established that the surrounding microenvironment not only aids tumour survival, but also the induction, selection and expansion of neoplastic cells for malignant progression[11,12]. When you consider all the required 'hallmarks' of cancer, seven noticeably involve contributions by immune and stromal cells of the tumour microenvironment[13]. How these cells contribute to these traits is discussed below.

2.1 Immune cells and their functions in cancer

The mammalian immune system is comprised of a repertoire of different cell populations and mediators that co-operate to instill protection against pathogens, whilst simultaneously maintaining tolerance against self-antigen[14] (**Figure 2.1**). The immune system is composed of two distinct compartments – adaptive and innate – differentiated by time of activation and antigen specificity[15]. Cells of the innate compartment, namely macrophages, mast cells, neutrophils, natural killer (NK) cells and dendritic cells (DCs) are first responders to sites of injury. Macrophages, mast cells and DCs serve as sentinel cells, residing in tissues and monitoring their environment for changes in tissue homeostasis. After homeostasis is perturbed, either by injury, infection or transformation, macrophages and mast cells secrete a number

of soluble factors that induce the mobilization and infiltration of other immune cells (leukocytes) to the site. These factors include cytokines, chemokines, reactive oxygen species (ROSs), matrix metalloproteinase (MMPs) and other extracellular matrix (ECM) remodeling enzymes[15]. This process is known as inflammation, and serves to mediate tissue repair mechanisms, kill any potential pathogens and readdress tissue homeostasis. DCs and macrophages act as antigen presenting cells (APCs), taking up foreign antigen and migrating to the lymph nodes in order to present their antigens to the adaptive immune response leading to its activation.

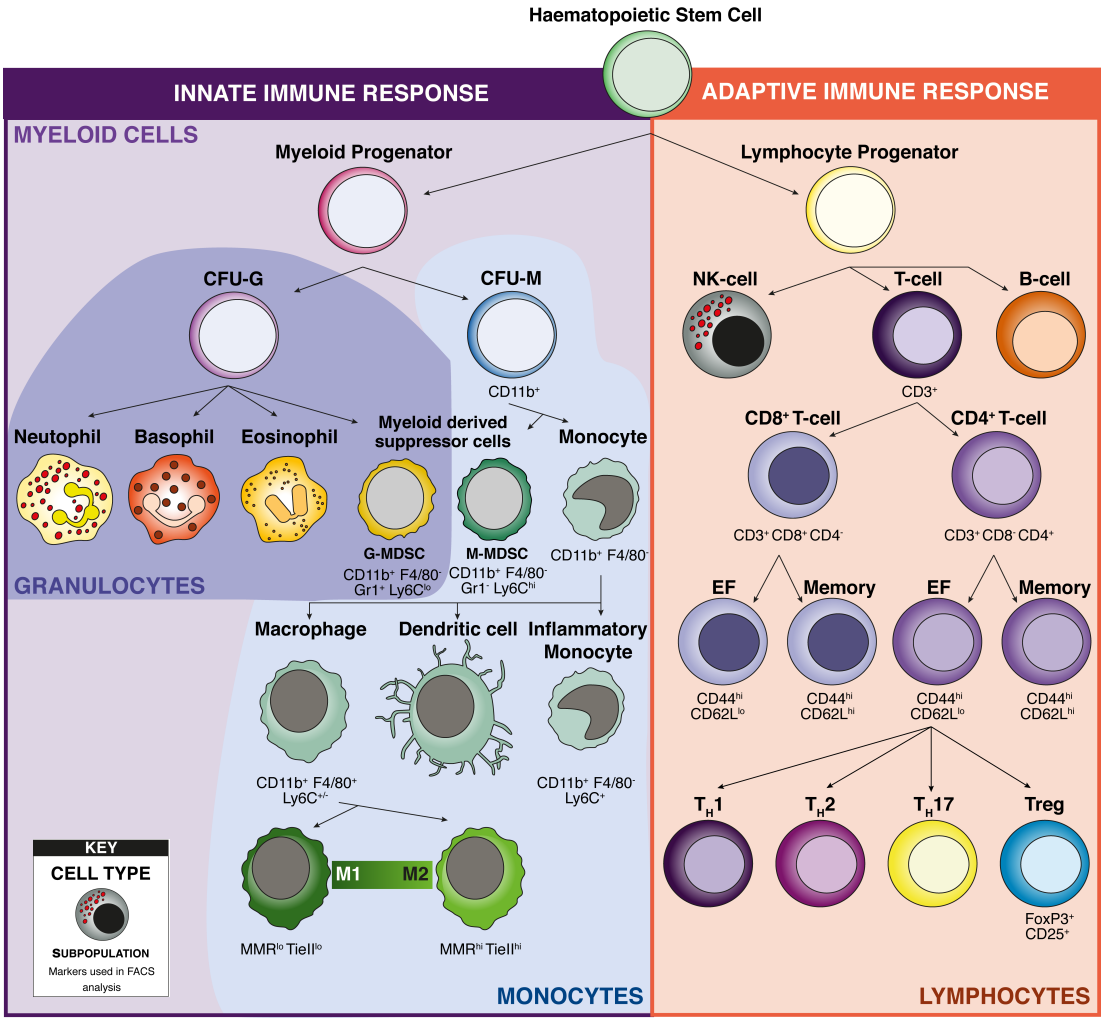

Figure 2.1 | Leukocyte Hierarchy within the innate and adaptive arms of the immune response. *left panel* Most cells of the innate immune response are derived form a shared myeloid progenitor cell and are therefore referred to collectively as myeloid cells. From this progenitor cell is derived the CFU-G and CFU-M from which granulocytes and monocytes are derived respectively. *right panel* All cells of the adaptive immune response are derived from the lymphoid progenitor cell and are referred to as lymphocytes. CFU-G = granulocytic colony forming unit; CFU-M = monocytic colony forming unit; MDSC = myeloid-derived suppressor cell; EF = effector

The adaptive immune compartment contains T lymphocytes, namely cytotoxic $CD8^+$ T-cells and $CD4^+$ T-cells, and B lymphocytes. The primary function of these cells is to identify and specifically destroy pathogen-infected cells or damaged cells as efficiently as possible, but also play roles in the host defense against pathogens such ass extracellular bacteria. However, these cells firstly require activation by direct interactions with mature APCs[14,15]. Each individual B and T lymphocyte are antigenically committed to a specific unique antigen[15], which if presented to them leads to the rapid clonal expansion of that T- or B-cell in order to attain the number of cells required to achieve an effective immune response. This delay is why the adaptive immune response is slower than the innate at responding to inflammation. Upon expansion and activation this compartment is highly sophisticated and efficient at destroying infected or damaged cells. This ability requires very stringent regulation however, as hyper-activated adaptive responses can lead to damage to adjacent tissues and autoimmune disease. A specialized regulatory $CD4^+$ T-cell called Tregs helps to suppress the activated adaptive response. How this occurs will be discussed in detail below (**2.1.3**).

The heightened and activated innate and adaptive immune responses are stopped by the resolution of inflammation. It was initially believed that inflammation was resolved by a passive catabolic mechanism and with the removal of the initial pro-inflammatory mediators the inflammation would simply 'burn itself out'[16]. However with the discovery of anti-inflammatory agents such as IL-10 and adenosine, and with the discovery of the anti-inflammatory roles of nitric oxide (NO) in the regulation of inflammatory myeloid cell apoptosis[17], it is now believed that inflammation is resolved through active mechanisms[16,18]. Key mediators of the resolution phase include anti-inflammatory cytokines such as IL-10, inhibitors of pattern recognition receptors, prostaglandins, resolvins and lipoxins[16]. The exact mechanisms by which resolution occurs, and how and when the resolution phase is initiated is still to be determined. However, what is clear is that the resolution of inflammation precedes the final stages of tissue repair, and leads to the return to tissue homeostasis. In normal physiological conditions, inflammation is resolved

shortly after tissue repair or pathogenic destruction. This is not the case in cancer, where inflammation is either not resolved, or is left unresolved long enough to aid tumour development.

Virchow was the first to identify a link between chronic inflammation and cancer in 1863[19], but since then three key lines of evidence have linked aberrant chronic inflammation to cancer development. Firstly, 16.1% of the global incidence of cancer can be attributed to inflammation-inducing infectious organisms[20], notably *Helicobacter pylori* in gastric cancer[21], human papilloma virus (HPV) in cervical and head and neck cancers[22,23], and hepatitis B and C in hepatocellular carcinoma[24]. Secondly, chronic inflammatory diseases such as inflammatory bowel disease (IBD)[25], chronic pancreatitis[26] and pelvic inflammatory disease[27] increase the risk of developing colorectal carcinoma, pancreatic cancer and ovarian cancer respectively[28]. Finally, treatment with non-steroidal anti-inflammatory drugs (NSAIDs) have shown to decrease the onset of cancer; prolonged intake of aspirin is associated with reduction in the incidence of colorectal cancer[29]; treatment with tolfenamic acid saw reduced incidence of pancreatic, esophageal and lung cancers[30]; treatment with COX2 inhibitor NSAID Celecoxib has been approved as an adjunctive therapy for the reduction of polyps in FAP. The type of inflammatory response associated with increased cancer risk is often referred to as 'smoldering inflammation', due to its low grade and lack of overt clinical concequences[31,32]. Growing evidence that inflammation is in fact the root cause of many cancers has lead to pro-tumorigenic inflammation to be included as a hallmark of cancer[3,32]

With growing interest in the contribution of inflammation in cancer development, work turned to the identification of leukocytes within the tumour microenvironment itself. Populations from both arms of the immune response have since been found in or adjacent to neoplastic tissue. Work has shown that these immune cells contribute to tumorigenicity in four ways; to facilitate cellular transformation, to prevent or regulate tumour outgrowth, to modulate tumour immunogenicity and to aid progression of tumour development and malignant conversion[33,34]. Whether a specific immune population will contribute to each of these functions is determined by the inflammatory state of the tumour, the stage of tumour development, the other

immune populations involved and the repertoire of tumour-associated antigens (TAAs) presented by APCs or expressed on tumour cells[33]. Thus immune cells may act in both a pro-tumorigenic and anti-tumorigenic capacity. Here I discuss the specific functions of immune cells within the tumour microenvironment, focusing on macrophages and DCs from the innate compartment, T-cells from the adaptive compartment, and the immunosuppressive cells that regulate these responses, myeloid-derived suppressor cells (MDSCs) and Tregs.

2.1.1 Macrophages: mediators of tissue repair to promote tumour survival

Macrophages ($CD45^+$ $CD11b^+$ $F4/80^+$ cells) are critical components of the tumour immune milieu. Two major subtypes of macrophages exist in the tumour microenvironment, resident macrophages and inflammatory macrophages[35]. It is worth identifying at this point that the work within this thesis discusses mouse macrophages and not human, and although both mouse and human macrophages do have a number of similarities, they are also distinct within the markers used to identify them, and in some cases within their mechanism of action[36]. As discussed above, resident macrophages act as sentinel cells within tissues and contribute to the initiation of inflammation. Inflammatory macrophages are recruited from the peripheral lymphoid tissues or are differentiated from $Ly6C^+$ inflammatory monocytes at the site of inflammation. Macrophages are highly plastic cells that can exist in two polar differentiated states, M1 (classical) macrophages and M2 (alternative) macrophages[37]. M1 macrophages are a anti-tumorigenic, highly phagocytic, pro-inflammatory population activated by lipopolysaccharide (LPS) or INF-γ and characterised by the expression of 'M1 genes' such as *Nos2, IL12b* and *Ciita*[37-41]. M2 macrophages show high expression of 'M2 marker genes' such as *MMR*, *Tie2*, *Arg1* and *Retnla*, and display pro–tumorigenic functions; they reduce inflammation and promote mechanisms of wound-healing such the activation of fibroblasts and angiogenesis[37-41]. Both M1 and M2 macrophages are polar differentiated populations that exist in constant state of flux determined by the surrounding microenvironment, resulting in intra-tumoural macrophages with aspects

from both M1 and M2 phenotypes (hence the term 'macrophage polarization'). The factors that mediate macrophage polarization remain unclear. However, M1 and M2 phenotypes are akin to T_H1 and T_H2 T-cell mediated inflammatory responses, requiring IFN-γ and IL-4 respectively. STAT signalling appears to direct a number of M1 and M2 differentiation specific genes, such as Stat1, an essential mediator of M1 polarization in the presence of IFN-γ, and Stat6, which is required for M2 polarization in response to IL-4and IL-13[39].

Macrophages are an abundant population of leukocytes in solid tumours[35] and $Ly6C^+$ macrophages appear phenotypically distinct in the tumour microenvironment from resident macrophages. The role of resident macrophages in cancer is unclear, but the roles of inflammatory macrophages have been better characterised in work investigating $CCR2^+$ tumour associated macrophages (TAMs). A large proportion of intra-tumoural inflammatory macrophages are $CCR2^+$ TAMs, and increased infiltration or the upregulation of TAM-associated gene signatures correlates with poor prognosis in many human cancers[31,35,38,42,43]. TAMs have many functions within the tumour microenvironment and at the distant metastatic site, and have been shown to regulate both tumorigenesis and the progression of the primary tumour.

2.1.1.1 Macrophages regulate inflammation that drives tumorigenesis

Macrophages and other myeloid cells induce inflammation at sites of injury, but macrophages are central to the 'smouldering inflammatory response' seen in cancer[44]. The inflammatory state of myeloid cells is controlled by NFκB and Stat3 mediated signalling which act in direct opposition to each other[45]. NFκB is a central signal transducer downstream of toll-like receptor (TLR) activation, which results in the expression of inflammatory mediating cytokines such as IL-12 and TNF-α[31,46,47]. The transcription factor Stat3 functions to suppress the inflammatory response, and acts as the major target of the immunosuppressive cytokine IL-10[31,46]. Myeloid specific ablation of Stat3 or NFκB signalling components induces or suppresses chronic inflammation respectively and has been shown to effect tumour initiation. Ablation of myeloid Stat3 induced inflammation in the colon results in chronic colitis and invasive colonic adenocarcinoma. Myeloid specific inhibition of NFκB

signalling by the ablation of IκB kinase α (IKKα) reduces inflammation and tumour progression in mouse models of intestinal cancer[48].

After the initial genotoxic-transforming event, macrophages are recruited to the tissue and adopt a M1 phenotype to induce an inflammatory response in order to restore tissue homeostasis. Part of the repertoire of inflammatory and cytotoxic molecules secreted by M1 macrophages, are reactive nitrogen and oxygen species (RNS and ROS respectively)[49], which play normal physiological roles in anti-microbial defence. However, the secretion of molecules such as ROS and RNS generates a mutagenic inflammatory environment in cancer[49]. Due to the highly mutagenic capacity of ROS and RNS, this environment induces mutations in adjacent epithelial cells and mediates genomic instability in the developing tumour[49,50]. The requirement of macrophages in the promotion of tumorigenesis can also be seen in mouse models of cancer using chemical carcinogenesis. The two-stage cutaneous DMBA (7,12-dimethylbenathracene) / TPA (2-O-tetradecanoylphorbol 13-acetate) skin carcinogenesis protocol[51] uses a low dose of the carcinogen DMBA to induce an oncogenic mutation in the skin. This mutation is not sufficient however to initiate tumorigenesis and frequent topical application of pro-inflammatory TPA is required. The inflammatory response generated by TPA is dominated by macrophages. This pro-tumorigenic inflammatory response mediated by TPA is caused by TNF-α signalling through NFκB, and acts directly on epithelial cells and on inflammatory cells, in particular macrophages within the surrounding microenvironment[52].

2.1.1.2 Macrophage functions in the primary tumour

As primary tumours progress and develop, intra-tumoural macrophage populations revert from the inflammatory phenotype seen in tumorigenesis, to trophic/M2 macrophages seen in tissue repair and development[31,53-55]. After the initial stages of tumorigenesis, NFκB signalling in TAMs become inhibited by the constitutive expression of p50 homodimers, which in turn inhibits M1 inflammatory responses and induces a M2 macrophage phenotypic switch[56]. The induction of an M2 phenotype by p50 can be seen *in vitro*[45], and can also be found in cancers that

lack the characteristic inflammatory response, such as breast cancer where M2 macrophages are recruited in high numbers before metastatic transition both in humans[57] and in mouse models[31,58].

Macrophages play a number of roles in the primary tumour. M2 Macrophages induce angiogenesis and mediate the 'angiogenic switch' (an enhancement of vascular density observed following benign to malignant transition)[59,60] (**2.2.1**). Evidence supporting this notion comes from a number of studies. Null mutations in the macrophage *CSF1* gene reduce vascular density[61], while overexpression of *CSF1* promotes a premature increase in the number of macrophages and leads to an early angiogenic switch that accelerates tumour malignant progression[59,61,62]. Work in mice reflects clinical observations seen in breast cancer that correlates increased macrophage infiltration with increased micro-vessel density and poor prognosis[31,63]. Tie2, a protein constitutively expressed on endothial cells and enriched on macrophages within the tumour[64,65], has been observed to mark a population of macrophages proximal to angiogenic vessels, and transcriptional profiling of $Tie2^+$ macrophages[65] highlighted an enrichment of pro-angiogenic molecules[66]. $Tie2^+$ macrophages have features of M2-polarized macrophages[32], promote both tumour and developmental angiogenesis[67,68] and are required for the formation of blood vessels[64,65,69].

Macrophages also function to aid tumour progression and contribute to increase tumour invasion, migration and intravasation. Macrophage-induced tumour cell invasion has been observed in the MMTV-PyMT mouse model of breast cancer using intravital optical imaging techniques, which correlate with work seen in human breast xerograph studies[70]. Macrophages aid tumour cell migration by a paracrine signalling axis that exits between tumour cells and macrophages; tumours secrete CSF-1, stimulating macrophage migration and secretion of epidermal growth factor (EGF), which in turn induces tumour cell migration[71]. Inhibition of either the macrophage restricted CSF-1 or the tumour cell restricted EGF results in the perturbation of migration and chemotaxis in both cell types in the tumour microenvironment[31,71,72]. Furthermore, in study of breast cancer by Qian *et el*[73], $CCR2^+$ macrophages promote the extravasation, seeding and growth of tumour cells

at distant metastatic sites[73]. Inhibition of CCR2 signalling reduces metastatic progression and the recruitment of inflammatory monocytes, associate with an increase in survival of tumour-bearing mice[74,75].

CCR2 has also been shown to be required for the recruitment of splenic-derived macrophages and macrophage progenitors[76]. The spleen may therefor act as reservoir for TAM recruitment and differentiation, and data suggests that it is source of most TAMS within the microenvironment, continuously supplying the tumour though out its development[76]. Although select roles for splenic-derived macrophages have not as yet been elucidated, their mobilization increases, mediated by chemotactic signals such as M-CSF, GM-CSF and IL-3[77-80] after chemotherapy and radiotherapy, and may also increase resisitance to DNA-damaging chemotheraeutics[81]

2.1.1.3 Macrophage involvement in tumour responses to anti-cancer therapies

A number of published works have studied the involvement of macrophages in determining the outcome of anti-cancer therapies. The effects of anti-cancer agents on macrophage polarization, recruitment and proliferation can determine tumour resistance or sensitivity to therapy. However, results are conflicting, and it is becoming clear that whether macrophages enhance or limit responses to chemotherapy depends on the cytotoxic agent and the mouse model used. Chemosensitivity is enhanced when cytotoxic agents increase the cytotoxic capacity of M1 macrophages or decrease the numbers of total macrophages, monocytes or M2 macrophages[82]. This can be seen in a number of mouse models; treatment with doxorubicin induces M1 cytotoxic activity in models immunogenic lymphoma[83]; docetaxel treatment promotes M1 macrophage expansion in 4T1 mammary transplantable mouse models[84]; trabectedin depletes protumoural monocytes and TAMs in 3-methylcholantrene induced and transplantable fibrosarcoma[85] models. In all three of these studies, macrophages enhance the efficacy of the respective chemotherapeutic agent through different mechanisms. However, treatment of MMTV-PyMT transgenic model of breast cancer with doxorubicin increased tumour infiltration of M2-macrophages, resulting in resistance to doxorubicin in this model, contrasting with results in immunogenic lymphoma. Resistance to chemotherapy

correlates with increased M2 macrophage tumour infiltration in a number of mouse models including paclitaxel, gemcitabine and 5-fluorouracil[86] treated EL4 transplantable model of lymphoma, and MMTV-PyMT transplanted and transgenic breast cancer models treated with paclitaxel[87,88].

High numbers of intra-tumoural TAMs also correlate with poor tumour responses to irradiation[82,89]. Following tumour-induced DNA damage, Abelson murine leukaemia viral oncogene homologue-1 (ABL-1) kinase activation promotes CSF1 gene transcription and increases levels of CSF1 within the tumour[90]. This in turn increases the recruitment of myeloid cells, including TAMs that express CSF1R, which induce tumour regrowth and repair following irradiation[90]. Inhibition of CSF1R[90] or antibody depletion of $CD11b^+$ myeloid cells[91] increased the efficacy of irradiation and reduced post-therapy tumour regeneration.

Further to this, it has since been established that M2 macrophages may help to stimulate tumour regrowth after chemotherapy. Tumour relapse after therapy is a major clinical problem, and Hughes *et al*[92] have identified a subpopulation of M2 TAMs ($MRC1^+$ $TIE2^+$ $CxCR4^{hi}$) which accumulate around blood vessels in tumours after chemotherapy. Here, they promote tumour revascularization and relapse by a mechanism, which in part involves the release VEGF, and pharmacological blockade of CxCR4 pathway reduce the number of M2 TAMs after chemotherapy, leading to a reduction in tumour revascularization and regrowth[92]. This offers an exciting clinical opportunity, and implies potentially novel roles for other immune populations in determining the frequency of cancer relapse.

2.1.2 The impact of T-cell activation and tolerance on tumour survival

T-cells ($CD45^+$ $CD3^+$ cells) are major contributors to the anti-tumour immune response. They exist in two major classes, $CD8^+$ cytotoxic T-cells and $CD4^+$ 'helper' T-cells. Following exposure to antigen, naïve T-cells activate and expand, becoming effector T-cells ($CD44^{hi}$ $CD62L^{lo}$)[93]. Effector T-cells secrete chemokines and cytokines such as IL-2, which binds its cognate receptor IL-2R in a paracrine signalling axis that leads to the activation of PI3K/AKT-mTOR proliferative

signalling pathways[94]. Effector T-cells thus begin to proliferate rapidly, reaching optimal density around 2 weeks after initial exposure to antigen, and subsequently play a number of critical functions in driving the anti-tumour immune response (discussed below)[95]. After peak effector T-cell proliferation, approximately 90-95% of cells undergo apoptosis, whilst the remaining effector population matures into memory T-cells ($CD44^{hi}$ $CD62^{hi}$)[93,96,97]. Memory T-cells are a long-term cell population that persist for several years or even decades after initial antigen exposure. Upon repeat exposure to a specific antigen, memory T-cells expand and regain higher effector functions. This occurs more rapidly than for naïve T-cells, typically resulting in an asymptomatic response[96,98]. This archetypal T-cell response is the basis of most vaccinations[96]; controlled exposure to a non-pathogenic or weakened strain of the pathogen is recognised by the immune system, destroyed and the resultant memory T-cells provide nascent asymptomatic protection against subsequent re-exposure.

Immunogenicity, the capacity to induce an adaptive immune response *in vivo*, has been widely investigated in cancer using transplantable mouse models. Cancer cell immunogenicity can be classified into three grades; 1) Highly immunogenic cancer cells that are rejected after transplantation into naïve syngeneic mice, 2) intermediate immunogenic cell models that require host mice to be immunized against the specific expressed antigen prior to transplantation in order for tumour regression, or 3) non-immunogenic cancer cells that are not rejected following immunization[99]. Tumours are generally weakly immunogenic due to the selective pressure of the immune system as the tumour progresses. Despite this, sporadic immunogenic tumours may still progress, indifferent to the presence of $CD8^+$ T-cells specific for that transplantable antigen[100]. These data imply that cytotoxic immune responses can be converted into non-destructive T-cell responses. These responses aid in tumour progression and in the evasion of the anti-tumour immune response. However, this also implies that seemingly non-immunogenic tumours may be converted to become immunogenic, a process that has gained great clinical interest[99].

2.1.2.1 Dendritic cells (DCs) orchestrate T-cell activation and anergy

DCs are pivotal to the anti-tumour immune response as they either prime or anergize naïve T-cells in primary lymphatic organs, leading to either anti-tumour immunity or peripheral tolerance[101,102]. DCs, as well as macrophages, act as antigen presenting cells (APCs) both at peripheral lymphoid tissues and at the tumour site. APCs present processed antigenic peptides via the major histocompatibility complexes (MHC) expressed on their surface[14]. Presented antigen is identified by antigenically committed T-cells, leading to their rapid clonal expansion, raising a highly specific and effective adaptive immune response. The multi-molecular complex between APCs and naïve T-cells, called the immunological synapse is a highly regulated complex of surface expressed ligands and concomitant receptors that simultaneously act not only to activate T-cells, but to control and suppress their activity[14] (called T-cell anergy; **Figure 2.2**). On the surface of APCs, MHC-presented antigen binds to its concomitant CD3/T-cell receptor (TCR) complex exclusively expressed on a specific T-cell subset. Concurrent binding of the TCR co-receptor CD8/CD4 is required for optimal TCR activation of $CD8^+$ cytotoxic T-cell or $CD4^+$ T-cells respectively[103]. DCs modulate the nature of the T-cell response within the immunological synapse by expressing of a series of co-stimulatory receptors that are required either promote a T-cell mediated immune response, or to restrict T-cell activity by inducing T-cell anergy and eventual apoptosis (**Figure 2.2**). APC-expressed B7 molecules CD80 and CD86 (B7.1 and B7.2 respectively) bind to T-cell CD28 in parallel with TCR stimulation, leading to T-cell activation and induction of T-cell effector functions. Induction of either CD28 or TCR signaling without activation of the other parallel pathway results in the induction of T-cell anergy. Activation of other receptor/ligand pairs directly induces T-cell anergy. These inhibitory pathways, called immune checkpoints are crucial for maintaining self-tolerance and modulating the duration and amplitude of physiological immune responses[104] (discussed below).

Further to antigen presentation by APCs, host cells present tolerized autologous or 'self' antigen of which the immune system is educated to disregard. All cell types express autologous antigens by MHC molecules, and foreign antigens can be detected directly by T-cells eliciting the activation of a cytotoxic $CD8^+$ T-cell

response. In this regard, autochthonous cancer cells have been shown to express repertoires of mutated or modified self-antigens and a number of these result from oncogenic mutations; mutant N-ras[105], B-raf[106] and CDK4[107] have all be found as TAA on melanoma cells, mutant K-ras[108] has been reported as a TAA on pancreatic ductal adenocarcinoma (PDAC) and the BCR-Abl fusion protein B3a2 has been shown to be expressed as four different TAA peptides in chronic myeloid leukemia[109-111]. This raises the question as to why these cancers are not destroyed by the adaptive immune response. T-cells with high avidity for self-TAAs are typically deleted during the thymic T-cell selection process[112], and thus T-cells within the tumour microenvironment are highly susceptible to mechanisms of peripheral tolerance and immunosuppression.

Downstream of TCR engagement, TCR-associated CD3 becomes phosphorylated by Src family kinases Fyn and Lck leading to binding of Zeta-chain-associated protein kinase 70 (ZAP-70)[113], and downstream activation of NFκB, NFAT and Ca^{2+} influx pathways. These pathways drive a variety of different T-cell effector functions within the tumour microenvironment.

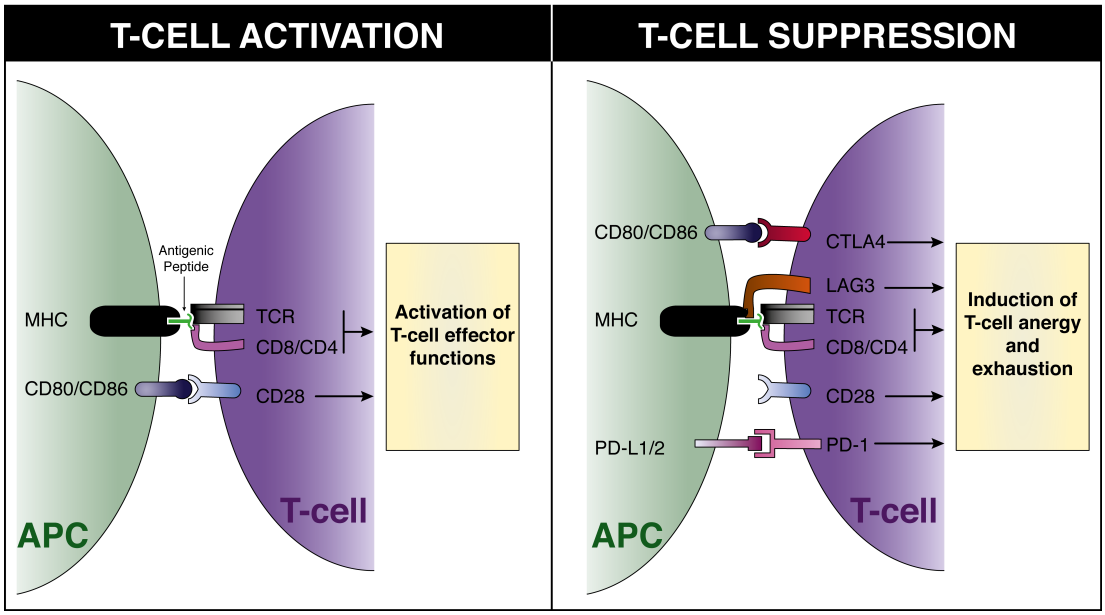

Figure 2.2 | The immunological synapse mediates T-cell activation, anergy and exhaustion. *Left panel* APCs present antigenic peptides via MHC molecules. T-cell activation requires the engagement of the concomitant T-cell TCR, stabilization of this signal by lineage dependent co-receptors CD8 and CD4 and binding of co-stimulatory molecule CD28 with APC expressed CD80/86. *Right panel* APC expressed co-stimulatory molecules may induce T-cell anergy / exhaustion. Lack of CD80/86 stimulation of CD28 after TCR engagement, sequestration of CD80/86 and activation of CTLA4 and PD-1 binding with its ligands PD-L1/2 all induce anergy and exhaustion in T-cells.

2.1.2.2 Effector T-cell functions within in the tumour microenvironment

Upon activation within the tumour microenvironment, $CD8^+$ and $CD4^+$ T-cells exhibit distinct effector functions (**Figure 2.3**). Effector $CD8^+$ T-cells are highly cytotoxic, and although all $CD8^+$ T-cells require MHC class I–antigen–TCR interactions to target a cell to be killed, a $CD8^+$ T-cell can kill a cell by engagement of Fas ligand with its receptor, or by the localised release of cytotoxins[14] (**Figure 2.3**). Direct induction of cell death occurs after surface expressed Fas ligand (FasL/ApoL1), which is upregulated on effector $CD8^+$ T-cells, binds to its concomitant receptor (Fas/Apo1) expressed on tumour cells. This induces the recruitment of the death-induced signalling complex (DISC) to Fas, which results in the caspase cascade and subsequent tumour cell apoptosis[14]. $CD8^+$ T-cells may induce cell death by the localized release of cytotoxins namely perforin, granzymes, and granulysin[14]. Perforin and granulysin form pores or increase the permeably of the target cell membrane respectively, which allows granzymes to enter the cytoplasm, causing the target cells serine proteases to induce the caspase cascade[14,114].

Upon activation, $CD4^+$ T-cells differentiate into a number of distinctive subpopulations including T_H1, T_H2, T_H17 and Tregs, determined by the presence of different chemokines and cytokines within the tumour microenvironment (**Figure 2.3**). Each of these effector $CD4^+$ T-cell sub-states function differently within the tumour microenvironment, and play very different roles in enhancing or suppressing immune mediated tumour destruction. T_H1 and T_H2 are the first-defined and best-characterised T-cell linages. Distinct chemokines, cytokines and membrane expressed molecules displayed by these cell types promote matched effector functions of other cells of the adaptive and innate arms of the immune response[115]. T_H1 lineage cells are the classical 'T-helper' cells, and are induced by IFN-γ and IL-12 mediated activation of the transcription factor T-Bet[116]. Activation of T-Bet upregulates IFN-γ and CCL2, that acts to increase the anti-tumour immune response in the tumour microenvironment. T_H1 cells enhance the cytotoxic activity of $CD8^+$ T-cells, increasing M1 macrophage activation and the recruitment of NK cells and macrophages to the tumour site[117]. T_H2 lineage cells are associated with allergic reactions and mediate humoral immune responses. GATA-3 activation by IL-4, IL-2

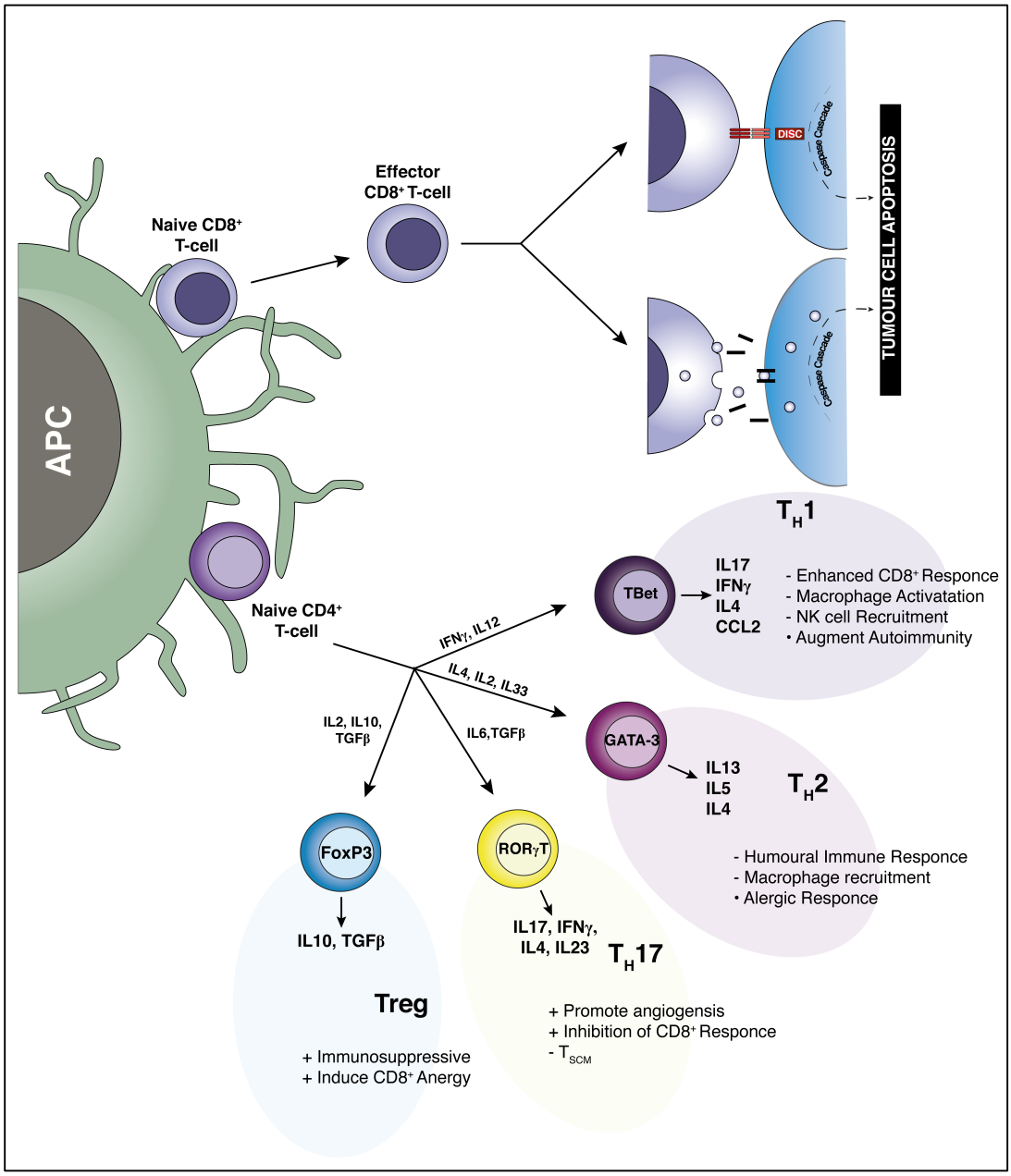

Figure 2.3 | Effector functions of CD8$^+$ and CD4$^+$ T-cells following activation by APCs. Following antigen presentation, effector CD8$^+$ T-cells have two distinct cytotoxic mechanisms and may induce tumour cell apoptosis either directly by Fas ligand or indirectly by the secretion of granzymes, perforin and granulysin. CD4$^+$ T-cells differentiate upon activation into a number of sub-sets with different pro-tumorigenic or anti-tumorigenic functions, depending on the presence of secreted inflammatory chemokines and cytokines within the tumour microenvironment. Each subset is regulated by a specific transcription factor that determines its phenotype. APC = antigen presenting cell, + = pro-tumorigenic function, - = anti-tumorigenic function, • = other function

and IL-33 induces the T_H2 phenotype, which leads to the upregulation of IL-13, IL-5 and IL-4[118]. The role of T_H2 cells in cancer is poorly understood, but anti-tumour effects of IL-4 have been attributed to an increase in intra-tumoural eosinophils and macrophages[119,120]. Contrary to this, the frequency of $CD4^+$ cells expressing IL-5 correlates with increased melanoma and renal cell carcinoma progression[121], suggesting that T_H2 mediated effects on tumour growth may be context dependant.

Identification and classification of T-cell subsets has helped to develop understanding of the functions of $CD4^+$ T-cells within the tumour microenvironment, beyond the archetypal T_H1 – T_H2 binary polarization models, and T_H17 cells and Tregs are examples of this. T_H17 subsets depend on the transcription factor $ROR_\gamma t$, and are characterized by the production of IL-17[122]. Induction requires stimulation by TGFβ and IL-6, but differentiated T_H17 populations are sustained and maintained by IL-23[123]. The functions of T_H17 cells within the tumour microenvironment are not yet fully understood, despite being identified in a number of human cancers including ovarian[124], gastric[125], prostrate[126], pancreatic and renal cell carcinomas[127]. T_H17 cells represent a polyfuctional $CD4^+$ effector T-cell phenotype that may both aid and hinder immune cell-mediated tumour destruction. IL-17 can induce the expression of CCL2, CxCL7 and CCL20 which act as pro-inflammatory and pro-angiogenic mediators to increase tumour growth and survival[128,129]. But IL-17 may also act in conjunction with IFN-γ to stimulate CxCL19 and CxCL10 production to increase anti-tumour effector $CD8^+$ T-cells and to stimulate T_H1 $CD4^+$ T-cell differentiation[127,130]. Some studies however have identified that the anti-tumour capabilities of T_H17 cells are in part due to genomic reprograming events that instil a longer life span, increased plasticity and ability to self renew in some T_H17 cells within the tumour microenvironment[131]. This re-programmed T_H17 cell population reassemble stem cell-like memory cells (T_{SCM}) which differs to other anti-tumour $CD4^+$ responses that display genetic signatures consistent with terminal differentiation[117,132]. This increase in plasticity implies that the functions of T_H17 cells with the microenvironment are potentially highly context dependant, with as yet unknown factors determining whether they adopt a state that aids or hinders tumour survival.

Tregs are a highly immunosuppressive population that depend on the expression of the FoxP3 transcription factor. Tregs are highly immunosuppressive cells that exist in two distinct subpopulations, tTregs and iTregs. Thymic-originated Tregs (tTregs) are derived during T-cell maturation and education. Immature single positive $CD4^+$ T-cells receive TCR stimulation from antigen presenting-APCs, and the avidity and response time of the TCR signal determines $CD4^+$ T-cell fate. Upon reception of a high TCR signal, most $CD4^+$ T-cells undergo apoptosis and low TCR signal induces maturation into a conventional $CD4^+$ T-cell[133]. However, immature $CD4^+$ T-cells that respond with an intermediate TCR avidity may induce FoxP3 expression and differentiate into tTregs in the presence of IL-2[133-136]. Indeed, if levels of IL-2 are high enough, $CD4^+$ T-cells with high avidity can escape destruction and become tTregs but this is rare[135,136]. tTregs are recruited to sites of inflammation by chemoattractant CCL5/CCR5 signalling axis[137], which also enhances there ability to suppress $CD8^+$ T-cells[138]. Disruption of this axis in mice, reduces the number of intra-tumoural Tregs leading to increased tumour survival and growth[137]. Peripherally induced Tregs (iTregs) differentiate withih the lymph node and at sites of inflammation from effector $CD4^+$ T-cells. The induction and maintenance of iTregs requires repeat antigenic exposure and cognate iTreg TCR activation, and also requires the chemokines and cytokines TGFβ and IL-10[139]. The effector functions of tTregs and iTregs appear to be the same, but tTregs can be distinguished by the expression of Neuropillin-1 (NRP-1) and Helios[140], although it is debated whether all tTregs express these markers. The immunosuppressive functions of Tregs are discussed in detail below (**2.1.3.2**), but they generally act to induce T-cell anergy and thus promote tumour survival and the evasion of an active anti-tumour immune response. Other types of $CD4^+$ regulatory T-cell also exhibit immunosuppressive capabilities, including $Foxp3^-$ type 1 regulatory (Tr1) cells that secrete immunosuppressive IL-10[141].

It is widely accepted that tumours are immunogenic, as tumour-mediated T-cell responses occur frequently in cancer in the autochthonous host, in both cancer patients and mouse models[99]. The behavior of T-cells in cancer is frequently compared with the adaptive response in chronic viral infection, which share the capacity to establish highly antigenic and immunosuppressive environments unseen

in acute conditions[93]. The fundamental differences between these two pathogeneses are that viral antigens are often exogenous and highly immunogenic, unlike the endogenous and weakly immunogenic TAAs. The immunogenicity of a tumour is dependant on the repertoire of tumour-associated antigens (TAA) expressed[142] but also on a number antigen-independent immunomodulatory factors. In a number of cases is the antigen-independent immunomodulatory factors which give tumours the capacity to avoid an activated cytotoxic $CD8^+$ response.

2.1.2.3 Mechanism of peripheral tolerance: T-cell anergy and exhaustion.

After lymphocytes encounter their cognate antigen, mechanisms of peripheral tolerance are critical in the restraint of the T-cell response in order to avoid potentially fatal autoimmune reactions. Tumours hijack these responses in order to evade immune mediated destruction by activated $CD8^+$ T-cells. Lack of adequate signalling from CD28 co-stimulatory receptors (**Figure 2.2)** with persistent MHC-TCR-antigen signalling induce T-cell anergy[143], a form of T-cell hyporesponsiveness characterised by the lack of IL-2 expression and downstream TCR activity[144]. An anergic state may also be induced by inhibition of mTOR[145], required for effector cell proliferation, or by the deprivation of nutrients or energy, determined by the activation of deprivation pathways such as the AMPK pathway[146]. Other T-cell co-stimulatory molecules can provide direct negative signals to inhibit T-cell responses and induce T-cell tolerance (**Figure 2.2**). Immune checkpoint mediator programmed cell death protein-1 (PD-1) and its ligands PD-L1 and PD-L2 are master regulators of T-cell anergy. Binding of T-cell expressed PD-1 with PD-L1/2 alongside concurrent TCR stimulation, increases the recruitment and activation of Src homology region 2 domain-containing phosphatase (SHP) 1 and 2, leading to the dephosphorylation of proximal signaling complexes. These dephosphorylation events attenuate the activation of PI3K/AKT proliferative pathways, reducing T-cell proliferation and inhibiting downstream mechanisms of TCR activation[117,147]. The impact of PD-1 regulation of T-cells can be see with genetic ablation of *PD-1 (Pdcd1-/-*) in mice, which live for approximately 1 year until they develop systemic lupus erythematosus-like autoimmune disease,

manifesting as glomerulonephritis or dilated cardiomyopathy on C57BL/6 and BALB/c backgrounds respectively[148,149]. Work in a number of mouse models has shown that PD-1 also plays critical roles in regulating T-cell effector functions and T-cell tolerance at later time points in peripheral tissue sites. The breakdown of PD-1 mediated tolerance can result in a number of tissue specific pathogeneses; PD-L1 upregulation in allogeneic pregnancies leads to fetal abortion[150], PD-1 regulates autoimmune diabetes in the pancreas of non-obese diabetic (NOD) mice[151,152] and experimental autoimmune encephalomyelitis (EAE) mouse models of human multiple sclerosis have shown that PD-1 and PD-L1/2 heavily influence EAE pathogenesis[153].

T-cell PD-1 expression is also indicative of T-cell exhaustion, which results after chronic TCR over-stimulation such as occurs in cancer[147]. T-cell exhaustion is a hierarchal multi-step process; as antigenic load increases, T-cells progress through various stages of dysfunction, reducing the expression of IL-2, TNF-α and IFN-γ, and progressively losing cytotoxic and proliferative potential, eventually subsiding to apoptosis[154]. This is accompanied by a progressive upregulation of immune-suppressive receptors, such as PD-1, LAG-3 and CD244 and secretion of immuno-modulating cytokines IL-10 and **TGF**β[154]. T-cell exhaustion is especially prevalent in cancer due to constant exposure of T-cells to antigen within the tumour microenvironment, and so it is likely that T-cell exhaustion is a major mechanism contributing to T-cell dysfunction in cancer patients[154,155]. T-cell exhaustion is not a terminal process, and reversing it has been achieved using PD-1 blocking therapy. However, PD-1 expression levels on exhausted T-cells is linked to the efficacy of these therapeutics. T-cells expressing low and intermediate levels of PD-1 are noted to respond to therapy, while those expressing higher levels of PD-1 did not[156]. Combinations of PD-1 and LAG-3 blocking therapies have shown better efficacy. However, again T-cells expressing high levels of PD-1 and LAG-3 were still unaffected[155], stressing the importance of early clinical intervention in achieving optimal response to therapy.

Cytotoxic T-lymphocyte-associated antigen 4 (CTLA4) is another well-characterised immune checkpoint protein that acts to regulate the amplitude of early T-cell

activation and also regulates T-cell exhaustion. Although CTLA4 and PD-1 belong to the same family of molecules and are both co-inhibitory, evidence suggests they use distinct non-redundant mechanisms to inhibit T-cell activation. CTLA4 knockout mice die after 4 weeks from a lethal hyper-lymphoproliferative disorder resulting in multi-organ tissue failure[157], compared with the less severe lupus-like symptoms seen after 1 year in PD-1 knockout mice. CTLA4 shares identical ligands with CD28 (CD80 and CD86) but with much higher affinity, thus outcompeting CD28 and reducing CD28-medaited T-cell activation (**Figure 2.2**). Downstream of CTLA4 activation, recruitment of SHP1/2 leads to the dephosphorylation of proximal signaling complexes as with PD-1, but the recruitment phosphatase PP2A is unique to CTLA4, which acts directly to inhibit AKT phosphorylation[104]. Thus, CTLA4 expression acts with dual-immunosuppressive capabilities, both to sequester cognate ligands of CD28 and to down-regulate T-cell proliferative and survival signalling pathways. Further more, *CTLA4* is a target gene for the transcription factor FoxP3[104], a critical factor in determining Treg lineage and is constitutively expressed on the surface of Tregs.

2.1.3 Tregs and MDSCs suppress anti-tumour immune response

Mechanisms of peripheral tolerance and the two-signal requirement for T-cell activation appear insufficient to counter the threat of autoimmune reactions, without the need for immunosuppressive cells. Acting in *trans*, Tregs and myeloid derived suppressor cells (MDSCs) suppress immune responses and aid in the active resolution of inflammation at sites of injury and distally within peripheral lymphoid tissues. In cancer, both these cell types provide tumours with the means of escaping immune mediated destruction, and tumour cells use a number of distinct mechanisms in order to subvert the physiological functions of Tregs and MSDCs to aid cancer survival and progression.

2.1.3.1 MDSCs inhibit anti-tumour immune responses

There are two populations of MDSCs that have been characterised; Granulocyte-derived MDSCs (G-MDSCs) and Monocyte-derived MDSCs (M-MDSCs)[158]. G-MDSCs are the most prevalent in tumour-bearing mice, but are only weekly immunosuppressive and suppress immune cells by secretion of ROS[159,160]. M-MDSCs suppress the anti-tumour T-cell response primarily by enzymes ARG1 and inducible nitric acid synthase (iNOS) as well as through the secretion of ROS[159,160]. Arg1 and iNos both induce T-cell proliferative arrest by inhibition of PI3K/mTOR signalling pathways. In human tumours, the levels of intra-tumoural M-MDSCs, but not G-MDSCs correlate with immune suppression and poor prognosis[161].

2.1.3.2 Tregs and Treg-mediated T-cell suppression

Tregs ($CD4^+$ $CD25^+$ $FoxP3^+$ cells) are characterized by the expression of the transcription factor FoxP3 that drives the upregulation of IL-2, IL10, TGFβ and other immunosuppressive associated factors. Genetic deletions, or loss-of-function mutations in FoxP3, result in hyper-lymphoproliferative disorder leading to multi-organ tissue failure in both humans and mice[162,163]. Tregs are highly immunosuppressive cells that exist in two distinct subpopulations, tTregs and iTregs described above (**2.1.2.2**). The transcriptional program of FoxP3 drives the immunosuppressive functions of Tregs, and maintenance of FoxP3 expression is critical to Treg linage stability[139]. FoxP3 suppresses the expression of pro-inflammatory mediators such as IL-2, TNF-α, IFN-γ, IL-17 and IL-4 by Tregs[139,164-166], and induces the constitutive expression of CD25 (a subunit of the IL-2 receptor), CTLA4, IDO, CD39 and CD73[139,167]. The understanding of the molecular mechanisms of Treg immune suppression is still limited, but some putative mechanisms have been described (**Figure 2.4**). IL-2 is required for T cell proliferation, and high levels of Treg-expressed CD25 may act to sequester and deprive T-cells of IL-2, subsequently inhibiting T-cell proliferation[168]. CTLA4 has also been implicated in Treg-mediated immune suppression. Treg-specific genetic deletion of CTLA4 in BALB/c mice results in greatly increased numbers of activated Tregs under inflammatory conditions, yet the immunosuppressive activity of the

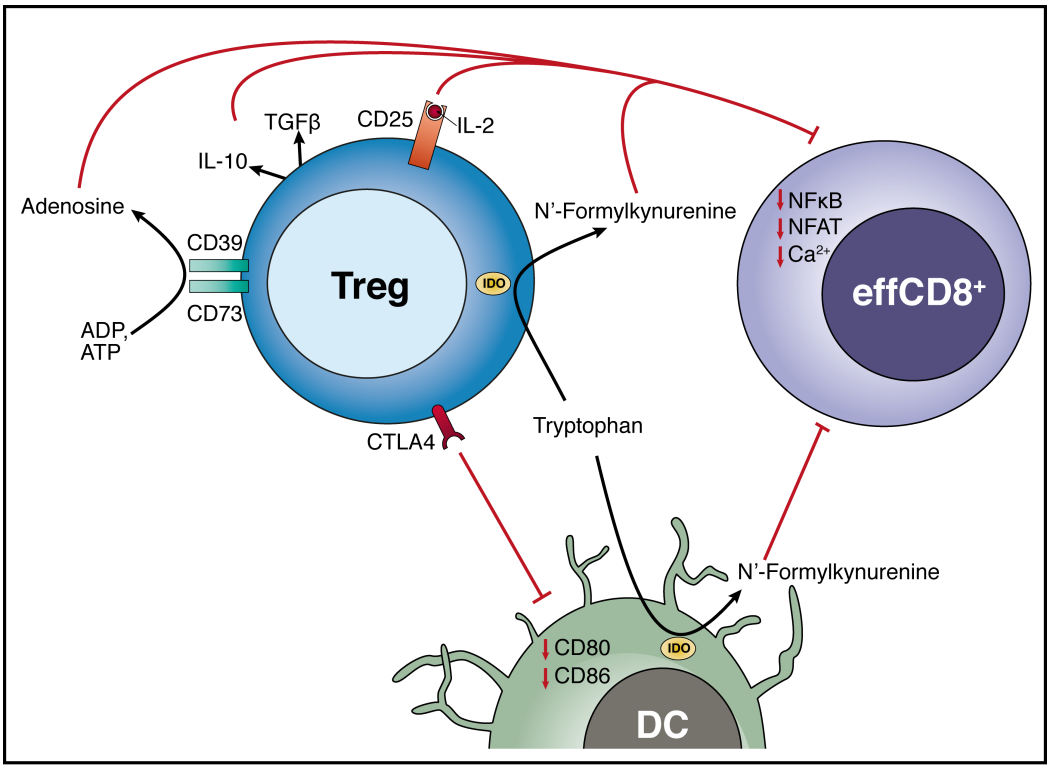

Figure 2.4 | The molecular mechanisms of Treg immunosuppression. Tregs can suppress effector $CD8^+$ T-cells ($effCD8^+$) either directly or indirectly. The hydrolysis of ATP and ADP to adenosine by CD39/73, secretion of immunosuppressive cytokines IL-10 and TGFβ, catabolism of tryptophan to N'-formylkynurenine by IDO and sequestration of IL-2 by CD25 suppresses $effCD8^+$ cytotoxic functions directly. Treg surface-expressed CTLA4 may reduce the APC surface expression of co-stimulatory molecules CD80 and CD86 and may induce the expression of IDO, both of which act to inhibit $effCD8^+$ activity indirectly

CTLA4-deleted Tregs was greatly impaired[139,169,170]. The reduction of Treg immunosuppressive function was associated with increased DCs[171], due to CTLA4-deleted Tregs inability to down-regulate DC-expressed CD80 and CD86 by trans-endocytosis (**Figure 2.4**)[170,172]. Furthermore, Tregs can induce the expression of indoleamine 2,3-dioxygenase (IDO) on DCs, which catalyzes the degradation of tryptophan to N′-Formylkynurenine, leading to starvation of effector T cells and direct cell cycle arrest[167,173,174]. However, BALB/c mice are known to be susceptible to various immune-mediated disorders. Treg-specific genetic deletion of CTLA4 in C56Bl/6 mice did not result in increased numbers of DCs and only partially impaired Treg immunosuppressive capacity[139], thus CTLA-4 contribution to Treg functions can be significantly modified on different genetic backgrounds. Other FoxP3

mediated CD25/CTLA4 independent mechanisms of Treg suppression have been described. Cell-surface molecules CD39 and CD73 are two ectoenzymes that are highly expressed on Tregs. These molecules hydrolyse extracellular ATP and ADP to adenosine, and as a result not only directly inhibit effector T-cell proliferation but also negatively impact on the function of DCs (**Figure 2.4**)[175,176]. Furthermore, Treg secreted cAMP may directly inhibit effector T-cell and DC fuction[177].

In cancer, Tregs have been found within tumours and peripheral draining lymph nodes in patients with liver[178], lung[179], head and neck[180], breast[181], pancreatic[181,182], gastrointestinal[183] and ovarian cancers[184,185]. Increased levels of Tregs are not necessarily indicative of poor prognosis, but rather the ratio between the number of effector $CD8^+$ T-cells and intra-tumoural Tregs (effCD8:Treg), where by a low ratio correlates with poor prognosis[184-186]. Tumour cells have developed a number of ways to recruit, induce and maintain Tregs (**2.4**)

2.2 Stromal contributions to the tumour microenvironment

2.2.1 Endothelial cells and angiogenesis within the tumour microenvironment

The availability of oxygen, nutrients and serum-derived growth factors are prerequisites for all tissues. The extensive vascular network has evolved to supply these demands and facilitate immune surveillance. The remodelling of established vessels and the production of new ones is a complex program of multiple mechanisms, referred to collectively here as angiogenesis. In adult tissues, quiescent endothial cells form a monolayer interconnected by juctional molecules such VE-cadherin and claudins[187]. This forms a hollow tube ensheathed by pericytes, a specialized cell type that maintains vessels and regulates endothelial cell (EC) proliferation. When the quiescent ECs sense a pro-angiogenic signal such as vascular endothelial growth factor (VEGF), angiopoietin-2 (ANG-2) or fibroblast growth factors (FGFs), pericytes detach themselves from the vessel walls and secrete proteases such as MMPs to degrade the basement membrane. Juctional adhesions between ECs begin to loosen and the nascent vessel dilates. The secretion of VEGF by the surrounding milieu increases vascular permeability allowing plasma proteins to extravasate and lay down a temporary extracellular matrix (ECM) scaffold[187]. In response to integrin activation by the newly assembled ECM, ECs migrate out and begin to remodel the ECM and surrounding milieu to establish a new niche, ready to support a developing vessel[187,188]. One EC is selected to become a tip cell, which drives the directional migration of the newly developing vessel in response to VEGF, neuropilins and FGFs. The remaining ECs assume subsidiary positions as stalk cells, which divide to elongate the developing vessel, and which form the vessel lumen[187-189]. Finally, for the newly developed vessel to become functional ECs resume a quiescent state, platelet-derived growth factor (PDGF) and TGFβ signaling recruits pericytes to ensheath the new vessel and EC juctional adhesions are established[187-189]. The matured vascular structure is maintained and protected from insult by VEGF,

NOTCH, angiopoietin-1 (ANG-1) and FGFs, emanating from supporting pericytes, proximal fibroblasts or autocrine signalling loops directly from ECs[187,190,191].

Established vessels also express oxygen-sensing mechanisms such as hypoxia-inducible factor-2α (HIF-2α) and prolyl hydroxylase domain 2 (PHD2) which precipitate vascular re-modelling to optimise blood flow to hypoxic areas[187,188]. This is most prevalent in cancer[192], where tumours are inherently hypoxic and often contain activated fibroblasts and immune cells which secrete pro-angiogenic factors. This induction of angiogenesis or 'angiogenic switch' increases tumour cell proliferation and metastatic progression[193,194]. Constitutive pro-angiogenic signalling in tumours results in a neoplastic vasculature architecture that is irregular, unstable and leaky[195,196]. The lack of matured vessels in tumours can impede immune cell function and the distribution of oxygen and anti-cancer therapeutics[189,197].

In adults, angiogenesis in the most part occurs only in neoplastic tissue and therefore has become the prime subject of microenvironment-targeted anti-cancer therapies. Treatment with monoclonal antibody antagonists of VEGF presented promise as an anti-tumour therapy in mice, but showed disappointing efficacy in the clinic. Numerous preclinical studies (ref. to [198] for full list) has shown a 25 – 90% inhibition of tumour growth in mice treatment with A.4.6.1, a monoclonal VEGF antibody. These results could not be replicated in humans however, and treatment with the human equivalent of A.4.6.1, Bevacizumab (trade name Avastin®) in clinical trails of non-small cell lung cancer (NSCLC)[199] and metastatic renal cancer[200] only showed modest improvement in patient outcome[201]. The lack of efficacy in human trials has been attributed to secondary angiogenic mechanisms which re-establish tumour vasculature after VEGF-depletion. In a number of cases the reoccurring vessels exceeded the pre-existing vasculature in both vessel quality and tumour coverage, increasing both tumor survival and progression[189,196]. The mechanisms of tumour vascular normalization are still unclear. However, angiopoietin receptor Tie2 expressing macrophages have been shown to improve neovascularization[202] and ECs can themselves produce other VEGF-independent angiogenic factors. These results highlight the fundamental requirement of a vascular network to support tumour

survival, growth and progression. Further work focuses on understanding the functional redundancy of VEGF in neovascularization and possible therapeutic combinations aimed at both VEGF and components of tumour normalization.

2.2.2 The ECM and fibroblasts in cancer

The extracellular matrix (ECM) was believed to be an inert structure involved in the compartmentalisation of cells for the delineation of tissue architecture[11]. It has since been shown to be a complex signalling mediator consisting of fibrillar collagens, fibronectins, hyaluronic acid and proteoglycans[203], which together provide contextual information for the surrounding cells[204]. This is especially the case in cancer as neoplastic ECM is distinct from normal tissue ECM[205], and contextualises transformed cells as 'tumour cells'. Without tumour-generated ECM, transformed-cells can integrate into normal tissue[206,207] and form tissue-specific structures in culture, losing their hyper-proliferative state and function as part of the tissue, effectively behaving as a 'normal' cell[204]. These cells still retain the capacity to behave as transformed cells (once removed from co-culture they proliferate rapidly and formed tumours *in vivo*) but in the presence of non-tumour ECM they are effectively non-tumorigenic[204].

Beyond providing contextual information to the tumour, both quality and quantity of ECM has been reported to influence tumour survival, proliferation and migration[208,209]. Tumour cells greatly influence their surrounding ECM both quantitatively, by increasing the deposition of matrix, and qualitatively by regulating the rigidity of the 3D matrix[210]. Three major components of the ECM distinctly regulate these properties:

i. **Collagens** are critical components of the ECM involved in modulating ECM stiffness and rigidity[210]. Tumour fibrillar collagen is linearized and matured in a mechanism that requires the covalent cross-linking of collagen by lysyl oxidase (LOX), expressed initially by fibroblasts but also later by

carcinomas in hypoxic conditions[211,212]. Matured fibres enhance both tumour cell migration and invasion, and inhibition of LOX family has been shown to reduce tumour growth, migration, invasion and progression[213]. Furthermore, LOX inhibition reduced metastatic spread in a number of different models, suggesting that LOX may act at distant metastatic sites to predispose the metastatic niche to seeding of circulating tumour cells[213,214].

Collagens within the ECM also mediate the migration, recruitment and activation of a number of stromal cells within the tumour microenvironment. It has been reported that linear fibrillar type I collagen induced invadosome structures on tumour cells, endothelial cells, fibroblasts and macrophages[212]. Invadosomes (referring collectively to invadopodia and podosomes) are actin based molecular complexes involved in ECM degradation associated with increased cellular migration and invasion[210,215].

ii. **Fibronectins** have been reported to be ligands for a number of integrin family members, including α5β1 integrin[216], and regulate a number roles involved in cell adhesion, migration and growth[210,217]. Upregulation of fibronectins has been associated with increased metastasis of A431 tumour cells[218], and has been shown to increase metastatic progression of ovarian cancer by promoting an association between α5β1 integrin and c-Met, leading to a ligand-independent activation of c-Met[210,219].

iii. **Hyaluronic acid** (Hyaluronan) expression has been shown positively regulate tumour neovascularisation and EC proliferation by increasing the recruitment of tumour-associated macrophages (TAMs)[220].

Although most cell types can produce ECM component proteins, fibroblasts are the major producers of both ECM components and ECM modulating enzymes. 'Normal' fibroblasts are typically embedded in the ECM of connective tissue. Upon tissue injury, fibroblast activation is induced by secreted growth factors released from injured epithelial cells or by infiltrating monocytes and macrophages[221]. These factors include transforming growth factor β (TGFβ), hepatocyte growth factor

(HGF) and PDGF[221]. Activation of fibroblasts in this way is characterised by the expression of smooth muscle actin (α-SMA), and these 'myofibroblasts' produce extensive ECM components and ECM remodelling enzymes. To facilitate this increase in protein translation, myofibroblasts undergo a morphological switch from the typical fusiform morphology of inactive fibroblasts, to a spindle cell morphology containing increased rough endoplasmic reticulum, peripherally located smooth-muscle type myofilaments, Golgi apparatus producing collagen-secretion granules and fibronexus junctions[222]. In this manner, myofibroblasts are distinct from other fibroblasts and can be identified pathologically. Myofibroblast infiltration has been associated with nodular pseudosarcomatous fasciits, inflammatory myofibroblastic tumours, dermatofibrosarcoma protuberans, myofibroblastic sarcoma, malignant fibrous histiocytoma and spindle-cell carcinoma[223].

A number of different fibroblastic cell types can be present within the developing tumour niche, referred collectively as cancer-associated fibroblasts (CAFs); tissue-resident fibroblasts proximal to the developing tumour can be recruited directly or become activated, alongside mesenchymal stem cells and myofibroblasts[203]. CAFs show distinct phenotypic differences to normal fibroblasts within the tumour microenvironment. These include the *de novo* expression of α-SMA and fibronectin as seen in myofibroblast activation, but unlike myofibroblast activation, cannot be de-activated and are much longer lived (are not removed through apoptosis)[210]. In breast cancer, normal fibroblasts promote an epithelial-like phenotype that suppresses metastasis; whereas CAFs induce a mesenchymal-like phenotype and enhance metastasis of both premalignant and malignant mammary epithelial cells[224,225]. CAFs can stimulate anti-apoptotic responses in tumour cell through the modulation of the ECM as CAF-derived ECM remodelling proteases have the capacity to generate ligands for anti-apoptotic integrins. Furthermore, CAFs have been shown to stimulate tumour cell proliferation through the secretion of growth factors such as the FGF, HGF, epithelial growth factors (EGFs) and insulin-like growth factors 1 and 2 (IGF1/2)[13,210,226,227]. CAFs may also secrete a range of pro-inflammatory cytokines[228] that can indirectly act as mitogenic signals by recruiting and activating pro-tumorigenic immune populations.

2.3 Remodelling the tumour microenvironment to promote tumour rejection

Given the influence of the tumour microenvironment on cancer biology and clinical outcome, the development of effective therapies that target components of the microenvironment is becoming increasingly important. Therapies that promote anti-tumour immune responses have shown great promise over the last few years, none more so than antibody-based therapies targeting immunosuppressive molecules CTLA4 and PD-1. CTLA4 antagonist Ipilimumab has been clinically assessed in a number of different cancer models, most notably metastatic melanoma. Anti-CTLA4 therapy has the potential to target and suppress the immunosuppressive functions of Tregs (**2.1.3.2**) and to re-activate anergic or exhausted T-cells. Ipilimumab monotherapy produced objective responses in approximately 15% of patients with metastatic melanoma, which include 3 patients who demonstrated complete responses[229]. However, in other instances, Ipilimumab caused severe autoimmune complications. Treatment schedules and dose escalation studies have identified optimal responses at the highest doses[230], which escalates the risk of developing autoimmune conditions, manifesting primarily as immune-related toxicity to the skin and gastrointestinal tract[231]. However the benefits to patient survival with Ipilimumab treatment in metastatic melanoma, a disease with very few effective front line therapies and an average patient-survival rate of 5-10%, vastly out-weigh the risk of developing chronic, unmanageable side effects.

Anti-PD1 therapy also targets exhausted and anergic T-cells to re-activate the anti-tumour cytotoxic $CD8^+$ T-cell response. PD-1 targeted anybody Nivolumab showed moderate success as a monotherapy, but excelled in combination with Ipilimumab. In a recently published study[232], 53 patients with advanced metastatic melanoma received concurrent therapy with Nivolumab and Ipilimumab, and 33 received sequential treatment. 53% of patients had an objective response and all showed a reduction in tumour size in excess of 80%.

The success of immunotherapy has been attributed, in part to the low-immunogenic nature of some cancers. The availability of TAA-specific $CD8^+$ T-cells is becoming accepted as an essential prerequisite for an objective response to immune checkpoint therapies; without the capacity for a $CD8^+$ T-cell response against a TAA, reactivation of immune cells by targeting immune checkpoints would not necessarily lead to immune-mediated destruction of tumours. The heterogeneity of TAA expression, including intratumoral variation and variation across different patients, may begin to explain why typically up to 40% of patients respond to immune checkpoint inhibitors, and a significant number do not. Although at this point little evidence exists to support this hypothesis, work involving immune checkpoint inhibition in combination with tumour vaccinations, both by the implantation of primed dendritic cells and the injection of tumour-specific antigenic peptides have begun to show promise in pre-clinical studies[104,233,234].

2.4 Tumour cells and the tumour microenvironment

When I consider 'the hallmarks of cancer', there are relatively few tumour cell autonomous properties (genome instability and mutation, and enabling replicative immortality). To survive and progress, the tumour must recruit, manipulate and subvert crucial cell populations. Transformed cells contribute to the generation of the tumour microenvironment by secreting signalling molecules or by direct cell:cell or cell:ECM contact. Tumour secreted growth factors and chemokines, such as TGFβ, PDGF, FGF and MCP1, activate CAFs present in the tumour microevironment[225,235,236], and tumour cell secreted VEGF can initiate angiogenesis. Secreted factors originating for the tumour cell allow the tumour to generate a more permissive niche as quickly and efficiently as possible.

In order to mount an effective adaptive immune response, T-cells require APC presented antigen. Tumour cells that undergo apoptosis may generate an antitumor immune response through different mechanisms collectively called immunogenic programmed-cell death (**Figure 2.5**). Apoptosis is a mechanism by which the cell in response to stress signalling or DNA damage can induce programed cell

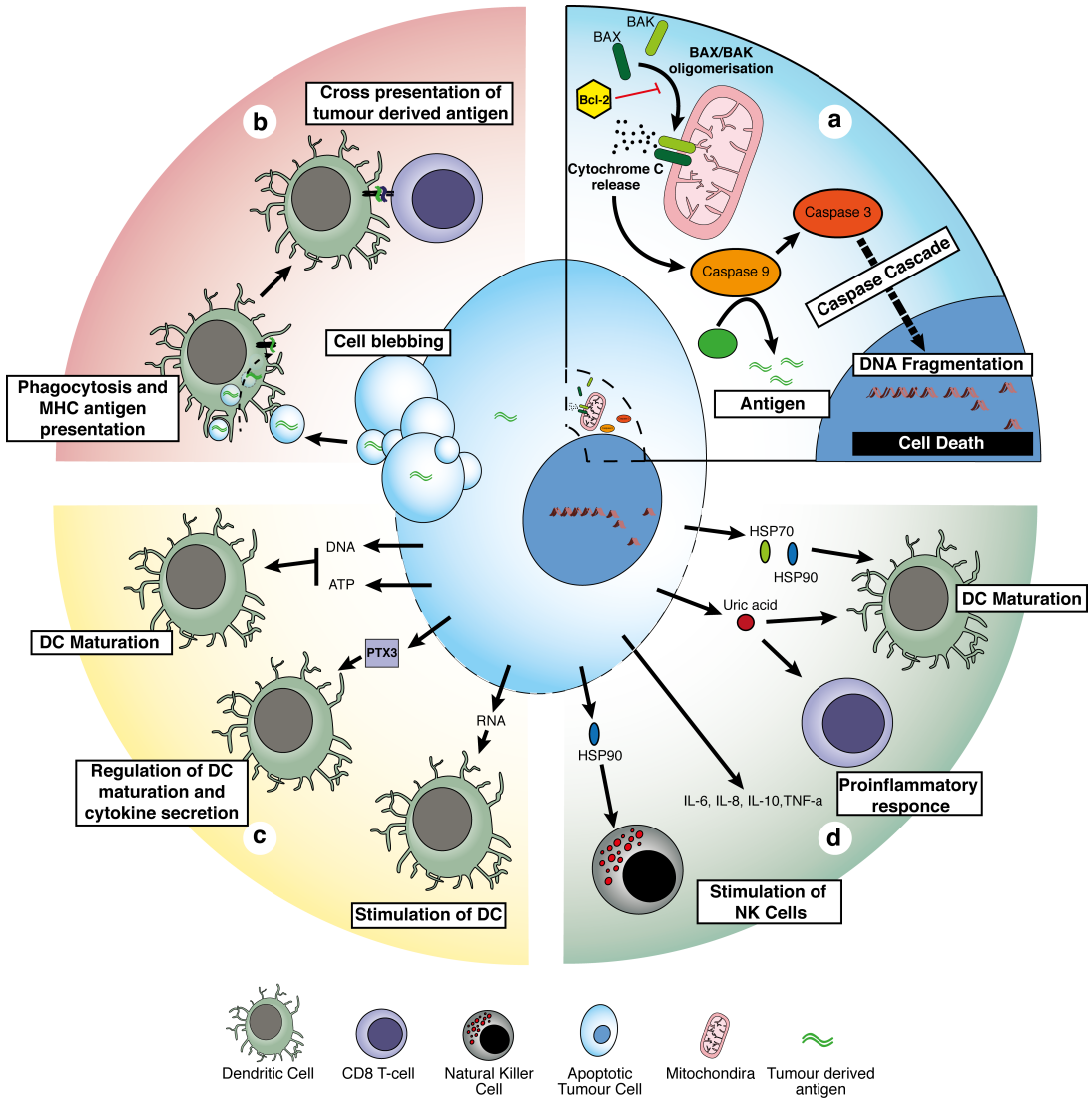

Figure 2.5 | Mechanisms of immunogenic cell death. Immunogenic cell death is a form of apoptosis that induces and primes an immune response. **a** Intrinsic apoptotic mechanisms generate new antigenic peptides. **b** New antigenic peptides may be released via cell blebbing and subsequently phagocytosed and presented by APCs. **c** Increased permeability of nuclear and cell membranes releases DNA, RNA and PTX3 which act to stimulate and regulate the maturation of DCs. **d** Finally further breakdown of cell membranes releases pro-inflammatory molecules into the microenvironment which act to increase anti-tumorigenic immune responses

death[237](**Figure 2.5a)**. Activation of the mitochondrial BAX/BAK pathway leads to the generation of the cytosolic apoptosome complex, and subsequently the activation of caspase 9, triggering the caspase cascade and the induction of apoptosis. A consequence of the induction of apoptosis is the up regulation of proteolysis, which under certain conditions can lead to the generation novel TAAs. TAAs can then be found in the 'cell blebs', extracellular vesicles formed in the final phase of apoptosis, which can be phagocytised by APCs and the TAAs presented[238] (**Figure 2.5b)**.

Furthermore, increased proliferation, recruitment and differentiation of APCs can be seen at sights of chemotherapy-induced apoptosis, in part due to the release of factors from dying cancer cells, such as ATP and DNA which induce DC maturation and RAN and PTX3 which stimulate and active DCs respectively[239] (**Figure 2.5c)**. Furthermore, in the final stages of apoptosis as the cell and nuclear membrane begin to break down and cellular components are released, HSP70, uric acid and HSP90 can induce DC maturation, $CD8^+$ T-cell mediated pro inflammatory responses and the stimulation of NK cells[240] (**Figure 2.5d)**.

Tumour cells hijack and manipulate both arms of the immune response in order to promote tumour survival and evade immune cell-mediated destruction (**Figure 2.6**). Secretion of chemokines and cytokines into the tumour microenvironment can act on multiple immune cell populations simultaneously, to increase pro-tumorigenic and immunosuppressive functions and suppress cytotoxic activity. Tumour-secreted TGFβ acts to polarize intra-tumoural neutrophils to adopt a more pro-tumorigenic phenotype, whilst alongside IL-10, induces Treg expansion from $CD4^+$ effector cells, maintains intra-tumoural Treg populations and suppresses $CD8^+$ cytotoxic effector functions[241-243]. IL-10 also acts with IL-1β, IL-6, IL-11 and VEGF to modulate MDSCs, macrophages and DCs. Each molecule may act alone or together to induce the expansion of MDSCs and increase their immunosuppressive capacity, polarize macrophages into a pro-tumorigenic immunosuppressive M2 phenotype and inhibit DC activation, all of which act to increase tumour survival[242]. Other tumour-secreted factors include IFN-γ and IL1-α that enhance iNOS and ARG1 immunosuppression by MDSCs and macrophages. Furthermore, GM-CSF, drives expansion of MDSCs, while IL-4 and IL-13 contribute to the recruitment and immunosuppressive capacity of MDSCs and macrophages respectively[242]. Furthermore, tumour cells can express TCR co-stimulatory molecules CTLA4, PD-1, PD-L1/2 and CD80/86, which act to induce effector T-cell anergy and exhaustion[241].

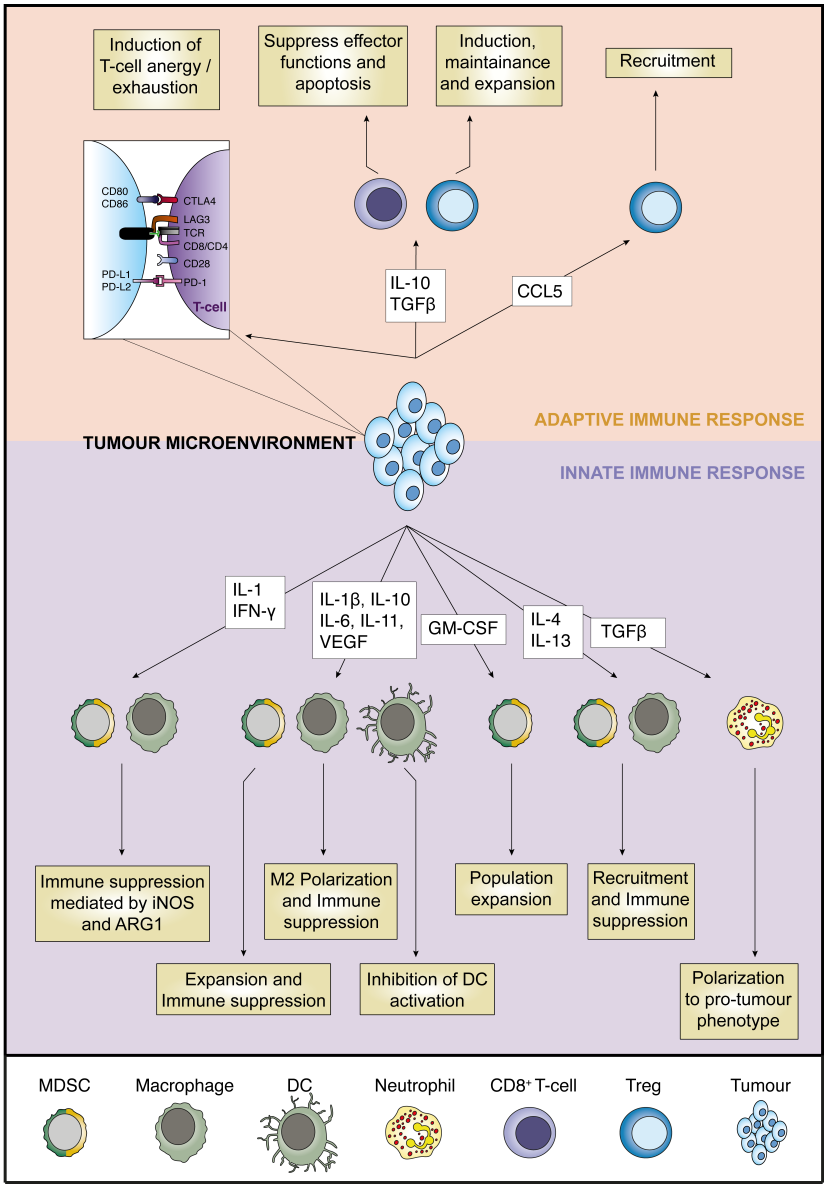

Figure 2.6 | Tumours subvert immune responses to aid tumour growth and survival. Tumour cell expressed and secreted molecules modulate aspects of the adaptive (*top*) and innate (*bottom*) arms of the immune response. Tumour cells may increase the expansion, recruitment or immunosuppressive capacity of pro-tumorigenic populations such as M2 macrophages, Tregs, MDSCs and polarized neutrophils and directly evade anti-tumour $CD8^+$ T-cell responses by the suppression of $CD8^+$ effector functions, the induction of T-cell anergy / exhaustion or by the inhibition of DC-mediated antigen presentation. *top* Tumour cell may express co-stimulatory molecules such as PD-1 and CTLA4 which act to induce T-cell anergy and exhaustion. Secreted factors such as IL-10, TGFβ and CCL5 act to suppress effector $CD8^+$ T-cell functions and increase the recruitment and the immunosuppressive capacity of Tregs. *bottom* Some factors act synergistically with both arms of the immune response, namely TGFβ and IL-10 which not only act to modulate the adaptive immune response, but may also enhance the pro-tumorigenic polarization of neutrophils and macrophages. Factors such as IL-1, IL-4, IL-6 and IL-11 act to increase the recruitment, expansion and immunosuppressive functions of MDSCs and M2 macrophages. Others may act to inhibit DC activation and thereby inhibit the $CD8^+$ T-cell response. MDSC = myeloid-derived suppressor cell; DC = dendritic cell

3 FAK is a central molecule in the regulation of key cancer cell phenotypes.

FAK is a non-receptor protein tyrosine kinase localised primarily at focal adhesions, where it acts a pivotal signalling integrator downstream of integrins and growth factor receptors. It consists of 3 functional protein domains; an N-terminal Four-point-one, Ezrin, Radixin, Moesin (FERM) domain, a central kinase domain and a C-terminal Focal Adhesion Targeting (FAT) domain[244] (**Figure 3.1**). Autophosphorylation of tyrosine residue 397 (Y397) reveals a high affinity SH2 Src family-binding domain. Upon Src binding, a transactivation mechanism results in the phosphorylation of other key tyrosine residues (Y576, Y577, Y862 and Y925), fully activating FAK and forming the FAK-Src signalling complex. Further to FAKs association with Src, other FAK binding partners include Arp2/3, talin and paxillin, VE-cadherin, PI3K/AKT, GRB2 and p53 (**Figure 3.1**). Through both kinase-dependant and independent protein:protein interactions such as these, FAK regulates a number of signalling pathways associated with tumour growth and metastasis (**Figure 3.2**) including regulation of invasion[245], cell morphology and polarization[246-248], motility[249-251], cell cycle progression[252] and proliferation[253,254]. Studies investigating the role of FAK in cancer have thus far identified elevated levels of FAK expression in a range of tumours, including breast[255-257], colon[255,256], prostate[258], oral[259], laryngeal[260], skin[245], and squamous cell carcinomas[261]. Thus FAK presents a therapeutic target that is both upregulated in a number of cancer models and is critically important in an array of cancer cell processes.

Tumour cell:ECM contact provides both contextual and survival signals to tumour cells. The ECM is commonly deregulated and disorganized in cancer which promotes cellular transformation and metastatic progression[262]. Tumour cells interact with the ECM at sites of integrin clustering, known as focal adhesions. Here, integrins mediate bi-directional signaling across the plasma membrane by virtue of their association with intra-cellular macro-molecular complexes, of which FAK is a key component. Downstream of integrins, FAK is known to regulate multiple processes in tumour biology, including the invasion, migration and metastasis, and tumour survival and growth.

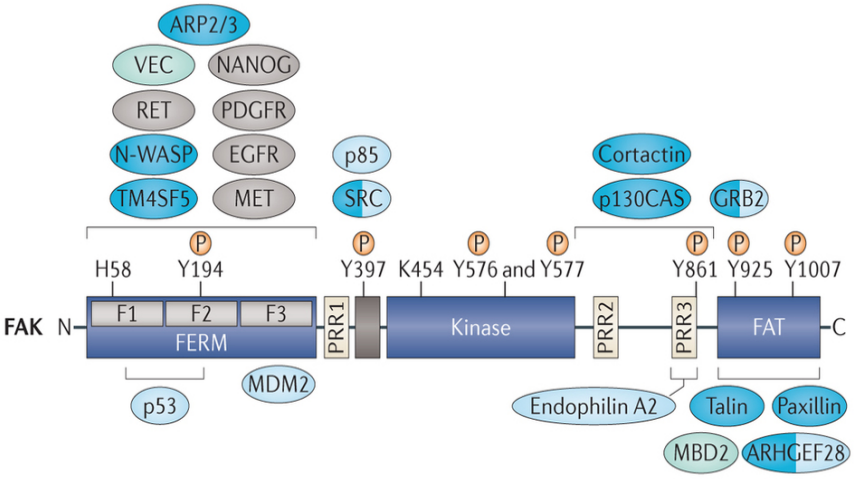

Figure 3.1 | The structure of FAK and key binding partners. The structure of FAK consists of three modular domains; an N-terminal four-point-one, ezrin, radixin, moesin (FERM) domain, a central kinase domain and a C-terminal focal adhesion targeting (FAT) domain. Activation of FAK requires the autophosphorylation of tyrosine (Y) 397, and the subsequent phosphorylation of key residues (as shown). Lysine (K) 454 is a critical molecule in the kinase activity of FAK and mutation of this residue generates a kinase-deficient FAK analogue. FAK complexes with a number of proteins involved in cell motility (dark blue), cell survival (light blue) or both functions (dark blue/light blue). Roles involving FAK activation are shown in grey, and important contributions to the tumour environment are shown in green. Figure adapted from *FAK in cancer: mechanistic findings and clinical applications*. Sulzmaier, F. J., Jean, C. & Schlaepfer, D. D. Nature reviews Cancer, 2014

3.1 FAK promotes tumour cell invasion and metastasis

Dynamic changes in focal adhesions and in cytoskeletal organisation and polymerisation allow tumour cells to polarize, transition to a motile state and invade. Canonical FAK signalling is associated with the maturation and turnover of focal adhesions[263-265]. The loss of FAK in cells increases the number of immature focal adhesions correlating with decreased cell migration[266]. Through the recruitment and activation of key adaptor proteins such as paxillin[267] and talin[268], and through an association with proteolysis complex CPN2 and Caspase-8[269], FAK regulates both the disassembly and maturation of focal adhesions at the cell leading and trailing edges (**Figure 3.2b**).

FAK further contributes to migration and cellular polarization by regulating cytoskeletal dynamics through interactions with complexes involved in actin polymerisation and Rho family signalling modulation[263]. In a kinase independent manner, the FAK-FERM domain binds the Arp2/3 complex, enhancing Arp2/3-depandant actin polymerisation. This results in increased protrusive lamellipodia formation and cell spreading[248]. In addition FAK regulates the activation of Rho family GTPases; GTPase regulator associated with FAK (GRAF, part of the RhoGAP family) and ARHGEF28 (also known as p190RhoGEF) bind to the c-terminal domain of FAK, and act to inhibit and activate Rho mediated signalling respectively[263]. Why FAK interacts with complexes that both activate and

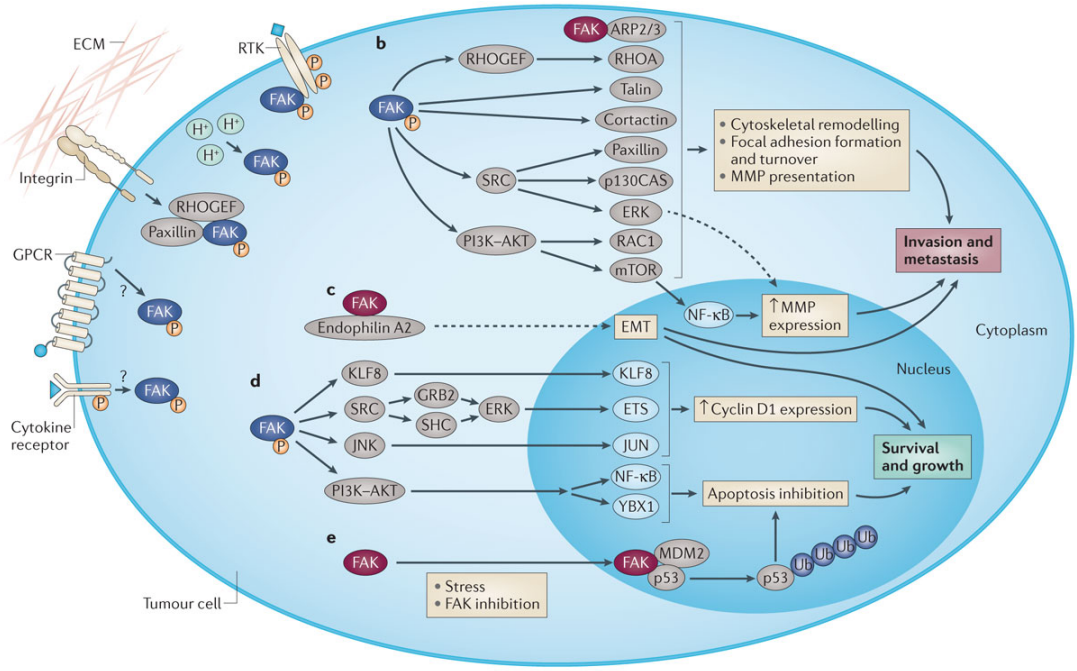

Figure 3.2 | Signaling pathways of FAK that regulate tumour growth and metastasis. FAK enhances tumour growth and metastasis through kinase-dependent (blue) or kinase-independent (red) functions. *Dashed lines* represent processes that have yet to be fully characterized. **a** FAK is activated downstream of receptor tyrosine kinases (RTKs), integrins, G-protein coupled receptors (GPCRs) and cytokine receptors. **b** Activated FAK increases tumour cell invasion and metastasis by remodeling the cytoskeleton, turnover of focal adhesions and the transcriptional upregulation and presentation of matrix metalloproteinases (MMPs). **c** FAK kinase-independent scaffolding functions interact with endophilin A2 increasing the expression of markers of endothelial-to-mesenchymal transition (EMT). **d** FAK activation increases the levels of cyclin D1 expression and enhances the inhibition of apoptosis subsequently increasing tumour cell survival and growth. **e** Under conditions of cellular stress, FAK may translocate to the nucleus where is acts as a scaffold for the p53/MDM2 complex, targeting p53 for polyubiquitination (Ub) and increasing tumour survival and growth. Figure taken from *FAK in cancer: mechanistic findings and clinical applications*. Sulzmaier, F. J., Jean, C. & Schlaepfer, D. D. Nature reviews Cancer, 2014

inhibit Rho signalling is not yet understood, but it raises an interesting hypothesis that FAK may act to both spatially and temporally regulate actin dynamics by alternately associating with both RhoGAPs and RhoGEFs[263,270].

What these data suggest is that FAK is a critical molecule in the regulation of cell polarization, motility and invasion. Epithelial to mesenchymal phenotype (EMT) is required for the migration and metastatic progression of some caner cells, where as come cells migrate collectively. FAK signalling promotes EMT-like transcriptional programmes and both TGFβ-[271] and SNAIL1-induced[272] EMT requires FAK expression. Moreover, inhibition of FAK or Src regulates E-cadherin internalization *in vivo*[249], stabilizing E-cadherin cell surface expression resulting in a suppression of E-cadherin-dependent collective cell migration[249,273]. Thus FAK plays an important role in EMT, invasion and metastatic progression, providing the basis for the development of a number of FAK kinase inhibitors as discussed in detail below.

3.1.1 FAK promotes tumour cell survival and growth

FAK promotes tumour cell survival through kinase dependant and independent mechanisms (**Figure 3.2d**). Those that require kinase activity include FAK signalling through the PI3K-AKT pathway[274]. Tumours can prevent death-inducing signals by the integrin-mediated activation of the FAK-AKT pathway[275]. Tumour cells may also activate this pathway in times of adhesion stress and inhibit the onset of anoikis[274]. Studies using a kinase deficient mutant of FAK have identified that FAK kinase activity is also a requirement for the anchorage-independent 3 dimensional growth of squamous cell carcinoma (SCC) cells *in vitro,* and their growth as xenografts in CD1 nude mice[276].

FAK activity also regulates cell cycle progression. Loss of FAK decreases levels of cyclin D1, and consequently genetic deletion of FAK in tumour cells inhibits G1 to S phase transition, reducing tumour cell growth[277]. FAK regulates levels of Cyclin D1 through three separate pathways. Firstly, FAK signals through ERK in a Src-dependant manner, and ablation or inhibition of FAK reduces Src-mediated p130CAS activation and signalling through ERK in models of breast cancer[278,279].

Activation of ERK leads to its nuclear translocation and the transcription of *CCND1* (gene encoding Cyclin D1)[280]. Secondly, FAK induces the expression of the transcription factor KLF8 through the activation of PI3K-AKT pathway, which leads the transcription of *KLF8* by SP1[281]. KLF8 directly transcribes *CCND1* enhancing cell cycle progression, but is also critical in EMT and oncogenic transformation[281]. Finally, FAK can increase levels of Cyclin D1 though interactions with JNK.

3.1.2 FAK and the nucleus

In addition to its signaling role at focal adhesions, FAK has also been shown to display nuclear localization and have distinct functions in the nucleus. The emergence of kinase-independent functions of FAK fueled investigation into other domains, leading to the discovery of a Nuclear Localization Sequence (NLS) within the FAK FERM domain and revealing some of FAK's nuclear functions[282]. It has been shown that nuclear FAK forms a tri-molecular complex with p53 and the E3 ubiquitin ligase mdm2, targeting p53 for degradation, promoting cell cycle progression[283] (**Figure 3.2e**). Further nuclear specific studies have shown FAK also targets GATA-4 for degradation[284], a transcription factor associated with the expression of pro-inflammatory protein VCAM-1 amongst others[284]. This relationship between nuclear FAK and transcription factors brings into focus numerous potential roles for FAK in direct transcriptional regulation.

3.1.3 FAK and Pyk2

Proline-rich tyrosine kinase 2 (Pyk2) is a closely related non-receptor tyrosine kinase to FAK, and shares approximately 60% sequence homology. Pyk2 and FAK share the same modular domain structure, an N-terminal FERM domain, central kinase domain and C-terminal FAT domain, with the phosphorylation of critical Pyk2 tyrosine residues Y402, Y579/580 and Y880 functioning synonymous to FAK Y397, Y576/577 and Y925 respectively[285]. However, Pyk2 displays perinuclear distribution and localization, and is only weakly present at focal adhesions. Both proteins do

share common protein binding partners, including Grb2, and are associated in a trans-activation mechanism with Src family kinases[286]. FAK is thought to be expressed a various levels in most tissues, whereas Pyk2 expression appears restricted to epithelial cells, neurons and hematopoietic cells[287-291]. Pyk2 has a small number of unique binding partners, such as the actin associated protein gelsolin, and Talin only associates with FAK C-terminal domain and not Pyk2. Pyk2 may act in a compensatory manner to FAK, although their expression and regulation are distinct[292]. Due to their sequence similarity many FAK kinase inhibitors also target Pyk2 with greater or lesser affinities.

3.2 FAK signalling within the microenvironment

Alongside FAKs roles in tumour cell biology, it is also a central molecule in a number of stromal cells within the microenvironment (**summarized in Figure 3.3**). A series of non-cellular microenvironmental cues that influence tumour growth, survival, progression and metastasis may act by increasing FAK activity in stromal cells in the tumour microenvironment[265]. Increases in pH correlate with the upregulation of FAK Y397 autophosphorylation and focal adhesion maturation[293], and increased FAK activation has been observed downstream of VEGF binding to its receptor. Upregulation of FAK expression in stromal cells can also be controlled by these factors. *FAK* gene expression is regulated in part by active NF-κB[294]. Signals related to cellular stress such as reactive oxygen species (ROS), TNFα[295], growth factors, and chemokines and cytokines such as IL-1β and IL-8[296] activate NF-κB, leading to the transcriptional upregulation of *FAK*. Thus, the influence of FAK signalling on tumour cell biology extends beyond the tumour cells themselves and into the stromal compartment of the microenvironment as discussed below.

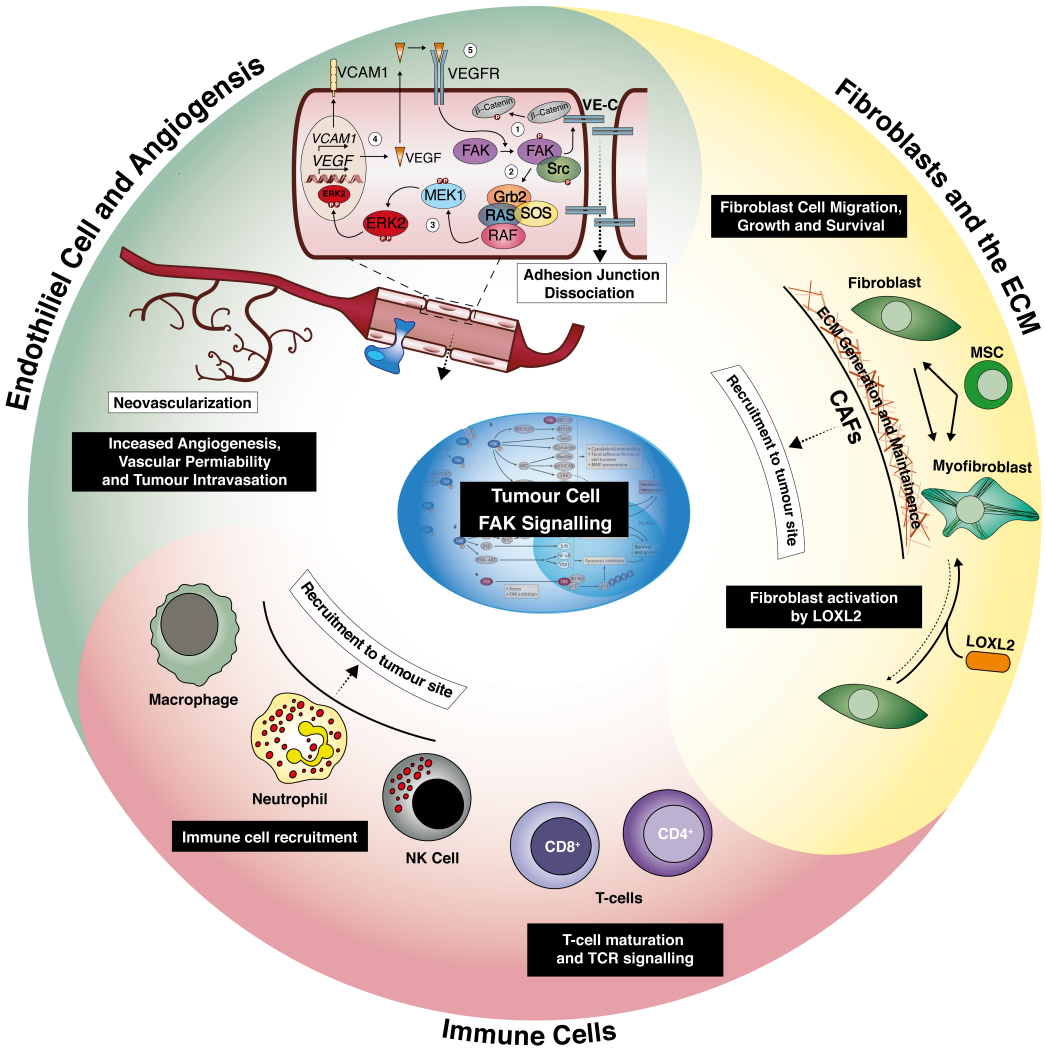

Figure 3.3 | The roles of FAK in the tumour microenvironment. FAK play numerous roles in the each compartment of the tumour microenvironment. In the immune compartment FAK is required for macrophage, natural killer (NK) cell and neutrophil migration and tumour recruitment (3.2.1). It may also play a role in signal transduction downstream T-cell receptor (TCR) activation on T-cells. In endothial cells FAK is involved in increasing angiogenesis, vascular permeability and tumour cell intravasation (3.2.2). FAK is also required for fibroblast migration, growth and survival, activation by LOXL2 and cancer associated fibroblast (CAF) recruitment into the tumour microenvironment (3.2.3). Adapted from *FAK in cancer: mechanistic findings and clinical applications*. Sulzmaier, F. J., Jean, C. & Schlaepfer, D. D. Nature reviews Cancer, 2014

3.2.1 FAK signaling in immune cells

FAK is expressed in a number of cells from both the adaptive and innate immune lineages, including macrophages, neutrophils and T-cells[297]. Macrophages and neutrophils are cell populations of the myeloid lineage, central in mediating the immune response at sites of heightened inflammation such as cancer. Typically, the first cells to respond to changes in inflammation, they act to phagocytose cell debris and aid in angiogenesis and tissue repair. In terms of cancer, the most extensively characterised of these cells are macrophages. FAK is upregulated in differentiating myeloid cells following GM-CSF stimulation[297], and macrophage motility requires FAK signaling downstream of α5β1 for haptotaxis toward fibronectin and for directional chemotaxis toward M-CSF1[298]. FAK knockout in macrophages also decreases monocyte recruitment to inflammatory sites *in vivo*[299]. Treatment with a FAK inhibitor in mouse models of breast cancer results in decreased levels of tumour associated macrophages (TAMs) and a reduction in primary tumour size[300,301]. Additionally in models of PDAC, without effecting angiogenesis, necrosis or apoptosis, FAK inhibition also resulted in a decrease in TAM recruitment[302].

The role of FAK in other myeloid lineages is controversial. In mice with a myeloid specific FAK deletion (a Lyzsozyme 2 knock-in cre; B6.129P2-Lyz2$^{tm1(cre)Ifo}$/J)[303], neutrophils demonstrated accelerated spontaneous cell death and reduced phagocytic activity[303]. Other work disputes the role of FAK in myeloid cell differentiation, indicating that FAK is decreased in haematopoietic stem cells before commitment toward a myeloid lineage, and this shift in haematopoietic homeostasis is linked to increased metastasis[304]. Furthermore, in a study of acute myeloid leukaemia (AML), FAK expression was upregulated in CD34$^+$ AML cells but not in CD34$^+$ normal cells[305], contradicting previous work identifying FAK upregulation in early myeloid progenitors[297]. Many of the problems associated with addressing the role of FAK in myeloid cells, and hence the conflicting data, are due to the involvement of Pyk2. In a number of studies involving myeloid cells, FAK upregulation correlates with an upregulation of phosphorylated Pyk2 (Y881)[305]. Therefore, the effects of Pyk2

activation need to be further dissected before the role of FAK in myeloid cells can be addressed definitively.

In T-cells, TCR signal transduction involves the Src family kinases Fyn and Lck (**2.1.2.1**), and therefore could imply due to the close association between FAK and Src family kinases, that FAK may play an important role in TCR signal transduction. However, some data suggests that FAK negatively regulates TCR signalling and FAK-/- Jurkat cells upregulate IL-2 production associated with increase ZAP70 phosphorylation[306]. In this purposed mechanism, FAK activation recruits C-terminal Src kinase (CSK) to the membrane, impairing CSK activation of Lck, and thus inhibiting TCR signalling down-stream of Lck[306]. FAK kinase inhibition with PF-562,271 reduces $CD4^+$ T-cell TCR activation, and reduced in the phosphorylation of ZAP70 downstream Erk1/2 activation, which was associated with a reduction in the proliferation of both murine and human T-cell was reduced following treatment with PF-562,271[307]. However, the conditional deletion of FAK in $CD4^+$ T-cells does not impair proliferation, and therefor the mechanism of PF-562,271 could be due to inhibition Pyk2.

What brings many of these finding in to question, is that most of these studies were performed in Jurkat cells, and to what extent cell signalling has been effected by the immortalisation of these cells has not yet been addressed. These concerns are heightened by primary and *in vivo* data in which FAK appears not to be expressed in T-cells. Furthermore, Pyk2 has distinct and better characterized roles in T-cells.Pyk2 overexpression in immortalised $CD4^+$ Jurkat cells identified that TCR- and CD28-induced JNK and p38 MAPK activation, and subsequent IL-2 production, was partially dependant on Pyk2[308]. T-cell specific deletion of Pyk2 reduced the proliferative capacity of T-cells *in vitro*, and reduced IL-2 and IFN-γ production in $CD8^+$ T-cells[309]. However, similar effects were not as evident *in vivo*, potentially linked to FAK upregulation upon T-cell activation[306] and subsequent compensation for loss of Pyk2. Pyk2 is also reported to mediate actin cytoskeletal dynamics downstream of TCR stimulation, and to play a role in the re-organisation of T-cell morphology during the formation of the immunological synapse[309,310].

3.2.2 FAK destabilizes EC cell junctions and promotes EC migration and angiogenesis

FAK in ECs is considered a therapeutic target for the treatment of vascular diseases including cancer[265]. Treatment with a FAK inhibitor reduces tumour angiogenesis in animal models of colon[311], hepatocellular[312] and ovarian carcinoma[313,314]. A number of animal models have identified that conditional knockout of FAK[315-317] or conditional knock-in of a kinase dead (KD) FAK[314,318] reduces tumour neovascularization, vascular permeability and angiogenesis. Both approaches resulted in early embryonic lethality due to multiple vascular defects. Primary ECs isolated from these mice exhibited defects in tubulogeneis, sprouting, migration, proliferation and survival *in vitro*. Further *in vitro* work identified that RACK1 and vimentin associate with FAK during endothelial migration through a 3D collagen matrix, and this RACK1-vimentin-FAK signalling complex is hypothesised to regulate EC polarization, motility and focal adhesion turnover during the initial phases of neovascularization[319]. Furthermore, FAK mRNA and protein levels are upregulated in cancer associated ECs[320] concomitant to an increase in FAK Y397 phosphorylation[314]. Thus FAK in ECs plays a critical role in establishing the neovascular architecture in a developing tumour.

As described above (**2.2.1**), the generation of the neovasculature leads to increased tumour progression and metastasis. For tumours to progress after local invasion, tumour cells must then enter the vasculature in order to circulate and metastasise to distant sites in the body. This intravasation requires increased vascular permeability, achieved by the dissociation of tight endothelial cell-cell junctions formed by the vascular endothial cadherin (VE-cadherin) complex (**Figure 3.4**). In ECs, FAK becomes phosphorylated and activated downstream of integrins and growth factor receptor signalling, forming the FAK-Src signalling complex. Following rapid localisation of this complex to cell-cell junctions, the FAK FERM domain binds to the cytoplasmic tail of VE-cadherin. FAK in turn directly phosphorylates Y142 of VE-cadherin associated β-catenin[321], leading to the breakdown of the VE-cadherin-β-catenin complex and the dissociation of EC adhesion junctions. The dissociation of EC adhesion junctions increases vascular permeably and concomitant

tumour cell intravasation. FAK inhibition reduces the phosphorylation of β-catenin and also inhibits the association of FAK to VE-cadherin[321]. Although the FERM domain of FAK mediates this association in a kinase independent-manner, the conformational change following FAK phosphorylation is required for VE-cadherin-FAK binding, which is blocked following FAK kinase inhibition.

Further to FAKs role in increasing vascular permeability, FAK mediates VEGF-induced angiogenesis in ECs via a paracrine signalling axis involving the MAPK pathway (**Figure 3.4**). Binding of Grb2 to FAK Y925 leads to the formation of the Grb2-RAS-RAF-SOS signalling complex and the activation of the MAPK pathway, upstream of ERK activation and nuclear translocation. Amongst other

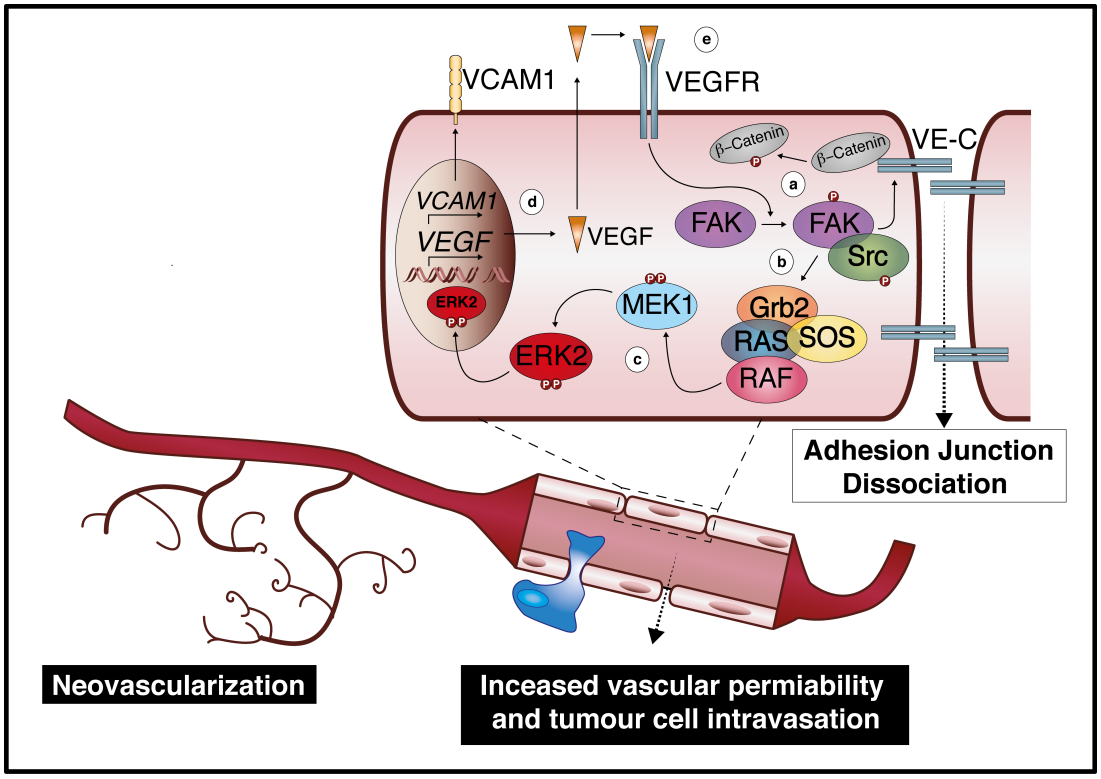

Figure 3.4 | The roles of FAK in endothelial cells. FAK plays multiple roles in endothelial cells in order to increase neovascularization, vascular permeability and tumour cell intravasation. **a** FAK is activated downstream of VEGF stimulation of VEGFR, leading to the formation of the FAK-Src signaling complex. FAK-Src signaling complex rapidly associates with VE-cadherin at cell-cell junctions, leading to the breakdown of the VE-cadherin-β-catenin complex and the dissociation of EC adhesion junctions. **b** activation of the FAK-Src signaling complex generated the formation of the Grb2-RAS-RAF-SOS signing complex, **c** resulting in the activation of the MAPK pathway and the nuclear translocation of active ERK. **d** activated ERK upregulates the transcription and secretion of VEGF, which **e** forms a paracrine signaling axis, binding to VEGFR and increasing the activation of FAK.

nuclear targets of activated ERK, VEGF is transcriptionally upregulated leading to increased VEGF secretion into the surrounding microenvironment. Secreted VEGF may then bind to its receptor (VEGFR) increasing levels of FAK phophorylation[322]. In this mechanism, ECs can initiate VEGF-directed angiogenesis quickly following the amplification of relatively small amount of VEGF, thus repairing damaged vessels or indeed establishing neovasculature, as efficiently as possible. Other nuclear targets of the ERK signalling cascade include vascular cell adhesion molecule 1 (VCAM1) following GATA4-dependant transcription[284], and E-selectin[323], proteins involved in immune cell and tumour cell binding to ECs respectively. Although the role of VCAM1 expression on ECs is unclear, E-selectin binds tumour cells to ECs mediating tumour cell intravasation. Although work continues in order to understand the role of FAK in ECs, what is clear is that FAK plays a substantial role in both the development of neovascular architecture and in linking tumour cells to ECs, both aiding tumour survival and progression through metastasis.

3.2.3 FAK is essential to fibroblast biology, fibroblast activation and CAF recruitment.

Much of what is currently known about the role of FAK in stromal cell biology originates from work in fibroblasts. In fibroblast cell models, FAK was shown to mediate migration, polarisation, cell cycle progression and survival in a manner akin to tumour cells (**3.1**). Fibroblasts exist in multiple different activated states within the tumour microenvironment (**2.2.2**) and FAK is involved in fibroblast differentiation and activation. Secreted proteins and growth factors mediate the regulation of nascent fibroblast activation resulting in the upregulation of α-SMA expression. Lysyl oxidase-like 2 (LOXL2) activates fibroblasts and promotes expression of α-SMA in a FAK dependant manner through activation of the AKT pathway[213,324]. Inhibition of LOXL2 greatly reduced metastasis and primary tumour cell invasion in both orthotropic and transgenic mouse mammary carcinoma models[324]. Although this study did not investigate these effects in FAK-/- fibroblasts, FAK inhibition was shown to reduce AKT activation and α-SMA production, and integrin-mediated FAK

Y397 phosphorylation increased in fibroblasts following treatment with recombinant LOXL2[324]. Other studies have shown that FAK may also regulate the 'deactivation' of myofibroblasts and their differentiation back into fibroblasts by enhancing FGF signalling which ultimately decreases α-SMA expression[325], which implies that the role of FAK in myofibroblast differentiation may be context dependant.. Further to FAKs role in fibroblast activation, the recruitment of CAFs into the tumour microenvironment is also dependant on FAK. FAK mediates the migration of fibroblasts downstream of α5β1 integrin engagement and inhibition of FAK in pancreatic ductal adenocarcinoma (PDAC) was associated with a reduction in CAF recruitment, associated with a reduction in tumour growth and metastasis[302].

3.3 Conclusion

As described in detail above, the role of FAK downstream of integrins has been, and continues to be, investigated in a number of cell types, many of which contribute to the composition of the tumour microenvironment. Thus, therapeutic targeting of FAK has the potential to impact directly on tumour cells, endothelial cells, fibroblasts, and some immune cells. However, little has been done to address whether FAK signalling in cancer cells has any influence over the composition or activation status of cells within the tumour microenvironment. Recently, FAK has been identified to translocate to the nucleus under conditions of stress, where its function remains largely unknown. Preliminary studies suggest that FAK may be able to influence the transcription of some secreted factors, including TGFβ, VEGF, angiopoeitin 1, and interleukin-6, implying that it may have an unappreciated function in regulating aspects of paracrine signalling between cell types. I therefore set out to test whether FAK signalling in tumour cells was involved in the regulation of chemokines and cytokines by tumour cells, and if so, whether this could influence the immune cell composition of the tumour microenvironment and ultimately tumour growth and survival.

4 Materials and methods

4.1 Materials

4.1.1 Cell culture reagents

Supplier*: ECRC Central Services*

Sterile PBS

Sterile PE

Supplier*: Life Technologies, Loughborough, UK*

HBSS

DMEM

GMEM

IMDM

MEM vitamins

MEM non-essential amino acids

200 mM L-glutamine

2.5% trypsin solution

Dispase II

Fetal bovine serum (FBS)

Supplier*: Merck Millipore, Hertfordshire, UK*

Hygromycin B

0.45 μM Millex-HA filter

Supplier: *Qiagen, Crawley, UK*

Miniprep DNA Kit

Maxiprep DNA Kit

RNAeasy Kit + On-column DNase addition

Gel purification Kit

PCR purification Kit

Supplier: *Sigma Chemical Co, Poole, UK*

Polybrene

Sodium pyruvate

Doxorubicin hydrochloride

Supplier: *ATCC, LGC Standards, Middlesex, UK*

TIB-207

TIB-210

4.1.2 Cell culture plastic-ware

Supplier: *Becton Dickinson Biosciences, Oxford, UK*

Falcon vented tissue culture flasks (T25, T150 and T175)

Falcon tissue culture dishes (60 mm, 90 mm and 120 mm)

Cell strainers (40 and 70 μm)

4.1.3 Cell Culture medium

4.1.3.1 SCC and Mel31

1x GMEM supplemented with

10% FBS

2 mM L-glutamine

1% Non Essential Amino Acids

1% MEM vitamins

1% Sodium Pyruvate

4.1.3.2 Panc043, Panc047, Panc117 and Met01

1x DMEM supplemented with

10% FBS

2 mM L-glutamine

4.1.3.3 *HEK293FT*

1x DMEM supplemented with

10% FBS

2mM L-glutamine

1% Non Essential Amino Acids

4.1.3.4 Phoenix Ecotropic

1x DMEM supplemented with

10% FBS

2mM L-glutamine

4.1.3.5 TIB-207

1 x IMDM supplemented with

2% FBS

4.1.3.6 TIB-210

1x DMEM supplemented with

2% FBS

4.1.3.7 Trypsin

0.25% trypsin in sterile PE

4.1.4 Animal experiments

Supplier: *Sigma Chemical Co, Poole, UK*

Tween 80

Carboxymethyl cellulose (CMC)

Supplier: *Verastem, MA, USA*

VS-4718

Supplier: *Charles River, Kent, UK*

FVB/Ncrl (FVB/N) mice

BALB/cAnNCrl (BALB/c) Mice

C57BL/6NCrl (C57BL/6) mice

Crl:CD1-Foxn1nu (CD-1 nude) mice

All mice were supplied as age matched, 5-week old females and isolated for one work after delivery.

4.1.5 Immunofluorescence

Supplier: *Sigma Chemical Co, Poole, UK*

Formaldehyde

Supplier: *Thermo Fisher, Loughborough, UK*

Circular 19mm glass cover slip

Prolong gold anti-fade mounting media

Supplier*: NIH*

ImageJ software

Supplier*: Olympus UK Ltd, Hertfordshire, UK*

Olympus FV1000 Confocal microscope

4.1.6 Western Blotting and electrophoresis

Supplier*: Bio-Rad Laboratories Ltd, Hertforshire, UK*

4–15% Mini-PROTEAN® TGX™ Precast Protein Gels

Precision Plus Protein™ WesternC™ Standards

Trans-Blot® Turbo™ Midi Nitrocellulose Transfer pack

Mini-PROTEAN® Tetra Cell gel electrophoresis tank

Trans-Blot® Turbo™ Transfer System

Clarity™ Western ECL Blotting Substrate

ChemiDoc MP Imaging System

Image Lab™ image acquisition and analysis software

10x TGS buffer

Supplier: *Beckman Coulter, Luton, UK*

Beckman DU 650 spectrophotometer

Supplier: *Chemicon International, Harrow, UK*

Re-blot kit

Supplier : *Sigma Chemical Co, Poole, UK*

Triton X-100

Sodium Chloride (NaCl)

Tris base

Sodium deoxycholate

Sodium dodecyl sulphate (SDS)

2-mercaptoethanol

Gycerol

Bromophenol blue

Tween 20

Supplier: *Thermo Fisher, Loughborough, UK*

Micro BCA protein assay kit

Supplier: *Merck Millipore, Hertfordshire, UK*

Bovine serum albumin (BSA)

Supplier : *Roche, Hertfordshire, UK*

protease inhibitor cocktail

phosphatase inhibitor cocktail

4.1.7 Western Blotting and electrophoresis buffers

4.1.7.1 RIPA buffer

50 mM Tris/HCl, pH 7.6

150 mM NaCl

1% Triton X-100

0.5% Sodium deoxycholate

0.1% sodium dodecyl sulphate (SDS)

Protease inhibitor cocktail

Phosphatase inhibitor cocktail

4.1.7.2 2x Sample buffer

800 µl 2-mercaptoethanol

1.3 ml Tris pH 6.8

2 ml glycerol

5 ml 10% SDS

1.3 ml H2O

Bromophenol blue to colour

4.1.7.3 Wash buffer

0.2% Tween 20 in Tris Base Solution

4.1.8 Western Blotting antibodies

Supplier: *New England Biolabs, Hertfordshire, UK*

Anti-mouse/horseradish peroxidase conjugate

Anti-rabbit/horseradish peroxidase conjugate

Anti-mouse Bcl-2

Anti-mouse PARP

Anti-mouse β-Actin

Anti-mouse Caspase 3

4.1.9 Antibody purification

Supplier: *Thermo Fisher, Loughborough, UK*

Melon™ Gel IgG Purification Kit

SnakeSkin™ Dialysis Tubing, 10K MWCO, 22 mm

Supplier: *Sigma Chemical Co, Poole, UK*

Whatman® qualitative filter paper, 110mm, Grade 1

4.1.10 FACS analysis

Supplier: *Becton Dickinson Biosciences, Oxford, UK*

BD FACS Aria II

Falcon® Round-Bottom Tubes, Polystyrene

10x Pharm Lyse red blood cell lysis buffer

70 μm Cell strainers

Supplier: *Thermo Fisher, Loughborough, UK*

Countess automated cell counter

Countess automated cell counter slide

0.4% Trypan Blue stain

RPMI

DMEM

FBS

Dispase II

Supplier*: ECRC Central Services*

Sterile PBS

Supplier: *StarLabs UK Ltd, Milton Keynes, UK*

Sterile 1.2ml Microtubes in Rack

Supplier: *Roche, Hertfordshire, UK*

Collagenase D

Supplier: *Sigma Chemical Co, Poole, UK*

Hyaluronidase

Sodium Azide

4.1.11 FACS analysis buffers

4.1.11.1 FACS buffer

Sterile PBS

1% FBS

0.1% Sodium Azide

4.1.11.2 Fc Block

1 in 200 CD16/CD32 (Fc Blocking anybody)

in FACS buffer

4.1.12 FACS analysis antibodies

Supplier: *eBioscience, Hatfield, UK*

Anti-mouse CD16/CD32 (Fc Blocking antibody)

eFluor® 506 conjugated fixable viability dye

Anti-mouse CD45 – eFluor 450 conjugated

Anti-mouse CD45 – eFluor 780 conjugated

Anti-mouse F4/80 – FITC conjugated

Anti-mouse F4/80 – PE-Cy7 conjugated

Anti-mouse CD11b – PerPC-Cy5.5 conjugated

Anti-mouse MMR – APC conjugated

Anti-mouse Tie2 – PE conjugated

Anti-mouse Ly6C – eFluor 450 conjugated

Anti-mouse CD3 – FITC conjugated

Anti-mouse CD8 – PE conjugated

Anti-mouse CD4 – eFluor 647 conjugated

Anti-mouse CD62L – PE-Cy7 conjugated

Anti-mouse CD44 – PerCP-Cy5.5 conjugated

Anti-mouse Gr1 – FITC conjugated

Anti-mouse PD-L1 – PE conjugated

Anti-mouse PD-L2 – PE conjugated

Anti-mouse CD80 – eFluor 780 conjugated

Supplier: *Biolegend, London, UK*

Mouse Treg Flow™ Kit (FOXP3 Alexa Fluor® 488/CD4 APC/CD25 PE)

4.1.13 Quantitative RT^2-PCR analysis

Supplier: *Miltenyi Biotec Ltd, Surry, UK*

Treg isolation kit (130-091-041)

LD columns

MidiMACS Separation Kit

Supplier: *Qiagen, Crawley, UK*

RotorGene qRT^2-PCR System

RotorGene qRT^2-PCR analysis software

RNAeasy Kit + On-column DNase addition

RT^2 Profiler™ PCR Array Mouse Cytokines & Chemokine (PAMM-150Z)

RT^2 Profiler™ PCR Array Mouse Chemokines & Receptors (PAMM-022Z)

Supplier: *Thermo Fisher, Loughborough, UK*

SuperScript first-strand cDNA synthesis kit

Supplier: *Bioline Reagents Limited*, *London*, *UK*

SensiFAST™ SYBR® Hi-ROX Kit

Supplier: *StarLabs UK Ltd, Milton Keynes, UK*

96-well semi-skirted PCR plate

4.1.14 Quantitative RT^2-PCR Primers

Supplier: *Thermo Fisher, Loughborough, UK*

CCL5 forward = CCCTCACCATCATCCTCACT

CCL5 reverse = CCTTCGAGTGACAAACACGA.

CxCL10 forward = CCCACGTGTTGAGATCATTG

CxCL10 reverse = CACTGGGTAAAGGGGAGTGA.

B2M forward = GGGAAGCCGAACATACTGAA

B2M reverse = TGCTTAACTCTGCAGGCGTAT

Supplier: *Qiagen, Crawley, UK*

RT² qPCR Primer Assay for Mouse Tgfb2 (PPM02992A)

4.1.15 shRNA mediated knockdown

Supplier: *Thermo Fisher, Loughborough, UK*

Lipofectamine 2000

Supplier: *Sigma Chemical Co, Poole, UK*

Polybrene

Supplier*: Merck Millipore, Hertfordshire, UK*

0.45 μM Millex-HA filter

Supplier*: GE Healthcare, Hertfordshire, UK*

pLKO lentiviral TRC library TGFβ2 shRNA (RMM4534-EG21808)

pLKO lentiviral TRC library CCL5 shRNA (RMM4534-EG20304)

4.2 Methods

All animal experiments were carried out in accordance with the United Kingdom Animal Scientific Procedures Act (1986).

4.2.1 Cell lines

4.2.1.1 SCC

SCC cells were previously developed in the lab by A. Serrels *et al*[276] following the two-stage 7,12-dimethylbenz[a]anthracene (DMBA) / 12-*O*-tetradecanoylphorbol-13-acetate (TPA) chemical carcinogenesis protocol[51,326]. Briefly, SCCs were induced in the skin of K14*Cre*ER FAK$^{flox/flox}$ transgenic FVB/N mice. Six-week-old mice were subjected to a single topical application of DMBA followed by twice weekly topical applications of TPA for a period of 20 weeks. Benign papillomas were observed approximately 6-10 weeks following the first treatment of TPA, with a small proportion of papillomas progressing to invasive SCC succeeding 15 weeks

onwards. Following surgical excision of carcinomas, small tissue pieces were adhered to plastic tissue culture plates and cells were allowed to grow out onto the surrounding plastic surface. Tumour pieces and cells were maintained in MEM at 37 °c / 5% CO_2. Outgrowth of cells was observed following one week under normal tissue conditions. The genetic knockout of FAK was achieved following treatment with 15 μM 4-OHT for 24 hours (SCC FAK-/- cells). Purity of the SCC population and efficiency of FAK knockout was determined by PCR and Western Blot analysis as shown in [276] (**Figure 5.1**). SCC FAK-/- cells re-expressing FAK-wt or a kinase dead form of FAK (FAK-kd) were generated using retroviral transfection. Phoenix Ecotropic cells were transfected with FAK-wt or FAK-kd constructs using lipofectamine 2000 (Thermo Fisher) as per manufacturers instructions, as described in [276]. 24 hours post transfection, cell culture supernatant was removed, filtered through a 0.45 μM Millex-HA filter (Merck Millipore), diluted at a 1:1 ratio with normal SCC cell culture medium, supplemented with 5 μg/ml polybrene and added to FAK-/- SCC cells for 24 hours. A total of two rounds of infection were performed to generate each cell line. Cells were cultured at 37 °C / 5% CO_2 in Minimum Essential Medium (MEM; Life Technologies) supplemented with 2 mM L-glutamine, MEM vitamins, 1 mM, MEM amino acids, and 10% fetal bovine serum (all Life Technologies), and sodium pyruvate (Sigma) and maintained under selection using 0.25 mg/ml hygromycin (Merck Millipore. Western blot analysis of partental SCC 7.1, SCC FAK-wt, FAK-/- and FAK-kd cells identified a reduction in FAK pY397 (see **Figure 3.1**), indicative of a reduction in kinase activity in SCC FAK-kd cells, validating published data idenifing this mutant and kinase dead (**Figure 5.1c**)[254,327].

SCC FAK-wt and SCC FAK-/- cell lines over-expressing GFP-tagged Bcl2 were generated using retroviral transfection as described above. The GFP-Bcl2 construct was a kind gift from Lesley Forrester (Center for Inflammation Research, University of Edinburgh).

4.2.1.2 Other cell lines

Mel31, Panc043, Panc047 and Panc117 cell lines were a kind gift from Owen Samson (The Beatson Institute for Cancer Research, Glasgow). Met01 were a kind gift from Bin-Zhi Qian (Centre for Reproductive Health, University of Edinburgh, Edinburgh).

Mel31 cells were cultured at 37 °C / 5% CO_2 in Glasgow Minimum Essential Medium (GMEM) supplemented with 2 mM L-glutamine, MEM vitamins, 1 mM ,MEM amino acids, and 10% FBS (all Life Technologies) and sodium pyruvate (Sigma)

Panc043, Panc047, Panc117 and Met01 cells were cultured at 37 °C / 5% CO_2 in Dulbecco's Minimum Essential Medium (DMEM) supplemented with 2 mM L-glutamine and 10% FBS (all Life Technologies)

4T1 cells were cultured at 37 °C / 5 % CO2 in RPMI medium supplemented with 10% FBS (Life Technologies)

TIB-207 hybridoma cells (ATCC) were cultured at 37 °C / 5 % CO2 in Iscove's Modified Dulbecco's Medium (IMDM) supplemented with 2% FBS (Life Technologies)

TIB-210 hybridoma cells (ATCC) were cultured at 37 °C / 5 % CO2 in Dulbecco's Modified Eagle's Medium (DMEM) supplemented with 2% FBS (Life Technologies).

4.2.2 Western blot analysis

To prepare whole cell lysates, cells were washed x2 in ice cold PBS and lysed in radioimmuno-precipitation assay (RIPA) buffer (50 mmol/L Tris (pH 7.6), 150 mmol/L sodium chloride, 1% Triton X-100, 0.5% deoxycholate, 0.1% SDS, protease inhibitor cocktail (Roche), phosphatase inhibitor cocktail (Roche)). Lysates were cleared by centrifugation at 13000 rpm for 15 minutes at 4 °C. Protein concentration was then determined using Micro BCA protein assay kit (Thermo Fisher). Absorbance was measured with a Beckman DU 650 spectrophotometer (Beckman

Coulter, Luton, UK) at 562 nm. A total of 20 µg of each sample were aliquoted and an appropriate volume of 2x Sample buffer was added and incubated at 95 °C for 5 minutes. Lysates were resolved by 4 - 15% Bis-Tris gel electrophoresis (Biorad) and proteins transferred to (Biorad) using Trans-Blot® Turbo™ Transfer System (Biorad). Membranes were then blocked (5% BSA/PBST) for 1 hour at room temperature and probed with either anti-Bcl2 (1:1000 in 5% BSA/PBST, Cell Signaling Technology), anti-PARP (1:1000 in 5% BSA/PBST, Cell Signaling Technology) or anti-caspase3 (1:1000 in 5% BSA/PBST, Cell Signaling Technology) primary antibodies over-night at 4 °C. After over-night incubation, membranes were washed 3x with PBST and bound antibody was detected by incubation with anti-rabbit or anti-mouse HRP-conjugated secondary antibody (1/5000 in 5% BSA/PBST; Cell Signaling Technology) for 1 hour at room temperature. Following 3x washes with PBST, membranes were prepared for chemiluminescent visualization by incubation for 1 minute in Clarity™ Western ECL Blotting Substrate (Biorad) and visualized using a ChemiDoc MP Imaging System (Biorad). Membranes were rinsed with TBST and distilled water before stripping with re-blot plus mild solution (Chemicon International). After washing with distilled water, stripped membranes were re-probed with 1:10000 anti-actin (Sigma) to check protein loading.

4.2.3 Confocal Immunofluorescence microscopy

SCC FAK-wt and SCC FAK-/- Bcl2-GFP expressing cells were grown on glass coverslips, rinsed in PBS and fixed with 3.7% (v/v) formaldehyde for 15 min. Cells were examined using an Olympus FV1000 confocal microscope (Olympus UK Ltd).

4.2.4 Purification of CD4 and CD8 depleting antibodies

Anti-mouse CD4 (GK1.5, ATCC TIB-207) and CD8 (2.43, ATCC TIB-210) depleting antibodies were purified in-house from conditioned supernatant using a Melon Gel IgG purification kit (Thermo Fisher) as per manufactures instructions.

Cells were removed from supernatants by centrifugation (1300 rpm at 4 °C for 3 minutes). 1 litre of conditioned supernatants were concentrated using 20 mL Pierce™ Protein Concentrators (9K MWCO; Thermo Fisher) to a final volume of 100 ml and dialyzed into 1x Melon Gel purification buffer by 2x 1 hour exchanges into fresh 1x Melon Gel purification buffer (SnakeSkin™ Dialysis Tubing, 10K MWCO, 22 mm; Thermo Fisher). 1x sample volume of Melon IgG Purification Support was equilibrated to room temperature, then added to conditioned supernatants and incubated at room temperature for 5 minutes. Mixture of Melon IgG Purification Support and conditioned supernatants were then applied to a Buchner flask with a pre-soaked 110mm Whatman® qualitative filter paper (Sigma), vacuum was applied and the eluted purified antibody was collected.

Antibody purification was validated by protein visualisation using TGX stain-free gel electrophoresis (Biorad). Samples were resolved by 4 – 15% TGX Bis-Tris gel electrophoresis (Biorad) and UV light was applied to each gel and gels were visualized using a ChemiDoc MP Imaging System (Biorad).

4.2.5 Animal experiments

4.2.5.1 Subcutaneous tumour growth

Cells were injected subcutaneously into both flanks of either CD-1 nude mice (2.5 x 10^5 cells) or FVB/N, BALB/c or c57BL/6 mice (1 x 10^6 cells) and tumour growth measured twice-weekly using calipers. Animals were sacrificed when tumours reached maximum allowed size, or more commonly when signs of ulceration were evident. Group sizes ranged from 3 – 5 mice each bearing two tumours, and tumour volume calculated in Excel using the formula $v = 4/3\pi r^3$. Statistics and graphs were calculated using Prism (Graphpad). For studies involving treatment with VS-4718, drug was prepared in 0.5% carboxymethyl cellulose (CMC) + 0.1% Tween 80 (Sigma) and mice treated at 75 mg/kg BID by oral gavage. Animals were visually monitored for signs of toxicity and weighed prior to each dose with VS-4718. No signs of toxicity were observed.

4.2.5.2 Tumour growth following re-challenge

1 x 10^6 SCC FAK-/- cells were injected subcutaneously into the left flank of FVB/N mice and tumour growth measured twice weekly as described above. Following tumour regression, mice were left for 7 days before being challenged with 1 x 10^6 SCC FAK-wt or SCC FAK-/- cells injected subcutaneously into the right flank. Tumour growth was measured twice-weekly using calipers. Control groups were injected subcutaneously into both flanks at day 28 using mice that had not been pre-challenged with SCC FAK-/- cells. Tumour volume was calculated in Excel using the formula $v = 4/3\pi r^3$. Statistics and graphs were calculated using Prism (Graphpad).

4.2.5.3 $CD4^+$, $CD8^+$ and $CD25^+$ T cell depletion

Anti-mouse CD4 (GK1.5, ATCC TIB-207) and CD8 (2.43, ATCC TIB-210) depleting antibodies were purified in-house (**3.2.3**) or purchased from eBioscience. Rat IgG isotype control antibody and CD25 depleting antibody was both purchased from eBioscience. T-cell depletion was achieved following intra-peritoneal (IP) injection of 150 μg of depleting antibody (same for all antibodies) into female age-matched FVB/N mice for 3 consecutive days, and maintained by further IP injection at 3 day intervals until the study was terminated. 1 x 10^6 SCC FAK-wt or SCC FAK-/- cells were injected subcutaneously into both flanks 6 days after initial antibody treatment and tumour growth measured twice weekly using calipers. The extent of T-cell depletion was determined at the end of the study using FACS analysis from disaggregated spleen and thymus tissue (see below)

4.2.6 FACS analysis of tissues

Tumours established following injection of 1 x 10^6 SCC cells into both flanks of an FVB/N mouse were removed at day 7 into RPMI (Sigma) supplemented with 10% fetal bovine serum (Life technologies). Tumour tissue was mashed into a pulp using a scalpel and re-suspended in DMEM (Sigma) supplemented with 2 mg/ml collagenase D (Roche). Samples were incubated for 1 hour at 37 °C, pelleted by

centrifugation at 1600 rpm for 5 minutes at 4°C, and re-suspended in 5 ml of 1x red blood cell lysis buffer (Pharm Lysis Buffer, Becton Dickinson). Samples were incubated for 5 minutes at 37 °C, then pelleted by centrifugation at 1600 rpm for 5 minutes at 4 °C, re-suspended in PBS and passed through a 70 μm cell strainer (Becton Dickinson). The resulting single cell suspension was pelleted by centrifugation at 1600 rpm for 5 minutes at 4 °C and re-suspended in FACS buffer (PBS + 1% FBS + 0.1% sodium azide). This step was repeated a total of three times. A sample of the suspension was counted using trypan blue exclusion and the remaining cell suspension pelleted by centrifugation at 1600 rpm for 5 minutes at 4 °C and re-suspended in FACS buffer at a concentration of 1 x 10^6 viable cells/ml. 100 μl of each sample was pipetted into each well of a 96-well plate and the plate centrifuged at 1600 rpm for 5 minutes at 4 °C. Cell pellets were re-suspended in 50 μl of Fc block (1 in 200 dilution of Fc antibody (eBioscience) in FACS buffer) and incubated for 15 minutes at 4 °C. 50 μl of antibody mixture was added to each well and the samples incubated for 30 minutes in the dark at 4 °C. All antibodies were from eBioscience and used at a concentration of 1 in 200. The plate was then centrifuged at 1600 rpm for 5 minutes at 4 °C and the cells re-suspended in FACS buffer and analyzed using a BD FACS Aria II (Becton Dickinson).

Treg staining was performed using a Treg staining kit (Biolegend) as per manufacturers instructions. Tumours were disaggregated and incubated in Pharm lysis buffer (Becton Dickinson) as above. Samples were then re-suspended in 1x FOXP3 Fix/Perm buffer and incubated in the dark for 20 minutes at room temperature. Samples were then washed 3 times by centrifuged at 1600 rpm for 5 minutes at 4 °C and re-suspension in 1x FoxP3 Perm buffer. Samples were then stained with antibody cocktail containing anti-mouse FOXP3 Alexa Fluor® 488, CD4 APC and CD25 PE conjugated antibodies for 1 hour in the dark at room temperature. Stained samples were washed 3x in FACS buffer prior to analysis using a BD FACS Aria II (Becton Dickinson).

Staining of spleen and thymus tissue was performed as above.

Data analysis was performed using FlowJo software. Statistics and graphs were calculated using Prism (Graphpad).

For absolute counting, the same protocol as above was used, except tumours were weighed following surgical removal, and prior to FACS analysis samples were resuspended in varying volumes of FACS buffer (dependent on weight) containing CountBright Absolute Counting Beads (Life Technologies).

4.2.7 FACS analysis of cultured cells

Cells were cultured in 90 mm Falcon tissue culture dishes (Becton Dickinson). Cells were removed using 1x non-enzymatic cell dissociation solution (Sigma) and pelleted by centrifugation at 1600 rpm for 5 minutes at 4 °C, re-suspended in PBS and passed through a 70 μm cell strainer (Becton Dickinson). The resulting single cell suspension was pelleted by centrifugation at 1600 rpm for 5 minutes at 4 °C and re-suspended in FACS buffer (PBS + 1% FBS + 0.1% sodium azide). This step was repeated a total of three times. A sample of the suspension was counted using trypan blue exclusion and the remaining cell suspension pelleted by centrifugation at 1600 rpm for 5 minutes at 4 °C and re-suspended in FACS buffer at a concentration of 1 x 10^6 viable cells/ml. 100 μl of each sample was pipetted into each well of a 96-well plate and the plate centrifuged at 1600 rpm for 5 minutes at 4 °C. Cell pellets were re-suspended in 50 μl of Fc block (1 in 200 dilution of Fc antibody (eBioscience) in FACS buffer) and incubated for 15 minutes at 4 °C. 50 μl of antibody mixture was added to each well and the samples incubated for 30 minutes in the dark at 4 °C. All antibodies were from eBioscience and used at a concentration of 1 in 200. The plate was then centrifuged at 1600 rpm for 5 minutes at 4 °C and the cells re-suspended in FACS buffer and analyzed using a BD FACS Aria II (Becton Dickinson).

Data analysis was performed using FlowJo software. Statistics and graphs were calculated using Prism (Graphpad).

4.2.8 Gene expression profiling

RNA was prepared from SCC FAK-wt and SCC FAK-/- cells using an RNAeasy kit (Qiagen) according to the manufacturer's instructions. RNA was analyzed using the GeneChip Mouse Genome 430 2.0 Array (Affymetrix). Array data were background corrected, quantile normalized and log transformed. Data for differentially expressed genes ($P < 0.01$) were median centered and subjected to unsupervised agglomerative hierarchical clustering on the basis of Euclidean distance computed with a complete-linkage matrix using Cluster 3.0 (C Clustering Library, version 1.37) [328]. Clustering results were visualized using Java TreeView (version 1.1.1) [329]. Functional enrichment analysis against the mouse genome background was performed using ToppGene [330].

4.2.9 Quantitative RT^2-PCR array analysis of cytokine, chemokine, and chemokine receptor expression

RNA was isolated and purified using RNeasy kit with on column DNAse digestion (Quiagen). RNA prepared from SCC cells using and was analyzed using the mouse cytokine and chemokine RT^2 Profiler PCR Array (PAMM-150Z; Qiagen) and that from isolated Tregs (isolated using Treg isolation kit, 130-091-041; Miltenyi Biotech) was analyzed using the mouse chemokine and receptor array (PAMM-22Z; Qiagen) according to the manufacturer's instructions. Relative gene expression ($2^{-\Delta Ct}$) values were log transformed, median centered and subjected to hierarchical clustering as for microarray analysis. For interaction network analysis, an interactome of chemokine ligands and receptors was constructed using the IUPHAR/BPS Guide to Pharmacology database [331,332] and curated from the literature [333], onto which expression data for detected genes were mapped and visualized using Cytoscape (version 3.0.2) [334].

In addition, expression of selected cytokine and chemokine genes was assessed by standard quantitative RT-PCR. cDNA was prepared from RNA using SuperScript first-strand cDNA synthesis kit, as per manufactures instructions. cDNA reaction

mix consisted of 5 µg of RNA, 1 µL random hexamer primers (50 ng/µL), 1 µL of 10 mM dNTP stock mix, 4 µL of 25 mM $MgCl_2$, 2 µL of 0.1 M DTT, 1 µL of RNaseOUT (40 U/µL) and 1 µL SuperScript® III RT (200 U/µL) + 1x RT buffer to a final volume of 20 µL. Reactions were incubated for 10 minutes at 25 °C followed by 50 minutes at 50 °C. Reactions were terminated by incubation at 85 °C for 5 minutes, followed by the addition of 1 µL of RNase H to each tube and a final incubation for 20 min at 37 °C, after which cDNA reaction were stored at -20 °C until used.

TGFβ2 specific primers were purchased from Qiagen (Cat Number PPM02992A). CCL5 primers used were: forward, CCCTCACCATCATCCTCACT and reverse, CCTTCGAGTGACAAACACGA. Cxcl10 primers used were: forward, CCCACGTGTTGAGATCATTG and reverse, CACTGGGTAAAGGGGAGTGA. B2M primers used were: forward, GGGAAGCCGAACATACTGAA and reverse, TGCTTAACTCTGCAGGCGTAT. Briefly, a reaction mix consisting of 10 µl SensiFAST SYBR Hi-ROX reagent (Bioline), 0.4 µl of 10 µM stock forward primer, 0.4 µl of 10 µM stock reverse primer, 4.4 µl water, and 4 µl of 20 ng/µl stock random hexamer primed cDNA was run on a Rotorgene qRT-PCR machine using the following cycling conditions: 94°C for 10 minutes; 40 cycles of 94°C for 10 seconds, 57°C for 20 seconds, 72°C for 20 seconds; and 72°C for 7 minutes. Analysis was performed using rotorgene software and expression relative to B2M calculated using Microsoft Excel.

4.2.10 Treg Isolation

Single cell suspensions were generated from both SCC FAK-wt tumours and mouse Thymus as described above. A sample of the suspension was counted using trypan blue exclusion and the remaining cell suspension pelleted by centrifugation at 1600 rpm for 5 minutes at 4 °C and re-suspended in FACS buffer at a concentration of 1 x 10^7 viable cells/40 µL. Tregs were isolated using Treg isolation kit (130-091-041; Miltenyi Biotech) as per manufacturers instructions, using LD columns and MidiMACS Separation Kit (Miltenyi Biotech).

4.2.11 shRNA mediated TGFb2 and CCL5 knockdown

To generate lentiviral particles 2 x 10^6 HEK293FT cells were transfected with a mixture of 10 μg shRNA (TGFβ2 = RMM4534-EG21808; CCL5 = RMM4534-EG20304; GE Healthcare), 6.5 μg HIV, and 3 μg VSVG plasmid DNA using Lipofectamine 2000 (Thermo Fisher) as per manufacturers protocol. 24 hours post transfection, media was removed and filtered through a 0.45 μM Millex-AC filter (Millipore) and mixed at a 1:1 ratio with normal SCC growth media. This mixture was supplemented with polybrene to a final concentration of 5 μg/ml and added to the SCC for 24 hours. Cells were subject to two rounds of lentiviral infection prior to selection with puromycin at a final concentration of 2ug/ml. All shRNA constructs used were part of the pLKO lentiviral TRC library (GE Healthcare).

4.2.12 Statistical analysis

To determine the number of mice required to reach statistical significance in tumour growth experiments, preliminary data for SCC FAK-wt and SCC FAK-/- tumour growth were used in power calculations. 1 x 10^6 SCC FAK-wt and SCC FAK-/- cells were implanted into both flanks of FVB animals (n=5) and tumour growth was measured twice weekly, and tumour volume was calculated as described in **4.2.5.1**. The means of SCC FAK-wt (mean = 237.3 mm^3) and SCC FAK-/- (mean = 47.3 mm^3) tumours, with a standard deviation of 47.1 were compared using a 2-sample, 2-sided equality power calculation (see [335]). Sample size was calculated as 3 mice when using a power of 0.99 and a Type I error rate of 1%.

The number of mice required to reach statistical significance in drug-treated and antibody-treated experiments were determined as above, with a final calculated sample size of 5. The number of experiment repeats in all cases equal 2.

All statistical analysis was calculated using GraphPad Prism 6.0c for Mac. Normality of data was determined using D'Agostino and Pearson omnibus normality test. For FACS analysis, unmatched, ordinary, one-way Anova with Sidak's multiple comparison test was used to determine statistical significance involving three or more populations (stacked bar graphs), or between SCC FAK-wt, SCC FAK-/- and SCC FAK-kd populations. When analyzing only two populations, an unpaired, parametric t test with Welch's correction was used. For growth curves, matched, two-way Anova with Tukey's multiple comparisons test was used to determine statistical significance. P values = Not significant>0.05, * <0.05, **<0.01, ***<0.001, ****<0.0001.

5 Identification of a novel role of FAK in enabling tumour cell evasion of an anti-tumour immune response

5.1 Introduction

I set out to investigate whether FAK signalling in tumour cells influences the immune compartment of the tumour microenvironment. To address this, I used a syngeneic mouse model of squamous cell carcinoma (SCC) previously developed in the lab by A. Serrels *et al*[276]. SCCs were induced in the skin of K14*Cre*ER $FAK^{flox/flox}$ mice by the two-stage 7,12-dimethylbenz[a]anthracene (DMBA) / 12-*O*-tetradecanoylphorbol-13-acetate (TPA) chemical carcinogenesis protocol[51,326]. These mice were developed on an FVB/N background due to the increased susceptibility of FVB/N mice to DMBA/TPA treatment[336]. DMBA is a topical carcinogen, which when applied to the skin induces an irreversible A to T transversion on codon 61 of proto-oncogene Harvey-ras (Ha-Ras). Treatment with DMBA alone is not sufficient to induce tumours and requires the repeat application of tumour-promoting agents such as TPA. The pro-inflammatory phorbol-ester TPA, binds and activates protein kinase C (PKC)[337] and induces the expression of pro-inflammatory cytokine IL-1α[338]. With repeated application after DMBA treatment, TPA activates stromal fibroblasts, increases macrophage and neutrophil recruitment and results in the generation of benign papillomas that, in some cases progress to carcinoma.

The coding exons of the *fak* gene span over 225 kb, and so it was not feasible to delete the entirety of the *fak* gene[339]. K14*Cre*ER $FAK^{flox/flox}$ mice were developed so that *loxP* sites flank a critical codon in the FAK kinase domain (amino acids 413-444), and *Cre*-mediated excision results in a frame shift mutation in the adjacent exon, that precludes the production of a functional FAK protein[339]. A K14 skin-specific promoter drives the expression of a modified estrogen receptor–Cre

fusion protein (*Cre*ER) that translocates to the nucleus only after exposure to 4-hydroxytamoxifen (4OHT). Previous studies in the lab have showed that DMBA/TPA treatment does not induce papillomas after the deletion of *fak* in K14*Cre*ER FAK$^{flox/flox}$ mice *in vivo*[339], and therefore to develop an SCC FAK-/- cell line, SCC cells were derived and *fak* deleted *in vitro*. Following DMBA/TPA treatment, carcinomas were surgically excised and SCC cells were derived using selective cell culture conditions[276]. SCC cells were then cultured in the presence of 4OHT for 48 hours, single cell cloned and screened for FAK deletion by immunoblotting and PCR[276]. FAK constructs were then re-expressed back into SCC FAK-/- clones and a clone pair was selected that stably expressed FAK in a manner similar to exogenous levels determined by immunoblotting and PCR. This approach produced two syngeneic cell lines that were genetically identical apart for the expression of FAK, called SCC FAK-wt and SCC FAK-/-. This approach also allows other FAK constructs to be expressed in SCC FAK-/- cells, in order to investigate the effects of mutant FAK protein, on an identical genetic background.

5.2 Aims

- To investigate whether SCC FAK-wt and SCC FAK-/- tumours exhibit host-dependant characteristics
- If so, to identify whether components of the adaptive immune system are involved in regulating tumour growth
- To determine whether FAK kinase activity is required for any growth differences observed

5.3 Results

5.3.1 SCC FAK-/- cells exhibit host-dependent growth characteristics

SCC cells were generated by A. Serrels as described in **4.2.1.1**. The purity and efficiency of FAK knockout in the selected SCC FAK-/- clone was determined by PCR (**Figure 5.1a**) and Western Blot anlysis (**Figure 5.1b**). A kinase-deficient form of FAK was first described and characterised by Schlaepher *et al*[340], and subsequently SCC FAK-kd cells were made as described above. The loss of kinases activity was determined by Western blot anlysis of FAK pY397 (**Figure 5.1c**).

Using the SCC cell model described above I first set out to determine the growth characteristics of SCC FAK-wt and SCC FAK-/- cells in both CD-1 nude immuno-deficient mice and immuno-competent FVB/N mice. 2.5 x 10^5 and 1 x 10^6 SCC FAK-wt and SCC FAK-/- cells were implanted using bilateral subcutaneous injection into CD-1 nude (**Figure 5.2a**) and FVB/N mice (**Figure 5.2b**) respectively, and tumour growth was measured twice weekly using callipers. Tumour volume was calculated using the formula $4/3\pi r^3$.

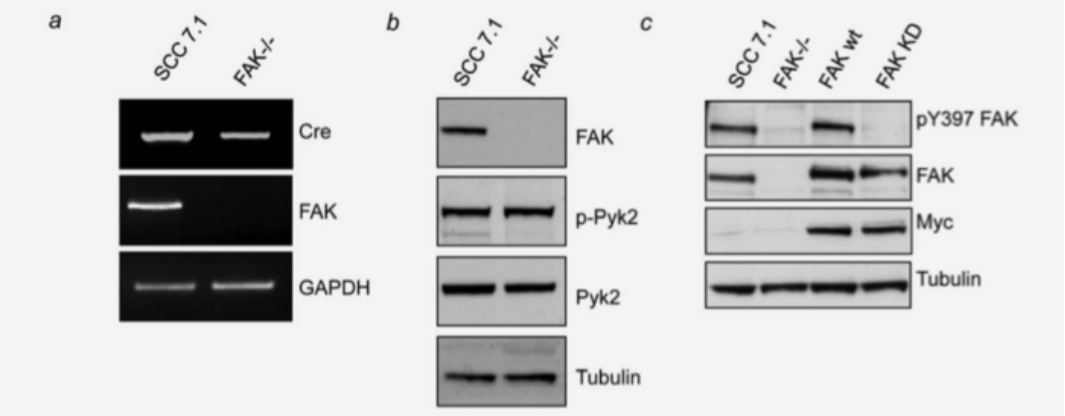

Figure 5.1 | Validation of SCC FAK-wt, SCC FAK-/- and SCC FAK-kd cell lines. *a* PCR of Cre and FAK in SCC 7.1 and SCC FAK-/- cells following 4OHT treatment. GAPDH was sued as a loading control**.** *b* Western blot of ACC FAK 7.1 and SCC FAK-/- cells. *c* Validation of the expression of FAK in SCC FAK-wt and SCC FAK-kd cells and the loss of pY397 FAK in SCC FAK-kd cells. Tubulin was used as a loading control Figure taken from *The role of focal adhesion kinase catalytic activity on the proliferation and migration of squamous cell carcinoma cells.* Serrels *et al.* Int J Cancer, 2012.

In CD1-nude mice (**Figure 5.2a**), SCC FAK-wt tumour growth reached an average tumour volume of 190.28 ± 24.246 mm^3 10 days post implantation, and a final average tumour volume of 407.35 ± 53.182 mm^3 after 14 days at which point the mice were sacrificed due to signs of ulceration. In comparison, SCC FAK-/- tumours showed a significant growth delay by day 10 and day 14 (average tumour volume = 93.759 ± 8.6705 mm^3, p value = 0.0091 and 207 ± 28.058 mm^3, p value = <0.0001 respectively), and continued to grow eventually reaching the same size as the SCC FAK-wt tumours (**Figure 5.2a**).

In contrast, bilateral subcutaneous injection of SCC FAK-wt or SCC FAK-/- cells in immune-competent FVB/N mice revealed a striking difference in tumour growth kinetics (**Figure 5.2b**). SCC FAK-wt tumours grew until day 14 reaching an average volume of 246.03 ± 55.544 mm^3, but also showing signs of ulceration requiring this experimental group to be terminated. In contrast, SCC FAK-/- tumours grew for an initial period of 7 days reaching an average volume of 71.745 ± 8.1837 mm^3, after which tumour growth stalled and complete regression occurred by day 21 (**Figure 5.2b)**. No tumour regrowth was observed following monitoring of these animals for a further 6 months (data not shown).

The observed difference in growth kinetics between SCC FAK-wt and SCC FAK-/- tumours on immune-competent and immune-deficient hosts suggested a potential role for the host immune status in dictating tumour outcome. CD-1 nude mice, via disruption of the *FOXN1* gene, are rendered athymic and as a consequence lack functional T-cells but retain functional B-cells, NK-cells and myeloid cells[341]. In contrast, FVB/N mice are fully immune-competent. Therefore, I hypothesised that FAK expression in SCC tumour cells may enable them to evade T-cell detection / destruction by one of 3 mechanisms; 1) FAK expression may protect cells from undergoing apoptosis leading to a reduction in the available antigen released into the microenvironment, 2) FAK may regulate the expression of tumour associated antigen (TAA) or 3) FAK expression in cancer cells may somehow influence the composition of the immunosuppressive milieu within tumours.

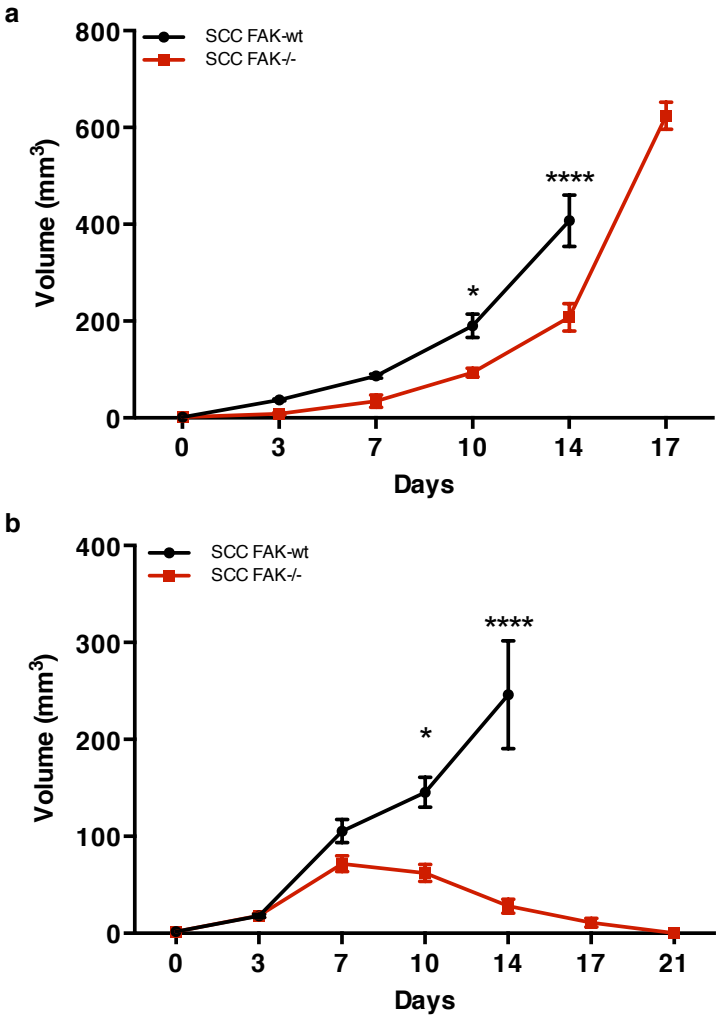

Figure 5.2 | SCC FAK-/- tumours show host-dependent growth characteristics. a SCC FAK-wt and SCC FAK-/- tumour growth in CD1-nude mice. 2.5 x 10^5 SCC FAK-wt and SCC FAK-/- cells were implanted into CD1-nude mice by bilateral subcutaneous injection (n = 6). SCC FAK-wt tumours grew until day 14 at which point the animals were sacrificed due to signs of ulceration. SCC FAK-/- tumours showed a significant growth delay compared to the SCC FAK-wt tumours. **b** SCC FAK-wt and SCC FAK-/- tumour growth in FVB/N mice. 1.0 x 10^6 SCC FAK-wt and SCC FAK-/- cells were implanted into FVB/N mice by bilateral subcutaneous injection (n = 6). SCC FAK-wt tumours grew until day 14 at which point signs of ulceration were observed and the animals were sacrificed. SCC FAK-/- tumours grew until day 7 at which point tumour growth stalled and was followed by complete regression by day 21. Tumours did not reoccur within 6 months post-regression (*data not shown*). Statistical significance was determined by matched, two-way Anova with Tukey's multiple comparisons. Data are represented as mean ± s.e.m. P-value = Not significant >0.05, * <0.05, ** <0.01, *** <0.001, **** <0.0001.

5.3.2 SCC FAK-/- tumour clearance is not due to increased Bcl-2-dependent apoptosis

FAK is known to promote cell survival under different conditions of adhesion stress[264,327], and apoptotic cell death can under certain conditions elicit an immune response (**2.4)**. I therefore hypothesised that SCC FAK-/- cells may be subject to increased apoptosis, resulting in greater availability of TAAs within the microenvironment. A key 'point of no return' during apoptosis is the release of Cytochrome C from the mitochondrial membrane through large pores generated by the oligomerization of BAX/BAK proteins. This is antagonised by the anti-apoptotic protein Bcl-2[342,343]. Thus, to test our hypothesis I stably overexpressed a Green Fluorescent Protein (GFP) tagged Bcl-2 in both SCC FAK-/- and SCC FAK-wt cells using retroviral transfection and antibiotic selection (**Figure 5.3**). The extent of GFP-Bcl-2 overexpression was visualised by confocal imaging (**Figure 5.3a**) and expression levels determined using immunoblotting (**Figure 5.3b**). To confirm that Bcl-2 overexpression was able to protect SCC cells from apoptosis, cells were treated with increasing concentrations of doxorubicin, a cytotoxic DNA intercalating agent, for 24 hours and the induction of apoptosis measured by immunoblotting for caspase 3 activation and PARP cleavage (**Figure 5.3c**). These results showed that treatment with doxorubicin increased levels of active caspase 3 and cleaved PARP in both SCC FAK-wt and SCC FAK-/- cell lines compared to untreated controls, and further highlighted that SCC FAK-/- cells exhibit greater sensitivity to doxorubicin-induced apoptosis, supporting the observations of others regarding the anti-apoptotic functions of FAK[344,345]. Bcl-2 over-expression in both cell lines resulted in a marked reduction in caspase 3 activation and PARP cleavage at all doxorubicin concentrations tested (**Figure 5.3c**). Thus, overexpression of Bcl-2 protected both SCC FAK-wt and FAK-/- cells from doxorubicin-induced apoptosis. Despite this, there were no differences observed in the tumour growth kinetics in FVB/N mice from either SCC FAK-wt or SCC FAK-/- Bcl-2 overexpressing tumours when compared to controls (**Figure 5.3d**). Furthermore, Fluorescent Activated Cell Sorting (FACS) of disaggregated SCC FAK-wt and SCC FAK-/- tumours formed at day 7 in FVB/N mice revealed no differences in cell viability (mean ± s.e.m. = FAK-wt,

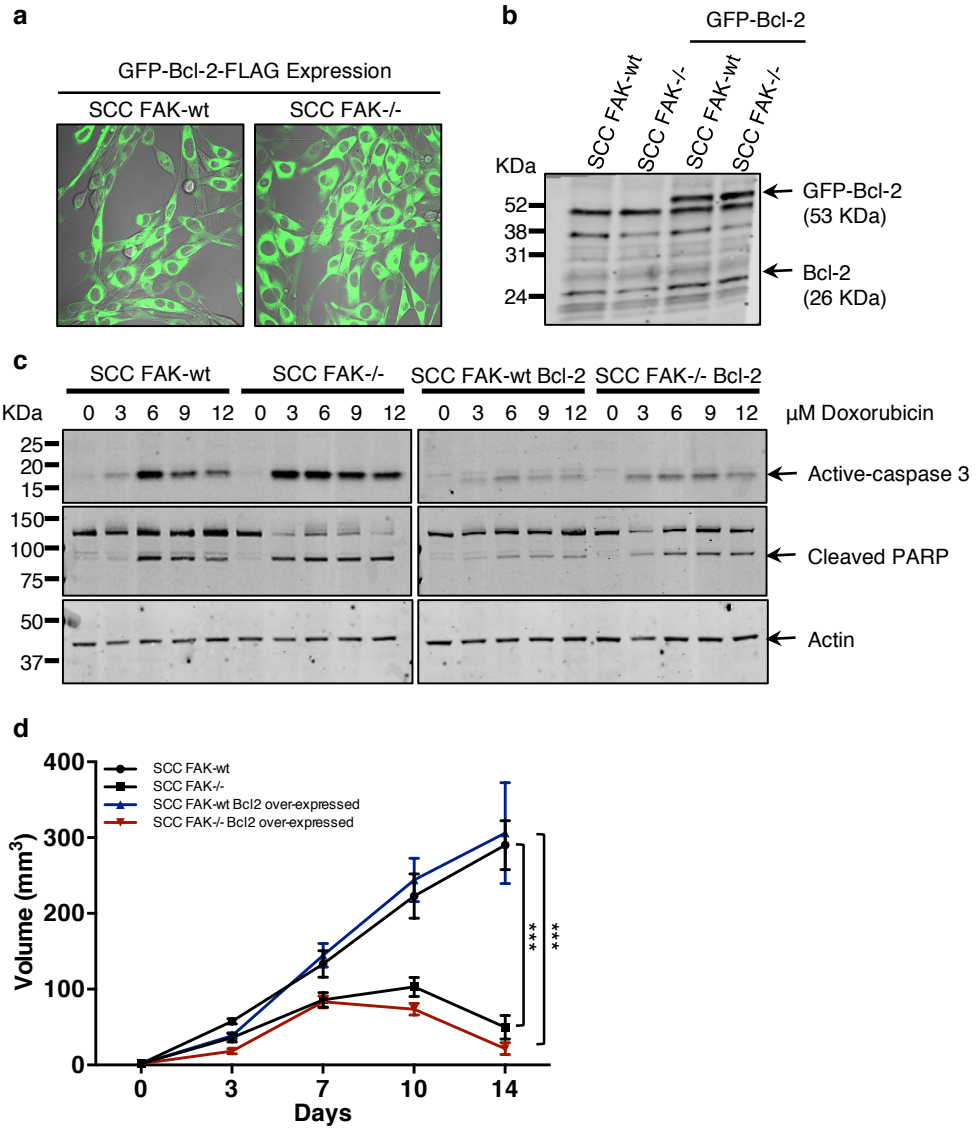

Figure 5.3 | Generation and characterization of GFP-Bcl-2 expressing SCC FAK-wt and SCC FAK-/- cells. a Representative confocal images of SCC FAK-wt and SCC FAK-/- cells expressing GFP-Bcl-2. **b** Western blot of endogenous Bcl-2 expression (26 KDa) and exogenous GFP-Bcl-2 (53 KDa) in SCC FAK-wt and SCC FAK-/- cells. **c** Validation of apoptotic protection of GFP-Bcl-2 expression in SCC FAK-wt and SCC FAK-/- cells after doxorubicin treatment**.** SCC FAK-wt, SCC FAK-/- and GFP-Bcl-2 expressing SCC FAK-wt and SCC FAK-/- cells were treated with increasing concentrations of doxorubicin. Doxorubicin-induced apoptosis was determined by immunoblotting for active caspase 3 and cleaved PARP. SCC FAK-wt and SCC FAK-/- cells expressing GFP-Bcl-2 showed lower levels of active-caspase 3 and cleaved PARP after doxorubicin treatment compared to controls. **d** GFP-Bcl-2 expression did not rescue SCC FAK-/- tumour clearance in FVB/N mice**.** 1.0 x 10^6 SCC FAK-wt, SCC FAK-/- and GFP-Bcl-2 expressing SCC FAK-wt and SCC FAK-/- cells were implanted into FVB/N mice by bilateral subcutaneous injection (n = 6). Tumour diameter was measured twice weekly and tumour volume calculated using the formula $4/3\pi r^3$. Statistical significance was determined by matched, two-way Anova with Tukey's multiple comparisons. Data are represented as mean ± s.e.m.

.

63.67% ± 0.6199; FAK-/-, 64.18% ± 0.3457), as measured by the uptake of an eFluor® 506 conjugated fixable viability dye (**Figure 5.4**). These data imply that Bcl-2-antagonized apoptosis is not responsible for, or a contributing factor to, the observed tumour regression characteristics of SCC FAK-/- tumours.

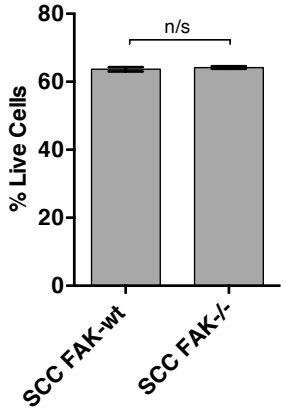

Figure 5.4 | Loss of FAK expression did not effect cell viability *in vivo*. FAK expression did not influence cell viability in early SCC FAK-wt and SCC FAK-/- tumours**.** 1.0 x 10^6 SCC FAK-wt and SCC FAK-/- cells were implanted into FVB/N mice by bilateral subcutaneous injection. SCC FAK-wt and SCC FAK-/- tumours were disaggregated at day 7, stained with fixable viability dye eFluor® 506 and analyzed by FACS (n = 12). Data are represented as mean ± s.e.m. SCC FAK-wt, 63.67% ± 0.6199; SCC FAK-/-, 64.18% ± 0.3457. Statistical significance was determined by an unpaired, parametric t test with Welch's correction. P-value = Not significant >0.05, * <0.05, ** <0.01, *** <0.001, **** <0.0001.

5.3.3 $CD8^+$ T-cells drive SCC FAK-/- tumour regression

Having ruled out Bcl-2-antagionised apoptosis, I next sought to definitively determine the role of T-cells in the clearance of SCC FAK-/- tumours. To do so, I utilised antibodies targeting $CD8^+$ and $CD4^+$ T-cells to deplete these populations in tumour bearing mice, and measure the impact on SCC tumour growth.

5.3.3.1 Purification and dose-optimization of T-cell depleting antibodies

Anti-mouse CD8 and CD4 depleting antibodies were purified from supernatants of rat hybridomas GK1.1 (ATCC TIB-207) and 2.41 (ATCC TIB-210) respectively using Melon IgG purification columns (Thermo Scientific) as described in the methods section. Briefly, hybridoma culture supernatant containing secreted antibody was concentrated, dialysed into 'binding buffer' and incubated with Melon IgG resin. Melon IgG resin contains a proprietary ligand that retains proteins found in cultured supernatants, allowing enrichment of IgG passing over it. Incubation of the beads in 'elution buffer' elutes a fraction containing purified IgG. The eluted fraction was collected and the efficiency of purification assessed using TGX stain-free protein gels (Biorad). These gels contain trihalo-compounds that react with tryptophan residues resulting in a fluorescent signal when activated by UV-exposure. Aliquots from each purification stage were visualised alongside concentrated supernatant and a commercially available Low Endotoxin Azide Free (LEAF) purified antibody control for both CD8 and CD4. A serial dilution BSA concentration standard was used to determine final antibody concentration. The resulting gels showed that both CD8 (**Figure 5.5a**) and CD4 (**Figure 5.5b**) antibodies were enriched in the final eluted fraction compared to the concentrated media in each case. Neither antibody was detected in the wash elutes (FT^1, FT^2 or FT^3), and the final concentration as determined by the BSA gradient was approximately 1 mg/ml. However, comparison of the eluted fractions with the commercial control antibody showed that purified elutes contained a number of high molecular weight species not found in the commercial preparations. To determine

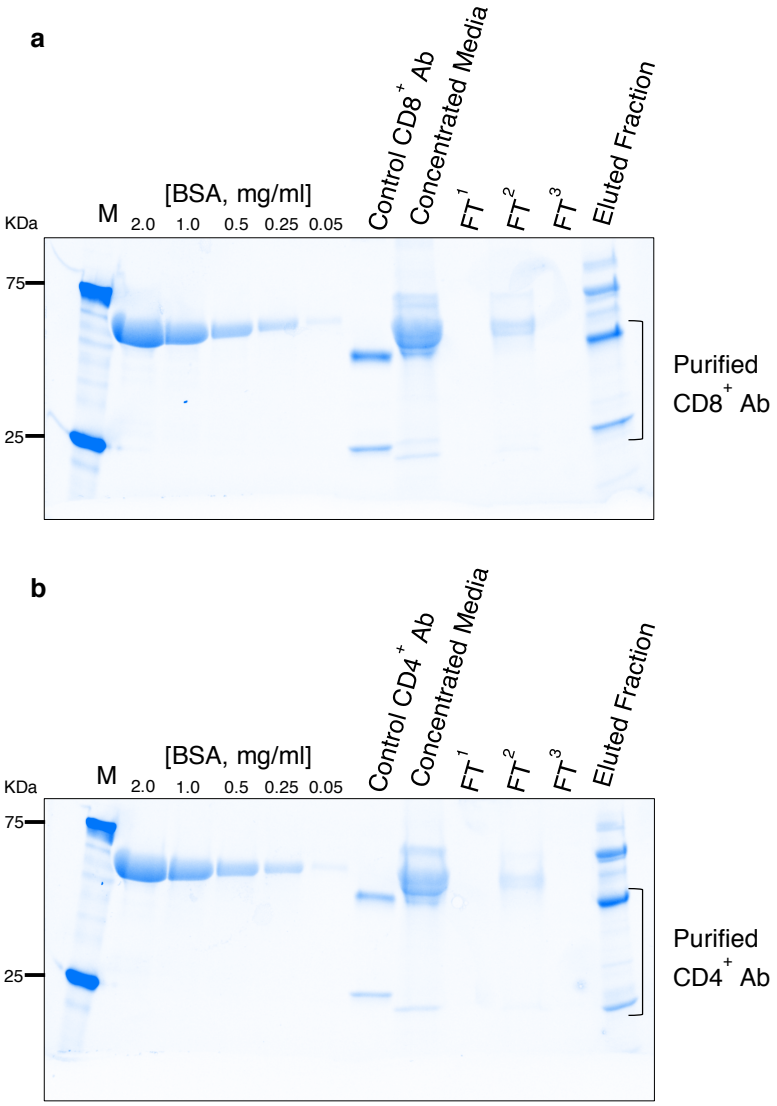

Figure 5.5 | Purification of anti-mouse CD8$^+$ and CD4$^+$ depleting antibodies. Image of UV activated TGX stain-free protein gel to determine the efficiency of the purification of **a** CD8$^+$ and **b** CD4$^+$ antibodies from cultured supernatants. Gels show each stage in the purification; concentrated media, flow through (FT) 1, 2 and 3 and the final eluted fraction. Also shown; BSA gradient to assess protein concentration, Control CD8$^+$ and CD4$^+$ antibodies (Ab) to determine correct protein size respectively and protein molecular weight markers (M). Both CD8$^+$ and CD4$^+$ antibodies purified alongside a number of high molecular weight species

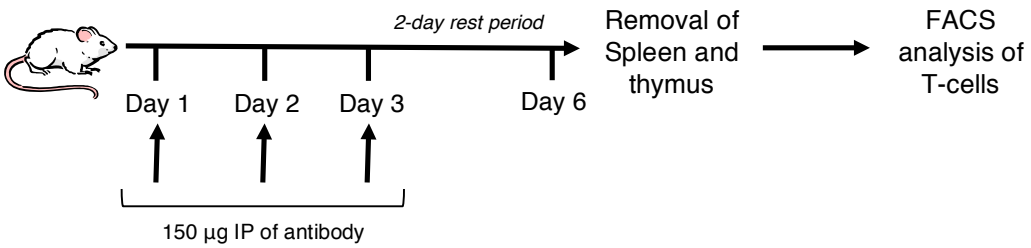

Figure 5.6 | Schematic describing the treatment schedule and dose validation for functional comparison of $CD8^+$ and $CD4^+$ depleting antibodies. Cohorts of FVB/N mice were treated for 3 consecutive days with 150 µg of $CD8^+$ or $CD4^+$ depleting antibodies, or a combination of both by IP injection. Antibodies were either purified in house or purchased commercially. After a 2 day rest period, the spleens and thymus were removed from each mouse and the number of each T-cell population was quantified using FACS.

whether the antibody preparations were functionally active and sufficient for purpose, or whether further purification would be required, I compared their capacity to deplete CD8 and CD4 T-cells with that of the commercial preparations. FVB/N Mice were treated for 3 consecutive days (**Figure 5.6**) with a single intraperitoneal (IP) injection of 150 µg of either commercial or purified individual antibodies, or a duel treatment of both CD4 and CD8 antibodies. Following a 2-day rest period, mice were culled and FACS analysis of disaggregated spleen and thymus used to determine the levels of $CD45^+CD3^+CD4^+CD8^-$ and $CD45^+CD3^+CD4^-CD8^+$ cells (**Figure 5.7**). Both the commercial and purified antibodies selectively depleted their target population from the spleen, without disrupting T-cell development in the thymus. The CD4 purified antibody depleted more $CD4^+$ cells in the spleens than the commercial antibody (**Figure 5.7** *red arrow*). The CD8 purified antibody lead to the substantial reduction of $CD8^+$ cells in the spleen but did not deplete the entirety of the $CD8^+$ cells unlike the commercial CD8 antibody (**Figure 5.7** *green arrow*). Also a $CD8^+$ $CD4^+$ T-cell population was retained after depletion with CD8 purified antibody (**Figure 5.7** *blue arrow*). I concluded that our own purified antibodies behaved similarly to the commercially available antibodies with respect to the depletion of T-cell sub-populations and thus I continued to use purified antibody for the remainder of our experiments. I hypothesised that the differences observed between the commercial and purified antibodies was likely due to the inaccuracies in determining the final concentrations of our purified antibodies.

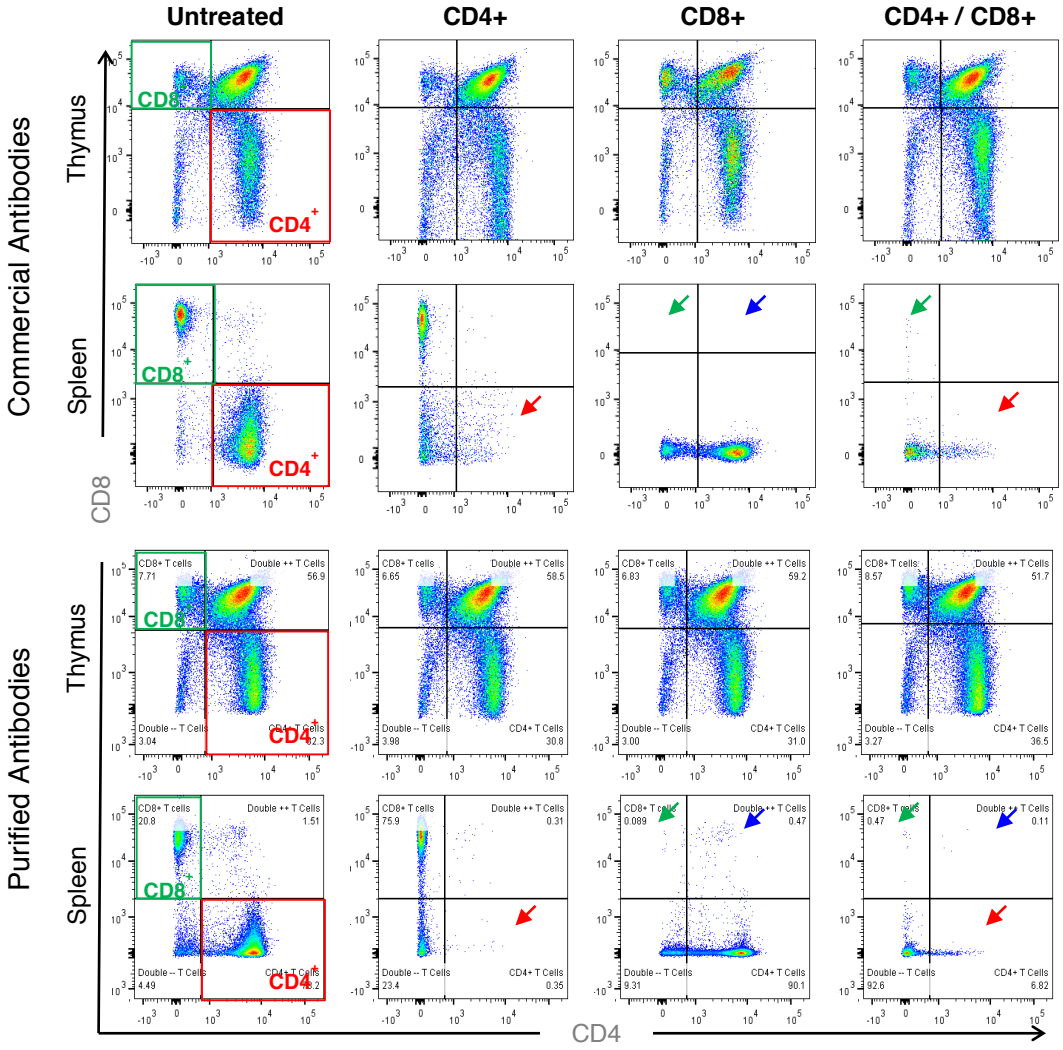

Figure 5.7 | Validation of CD8$^+$ and CD4$^+$ antibodies antibody-mediated T-cell depletion in FVB/N mice from both commercially available antibodies and in-house purified antibodies. FACS analysis of spleen and thymus tissue from non-tumor bearing animals 6 days after commencing antibody treatment. Cohorts of FVB/N mice (n = 5) were treated for 3 consecutive days with 150 µg of CD8$^+$ or CD4$^+$ depleting antibodies, or a combination of both, by IP injection. After a 2 day rest period, the spleens and thymus were removed and processed for FACS analysis. Both commercially available and in-house purified CD8$^+$ and CD4$^+$ antibodies selectively depleted each T-cell population respectively and in combination depleted all circulating T-cells in the spleen without affecting T-cells in the thymus; *green arrows* CD8$^+$ T-cells; *red arrows* CD4$^+$ T-cells; *blue arrow* CD8$^+$ CD4$^+$ cells

5.3.3.2 Effects of T-cell depletion on SCC tumour growth

Using purified antibody preparations, I set out to address whether T-cell depletion in FVB/N mice could rescue SCC FAK-/- tumour growth. Mice were treated for 3 consecutive days with a single IP injection of 150 µg of CD8, CD4 or a combination of both depleting antibodies, or with a rat IgG Isotype control antibody (eBioscience; **Figure 5.8**). After a 2-day rest period, 1 x 10^6 SCC FAK-wt or SCC FAK-/- cells were implanted by bilateral subcutaneous injection in to both flanks of FVB/N mice and tumour growth measured twice weekly. T-cell depletion was maintained by IP injection of 150 µg of antibody every 3 days. Sustained T-cell depletion was validated after each study had terminated by FACS analysis of the spleen and thymus of tumour bearing animals (**Figure 5.9**). Depletion of $CD4^+$ and $CD8^+$ T-cells was less in tumour-bearing mice than in non-tumour bearing animals seen previously, possibly due to the heighted inflammatory response induced following tumour cell implantation. However comparison of CD4 and CD8 depleting antibody-treated mice with untreated controls showed that a substantial proportion of both $CD4^+$ and $CD8^+$ T-cells were depleted (**Figure 5.9**).

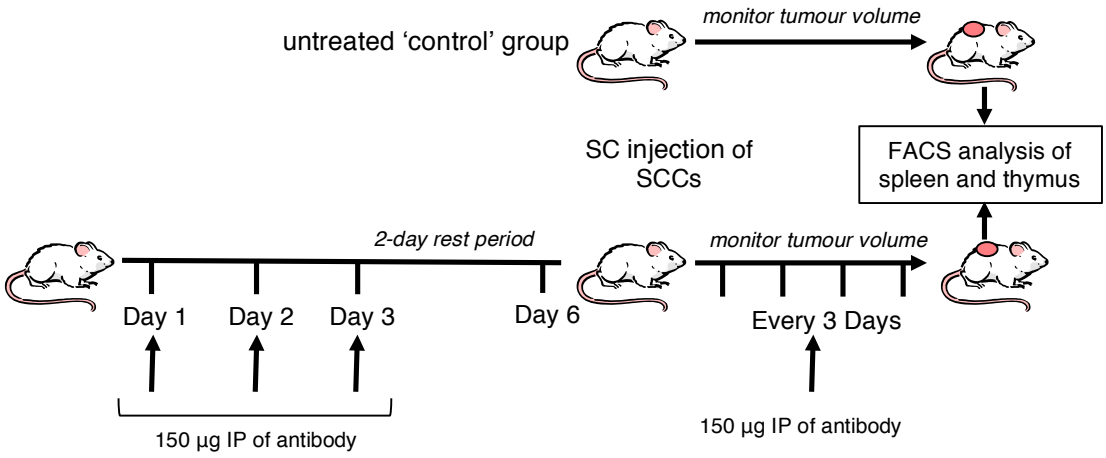

Figure 5.8 | Schematic describing the treatment regime for FVB/N antibody-mediated T-cell depletion during a tumour growth experiment. To determine whether $CD8^+$ and $CD4^+$ T-cells influence SCC tumour growth, cohorts of FVB/N mice were treated daily for 3 consecutive days with 150 µg of $CD8^+$ and $CD4^+$ depleting antibodies or a combination of both by IP injection. After a 2 day rest period, 1 x 10^6 SCC FAK-wt or SCC FAK-/- cells were implanted by bilateral subcutaneous injection into each flank. Tumour diameter was measured twice weekly and tumour volume calculated using the formula $4/3\pi r^3$. T-cell depletion was maintained by 150 µg IP injection of antibody every 3 days until the end of the experiment, at which point T-cell depletion was confirmed following FACS analysis of disaggregated spleen and thymus of each animal. SC = subcutaneous.

In FVB/N mice treated with CD4 depleting antibodies SCC FAK-/- tumour growth was unaltered (**Figure 5.10a**). In contrast, depletion of $CD8^+$ T-cells alone or in combination with $CD4^+$ T-cells was sufficient to restore SCC FAK-/- tumour growth. Therefore I conclude that $CD8^+$ T-cells are responsible for the clearance of SCC FAK-/- tumours (p value = <0.0001; **Figure 5.10a**), and that $CD4^+$ T-cells are not required for SCC FAK-/- immune clearance.

T-cell depletion in FVB/N mice bearing SCC FAK-wt tumours (**Figure 5.10b**) highlighted two observations; 1) $CD8^+$ depletion alone or in combination with $CD4^+$ T-cell depletion significantly increased SCC FAK-wt tumour growth when compared to either the Isotype treated or untreated control groups at day 14 (p value = <0.0001), and 2) depletion of $CD4^+$ T-cells alone resulted in the clearance of SCC FAK-wt tumours in a manor akin to SCC FAK-/- tumour clearance. These data indicate that SCC FAK-wt tumours are under negative pressure from $CD8^+$ T-cells and are thus likely subject to an underlying immune response. Further, they imply a role for the $CD4^+$ T-cell compartment in conferring protection of SCC FAK-wt tumours from the cytotoxic $CD8^+$ T-cell response.

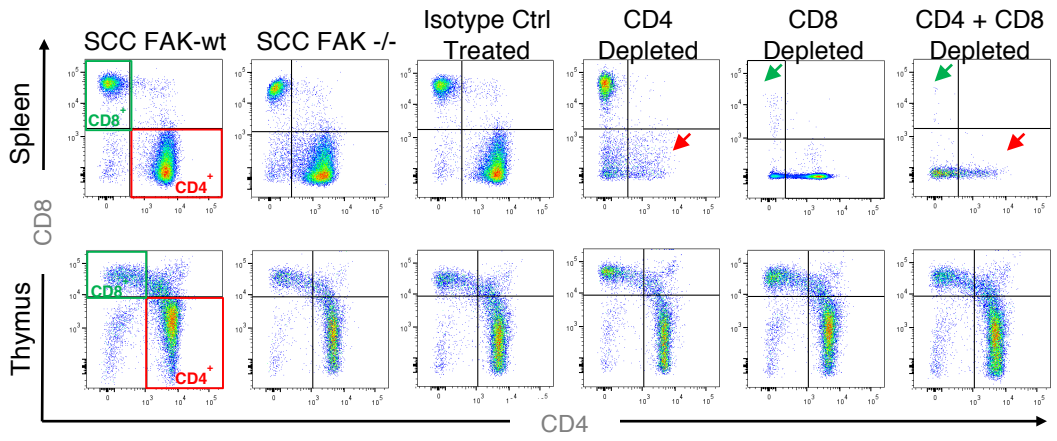

Figure 5.9 | Validation of sustained CD8 and CD4 T-cell depleting antibodies in tumour bearing FVB/N mice. FACS analysis of T-cell populations from spleen (*top*) and thymus (*bottom*) tissue from tumour bearing animals at the end of T-cell depletion studies described in **Figure 5.10**; *green arrows* $CD8^+$ T-cell depletion; *red arrows* $CD4^+$ T-cell depletion.

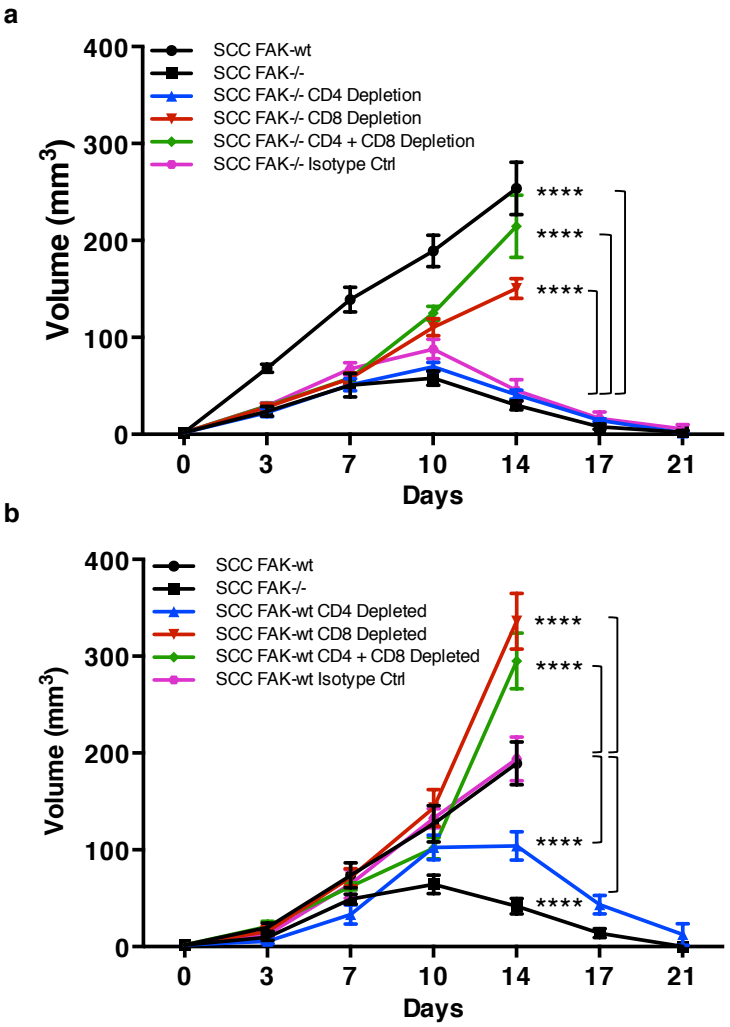

Figure 5.10 I SCC tumour growth +/- CD8$^+$ and CD4$^+$ T-cell depletion. a SCC FAK-/- and **b** SCC FAK-wt tumour growth in T-cell depleted FVB/N mice. Cohorts of FVB/N mice (n = 5) were treated with either CD8$^+$, or CD4$^+$ depleting antibody, or with both CD8$^+$ and CD4$^+$ antibodies in combination as per the dosage scheduled referred to in **Figure 5.8.** Both untreated and isotype control treated groups were included. 1 x 10^6 SCC FAK-wt or SCC FAK-/- cells were implanted by bilateral subcutaneous injection into each flank. Tumour diameter was measured twice weekly and tumour volume calculated using the formula $4/3\pi r^3$. Statistical significance was determined by matched, two-way Anova with Tukey's multiple comparisons. Data are represented as mean ± s.e.m. P-value = Not significant >0.05, * <0.05, ** <0.01, *** <0.001, **** <0.0001.

5.3.3.3 SCC FAK-/- tumour cells induce immunological memory that does not permit regrowth of SCC FAK-/- or SCC FAK-wt tumours after rechallenge

Having characterised that SCC FAK-/- tumour regression was $CD8^+$ T-cell dependent, and that increased apoptosis was not a contributing factor in priming the anti-tumour immune response, I set out to test whether FAK expression resulted in regulation of TAA that could enable SCC FAK-wt cells to evade immune recognition. To do so, I took advantage of the SCC FAK-/- tumour regression characteristics, and performed a rechallange experiment in animals following SCC FAK-/- tumour clearance (**Figure 5.11**). I hypothesised that following SCC FAK-/- tumour clearance the host would remain immunised against further challenge with tumour cells expressing the same antigen, and as a consequence would mount a strong and fast secondary response that would not permit tumour growth. Thus, if

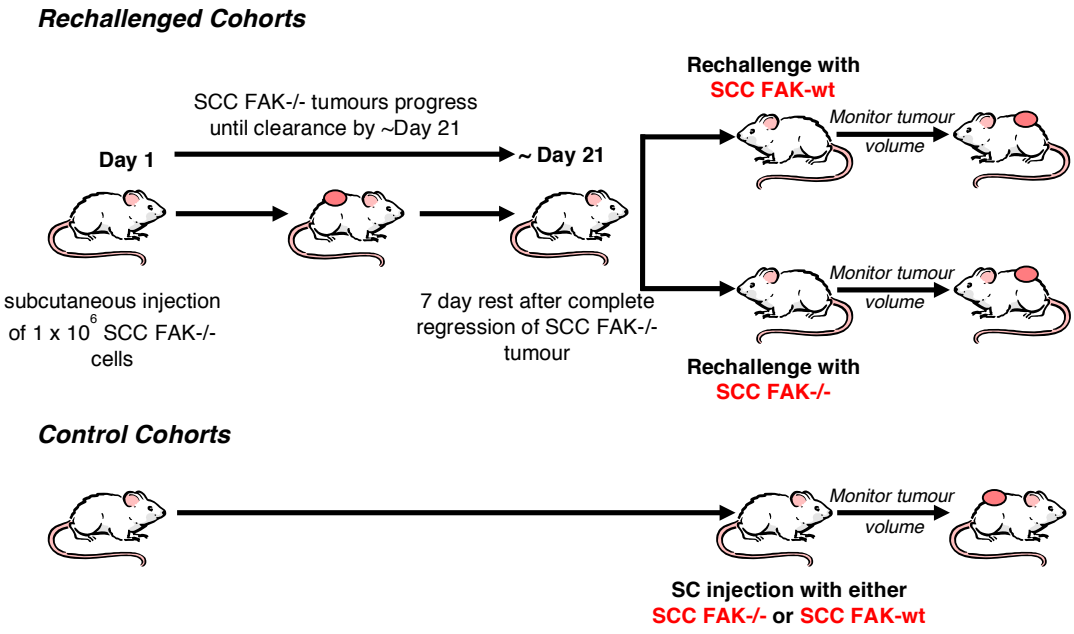

Figure 5.11 | Schematic detailing SCC FAK-/- rechallenge experimental setup. FVB/N mice were split into rechallenged and control cohorts for SCC FAK-wt and SCC FAK-/-. *Rechallenged cohorts* were first implanted with 1 x 10^6 SCC FAK-/- cells by subcutaneous implantation in to the left flank of each mouse. SCC FAK-/- tumours were allowed to grow and completely regress (by ~ Day 21). After 7 days tumour-free rest period, these cohorts were rechallenged with either 1 x 10^6 SCC FAK-wt (n = 5) or SCC FAK-/- cells (n = 5) by subcutaneous implantation in to the right flank. Resulting tumour volume was measured twice weekly. *Control cohorts* were not exposed to initial SCC FAK-/- tumour implantation. 1 x 10^6 SCC FAK-wt (n = 5) or SCC FAK-/- cells (n = 5) were implanted by subcutaneous implantation into the left flank. Resulting tumour volume was measured twice weekly. SC = subcutaneous.

SCC FAK-wt cells share a common antigen with SCC FAK-/- cells, then growth of these tumours will not be permitted in animals immunised using a primary challenge with SCC FAK-/- cells. To test this, I subcutaneously implanted 1 x 10^6 SCC FAK-/- cells into the left flank of FVB/N mice, and allowed the tumours to undergo complete regression. I then re-challenged these mice with either 1 x 10^6 SCC FAK-wt cells or 1 x 10^6 SCC FAK-/- cells on the right flank and monitored tumour growth (**Figure 5.12**). After the initial regression of the primary SCC FAK-/- tumour, and following a tumour-free period of 7 days, animals re-challenged with SCC FAK-wt (*middle graph*, **Figure 5.12**) or SCC FAK-/- cells (*bottom graph*, **Figure 5.12**) did not develop tumours. SCC FAK-wt and SCC FAK-/- cells implanted into unchallenged mice at day 28 grew as expected (*top graph*, **Figure 5.12**). In all cases except the SCC FAK-wt controls, animals were subsequently monitored for a further 6 months for tumour growth, and no tumour reoccurrence was observed (data not shown).

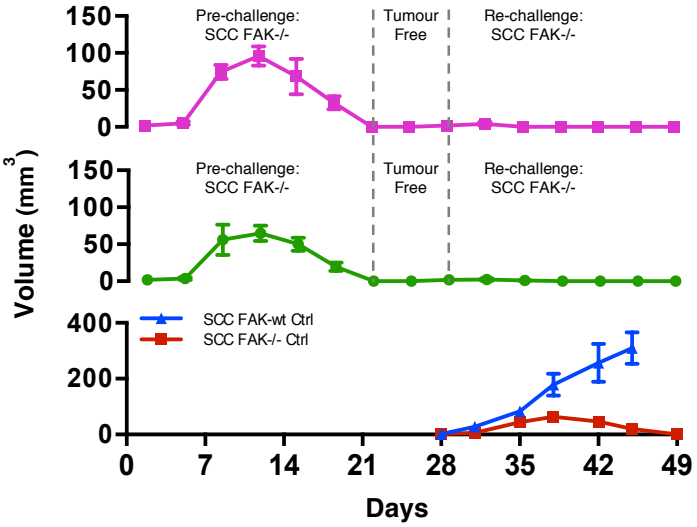

Figure 5.12 | Tumour rechallenge implies common antigen between SCC FAK-wt and SCC FAK-/- cells. Growth of rechallenged SCC FAK-wt and SCC FAK-/- tumours in FVB/N mice after clearance of SCC FAK-/- tumours. Experimental outline referred to in **Figure 5.11**.. *Top and center panels* Tumour growth of FVB/N mice rechallenged with SCC FAK-wt or SCC FAK-/- cells. 1 x 10^6 SCC FAK-/- cells were implanted into cohorts of FVB/N in the left flank by subcutaneous injection (day 0) and resultant tumours were allowed grow and regress (day 21). After a 7 day rest period, 1 x 10^6 SCC FAK-wt (*top*; n = 5) or SCC FAK-/- (*center*; n = 5) cells were implanted into the right flank by subcutaneous injection (day 28). *Bottom panel* SCC FAK-wt and SCC FAK-/- tumour growth controls. 1 x 10^6 SCC FAK-wt (n = 5) or SCC FAK-/- (n = 5) cells were implanted by bilateral subcutaneous injection in to the flanks of FVB/N mice at day 28 Tumour diameter was measured twice weekly and tumour volume calculated using the formaula $4/3\pi r^3$. Data are represented as mean ± s.e.m.

Together, these data imply that both SCC FAK-wt and SCC FAK-/- tumours share a common antigen. The heightened immune mediated clearance of SCC FAK-wt and SCC FAK-/- tumour cells after initial exposure to SCC FAK-/- cells, and the subsequent lack of any tumour-reoccurrence after 6 months, also suggests that regression of SCC FAK-/- tumours results in the generation of immunological memory that recognises both SCC FAK-/- and SCC FAK-wt cells.

5.3.4 FAK kinase activity is required for SCC tumour survival

FAK is a non-receptor protein tyrosine kinase of current clinical interest due to its role in regulating a number of tumour promoting processes, including proliferation, apoptosis, migration, invasion, EMT and angiogenesis. Small molecule FAK kinase inhibitors are being developed, with a number already being tested in early (phase 1 and 2) clinical trials. Hence, I set out to determine whether the survival of SCC FAK-wt tumours required FAK kinase activity and could therefore potentially be targeted with FAK kinase inhibitors. To address this, I used a previously reported lysine (K) $454^{254,327}$ kinase-deficient mutant of FAK, re-expressed in SCC FAK-/- cells (SCC FAK-kd cells). 1×10^6 SCC FAK-wt, SCC FAK-/- and SCC FAK-kd cells were implanted by bilateral subcutaneous injection in to both flanks of FVB/N mice and tumour growth was measured twice weekly (**Figure 5.13**). SCC FAK-wt and SCC FAK-/- tumours grew in a similar manner to previous experiments; however, SCC FAK-kd tumours grew in a manor akin to SCC FAK-/- tumour growth. These data suggest that FAK kinase activity is required for sustained SCC FAK-wt tumour survival and growth, and therefore treatment with a FAK kinase inhibitor may result in immune mediated tumour regression.

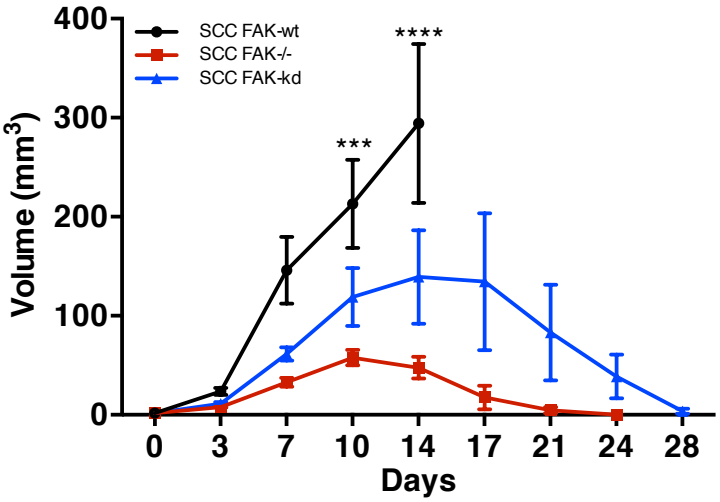

Figure 5.13 | FAK kinase activity is required for SCC tumour growth and survival. Tumour growth of SCC FAK-wt, SCC FAK-/- and SCC FAK-kd tumours in FVB/N mice. 1 x 10^6 SCC FAK-wt, SCC FAK-/- or SCC FAK-kd cells were implanted by bilateral subcutaneous injection into both flanks of FVB/N mice (n = 6). Tumour diameter was measured twice weekly and tumour volume calculated using the formula $4/3\pi r^3$. Statistical significance was determined by matched, two-way Anova with Tukey's multiple comparisons. Data are represented as mean ± s.e.m. P-value = Not significant >0.05, * <0.05, ** <0.01, *** <0.001, **** <0.0001 eekly and tumour volume calculated using the formaula $4/3\pi r^3$. Data are represented as mean ± s.e.m.

5.4 Conclusion

In immune-competent FVB/N mice, SCC FAK-/- tumours undergo immune-mediated tumour regression in a manner dependent on $CD8^+$ T-cells. Further, following complete regression host mice remain immunised against further tumour challenge, including when this secondary challenge is with SCC FAK-wt cells, implying expression of a common antigen that is independent of FAK expression levels. FAK kinase activity is required for SCC cells to evade immune mediated tumour clearance, raising the possibility that FAK kinase inhibitors may drive FAK-wt tumour regression.

The primary model used in this thesis is the DMBA/TPA generated model of SCC[276]. As described in [276], **4.2.1.1** and **5.1**, SCC FAK-/- and SCC FAK-wt cells originate from the same clone of a heterogeneous parental SCC population, which generates a genetically identical background into which FAK-wt is stably expressed at

comparable levels to endogenous expression. The selection and purification of the parental SCC population is achieved by selective cell culture conditions, which aim to sustain the growth of the transformed population, and not the un-transformed stromal populations such as fibroblasts, endothelial cells etc. Although this technique is well characterised and has led to a large number of publications with this model, more stringent purification could have been achieved using FACS. However, due to the length of time required not only to generate but also to maintain cells in culture, it is highly unlikely that an untransformed population could have survived within the parental population. Furthermore, the single cell cloning of the SCC FAK-/- and FAK-wt cells further increases the likelihood of a pure SCC population within both the SCC FAK-/- and SCC FAK-wt cell lines.

One potential caveat regarding the generation of the SCC FAK-wt and SCC FAK-/- cells is that a sham transfection was not undertaken when expressing the FAK-wt construct. A sham transfection exposes SCC FAK-/- cells to the same transfection protocol as the resulting FAK expressing cells, without the expression of FAK. This controls for possible phenotypic changes induced by the transfection reagent or transfection protocol that would not have occurred in untreated SCC FAK-/- cells. Although it is therefore a valid assumption that the phenotypic defences observed between SCC FAK-wt and SCC FAK-/- cells could be as a result of SCC FAK-wt cell transfection and not due to the expression of FAK, SCC FAK-kd cells have undergone transfection, and appear to mimic the SCC FAK-/- phenotype in all experiments undertaken throughout this thesis. Although it would have been more scientifically sound to produce sham transfected SCC FAK-/- cells, in this case, the contribution of FAK kinase activity to tumour growth and survival appear genuine.

Although the clonal nature of this model increases the confidence of a pure SCC population, one criticism of this technique is that the cell culture conditions and single cell cloning may be selective for the more aggressive SCC clones. These clones would be more likely to survive in time of stress (the transition to cell culture), at times of low confluence (during single cell cloning) and would be the first population to migrate out onto plastic cell culture plates. Heterogeneity within the isolated clones must also be considered, and thus a single clone may not be

representative of the heterogeneous population. Multiple clones from the parental population should be taken forward to compare the response to our SCC model, or alternatively other inducible transgenic models may offer the opportunity to study the of roles of FAK in an autochthonous host.

One further complication with the DMBA/TPA SCC model involves whether the resultant chemically induced SCC tumours are atypical of non-chemical induction. As stated above, TPA is a phorbol ester which induces a macrophage-dominated inflammatory response required to induce tumorigenesis in this model. TPA also acts to inhibit macrophage metabolic activity, which in turn reduces the phagocytic activity of macrophages[346]. The phagocytic activity of macrophages not only acts to kill tumour cells, but is also required for macrophage APC activity through the phagocytic ingestion and presentation of antigen[14]. This raises the question as to whether the clonal and antigenic heterogeneity of the DMBA/TPA model is less restricted than in other non-chemical models which may contain phagocytic macrophages. Without the selective pressure ensued by a competent macrophage response, both in its anti-tumour activity and in the presentation of antigen to the innate immune response, immunogenic neoantigens could survive in in a DMBA/TPA induced microenvironment, but not in a non-chemically induced microenvironment. Although macrophage APC activity is sustainably less than that of DCs which are unaffected by TPA, the potential for the selection of an atypically immunogenic cell line should be considered.

Furthermore, the restriction of neoantigen through single-cell cloning of this model may enhance the anti-tumour efficacy of immunomodulatory therapies. The evolution of tumour neoantigen heterogeneity determines how the immune system responds to tumour cells throughout tumour development and the efficacy of immunotherapy[347]; a more restricted range of immunogenic neoantigens increases the chance of an effective response to immunotherapy, where as a more diverse range creates a more resilient tumour. This is due to the evolution of neoantigens within a developing tumour, and the retention of mutated proteins which provide survival benefits for tumour cells, but which may also be recognized by an immune response[347]. This response is based on APC presentation of antigens early within

tumour development, therefore limiting the number of tumour cells that can rebuff the anti-tumour immune response. In this regard, it could also be possible that SCC tumours from this model appear more immunogenic due to the restriction of neoantigen through single cell cloning. This could be investigated by returning to the parental SCC cell line form which the SCC FAK-wt and SCC FAK-/- cell originate (SCC 7.1) and determining how this cell line responds to the potential immunomodulatory effects of FAK inhibition.

Using the SCC model, SCC FAK-wt and SCC FAK-/- tumours display different immune-mediated host-dependant growth kinetics. It should be noted that although CD1-nude mice are considered immune-deficient animals, partly due to the fact that this model mirrors immune-suppressed patients, CD1-nude mice still retain the capacity for an innate immune response. As SCC FAK-/- tumour growth is characterised by a growth delay in this host, contrasting the tumour regression observed in an FVB/N animal, the involvement of the innate immune system in immune-mediated regression of SCC FAK-/- tumours should not be disregarded. Cross-talk between the innate and adaptive immune responses has been shown to be required for optimal activation of both arms of the immune response, and as such the innate immune response could play a significant role in the immune-mediated clearance of SCC FAK-/- tumours. Furthermore, CD1-nude mice lack functional B-cell responses due to the lack of T-cell involvement in B-cell activity, which should also be considered when assessing tumour growth characteristics in CD1-nude mice.

Generation of the SCC model on a FVB/N background has the advantages of being more efficient, due to the highly susceptible nature of FVB/N mice to DMBA/TPA treatment compared to other genetic backgrounds such as c57BL/6 mice, which are inherently resistant to DMBA/TPA treatment. One disadvantage to using FVB/N mice however is the lack of available genetic and inducible knockout models for immune cell populations, such as the diphtheria toxin-inducible knockout systems that are almost exclusively on a c57BL/6 background. Although antibody-mediated depletion used throughout this thesis is a competent method of depletion as shown in **Figure 5.9**, it should still be noted that antibody-mediation depletion is not specific.

As such depletion of $CD8^+$ and $CD4^+$ population may not only deplete $CD8^+$ and $CD4^+$ T-cells, but may also deplete DCs, which have been shown to express both CD8 and CD4[348]. One may expect that depletion of DCs would cause tumour to survive, as a lack of DCs would reduce antigen presentation and therefor inhibit $CD8^+$ T-cell activation. The clearance of SCC FAK-/- tumours following CD4 antibody treatment indicates that $CD4^+$ DCs are not involved in this phenotype however, but $CD8^+$ DCs cannot be disregarded. Treatment with an anti-CD3 antibody would deplete both $CD8^+$ and $CD4^+$ T-cells simultaneously, but also would provide a control for the possible involvement of $CD8^+$ DCs.

Further to this, following antibody-mediated depletion of $CD8^+$ and $CD4^+$ T-cells, $CD8^+$ cells were shown to be responsible for the clearance of SCC FAK-/- tumours, independent of $CD4^+$ cells. Considering the role of $CD4^+$ T-cells in facilitating and increasing the effectiveness of the cytotoxic $CD8^+$ T-cell response, it was surprizing that CD4 depletion did not affect SCC FAK-/- tumour clearance. Although $CD8^+$ T-cell activation is not dependant on $CD4^+$ T-cell involvement[349], these data may indicate that $CD8^+$ T-cells help themselves, or interact with pre-activated DCs activated directly by SCC cells without $CD4^+$ T-cell involvement[350]. $CD8^+$ T-cells can self-activate by responding to antigen presented on MHC class I. Following the subsequent observation of CD8 directly binding to MHC class I proteins[351], it has become accepted that that the colligation of CD8 with the TCR alone, independent of DC or $CD4^+$ T-cell activation, can augment the effectiveness of $CD8^+$ T-cell TCR engagement and subsequent activation[352]. However, as determined in **Figure 5.12**, FAK does not regulate the expression of antigen and it would therefore seem unlikely that FAK would regulate CD4-independant activation of DCs, a process highly regulated by, and dependant on the availability of antigen. Also, although FAK may regulate MHC class I proteins, this also seems unlikely, both by the selective pressure of $CD8^+$ T-cells to SCC FAK-wt tumours and their requirement for the immune-mediated clearance of SCC FAK-/- tumours (**Figure 5.10**), and the clearance of SCC FAK-wt tumours in SCC FAK-/- challenge mice (**Figure 5.12**). Therefor it appears that the $CD8^+$ T-cell responses seen in both SCC FAK-wt and SCC FAK-/- tumours are activated by $CD4^+$ T-cell independent mechanisms, most

likely due to the direct binging of antigen primed MHC class I molecules to $CD8^+$ T-cells, a process that is independent of FAK expression.

Furthermore, considering the requirement for $CD4^+$ T-cells in SCC FAK-wt tumour growth, and that the depletion of $CD8^+$ T-cell alone or in combination with $CD4^+$ T-cells increased SCC FAK-wt tumour growth, these data indicate that the selective pressure by the immune system on SCC FAK-wt tumours is dependant on $CD8^+$ T-cells, and the presence of $CD4^+$ T-cells does not increase $CD8^+$ T-cell activity, but drastically inhibits it. These results identify a novel role for FAK in regulating the anti-tumour immune response, and highlight the need to investigate the composition of the immune cell infiltrate within the tumour environment. Thus, further work focused on the generation and optimisation of a tumour disaggregation and staining protocol for FACS, which included a number of multicolour FACS stains targeting a wide range of adaptive and innate immune populations.

6 Optimisation of a tumour disaggregation and staining protocol for FACS analysis of immune populations in SCC tumours

6.1 Introduction

Fluorescence activated cell sorting (FACS) is a specialized type of flow cytometry that provides a method of sorting a heterogeneous mixture of cells, one cell at time, based on the specific fluorescent and light-scattering properties of each cell. Each cell that passes through the flow cytometer will scatter light from an incoming laser by different degrees, in different directions, proportional to the dimensions of that cell; large round cells will scatter more light in all directions than smaller round cells, but elliptical cells will scatter more light in only one dimension than small round cells. In this regard, cells can be analysed based on size alone, but this is not sufficient to identify specific cell populations from a heterogeneous mixture of cells. Thus, cells are stained with fluorescently labelled antibodies that corresponded to specific lineage expressed proteins or proteins expressed upon cell activation (**Table 6.1**). In terms of immune cells, all leukocytes express CD45 and can be differentiated by this marker. Others include CD3 that is primarily expressed on lymphocytes, and CD11b, a marker for monocytic cells. Using this strategy it is possible to identify a variety of cell populations within each sample and quantified their abundance and relative proportions, enabling comparisons between different sample conditions, such as different tumours or different time points within tumour progression.

One caveat of FACS analysis is that samples must be prepared and disaggregated into single cell suspensions. There a number of possible methods for tissue disaggregation; mechanical disaggregation involves samples being forced through filters, enzymatic disaggregation involves the digestion of a sample by proteases that degrade key proteins found in the ECM, or a mixture of both. Mechanical disaggregation is the more gentle approach, but often leaves large sections of sample

whole. Enzymatic disaggregation is much more efficient and disaggregates the entire sample, but proteases may also cleave cell surface expressed molecules which in some instances might not be desirable. Therefore I set out to optimise a disaggregation protocol based on a combination of mechanical and enzymatic disruption for FACS analysis of SCC FAK-wt, SCC FAK-/- and SCC FAK-kd tumours for subsequent analysis of immune cell populations.

6.2 Aims

- To evaluate and optimise tumour disaggregation protocols
- Design multi-colour FACS stains that cover a wide range of immune populations
- Determine a time point for further tumour studies by measuring inherent changes in immune cell infiltration over time

6.3 Results

6.3.1 Collagenase D treatment of FVB/N spleens required for $CD11b^+$ cell detachment

In order to optimise a tissue disaggregation protocol suitable for FACS analysis of immune cell populations I used the spleens of naïve mice. Initially I tested mechanical disaggregation by mashing spleens from FVB/N mice through 70 μm filters to generate single cell suspensions. These suspensions were stained with fluorescent antibodies for CD45, CD11b, F4/80, CD3, CD8 and CD4, in order to identify a number of immune cell populations from both the adaptive and innate immune systems (**Table 6.1**). Samples were then analysed by FACS (**Figure 6.1**). Using this protocol I observed a number of $CD45^+$ $CD3^+$ $CD8^-$ and $CD45^+$ $CD3^+$ $CD8^+$ T-cells in the FVB/N spleens. However, only a small number of $CD45^+$

Population	Markers
Monocyte	$CD45^+$ $CD11b^+$
Macrophage	$CD45^+$ $CD11b^+$ $F4/80^+$
T-cell	$CD45^+$ $CD3^+$
$CD4^+$ T-cell	$CD45^+$ $CD3^+$ $CD8^-$
$CD8^+$ T-cell	$CD45^+$ $CD3^+$ $CD8^+$

Table 6.1 | Markers used for FACS analysis to determine how different tissue disaggregation protocols affected immune cell recovery.

$CD11b^+$ monocytes, and no $CD45^+$ $CD11b^+$ $F4/80^+$ macrophages, were detected (**Figure 6.1**). Thus, either FVB/N spleens contained few $CD11b^+$ monocytes and no $CD11b^+$ $F4/80^+$ macrophages, or alternatively, additional disaggregation methods were required to release these cell populations from the spleen.

Enzymatic disaggregation with Collagenases degrades collagen fibres leading to the, helping to release myeloid cells into suspension[353]. Of the available Collagenases, Collagenase D has the lowest tryptic activity, a key property that needs to be considered when staining for surface exposed proteins and retaining cell viability[354]. Indeed, tryptic activity is known to cleave some cell surface markers, and if not carefully validated could inadvertently yield misleading results. Thus, I tested a combination of mechanical and enzymatic disaggregation. Spleens from FVB/N

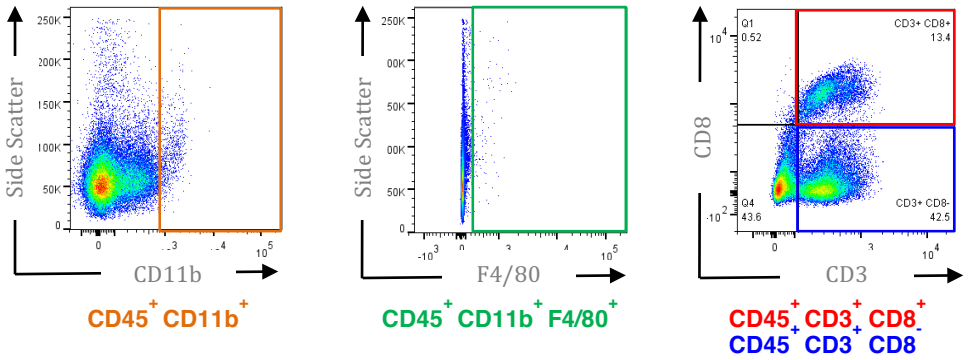

Figure 6.1 | Mechanical disaggregation was not sufficient to release monocytes and macrophages from FVB/N mice spleens. FVB/N spleens were mashed through a 70 µm filter to generate single cell suspensions, and stained for CD45, CD11b, F4/80, CD3 and CD8 (**Table 6.1**). FACS analysis determined the number of monocytes ($CD45^+CD11b^+$), macrophages ($CD45^+$ $CD11b^+$ $F4/80$) $CD8^+$ T-cells ($CD45^+$ $CD3^+$ $CD8^+$) and $CD4^+$ T-cells ($CD45^+$ $CD3^+$ $CD8^-$) released from the spleen after disaggregation.

mice were filtered through 70 µm filters, and samples split into two groups: 1) an untreated control group, and 2) a group treated with 2 mg/ml Collagenase D for 1 hour at 37 °C. Both treated and untreated samples were stained with fluorescent antibodies for CD45, CD11b, F4/80, CD3, CD8 and CD4, (**Table 6.1**) and samples analyzed by FACS (**Figure 6.2**). I observed substantially higher levels of $CD45^+$ $CD11b^+$ monocytes and $CD45^+$ $CD11b^+$ $F4/80^+$ macrophages in the Collagenase D treated samples when compared with untreated controls. Levels of $CD45^+$ $CD3^+$ $CD8^-$ and $CD45^+$ $CD3^+$ $CD8^+$ T-cells were unaffected by enzymatic treatment. Thus, I conclude that a combination of mechanical and Collagenase-D-based enzymatic disaggregation results in improved release of immune cells from the spleen.

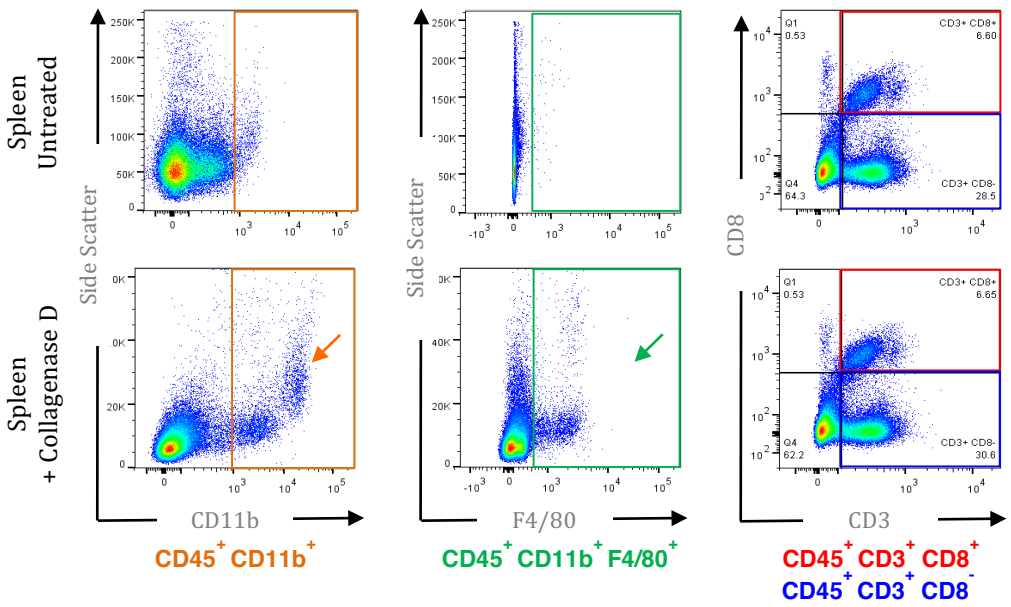

Figure 6.2 | Collagenase D treatment released monocytes and macrophages from FVB/N spleens. FVB/N spleens (n = 3) were mashed through 70 µm filters and treated with 2 mg/ml Collagenase D for 1 hour at 37 °C. Controls (n = 3) were mashed through 70 µm filters only. Both collagenase D treated and untreated samples were stained for CD45, CD11b, F4/80, CD3 and CD8 (**Table 6.1**). FACS analysis determined the number of monocytes ($CD45^+CD11b^+$), macrophages ($CD45^+$ $CD11b^+$ $F4/80$) $CD8^+$ T-cells ($CD45^+$ $CD3^+$ $CD8^+$) and $CD4^+$ T-cells ($CD45^+$ $CD3^+$ $CD8^-$) released from the spleen after disaggregation with and without collagenase D treatment.

6.3.2 Disaggregation of FVB/N spleen and thymus with Collagenase D, Dispase and Hyaluronidase resulted in the loss of T-cell markers.

As described in the introductory section **2.2.2,** tumours contain a complex network of extracellular matrix (ECM) proteins including collagen, fibronectin and hyaluronic acid. Treatment with Collagenase D, Dispase, and Hyaluronidase has been shown to degrade these, and provide an efficient method of tumour disaggregation[355]. Thus, I sought to determine the impact of this disaggregation cocktail on immune cell release and surface marker retention using both spleen and thymus tissue from FVB/N mice. Tissues were mashed through 70 μm filters then treated with either 2 mg/ml Collagenase D + 4 mg/ml Dispase + 0.1% Hyaluronidase, or 2 mg/ml Collagenase D alone, and incubated for 1 hour at 37 °C. Samples were then stained with fluorescently conjugated antibodies for CD45, CD11b, F4/80, CD3, CD8 and CD4, (**Table 6.1**) and analysed by FACS (**Figure 6.3**). Treatment of both the spleen and thymus with a cocktail of Collagenase D, Dispase and Hyaluronidase resulted in a marked reduction in $CD3^+$ T-cells, resulting in no $CD45^+$ $CD3^+$ $CD4^+$ $CD8^-$ (**Figure 6.3** *blue arrows*) or $CD45^+$ $CD3^+$ $CD4^-$ $CD8^+$ T-cells (**Figure 6.3** *red arrows*) being detected when compared to the Collagenase D only treated controls. $CD45^+$ $CD11b^+$ monocytes and $CD45^+$ $CD11b^+$ $F4/80^+$ macrophages were unaffected (**Figure 6.3**). Thus, I conclude that treatment with a cocktail of Collagenase D, Dispase and Hyaluronidase results in cleavage of important surface exposed T-cell markers, and that a combination of mechanical disaggregation alongside 2 mg/ml Collagenase D treatment represents a more optimal strategy for tissue disaggregation prior to immune cell FACS staining.

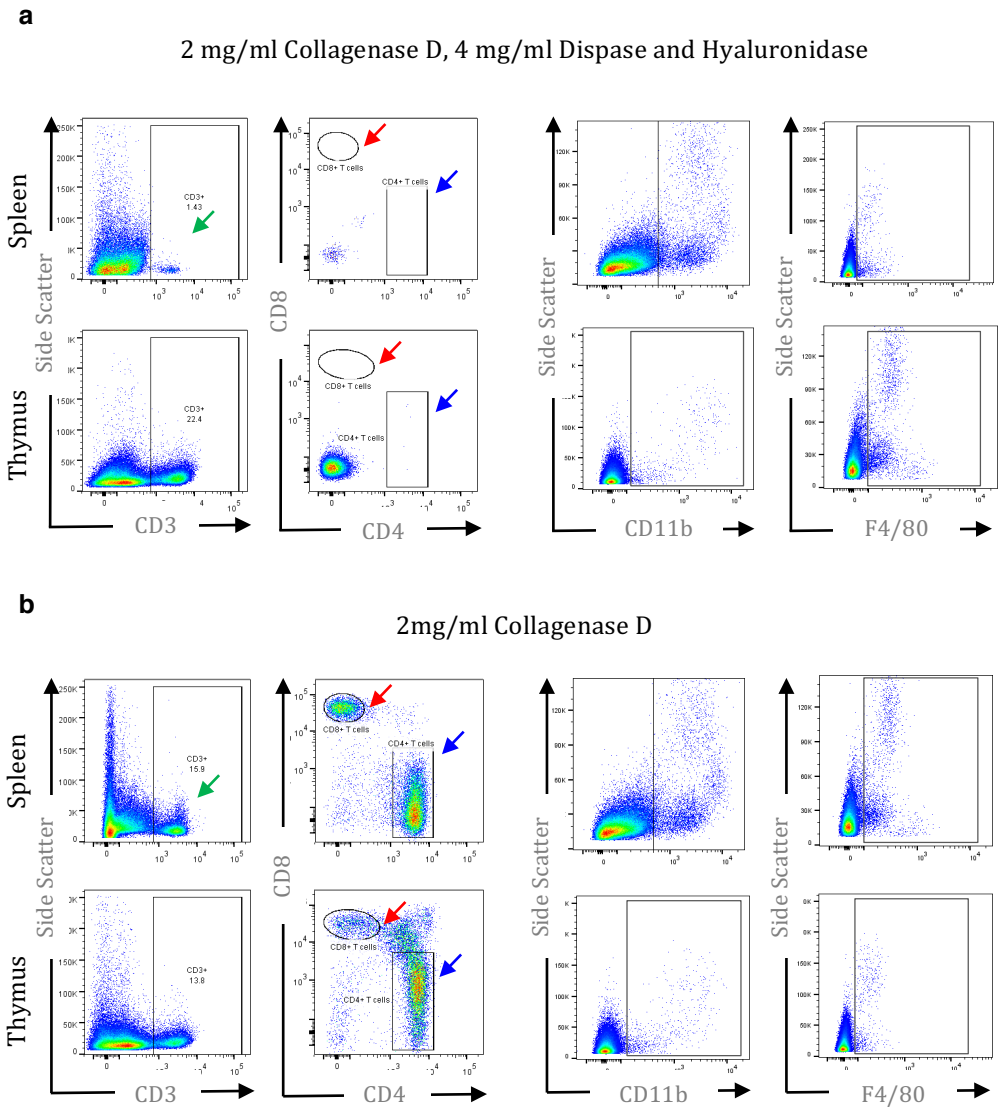

Figure 6.3 | Tissue disaggregation with Collagenase D, Dispase and Hyaluronidase reduced CD3, CD4 and CD8 expressing cells. FVB/N spleens and thymus (n = 3) were mashed through a 70 µm filter and treated with either 2 mg/ml collagenase D, 4 mg/ml dispase and 0.1% hyaluronidase (**a**) or 2 mg/ml Collagenase D (**b**). Samples were stained for CD45, CD11b, F4/80, CD3 and CD8 (**Table 6.1**). *green arrow* $CD3^+$, *red arrow* $CD8^+$ and *blue arrow* $CD4^+$ T-cells

6.3.3 FACS analysis of SCC FAK-wt tumours indicate an inflammatory switch 10 days post implantation

Tumour ulceration represents a recognized stage of SCC progression, occurring after increased necrosis causes the primary tumour nodule to slough, forming an ulcer which commonly does not heal[356]. I observed that SCC FAK-wt tumours appeared redder in colour around day 10, and that signs of ulceration began to show at day 14. Thus, I set out to investigate whether SCC progression and ulceration influenced the tumour immune infiltrate, and if so to identify any changes that correlated with the visual onset of ulceration. This information was important, as no ulceration was visually evident in SCC FAK-/- tumours at days 10 and 14. Therefore it was important to define a time-point with the following criteria: 1) little to no ulceration in any tumour samples, 2) sufficiently developed to contain an established and activated T-cell population, and 3) large enough in size to enable sufficient cell numbers to be released for FACS analysis. This was so that enough of each sample could be collected and processed, and comparisons could be made between SCC FAK-wt and SCC FAK-/- tumours. Furthermore, I wanted to expand our analysis to

Population	Markers
Blood Monocyte	$CD45^+$ $CD11b^+$ $F4/80^-$ $Ly6C^-$
Inflammatory Monocyte	$CD45^+$ $CD11b^+$ $F4/80^-$ $Ly6C^+$
Inflammatory Macrophage (polarization)	$CD45^+$ $CD11b^+$ $F4/80^+$ $Ly6C^+$ ($Tie2^{hi/lo}$ $MMR^{hi/lo}$)
Macrophage (polarization)	$CD45^+$ $CD11b^+$ $F4/80^+$ $Ly6C^-$ ($Tie2^{hi/lo}$ $MMR^{hi/lo}$)
$CD4^+$ T-cell	$CD45^+$ $CD3^+$ $CD4^+$ $CD8^-$
$CD4^+$ Central Memory T-cell	$CD45^+$ $CD3^+$ $CD4^+$ $CD8^-$ $CD62L^+$ $CD44^+$
$CD4^+$ Effector Memory T-cell	$CD45^+$ $CD3^+$ $CD4^+$ $CD8^-$ $CD62L^-$ $CD44^+$
$CD8^+$ T-cell	$CD45^+$ $CD3^+$ $CD4^-$ $CD8^+$
$CD8^+$ Central Memory T-cell	$CD45^+$ $CD3^+$ $CD4^-$ $CD8^+$ $CD62L^+$ $CD44^+$
$CD8^+$ Effector Memory T-cell	$CD45^+$ $CD3^+$ $CD4^-$ $CD8^+$ $CD62L^-$ $CD44^+$

Table 6.2 | Immune populations and the markers used to identify them by FACS analysis.

include a number of activation states for each population of immune cells (**Table 6.2**). Incorporation of Ly6C, MMR and Tie2 allowed us to differentiate between different monocyte populations and to investigate changes in macrophage polarization. The inclusion of CD62L and CD44 allowed us to determine any potential differences in T-cell effector, central memory and naïve activation states. Thus, I implanted 1 x 10^6 SCC FAK-wt cells by bilateral subcutaneous injection in to both flanks of FVB/N mice, and sacrificed cohorts of animals 7 days, 10 days or 14 days post implantation. Tumours were removed, disaggregated, and stained with Stains 1 and 2 (**Table 6.3**). Cell viability marker eFluor® 506 conjugated fixable viability dye was also included enabling dead cells to be excluded from the analysis; due to the break down of surface proteins, dead cells can adhere to antibodies resulting in false positive staining and so must be excluded. Samples were then analysed by FACS. Due to the more complex nature of the FACS analysis, a hierarchal gating strategy was required for both Stains 1 and 2 (**Figure 6.4 and 6.5** respectively).

Stain 1	
	Fluorophore
Viability	Viability e506
CD45	e780
F4/80	FITC
CD11b	PerCP-Cy5.5
MMR	APC
Tie2	PE
Ly6C	e450

Stain 2	
	Fluorophore
Viability	Viability e506
CD45	e450
CD3	FITC
CD8	PE
CD4	e647
CD62L	PE-Cy7
CD44	PerCP-Cy5.5

Table 6.3 | FACS stains used to identify immune populations described in Table 6.2. Stain 1 (*left panel)* was used to determine the number of blood monocytes, inflammatory monocytes, inflammatory macrophages and resident macrophages. Both inflammatory and resident macrophage polarization was determined using MMR and Tie2 expression (MMR^{lo} $Tie2^{lo}$ = M1 macrophage; MMR^{hi} $Tie2^{hi}$ = M2 macrophage). Stain 2 (*right panel*) was used to determine the number $CD8^+$ and $CD4^+$ T-cells and the activation status (effector memory and central memory) of both populations.

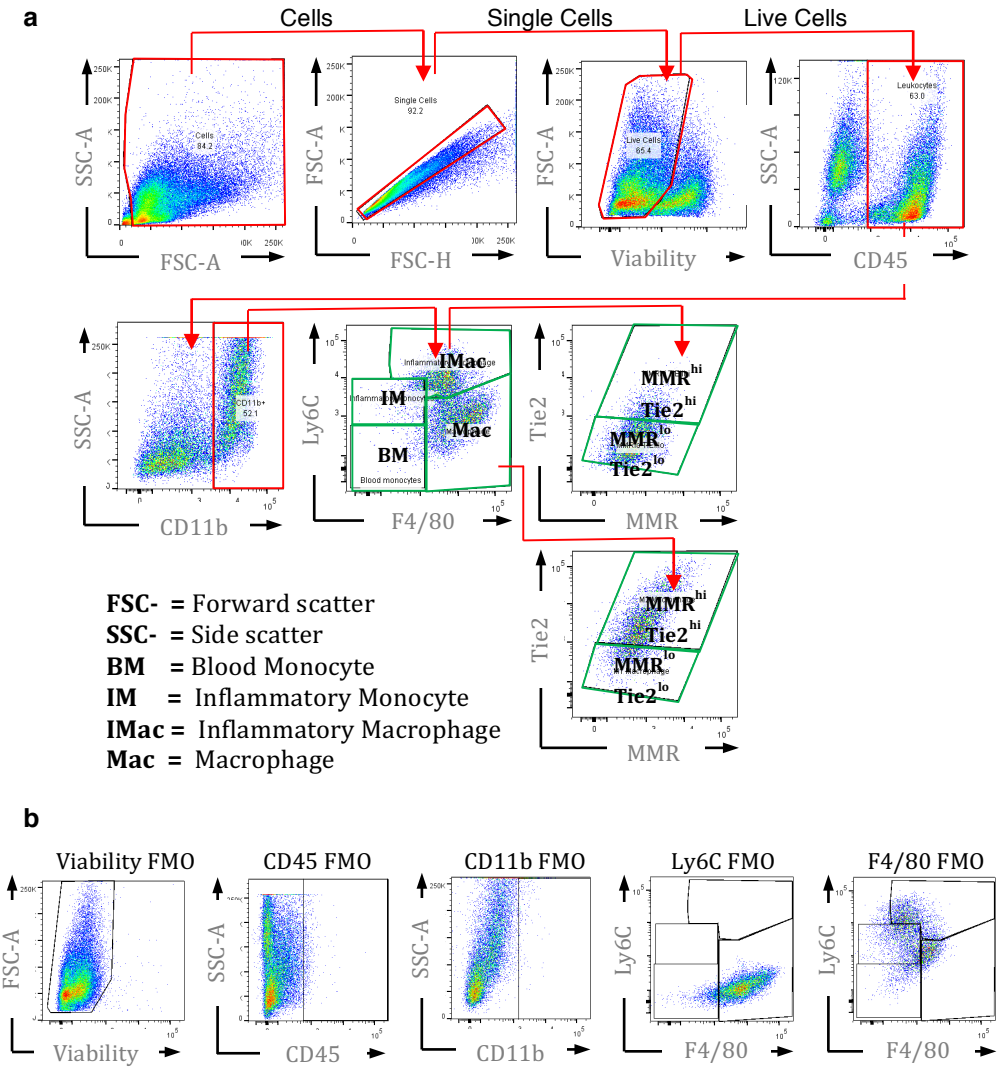

Figure 6.4 | Gating strategy and FMO controls for FACS analysis of myeloid cells and their polarization status. a Gating strategy applied to Stain 1 (**Table 6.3**), which was used to determine the number of blood monocytes, inflammatory monocytes, inflammatory macrophages and resident macrophages. Both inflammatory and resident macrophage polarization was determined using MMR and Tie2 expression (MMR^{lo} $Tie2^{lo}$ = M1 macrophage; MMR^{hi} $Tie2^{hi}$ = M2 macrophage). See **Table 6.2** for full list of immune populations and their respective markers markers. **b** FMO control samples used to determine macrophage sub-populations. Each FMO control sample contains every marker in Stain 1 (**Table 6.3**) except for the named marker. FMO controls were used to determine the correct gating positions in FACS analysis to exclude false positive results. *FMO* = Fluorescence minus one; *SCC* = side scatter; *FSC* = forward scatter

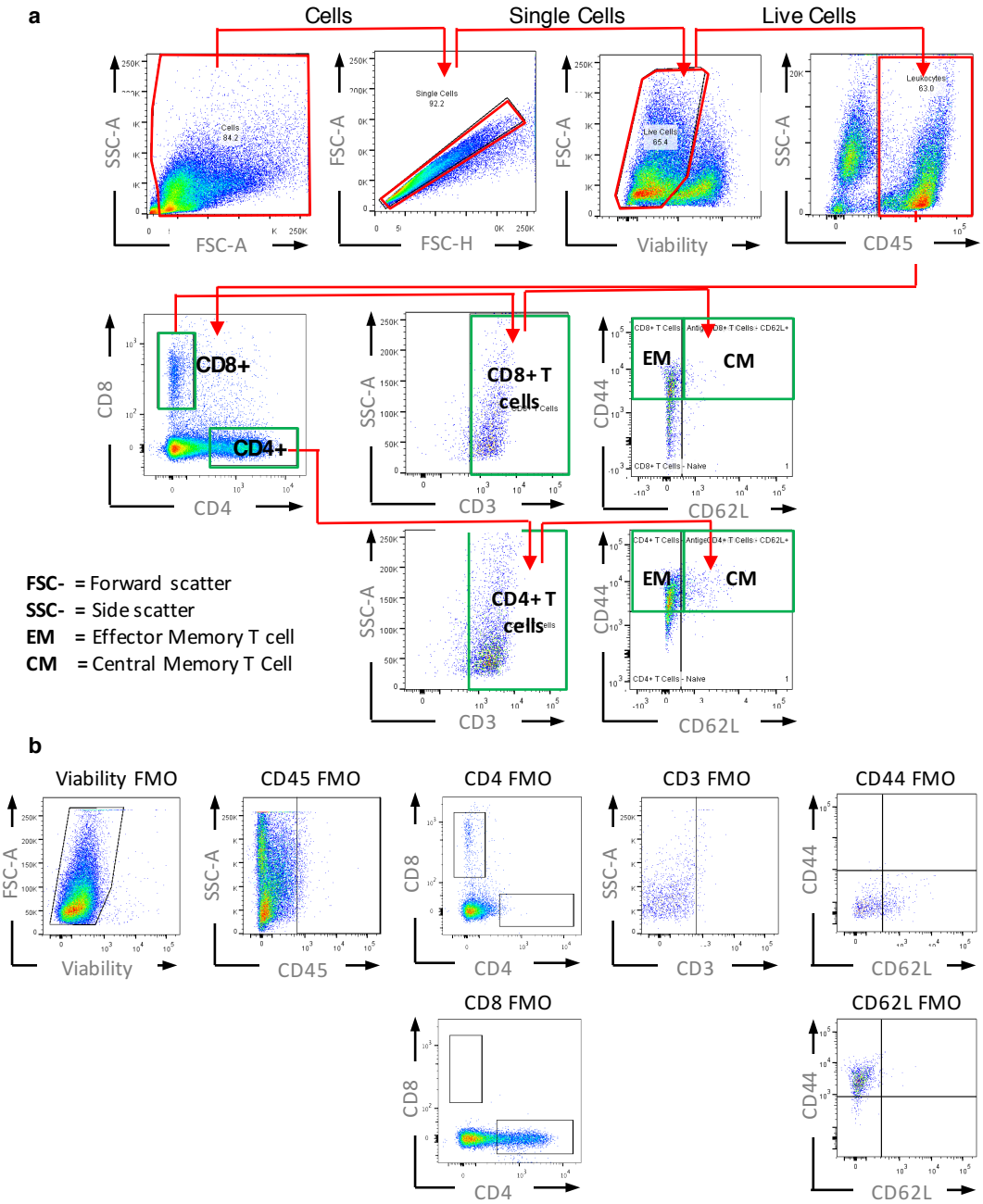

Figure 6.5 | Gating strategy and FMO controls for FACS analysis to identify T-cells and their activation status. **a** Gating strategy applied to Stain 2 (**Table 6.3**), which was used to determine the number of $CD8^+$ and $CD4^+$ T-cells and the activation status (effector memory and central memory) of both populations. See **Table 6.2** for full list of immune populations and their respective markers. **b** FMO control samples used to determine T-cell sub-populations. Each FMO control sample contains every marker in Stain 2 (**Table 6.3**) except for the named marker. FMO controls were used to determine the correct gating positions in FACS analysis to exclude false positive results. *FMO* = Fluorescence minus one; *SCC* = side scatter; *FSC* = forward scatter

FACS analysis of SCC FAK-wt tumours highlighted an increase between days 7 and 10 in $CD45^+ CD11b^+ F4/80^- Ly6C^+$ inflammatory monocytes (mean ± s.e.m = 2.427% ± 0.2339 and 4.612% ± 0.3805) and $CD45^+ CD11b^+ F4/80^+ Ly6C^+$ inflammatory macrophages (mean ± s.e.m. = 18.62% ± 0.849 and 25.57% ± 1.509) as a percentage of total $CD45^+$ cells (**Figure 6.6**). This correlated with a 10% decrease in $CD45^+ CD11b^+ F4/80^+ Ly6C^-$ resident macrophages between days 7 and 10 (mean ± s.e.m = 31.89% ± 1.324 and 21.48% ± 0.7170; **Figure 6.6**). Both inflammatory and resident macrophage populations showed a marked increase in MMR^- and $Tie2^-$ M1 polarized macrophages between these time points (inflammatory macrophage = mean ± s.e.m = 32.96% ± 1.967 and 89.32% ± 0.8048;

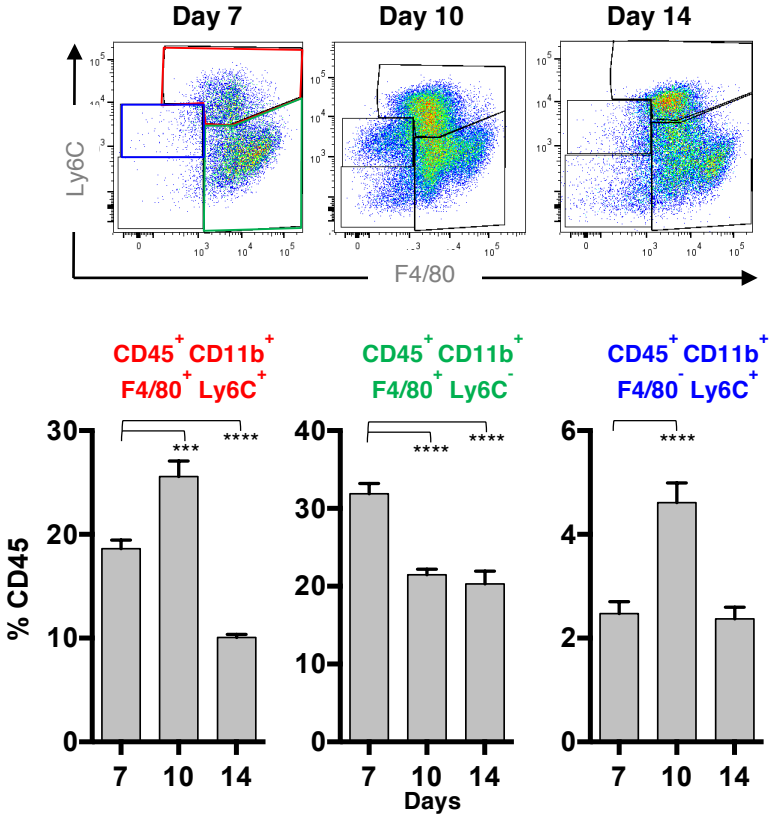

Figure 6.6 | Increase in intra-tumoural $Ly6C^+$ myeloid cells in SCC FAK-wt tumours. 1 x 10^6 SCC FAK-wt cells were implanted into the flanks FVB/N mice by bilateral subcutaneous injection. Tumours were removed from mice (n = 3) 7, 10 and 14 days post-implantation. Tumours were disaggregated and stained for FACS analysis (**Table 6.3**). Gating was as described in **Figure 6.4,** FACS plots of Ly6C and F4/80 expression on $CD45^+$ $CD11b^+$ populations (*upper panel*) and their quantification (*lower panels*). The number of each cell population was determined and the statistical significance between each time point was calculated by one-way Anova with Tukey's multiple comparisons. *Bar height* = mean, *Error bars* = s.e.m. Comparison between days 10 and day 14 not shown. P-value = Not significant >0.05, * <0.05, ** <0.01, *** <0.001, **** <0.0001.

resident macrophages = mean ± s.e.m = 15.47% ± 1.255 and 73.58% ± 2.095 respectively; **Figure 6.7**). An increase in $CD45^+$ $CD3^+$ $CD4^-$ $CD8^+$ T-cells of approximately 20% were seen across all three time points (mean ± s.e.m = 7.33% ± 0.8017, 13.38% ± 0.7457 and 27.43% ± 1.843 for days 7, 10 and 14 respectively; **Figure 6.8b**), but levels of $CD45^+$ $CD3^+$ $CD4^-$ $CD8^+$ $CD44^+$ $CD62L^-$ effector $CD8^+$ T-cells peaked at day 10 indicative of an activated cytotoxic population (**Figure 6.8c**). Althogh tthere was no significant difference between the levels of $CD45^+$ $CD3^+$ $CD4^+$ $CD8^-$ (**Figure 6.8d**), $CD45^+$ $CD3^+$ $CD4^+$ $CD8^-$ $CD44^+$ $CD62L^-$ effector $CD4^+$ T-cells increased significantly at day 10 (**Figure 6.8e**). SCC FAK-wt tumours showed obvious signs of ulceration at day 14 and the loss of inflammatory macrophages and monocytes at this time point is likely due to the increased proportion of $CD8^+$ T-cells as a consequence of increased ulceration. Therefore, I hypothesised that the increases in inflammatory $Ly6C^+$ immune cell populations, along side the increase in effector $CD8^+$ T-cells at day 10 of SCC FAK-wt tumour growth, were indicative of the initial stages of tumour ulceration. Therefore day 7 was selected as the most suitable time point for valid comparison between SCC FAK-wt and SCC FAK-/- tumours.

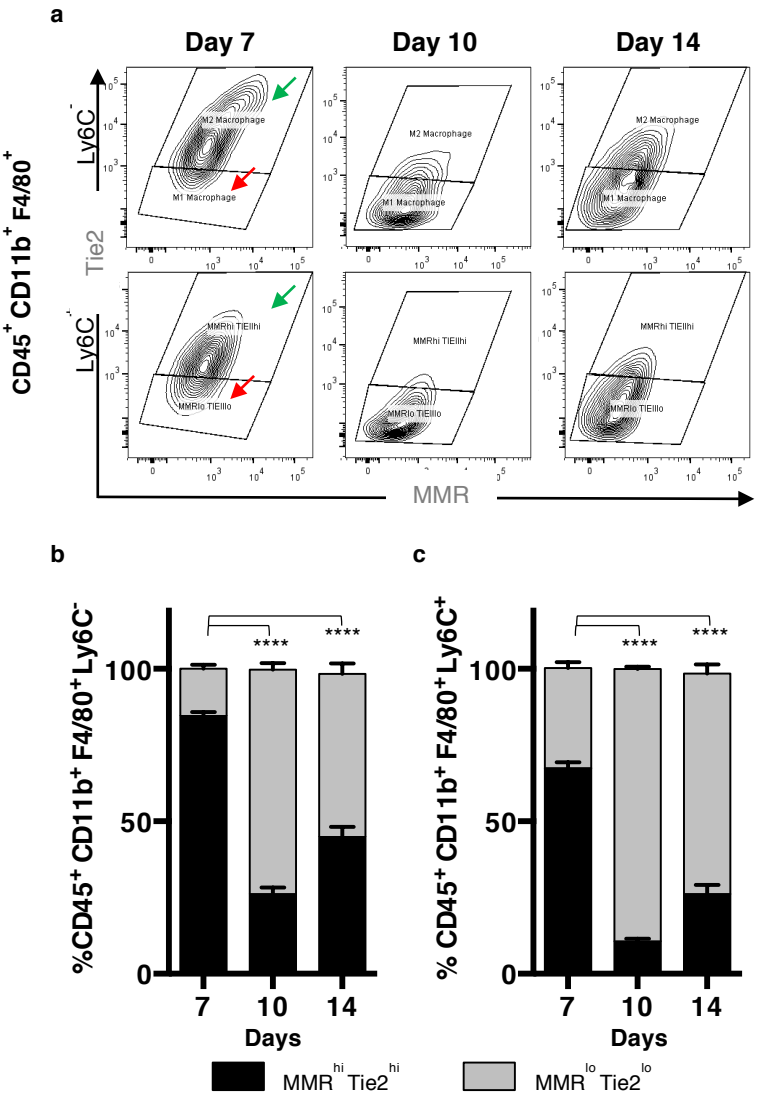

Figure 6.7 | Increase in intra-tumoural MMR^{lo} Tie2^{Lo} polarized Ly6C^{+} and Ly6C^{-} macrophages in SCC FAK-wt tumours. a FACS plots of MMR and Tie2 expression on CD45^{+} CD11b^{+} F4/80^{+} - Ly6C^{+} and – Ly6C^{-} populations and the quantification of **b** CD45^{+} CD11b^{+} F4/80^{+} Ly6C^{+} polarization and **c** CD45^{+} CD11b^{+} F4/80^{+} Ly6C^{-} polarization . 1 x 10^{6} SCC FAK-wt cells were implanted into the flanks FVB/N mice by bilateral subcutaneous injection. Tumours were removed from mice (n = 3) 7, 10 and 14 days post-implantation. Tumours were disaggregated and stained for FACS analysis (**Table 6.3**). Gating was as described in **Figure 6.4.** The number of each cell population was determined and the statistical significance between each time point was calculated by one-way Anova with Tukey's multiple comparisons. *Bar height* = mean, *Error bars* = s.e.m. Comparison between days 10 and day 14 not shown. P-value = Not significant >0.05, * <0.05, ** <0.01, *** <0.001, **** <0.0001. *Green arrow* = MMR^{hi} Tie2^{hi}; *Red arrow* = MMR^{lo} Tie2^{lo}

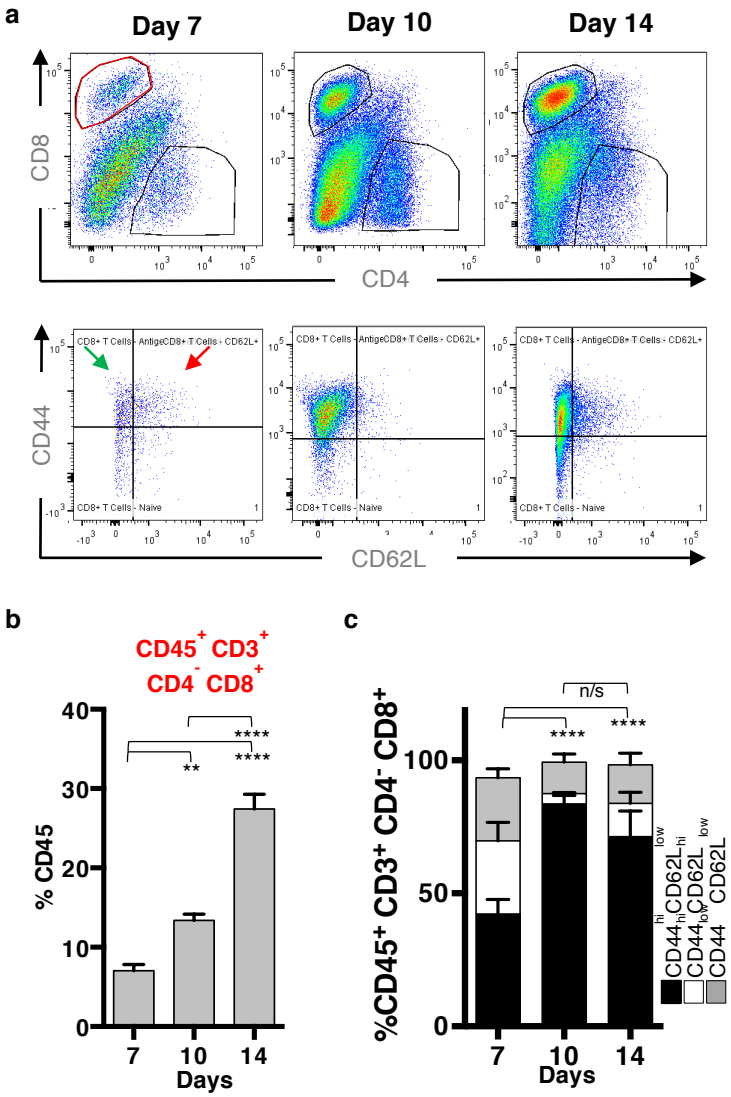

Figure 6.8 | Effector CD8^{+} T-cells were increased 7, 10 and 14 days post implantation. 1 x 10^{6} SCC FAK-wt cells were implanted into the flanks FVB/N mice by bilateral subcutaneous injection. Tumours were removed from mice (n = 3) 7, 10 and 14 days post-implantation. Tumours were disaggregated and stained for FACS analysis (**Table 6.3**). Gating was as described in **Figure 6.5.** **a** FACS plots of CD8 and CD4 expression on CD45^{+} CD3^{+} populations (*upper left panel*), the activation status of **CD45^{+} CD3^{+} CD8^{+}** population (*lower left panel*). **b** FACS quantification of total intra-tumoral CD8^{+} T-cells. **c** FACS quantification of CD8^{+}CD44^{hi}CD62L^{low}, CD8^{+}CD44^{hi}CD62L^{hi}, CD8^{+}CD44^{low}CD62L^{hi} T-cell subpopulations (statistics shown for CD44^{hi}CD62L^{low} only).The number of each cell population was determined and the statistical significance between each time point was calculated by one-way Anova with Tukey's multiple comparisons. P-value = Not significant >0.05, * <0.05, ** <0.01, *** <0.001, **** <0.0001 *Bar height* = mean; *Error bars* = s.e.m. EF = effector = CD44^{hi}CD62L^{hi}; M = central memory = CD44^{low}CD62L$^{hi.}$

6.4 Conclusion

Together these data show that tissue disaggregation with collagenase D, dispase and hyaluronidase appears to cleave surface-expressed markers, and thus tissue disaggregation with collagenase D alone was best suited for use with FACS analysis. Using this protocol, a number of immune populations could be identified within SCC FAK-wt tumours and changes in these populations at different time points of tumour growth could be quantified.

So that valid comparisons between two different tumours can be made using FACS analysis, tumours are matched by age and size in order to account for factors that may adversely influence the tumour immune milieu, including signs of tumour ulceration, bias in tumour size, different tumour histopathological stage etc. Ulceration of SCC tumours is a recognised histopathologicical indicator of disease progression[356] and early signs of the onset of ulceration was observed in SCC FAK-wt tumours 10 days post implantation into FVB/N mice. In a number of cases, SCC FAK-wt tumours appeared redder in colour, an observation that crucially was absent from SCC FAK-/- tumours at the same time point. Although the changes in the immune mileau of SCC in response to ulceration have not as yet been characterised, increases in $Ly6C^+$ immune populations and increases in $CD8^+$ T-cell populations have been observed concurrent with the onset of ulceration in melanoma[357] and in a number of different skin ulcerative diseases[358-360].

FACS analysis of SCC FAK-wt tumours dectected an increase in the levels of inflammatory $Ly6C^+$ immune populations and revealed a switch in the polarisation of both inflammatory and resident macrophage populations from pro-tumorigenic M2 to an anti-tumorigenic M1 phenotype[45,361]. Increasing numbers of total numbers of $CD8^+$ T-cells were observed across the time course. CD62L[362] and CD44[363] are adhesion proteins required for T-cell homing to non-lymphoid peripheral tissue, and are used to differentiate between effector ($CD44^+$ $CD62L^-$) and memory ($CD44^+$ $CD62L^+$) due to the requirement of CD44 alone or both CD44 and CD62L for homing respectively. This analysis indicated that effector $CD8^+$ T-cell population increased across the time course, indicative of increased cytotoxic activity in SCC

FAK-wt tumours that may not be present in SCC FAK-/-. It was concluded that these data were indicative of tumour ulceration and thus any potential changes in the immune milieu driven by FAK would be masked. Thus, day 7 was the optimal time point to provide the most valid comparison between SCC FAK-wt and SCC FAK-/- tumour immune milieu.

These data presented in this chapter identified that proteolytic degradation of surface expressed markers can result in the detection of very different immune landscapes. Both thymus and spleen predominantly contain T-cell populations[14], which were undetectable in samples prepared with collagenase D, dispase and hyaluronidase. This therefore highlights the need to include a selection of immune markers, capable of identifying a broad number of immune populations from both the adaptive and innate arms of the immune response. Furthermore, if this analysis had been conducted exclusively on tumour tissue, would would have been unable to elucidate the prescience of T-cells in our phenotype. This not only highlights the essential requirement to validate disaggregation techniques on tissues where the inflammatory landscape is known (i.e the large T-cell populations in both the spleen and thymus), but also emphasizes the need for further evaluation of the enzymes used for tissue disaggregation, and their potential to degrade surface-expressed targets.

As shown here, there is a requirement to use enzymatic disaggregation to release monocytes and other immune cells for tissue, but the effect on surface-expressed markers has to be considered. Therefore, a broad immunophenotyping approach alongside tissue disaggregation with collagenase D appears to be the most valid, one which incorporates markers for the identification and characterisation of a wide range of immune populations, and therefore can determine whether disaggregation has any effect on these targets, especially within tumours where the immune landscape is unknown. This approach has been used in a number of human studies, in which tissue sample is less abundant than in animal studies, to immunophenotype breast tumours[35,87]. Although the differences in sequences between mouse and human immune markers means that they are differentially effected by enzymatic degradation, and therefor a marker cleaved in a human sample may not be cleaved in

a mouse tumour, these studies highlight the capabilities of larger immunophenotyping approaches.

One potential caveat within the FACS analysis presented in this chapter is the presentation of FACS data as a percentage of $CD45^+$ cells, and not as the absolute number of cells within the sample. This method of presenting FACS data can suffer from changes in immune populations being observed not because they themselves change, but because another population has changed. For example, an increase in $CD8^+$ T-cells may be observed, but in fact the macrophage population has decreased and thereby increasing the proportion of $CD45^+$ cells that are $CD8^+$ T-cells, without actually effecting the total number of $CD8^+$ T-cells within the tumour. Changes such as these can be identified, but nevertheless must be considered when drawing conclusions from data presented in this manner.

This is not the case when presenting data as the absolute number of immune cells within a sample; populations will not change proportionally to each other and therefore a reduction in macrophages will not change the proportion of T-cells. However, one of the main issues with presenting data in this manor is that the absolute number of cells is directly related to the volume of the tumour and the tumour mass, and therefore surgically excised tumours must be weighted and measured after excision, and the FACS results normalized to these values. Another issue with this method is that counting beads have to be used to ensure that the sample concentration can be determined; if a greater volume of one sample is analysed when compared to another, this will not represent the absolute number of cells, and therefore invalidate the experiment.

The requirement for both tumour weight post-excision and the inclusion of counting beads means that analysis of the absolute number cannot be performed retrospectively, and although would have been beneficial to conduct a comparison of both percentage $CD45^+$ and absolute number methods here, this could not be completed. However, even though at day 7 SCC FAK-wt and SCC FAK-/- tumours are approximately the same volume, any increase in the tumour size of SCC FAK-wt tumours compared to SCC FAK-/- will introduce bias into the analysis, and therefor FACS data is presented as a percentage of $CD45^+$ cells within this thesis.

7 FAK expression results in generation of an immuno-suppressive microenvironment

7.1 Introduction

Following the observation that SCC FAK-/- tumour clearance was dependent on $CD8^+$ T-cells, and that cells of the $CD4^+$ T-cell compartment played a role in protecting SCC FAK-wt tumours from clearance, I set out to understand in more detail the composition of the tumour immune infiltrate. In doing so, I sought to identify whether $CD8^+$ T-cells were present in all tumour types, and if so, whether there was any evidence of other immune cell types within the tumour that had the potential to modulate $CD8^+$ T-cell function. A number of immune cell types with intrinsic immuno-suppressive capabilities are known to infiltrate extensively into tumours, including macrophages, myeloid derived suppressor cells (MDSCs), and regulatory T-cells (Tregs). Through a variety of mechanisms (described in detail in section 2.1.3) these cells can disarm the cytotoxic functions of antigen-primed $CD8^+$ T-cells and promote tumour survival and progression. Therefore I set out to study these populations in SCC FAK-wt, FAK-/-, and FAK-kd tumours 7 days post-implantation, with the aim of identifying changes that may be responsible for the observed regression phenotype.

7.2 Aims

- To characterise the T-cell response and determine T-cell activation status
- To determine whether FAK regulates the recruitment of immunosuppressive immune cell populations

7.3 Results

7.3.1 SCC FAK-wt tumours contain infiltrating activated T-cells

Having established a role for T-cells in the SCC tumour growth, I wanted to further characterise the T-cell population in our model. To address this, 1 x 10^6 SCC FAK-wt, SCC FAK-/- and SCC FAK-kd cells were implanted into the flanks of FVB/N mice by bilateral subcutaneous injection. Tumours were grown for 7 days, removed and disaggregated. Samples were then stained with Stains 1 and 2 (**Table 6.3**) and analysed by FACS. This analysis revealed T-cells in SCC FAK-wt, SCC FAK-/- and SCC FAK-kd tumours (**Figure 7.1a**). The levels of $CD8^+$ T-cells were significantly increased in SCC FAK-/- (mean ± s.e.m. = 3.272% ± 0.423%)) and SCC FAK-kd (mean ± s.e.m. = 3.066% ± 0.329%) tumours compared to SCC FAK-wt (mean ± s.e.m. = 1.76% ± 0.18%; **Figure 7.1b**). Further in-depth analysis into the activation status of the $CD8^+$ T-cell populations, highlighted a significant increase in $CD45^+$ $CD3^+$ $CD4^-$ $CD8^+$ $CD44^+$ $CD62L^-$ cells in SCC FAK-/- (mean ± s.e.m. = 48.39% ± 1.591) and SCC FAK-kd (mean ± s.e.m. = 67.04% ± 1.942) tumours, when compared to SCC FAK-wt tumours (mean ± s.e.m. = 42.28% ± 1.798; **Figure 7.1c**). This increase was greater after effector $CD8^+$ T-cell numbers were normalized to account for the observed changes in total $CD8^+$ T-cells and presented as a 'fold change' (**Figure 7.1d**). Normalized effector $CD8^+$ T-cells were 2-fold increased in SCC FAK-/- tumours, and approximately 3-fold increased in SCC FAK-kd tumours when compared to SCC FAK-wt tumours.

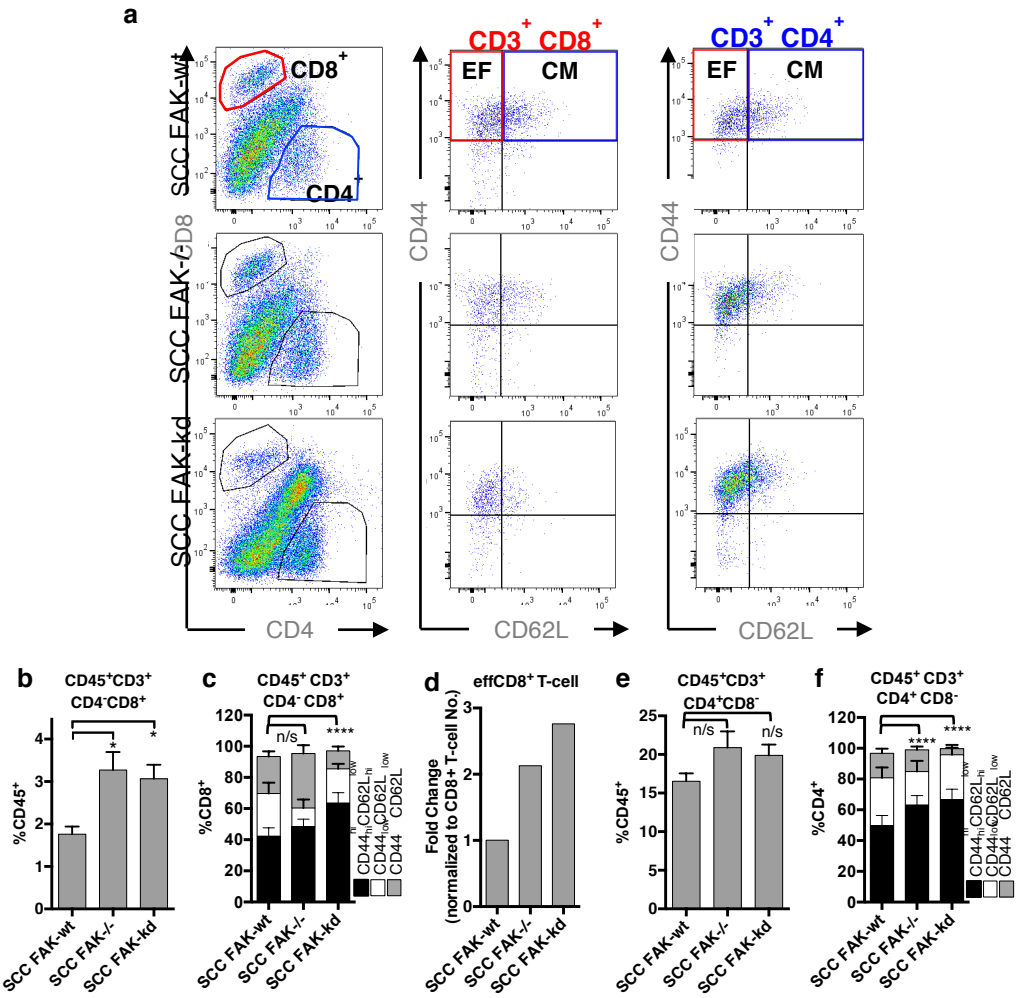

Figure 7.1. FAK-depleted tumours exhibit a heightened CD8$^+$ T-cell response. 1 x 10^6 SCC FAK-wt, SCC FAK-/- or SCC FAK-kd cells were implanted into the flanks of FVB/N mice by bilateral subcutaneous injection (n = 3). Tumours were removed after 7 days, disaggregated and stained for FACS analysis with Stain 1 (**Table 6.3**). Gating was as described in **Figure 6.5. a** FACS plots of CD8 and CD4 expression on CD45$^+$ CD3$^+$ cells (*left panel*) from SCC FAK-wt, SCC FAK-/- and SCC FAK-kd tumours. The activation status of CD8$^+$ T-cell (*center panel*) and CD4$^+$ T-cells *(right panel*) is also shown. **b** FACS quantification of total intra-tumoral CD8$^+$ T-cells. **c** FACS quantification of CD8$^+$CD44^{hi}CD62L^{low}, CD8$^+$CD44^{hi}CD62L^{hi}, CD8$^+$CD44^{low}CD62L^{hi} T-cell subpopulations (statistics shown for CD44^{hi}CD62L^{low} only). **d** Fold-change in effector (CD8$^+$CD44^{hi}CD62L^{low}) CD8$^+$ T-cells when normalized to total CD8$^+$ T-cell percentage. **e** FACS quantification of total intra-tumoral CD4$^+$ T-cells. **f** FACS quantification of CD4$^+$CD44^{hi}CD62L^{low}, CD4$^+$CD44^{hi}CD62L^{hi}, CD4$^+$CD44^{low}CD62L^{hi} T-cell subpopulations (statistics shown for CD44^{hi}CD62L^{low} only). The number of each cell population was determined and the statistical significance between each cell type was calculated by one-way Anova with Tukey's multiple comparisons. Comparision of SCC FAK-/- and SCC FAK-kd not shown P-value = Not significant >0.05, * <0.05, ** <0.01, *** <0.001, **** <0.0001 *Bar height* = mean; *Error bars* = s.e.m. EF = effector = CD44^{hi}CD62L^{hi}; M = central memory = CD44^{low}CD62L^{hi}

$CD4^+$ T-cell levels did not change between SCC FAK-wt, SCC FAK-/- and SCC FAK-kd tumours (mean ± s.e.m. = SCC FAK-wt, 16.54% ± 1.022; SCC FAK-/-; 20.88% ± 2.099; SCC FAK-kd, 19.88%; **Figure 7.1e**). However, I did observe a significant increase in the proportion of effector $CD4^+$ T-cells in SCC FAK-/- and FAK-kd tumours (SCC FAK-/- = mean ± s.e.m. = 63.12% ± 2.037; SCC FAK-kd = mean ± s.e.m. = 70.84% ± 1.816; p value = <0.0001<0.0001) when compared to FAK-wt tumours (mean ± s.e.m. = 49.78% ± 2.164; **Figure 7.1f**).

These data imply that an activated $CD8^+$ and $CD4^+$ T-cell response is present in all tumour types, raising the question as to why SCC FAK-wt tumours do not succumb to $CD8^+$ T-cell mediated clearance.

7.3.2 FAK expression promotes an immunosuppressive microenvironment

Recruitment of immune cell populations with intrinsic immuno-suppressive capabilities, including M2 macrophages, MDSCs and Tregs has been shown to suppress the anti-tumour immune response and promote tumour deveoplement[364,365,366] (**2.1.3**). Thus, I set out to identify whether changes in these populations could explain the tumour growth characteristics of the SCC FAK-wt, FAK-/-, and FAK-kd tumours. 1 x 10^6 SCC FAK-wt, SCC FAK-/- or SCC FAK-kd cells were implanted into the flanks of FVB/N mice (n=5). Tumours were removed after 7 days and disaggregated. To identify M2 Macrophages ($CD45^+$ $CD11b^+$ $F4/80^+$ MMR^{hi} $Tie2^{hi}$; **Table 6.2**), both subpopulations of MDSCs, G-MDSCs ($CD45^+$ $CD11b^+$ $F4/80^-$ $LyC6^{lo}$ $Gr1^{hi}$) and M-MDSCs ($CD45^+$ $CD11b^+$ $F4/80^-$ $LyC6^{hi}$ $Gr1^{lo}$) and Tregs ($CD4^+$ $CD25^+$ $FoxP3^+$; **Table 7.1a**), samples were stained with Stain 1 (**Table 6.3**), Stain 3 and Stain 4 (**Table 7.1b**) respectively. Samples were then analysed by FACS.

a

Population	Markers
M-MDSC	$CD45^+$ $CD11b^+$ $F4/80^-$ $Ly6C^{hi}$ $Gr1^{lo}$
G-MDSC	$CD45^+$ $CD11b^+$ $F4/80^-$ $Ly6C^{lo}$ $Gr1^{hi}$
Treg	$CD4^+$ $FoxP3^+$ $CD25^+$

b

Stain 3	
	Fluorophore
Viability	Viability 506
CD45	e780
CD11b	PerCP - Cy5.5
F4/80	PE-Cy7
Ly6C	e450
Gr1	FITC

Stain 4	
	Fluorophore
CD4	PerCP - Cy5.5
CD25	PE
FoxP3	FITC

Table 7.1 | Markers and FACS stains used to identify immunosuppressive intra tumoural MDSC and Treg populations. **a** Markers required to identify both subpopulations of immunosuppressive MDSCs (M-MDSCs and G-MDSCs) and Tregs. **b** Stain 3 (*left panel*) was used to identify MDSCs and Stain 4 (right panel) was used to identify Tregs.

7.3.2.1 Changes in macrophage polarization do not correlate with the tumour regression phenotype.

SCC FAK-wt, SCC FAK-/- and SCC FAK-kd tumours stained with Stain 1 (**Table 6.3**) were analysed as described in **Figure 6.4**. Levels of total macrophages were unchanged across SCC FAK-wt, SCC FAK-/- and SCC FAK-kd tumours (**Figure 7.2** *height of stacked bar graph*; mean ± s.e.m. = 50.511% ± 5.905, 50.456% ± 4.307 and 49.845% ± 3.984 respectively). The proportion of inflammatory macrophages within the total population significantly increased in SCC FAK-/- and SCC FAK-kd tumours compared to SCC FAK-wt (mean ± s.e.m. = 22.900 ± 3.200, 27.989 ± 5.600 and 18.622 ± 2.550 respectively; p value = <0.05 and <0.001 respectively; **Figure 7.2** *black bars*).

Analysis of macrophage polarization indicated that both inflammatory and resident macrophage populations were highly M2 polarised in both the SCC FAK-wt and SCC FAK-kd tumours compared to the SCC FAK-/- tumours (**Figure 7.3** *centre and right panels respectively, grey bars*). Levels of M2 inflammatory macrophages were equivalent in SCC FAK-wt and SCC FAK-kd tumours (mean ± s.e.m. = 67.300 ±

1.989% and 68.056 ± 1.202% respectively; **Figure 7.3** *centre panel, grey bars*). Significantly lower levels were seen in SCC FAK-/- tumours (mean ± s.e.m. = 37.611 ± 4.249%; p value = <0.0001). This same trend was also observed in the resident macrophage population. SCC FAK-wt and SCC FAK-kd tumours showed equivalent levels of M2 polarised resident macrophages (mean ± s.e.m. = 84.589 ± 1.231 and 86.033 ± 0.971 respectively; **Figure 7.3** *right panel, grey bars*), and this population was significantly decreased in SCC FAK-/- tumours (mean ± s.e.m. = 59.000 ± 3.92; **Figure 7.3** *right panel, grey bars*; p value = <0.0001).

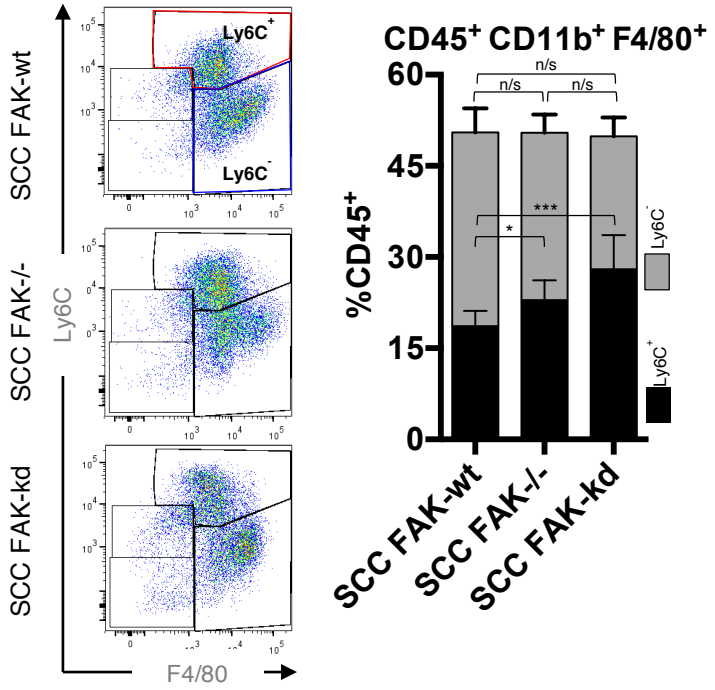

Figure 7.2. Intra-tumoural macrophages in SCC FAK-wt, SCC FAK-/- and SCC FAK-kd tumours. FACS plots of Ly6C and F4/80 expression on $CD45^+$ $CD11b^+$ populations (*left panel*) and their quantification (*right panel*). 1 x 10^6 SCC FAK-wt, SCC FAK-/- or SCC FAK-kd cells were implanted into the of flanks FVB/N mice by bilateral subcutaneous injection. Resulting tumours were removed from cohorts of mice (n = 3) 7 days post-implantation. Tumours were disaggregated and stained for FACS analysis (**Table 6.3**). Gating was as described in **Figure 6.4**. The number of each cell population was determined and the statistical significance between each cell type was calculated by one-way Anova with Tukey's multiple comparisons. *Bar height* = mean, *Error bars* = s.e.m. P-value = Not significant >0.05, * <0.05, ** <0.01, *** <0.001, **** <0.0001; *height of stack* = Mean total number of macrophages; Statistics shown for comparisons of $Ly6C^+$ and mean total number of macrophages. Statistics for $Ly6C^-$ not shown

These data showed that increased polarization towards M2 macrophages occurred in SCC FAK-wt and SCC FAK-kd tumours but not SCC FAK-/-. Two conclusions were drawn from this. Firstly, this implied that the presence of M2 macrophages were not sufficient to prevent SCC FAK-kd tumour regression, and therefore these cells were not the primary immunosuppressive population capable of evading a $CD8^+$ T-cell response. Secondly, this highlighted a potential kinase-independent role of FAK in modulating macrophage polarization. Although I chose not to investigate this further as these results did not correlate with tumour regression, this could potentially provide a novel therapeutic opportunity. The disruption of M2 macrophages and TAMs is of great clinical interest due to their multiple roles in tumour growth, survival and malignant progression (**2.1.1**).

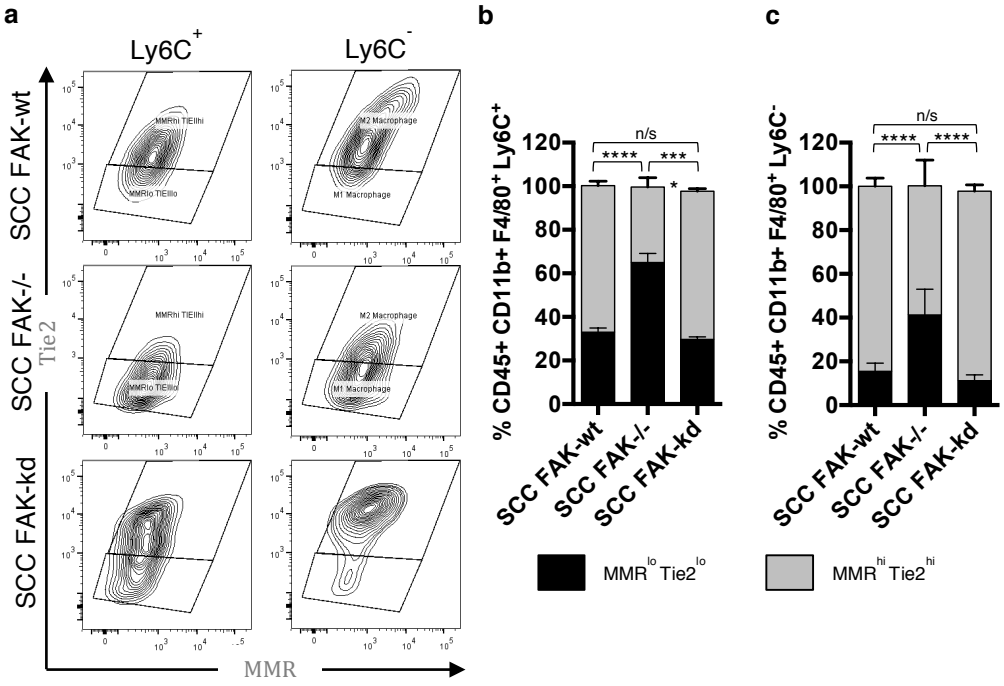

Figure 7.3 | M2 polarized macrophage populations did not correlate with tumour clearance characteristics. 1 x 10^6 SCC FAK-wt SCC FAK-/- or SCC FAK-kd cells were implanted into the flanks FVB/N mice by bilateral subcutaneous injection. Tumours were removed from mice (n = 3) 7 days post-implantation. Tumours were disaggregated and stained for FACS analysis (**Table 6.3**). Gating was as described in **Figure 6.4.** **a** FACS plots of MMR and Tie2 expression on $CD45^+$ $CD11b^+$ $F4/80^+$ $Ly6C^+$ and -$Ly6C^-$ populations and their quantification (*right panel*). The number of each cell population was determined and the statistical significance between each cell type was calculated by one-way Anova with Tukey's multiple comparisons. P-value = Not significant >0.05, * <0.05, ** <0.01, *** <0.001, **** <0.0001 *Bar height* = mean; *Error bars* = s.e.m. Statistics for MMR^{lo} $TieII^{lo}$ not shown

7.3.2.2 Intra-tumoural MDSC levels did not correlate with tumour regression characteristics.

I next focused on both subsets of MDSCs. M-MDSCs and G-MDSCs have been shown to have distinct functions, but M-MDSCs have been shown to have greater immunosuppressive capabilities[159] (**2.1.3.1**). Samples were stained with Stain 3 (**Table 7.1**) and analysed by FACS as described in **Figure 7.4**. Intra-tumoural M-MDSCs significantly increased in SCC FAK-/- tumours (means ± s.e.m. = 11.044 ± 1.937 compared to SCC FAK-wt (means ± s.e.m. = 7.9717 ± 3.255 and 8.5655 ± 2.803 respectively; p value = <0.0001; **Figure 7.5**). No significant difference was observed between SCC FAK-wt and SCC FAK-kd tumours (p value = >0.05).

The levels of intra-tumoural G-MDSCs were considerably less than M-MDSCs, but the comparison across all three-tumour types followed a similar trend. G-MDSCs were significantly increased in SCC FAK-/- tumours (means ± s.e.m. = 4.0125 ± 1.4477) compared to SCC FAK-wt (means ± s.e.m. 1.082 ± 0.667; p value = <0.0001) and SCC FAK-kd tumours (means ± s.e.m. = 1.9425 ± 0.604; p value = <0.001; **Figure 7.5**). No significant difference was observed between SCC FAK-wt and SCC FAK-kd tumours (p value = >0.05).

These data showed that both MDSC subpopulations were elevated in SCC FAK-/- tumours compared to SCC FAK-wt and SCC FAK-kd tumours. I concluded therefore, that neither M-MDSCs not G-MDSCs cells were the primary immunosuppressive population capable of evading a $CD8^+$ T-cell response. However, as levels of both populations in SCC FAK-kd tumours were comparable to the levels in SCC FAK-wt tumours, it was possible the FAK negatively regulated levels of intra-tumoural MDSCs in a kinase independent manner, or as a consequence of Kinase-independent regulation of other immune component, MDSCs represented a smaller proportion of leukocyte infiltrate.

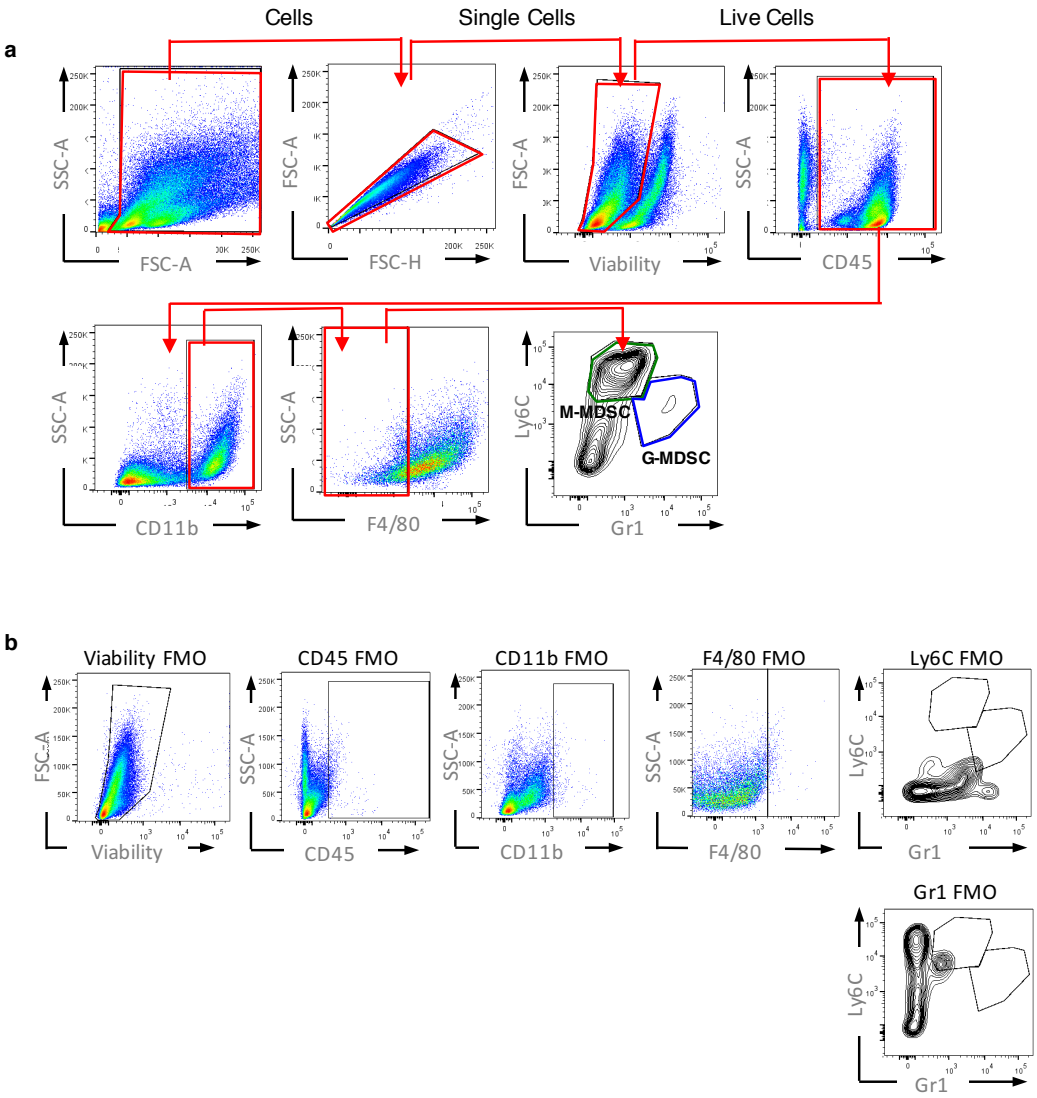

Figure 7.4 | MDSC FACS gating strategy. a Stain 3 (**Table 7.1**) was used to determine the total number of MDSCs and M-MDSCs and G-MDSCs subpopulations. See **Table 7.1** for full list of immune populations and their respective markers. **b** FMO control samples used to determine correct gating for MDSC sub-population identification. . M-MDSC = Monocytic Myeloid Derived Suppressor Cell; G-MDSC = Granulocytic Myeloid Derived Suppressor Cell; FMO = Fluorescence minus one

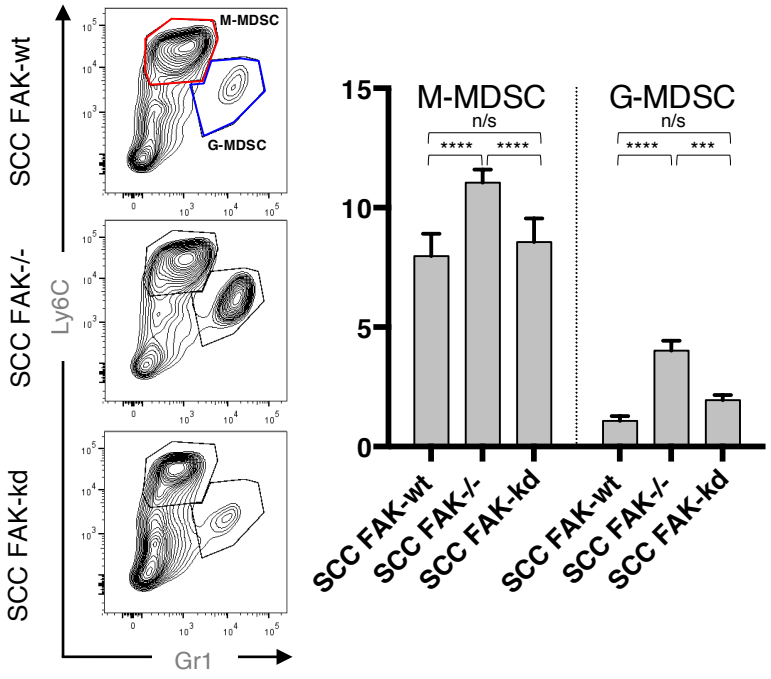

Figure 7.5 | FACS analysis of MDSC populations did not correlate with tumour clearance characteristics. 1 x 10^6 SCC FAK-wt, SCC FAK-/- or SCC FAK-kd cells were implanted into the flanks FVB/N mice by bilateral subcutaneous injection. Resulting tumours were removed from cohorts of mice (n = 3) 7 days post-implantation. Tumours were disaggregated and stained for FACS analysis with Stain 4 (**Table 7.1**). FACS analysis was gated as described in **Figure 7.4.** FACS blots of Ly6C and Gr1 expression on intra-tumoural $CD45^+$ $CD11b^+$ $F4/80^-$ populations (*left panel*) and their quantification (*right panel*). The number of each cell population was determined and the statistical significance between each cell type was calculated by one-way Anova with Tukey's multiple comparisons. P-value = Not significant >0.05, * <0.05, ** <0.01, *** <0.001, **** <0.0001 *Bar height* = mean; *Error bars* = s.e.m

7.3.2.3 Intra-tumoural Tregs were increased in SCC FAK-wt tumours and are required for SCC FAK-wt tumour growth.

Having ruled out M2 macrophages and MDSCs, I next focused on Tregs. Samples were stained with Stain 4 (**Table 7.1**) and prepared for FACS analysis. Samples were analysed as described in **Figure 7.6**. Stain 4 is a commercially available stain that includes cell permeablising buffers required for intracellular FoxP3 staining, and thus, FMO controls were not possible with this stain. SCC FAK-wt tumours showed a significant increase in the number of intra-tumoural Tregs (mean ± s.e.m. = 22.973 ± 2.614) compared to SCC FAK-/- and SCC FAK-kd tumours (mean ± s.e.m. = 6.8989 ± 5.2165 and 6.3800 ± 2.299 respectively; p value = >0.0001; **Figure 7.7a**). This increase resulted in a decrease in the ratio between effector $CD8^+$ and Tregs (**Figure 7.7b**; levels of $CD8^+$ effector cells shown in **Figure 7.1**). Changes in

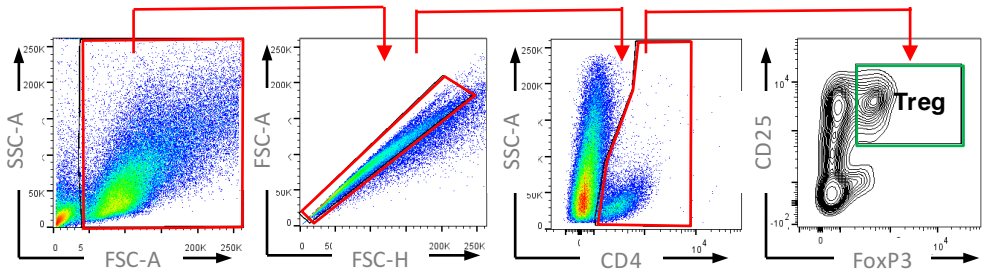

Figure 7.6 | Treg FACS gating strategy. Stain 4 (**Table 6.1**) was used to determine the number of $CD4^+$ $CD25^+$ $FoxP3^+$ Tregs. Stain 4 is a commercially available antibody cocktail, which incorporates cell permeablising buffers required for intracellular FoxP3 staining, and thus, FMO controls were not possible with this stain

the proportion of Tregs correlated with tumour regression characteristics, suggesting that this may be a potentially important population in mediating SCC FAK-wt tumour survival. There is an ever-expanding body of evidence that implicates Treg involvement in tumour immune evasion (**2.1.3.2**). Tregs ($CD4^+$ $CD25^+$ $FoxP3^+$ cells) are a highly immunosuppressive population whose primary function is to suppress activated $CD8^+$ T-cells in order to limit harmful immune responses to self-antigen. Thus, I wanted to further investigate whether Tregs were the immunosuppressive population that instilled SCC FAK-wt tumours with the capacity to evade a $CD8^+$ T-cell response. I had previously established that $CD4^+$ T-cells were required for SCC FAK-wt tumour survival (**Figure 5.10**). Treatment with CD4 depleting antibodies would reduce levels of Tregs, further supporting a role for Tregs in SCC FAK-wt survival. However, I wanted to take a more Treg-specific approach, and therefore used a CD25 depleting antibody. FVB/N mice were treated with 150 µg of CD25 depleting antibody (n = 5) or with Isotype control (n=5) by IP injection, and dosed as described in **Figure 5.8**. 1 x 10^6 SCC FAK-wt cells were implanted into mice after 5 days of treatment, and into an untreated control group, by bilateral subcutaneous injection in to both flanks. 1 x 10^6 SCC FAK-/- cells were also implanted into untreated animals as a control. Tumour diameter was measured twice weekly and tumour volume calculated using the formula $4/3\pi r^3$.

Untreated SCC FAK-wt and SCC FAK-/- tumours, and Isotype control treated SCC FAK-wt tumours grew as expected (**Figure 7.8**) and no significant difference was observed between SCC FAK-wt untreated and Isotype control treated animals (p value = >0.05). SCC FAK-wt tumours treated with CD25 depleting antibody grew

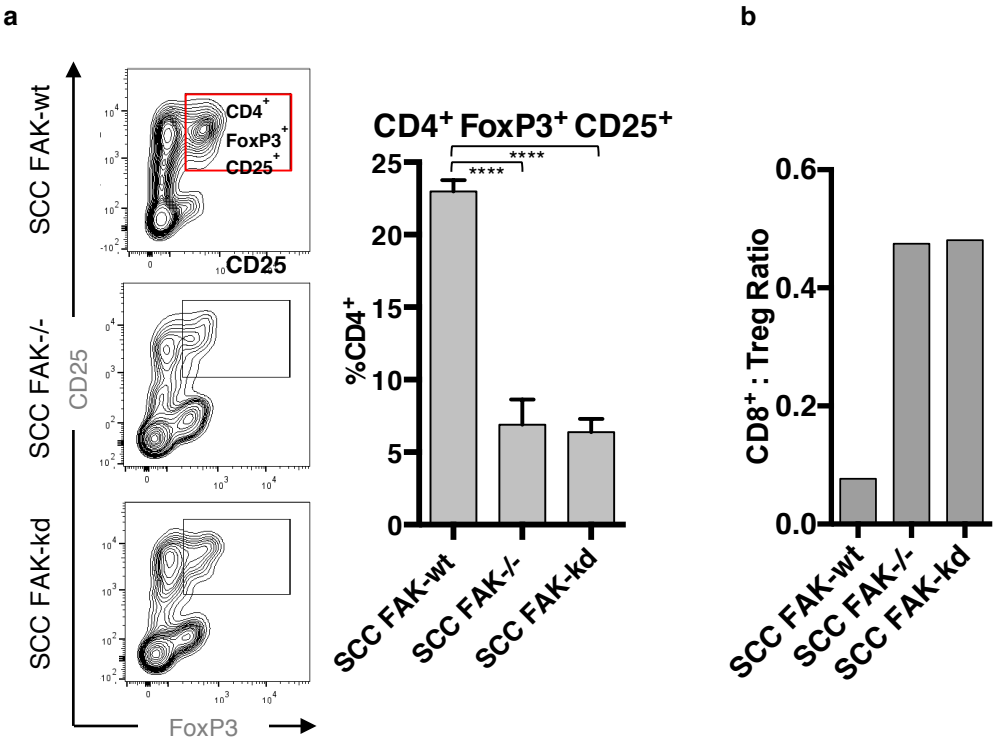

Figure 7.7 | Increase in the number of intra-tumoural Tregs in SCC FAK-wt tumours. 1 x 10^6 SCC FAK-wt, SCC FAK-/- or SCC FAK-kd cells were implanted into the flanks FVB/N mice by bilateral subcutaneous injection. Resulting tumours were removed from cohorts of mice (n = 3) 7 days post-implantation. Tumours were disaggregated and stained for FACS analysis with stain 4 (**Table 7.1**). FACS analysis was gated as described in **Figure 7.6**. **a** FACS plots of intra-tumoural Treg populations (*left panel*) and their respective quantification (*right panel*). **b** $CD8^+$ T-cell to Treg ratio calculated using mean values from **Figures 7.1** and **7.7**. The number of each cell population was determined and the statistical significance between each cell type was calculated by one-way Anova with Tukey's multiple comparisons. P-value = Not significant >0.05, * <0.05, ** <0.01, *** <0.001, **** <0.0001; *Bar height* = mean; *Error bars* = s.e.m

normally until day 7, where tumour growth stalled, leading to complete tumour regression by day 21 (**Figure 7.8**). Following cessation of antibody treatment 25 days post tumour-cell implantation, tumours did not reappear after 6 months of observation (data not shown).

Having established that SCC FAK-wt tumour growth required $CD25^+$ and $CD4^+$ cells, I concluded that Tregs were the cell population responsible for SCC FAK-wt tumour escape of immune-meditated tumour regression.

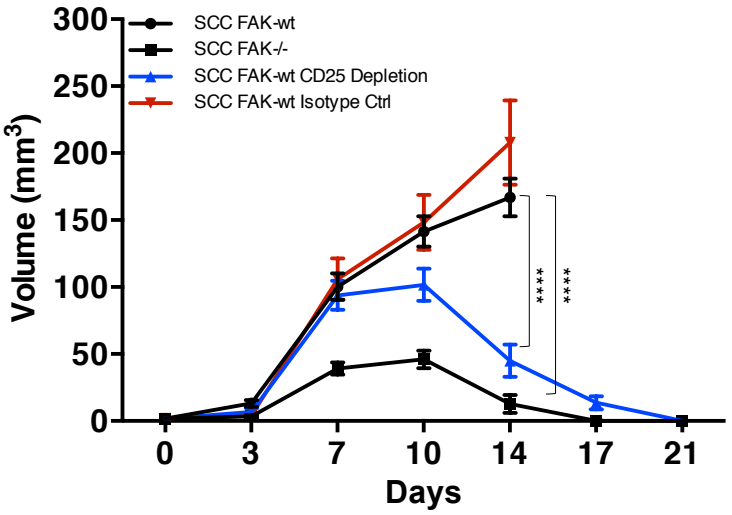

Figure 7.8 | SCC FAK-wt tumour clearance after antibody depletion of CD25$^+$ cells. SCC FAK-wt tumour growth in CD25 depleted FVB/N mice. FVB/N mice (n = 5) were treated with CD25$^+$ depleting antibody as per the dosage scheduled referred to in **Figure 5.7.** Control animals were treated with Isotype control antibody or were untreated. 1 x 10^6 SCC FAK-wt or SCC FAK-/- cells were implanted by bilateral subcutaneous injection into each flank. Tumour diameter was measured twice weekly and tumour volume was determined by $4/3\pi r^3$. Statistical significance was determined by matched, two-way Anova with Tukey's multiple comparisons. Data are represented as mean ± s.e.m. P-value = Not significant >0.05, * <0.05, ** <0.01, *** <0.001, **** <0.0001.

7.4 Conclusion

These data imply that antigen-primed CD8$^+$ T-cells infiltrate into all tumour types and therefore the lack of CD8$^+$ T-cell infiltration is not the underlying mechanism for continued growth of SCC FAK-wt tumours. Treg levels were observed to be elevated in SCC FAK-wt tumours when compared to SCC FAK-/- and FAK-kd tumours, and specific depletion of these cells using anti-CD25 antibodies led to complete regression of SCC FAK-wt tumours. Thus, increased Treg infiltration is required to protect SCC FAK-wt tumours from immune-mediated clearance. The ratio of CD8$^+$ T-cells to Tregs has been reported as a prognostic indicator of clinical outcome, with a low ratio linked to poor prognosis. Comparing the ratio of CD8$^+$ T-cells to Tregs in SCC FAK-wt, FAK-/- and FAK-kd tumours revealed a substantially lower ratio in SCC FAK-wt tumours, which in our model correlated with poor prognosis.

Therefore, one outcome of elevated FAK expression in tumours may be to alter the ratio of $CD8^+$ T-cells to Tregs in favour of tumour tolerance. Further work will be required to understand the broad relevance of these findings and to identify how FAK can influence Treg levels within tumours.

Levels of inflammatory and resident macrophages were unchanged across SCC FAK-wt, SCC FAK-/- and SCC FAK-kd tumours, but approx. 70% were M2 polarised in SCC FAK-wt and SCC FAK-kd tumours, and M1 polarised in SCC FAK-/-. While these changes in the polarity of macrophages were observed, they did not correlate with the regression phenotype and thus are unlikely to be the primary factor supporting continued growth of SCC FAK-wt tumours. However, these changes may be clinically relevant as M2 macrophages have been shown to be a pro-tumorigenic population indicative of poor clinical outcome, and may provide the tumour protection from chemotherapy and radiotherapy[43,57,82,85,92]. The difference between SCC FAK-/- tumours and SCC FAK-wt and SCC FAK-kd tumours can be attributed to the presence of FAK kinase-independent functionality, which is still retained in SCC FAK-kd cells. The kinase-independent roles of FAK have been shown to influence cell migration, adhesion, invasion, metastasis, growth and survival[244,247,249,264,339,367,368] (**Figure 3.2**), and do so through the scaffolding functions of the FAK FERM domain[244,274,284,321,369-373] (**Figure 3.1**). A number of these functions have been shown to be modulated by chemokines and cytokines. Therefore, it's possible to speculate that FAK FERM domain-mediated regulation of chemokines and cytokines may attribute to the differences observed between SCC FAK-/- and SCC FAK-kd tumours, and that the FERM domain regulates the expression of mediators of macrophage polarization.

The factors leading to the differential polarization of macrophages, and indeed MDSCs, are to date poorly characterised. However, some work has identified factors such as IFNγ and IL-4 to differentially stimulate M1 and M2 macrophage polarization respectively[361,374]. IFNγ and IL-4 are two of the main drivers of Th1 and Th2 immune responses respectively, and many of FAK kinase-independent functions lead to the upregulation of growth factors and chemokine and cytokine signalling[265,282,284]. This therefore raises the possibly that FAK kinase-independent

functions play a role in the modulation of these factors, which could have greater implications as to the inflammatory environment of a FAK-expressing tumour. Indeed, it may be possible that FAK-expression within tumours infer a Th2 inflammatory microenvironment, which in the absence or downregulation of Th1 mediating factors such as IFNγ could generate a more permissive environment for tumour development[375].

Although this hypothesis is intriguing, no significant differences were observed in the total numbers or the activation status of $CD8^+$ T-cells between SCC FAK-/- and SCC FAK-kd tumours (**Figure 7.1 b-d**). Thus, the more likely hypothesis is that FAK may regulate the expression other chemokines and cytokines that affect macrophage polarization without the major effects on Th2 immunity. IL-21 has been shown to be an inducer of M2 polarization through the activation of STAT-3 signalling in macrophages, but only moderately mediates Th2 induction[376]. The lack of an induced Th2 response by Il-21 is attributed to its effects in increasing the frequency of a subset of antigen-specific $CD8^+$ T-cells, which produce IL-2 in response to IL-21, and thus increase Th1 mediated immunity[377].

Although further work must be done to investigate the mechanisms by which the kinase-independent function of FAK may regulate macrophage polarization, few tools exist which are capable of inhibiting scaffolding functionality. To interrogate this phenotype further however, the disruption of FAK FERM domain interactions would be required, and this could be achieved using nanobodies. Nanobodies are short, single chain immunoglobulins found in camelids (such as llamas), which contain only heavy and light immunoglobulin variable domains[378]. The lack of the immunoglobulin constant domains (seen in most other mammalian immunoglobulins) generates antibodies which are small enough to perturb protein:protein interactions directly with high avidity and specificity[378]. Modified derivations of these antibodies have been used in the clinic in the form of bispecific t-cell engaging antibodies (BiTEs) targeting both CD3 and TAA (CD19) in B-cell lymphomas, and have been shown to have excellent pharmacodynamics properties, specificities and anti-cancer properties[379-383]. Although using these molecules as inhibitors of protein:protein interactions has yet to be trialled *in vivo* in either humans

or mice[384], they have been shown to have excellent inhibiting capacity *in vitro*[385-387] . Thus, it may be possible to disrupt FAK kinase-independent FERM interactions with nanobodies, and begin to interrogate the mechanisms by which the FAK FERM domain has the capacity to polarize macrophages. This may prove to be highly important in the long-term implications of FAK-based therapies.

Kinase-independent polarisation is also observed in both MDSC populations of SCC FAK-wt and SCC FAK-kd tumours, but it should be noted that the interpretation of the MDSC data is more difficult than for macrophages. Current definitions of immunosuppressive cell populations by FACS are not always specific. This is the case for MDSCs; M-MDSCs cannot be defined specifically at this point, and currently share the same markers are inflammatory monocytes ($CD45^+$ $CD11b^+$ $F4/80^-$ $Ly6C^{hi}$; **Table 7.1**). New methods, such as NanoString® aims to improve on this by combining both RNA sequencing and protein profiling into a single reaction, allowing immune cell populations to be more accurately identified by both the expression of proteins and RNA[388,389]. This technology increases the specificity of detecting immune populations by analysis of specific transcriptional and proteomic profiles consisting of many more markers than FACS, and therefor allows for a more accurate definition of immune populations. Although this is a significant advancement for immunoprofiling, this technology still relies on current identifiable markers, and for immune populations such as MDSC and DCs that have no unique identifiable markers, identification of these population will always be demanding until more work has been done on characterising them.

Having excluded both M2 macrophages and MDSCs as the immunosuppressive populations responsible for SCC FAK-wt tumour survival, work turned to identification and characterisation of the Treg population ($CD4^+$ $CD25^+$ $FoxP3^+$). It has been shown however that $CD4^+$ $FoxP3^+$ cells also have immunosuppressive capabilities, and are often referred to as Tregs in the literature. Although these cell can be immunosuppressive, due to the lack of CD25 they may not have the same suppressive capacity as double positive $FoxP3^+$ $CD25^+$ cells. Because of this, Tregs are defined only as $CD4^+$ $FoxP3^+$ $CD25^+$ cells within this thesis, and are stained by a commercially available kit that allows for the intracellular staining of FoxP3. This

does raise question as to whether the use of CD25 depleting antibodies (**Figure 7.8**) is an effective method to depleting Tregs. Indeed, $CD4^+$ $FoxP3^+$ cells will not be affected by this treatment, leaving the potential for residual immunosuppressive cells to be retained after CD25 depletion[390]. CD25 has also been shown to be upregulated on activated $CD8^+$ T-cells, and thus depletion of Tregs in this manner may also reduce cytotoxic activity[391]. Although both of these possibilities appear unlikely, as residual immunosuppression or reduction in cytotoxic activity would retain tumour tolerance after CD25 treatment, other possibilities would in fact lead to tumour rejection. For example, $CD25^+$ $CD8^+$ suppressor cells ($CD8^+$ T_{Sups}) would also be depleted by CD25 treatment; $CD8^+$ T_{sups} are a functionally defined, immunosuppressive population, and therefore CD25 depletion could cause tumour rejection if targeting this populations[392]. Many of the issues surrounding CD25 antibody-meditated depletion of Tregs would be resolved, albeit only transiently by using *FoxP3*^{DTR} knockin mouse, whereby Treg ablation follows treatment with diphtheria toxin (DT)[393]. Although these points must be considered when evaluating the data presented in this chapter, $CD8^+$ T_{sups} are typically found at very low abundance in tumours, and so the hypothesis that the rejection of SCC FAK-wt tumours after anti-CD25 is due to the lost of Tregs appears most likely.

The work presented in this chapter focuses on SCC FAK-wt tumours in order to better understand the immunomodulatory roles of FAK in SCC FAK-wt tumour survival. This work identifies the essential role of Tregs in SCC FAK-wt tumour tolerance, and correlates the absence of Tregs with SCC FAK-/- and SCC FAK-kd tumour rejection. However, to further substantiate this hypothesis, experimental evidence is required to show a stronger functional link between the lack of Tregs and the clearance of SCC FAK-/- and SCC FAK-kd tumours. This could be achieved by increasing the number of Tregs within SCC FAK-/- and SCC FAK-kd tumours by adoptive transfer of Tregs from SCC FAK-wt tumours. Two caveats with this technique are the requirement for *in vitro* expansion, which can prove difficult with Tregs and isolating a pure Treg population. As discussed above, the transcription factor FoxP3 is established as the best marker for Tregs, as CD25 expression is not restricted to Tregs alone. However, due to the permeabilization and fixation required for intracellular FoxP3 staining, purification by CD25 expression must be used to

achieve a final viable cell population. This raises difficulties around attaining a pure Treg population. Other methods of increasing Tregs include anti-CD45RB treatment, which increases endogenous splenic Tregs *in vivo*. Although the mechanism of action of anti-CD45RB treatment has been shown to act due to the specific enhancement of tTreg proliferation in response to antigen[394], this work is unsubstantiated and has yet to be tried in cancer setting, but offers an opportunity to increase Tregs *in vivo* without the requirement for expansion or purification.

8 FAK regulates chemokines and cytokines that increase the levels of intra-tumoural Tregs.

8.1 Introduction

Having established that intra-tumoural Tregs were increased in SCC FAK-wt tumours, and that they were required to avoid SCC FAK-wt tumour regression, I set out to investigate the molecular mechanisms by which FAK could regulate intra-tumoural Treg levels. Tumour cells have been shown to upregulate a number of factors that act to increase the differentiation of Tregs from effector $CD4^+$ T-cells (TGFβ and IL-10; **Figure 2.6**) or to increase the recruitment of tTregs and their retention within the microenvironment (CCL5; **Figure 2.6**). Thus, working with Dr Adam Bryon and Dr Alan Serrels (Frame Group) we undertook a screening approach in order to determine transcriptomic changes between SCC FAK-wt and SCC FAK-/- cells, focussing on differentially expressed cytokines and chemokines, and then concentrated our experiments on selected chemokines and cytokines that are known to regulate intra-tumoural Tregs.

8.2 Aims

- To determine whether FAK regulates the expression of factors that could influence Treg levels in tumours
- If so, to identify the factors involved in driving elevated Treg levels in SCC FAK-wt tumours

8.3 Results

8.3.1 FAK regulates the transcription of chemokines and cytokines involved in the peripheral induction, recruitment and retention of Tregs

To further investigate how FAK expression was linked to elevated intra-tumoural Treg levels, we used global transcriptional profiling of SCC cells. Using Affymetrix GeneChip Mouse Genome 430 2.0 microarrays that cover over 39000 transcripts, we compared the transcriptome of SCC FAK-wt cells *in vitro* to that of SCC FAK-/- cells *in vitro* (**Figure 8.1**). Analysis of the resulting data identified a set of 498 upregulated genes, and 598 downregulated genes in the SCC FAK-wt cells compared to SCC FAK-/- (**Figure 8.1a**). Gene ontology analysis on the upregulated gene set indicated that FAK expression was significantly associated with a number of biological processes including cell migration, secretion, wounding, and ovulation, and that the most overrepresented gene family within this gene set was chemokine ligands (**Figure 8.1b**).

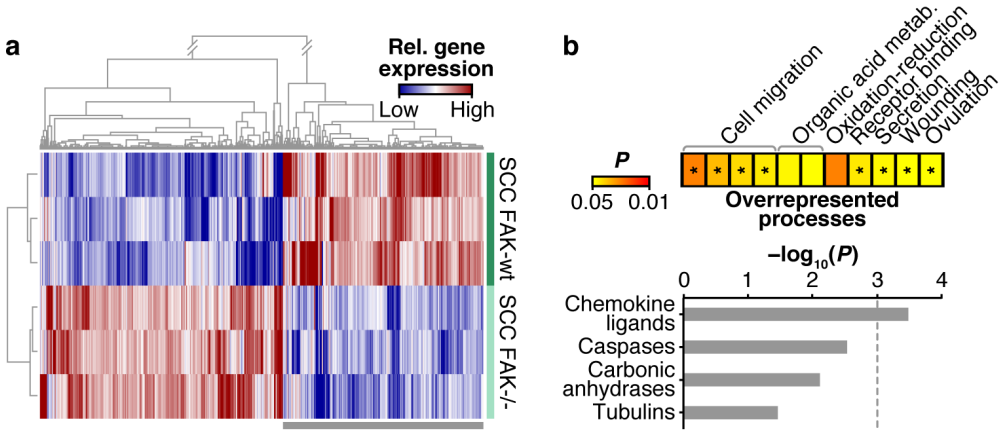

Figure 8.1 | Transcriptional profiling of SCC FAK-wt and SCC FAK-/- cells reveled a number of upregulated chemokine ligands in SCC FAK-wt tumours. a Heat map of transcriptional changes between SCC FAK-wt and SCC FAK-/- cells. **b** Functional enrichment analysis of genes upregulated in SCC FAK-wt cells (grey bar in **a**). Overrepresented biological processes are displayed as a heat map (log_{10}-transformed color scale) (*top panel*); asterisks indicate presence of cytokine-related genes. Overrepresented gene families are displayed as a bar chart (*bottom panel*); dashed line indicates $P = 0.001$. Displayed terms satisfy $P < 0.05$ (Benjamini–Hochberg-corrected hypergeometric tests). *Figure courtesy of Dr Adam Byron.*

To further establish which chemokines and cytokines were regulated by FAK, and to confirm the results from the microarray analysis, we used a focussed chemokine / cytokine qRT-PCR array to compare transcript expression between SCC FAK-wt and SCC FAK-/- cells (**Figure 8.2a**). We identified a subset of chemokines and cytokines that were upregulated more than two-fold in the SCC FAK-wt cells, of which a number have been reported to play a role in Treg induction, expansion[395] (*TGFβ2*; **Figure 8.2a** *red arrow*) and recruitment[396] (*CCL5, CxCL10, CCL1 and*

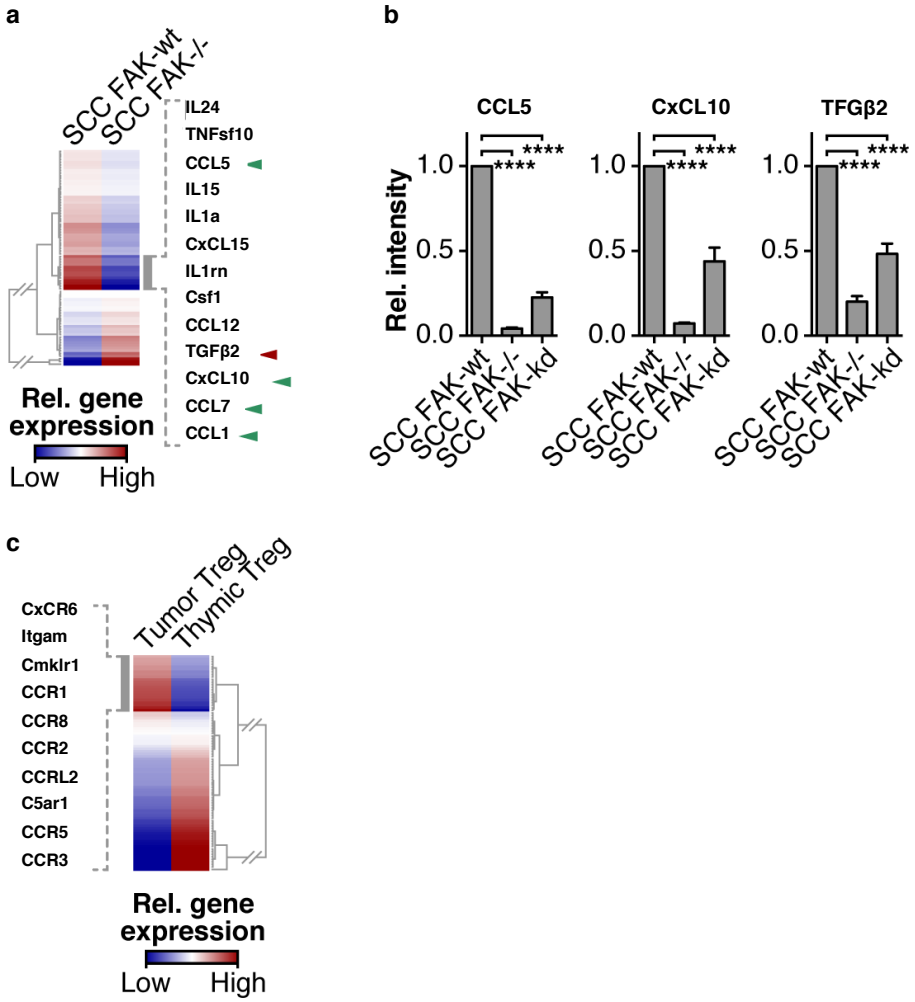

Figure 8.2 | FAK regulates transcription of chemokines and cytokines implicated in Treg recruitment and expansion. a qRT-PCR array analysis of cytokine and chemokine expression in SCC FAK-wt and SCC FAK-/- cells. Cytokine and chemokine gene names within cluster upregulated in SCC FAK-wt cells are listed. *Green arrows* indicate reported roles in Treg recruitment; *red arrow* indicates reported role in peripheral Treg induction. **b** qRT-PCR analysis of selected cytokine and chemokine gene expression in SCC cells. **c** qRT-PCR array analysis of chemokine receptor expression in tumor- and thymus-derived Tregs. Grey bar indicates cluster of genes upregulated in tumor-derived Tregs; receptor gene names are listed. ****$P < 0.0001$ (Sidak-corrected one-way ANOVA). Data are represented as mean ± s.e.m. *Figures courtesy of Dr Adam Byron and Dr Alan Serrels.*

CCL7; **Figure 8.2a** *green arrows*).

Having identified CCL5, CxCL10 and TGFβ as being upregulated in SCC FAK-wt cells compared to SCC FAK-/- cells, we next wanted to determine the relative quantity of these three chemokines and cytokines in SCC FAK-kd cells. qRT-PCR analysis of SCC FAK-wt, SCC FAK-/- and SCC FAK-kd cells showed that *CCL5* was down-regulated 10-fold in SCC FAK-/- cells and 4-fold in SCC FAK-kd cells compared to SCC FAK-wt (p value = <0.0001; **Figure 8.2b**). *CxCL10* was down-regulated 10-fold in SCC FAK-/- cells and approximately 2-fold in SCC FAK-kd cells compared to SCC FAK-wt (p value = <0.0001) and *TGFβ2* was down-regulated 5-fold in SCC FAK-/- and 2-fold in SCC FAK-kd cells compared to SCC FAK-wt (p value = <0.0001; **Figure 8.2b**). We conclude that the FAK kinase activity is required for the transcriptional upregulation of *CCL5, CxCL10* and *TGFβ2*. FAK has been shown previously to regulate the transcriptional levels TGFβ in other cell models[397,398], validating our findings. Further, it is possible that the differences observed between SCC FAK-/- and SCC FAK-kd cells were due to the fact that SCC FAK-kd cells are 'kinase deficient' not kinase-dead, and therefore retain some residual kinase activity.

To compliment this analysis, and to identify whether there was a relationship between FAK-dependent chemokine expression and Treg chemokine receptor profile, we isolated both intra-tumoural Tregs and thymic derived Tregs and compared their chemokine receptor expression using qRT-PCR (**Figure 8.2c**). Analysis of this data identified a subset of chemokine receptors that were greater than two-fold upregulated on intra-tumoural Tregs when compared to thymic derived Tregs, indicating a switch from lymphoid homing receptors, including CCR7[399] and CxCR4[400], towards expression of memory / effector-type chemokine receptors involved in recruitment to non-lymphoid tissues and sites of inflammation, including CCR2, CCR5, CCR8, and CxCR6[401].

Network analysis identified a FAK-driven paracrine-signaling axis between cancer cells and intra-tumoural Tregs based on chemokine ligand-receptor interactions. Indeed, 5 of the chemokine receptors upregulated on intra-tumoural Tregs were the

cognate receptors for the chemokine ligands upregulated in response to FAK expression in SCC cells (**Figure 8.3**).

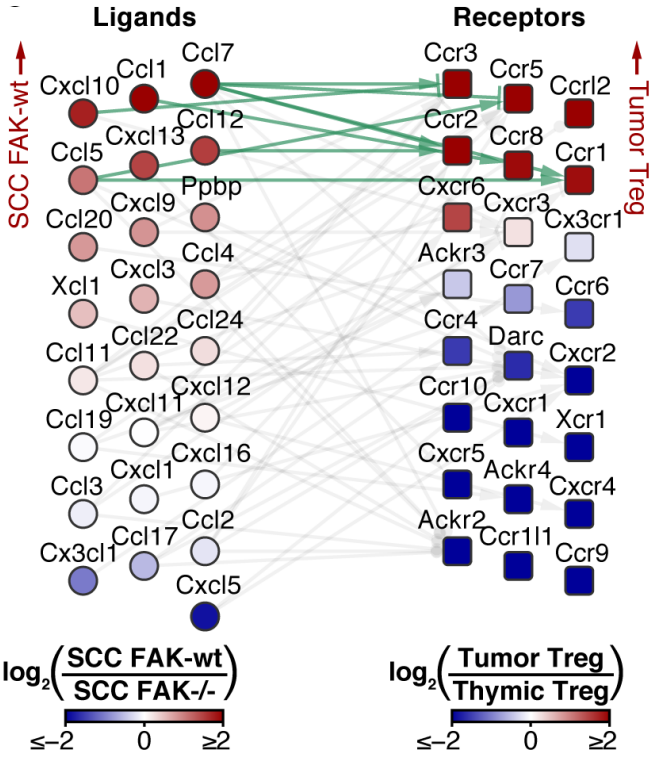

Figure 8.3 | Upregulation of chemokine ligands in SCC FAK-wt cells correlate with the upregulation of cognate receptors on SCC FAK-wt intra-tumoural Tregs. Interaction network analysis of chemokine ligand gene expression detected in SCC cells (*circles; left*) and corresponding receptor gene expression detected in intra-tumoural Tregs (*squares; right*). Genes are ordered vertically by fold change. Light gray lines connect receptor–ligand pairs; green lines indicate pairs upregulated at least two-fold in SCC FAK-wt cells and tumor-derived Tregs. *Figure courtesy of Dr Adam Byron.*

8.3.2 SCC FAK-wt tumour survival and growth requires TGFβ2 and CCL5, associated with an increase in intra-tumoural Tregs.

Following identification of a subset of chemokine and cytokine ligands upregulated in response to FAK expression, I sought to prioritise a small number for further testing. TGFβ2 and CCL5 have been previously reported to be important for Treg induction and recruitment to non-lymphoid tissues respectively[137,138,243,402]. Indeed, disruption of the CCL5 / CCR5 axis has been reported to result in reduced intra-tumoural Tregs and slowed tumour growth implying that FAK-dependent regulation of this paracrine signaling axis may be important[137]. I therefore used shRNA to knockdown TGFβ2 and CCL5 in SCC FAK-wt cells, and tested the impact of this on tumour growth and intra-tumoural Treg levels.

TGFβ2 knockdown was validated using qRT-PCR, and a single clone was chosen with reduced expression levels of TGFβ2 (**Figure 8.4a**). 1 x 10^6 TGFβ2 shRNA expressing SCC FAK-wt cells (SCC FAK-wt shRNA-TGFβ2) were implanted in to the flanks of FVB/N mice (n=3) by bilateral subcutaneous injection, along side SCC FAK-wt pLKO vector only controls and SCC FAK-/- cells for comparison. Tumour growth was measured twice weekly. SCC FAK-wt pLKO and SCC FAK-/- tumours grew as expected (**Figure 8.4b**). SCC FAK-wt shRNA-TGFβ tumour growth appeared to split into two groups (**Figure 8.4b**). Tumours which were observed to have initial increase in tumour growth compared to the SCC FAK-wt pLKO control, subsequently ulcerated prematurely (**Figure 8.4b** *blue dash*). Tumours that did not have this initially increase in growth did not ulcerate, and these tumours were cleared after 27 days (**Figure 8.4b** *red dash*). TGFβ signalling has been shown to have pleiotropic effects on tumour growth[138,243,403,404] and this could account for high variability in tumour growth observed. I concluded that, as a subset of SCC FAK-wt TGFβ2 shRNA expressing tumours were cleared, which was not seen in the SCC FAK-wt pLKO controls, that TGFβ2 was required for the survival of SCC FAK-wt tumours.

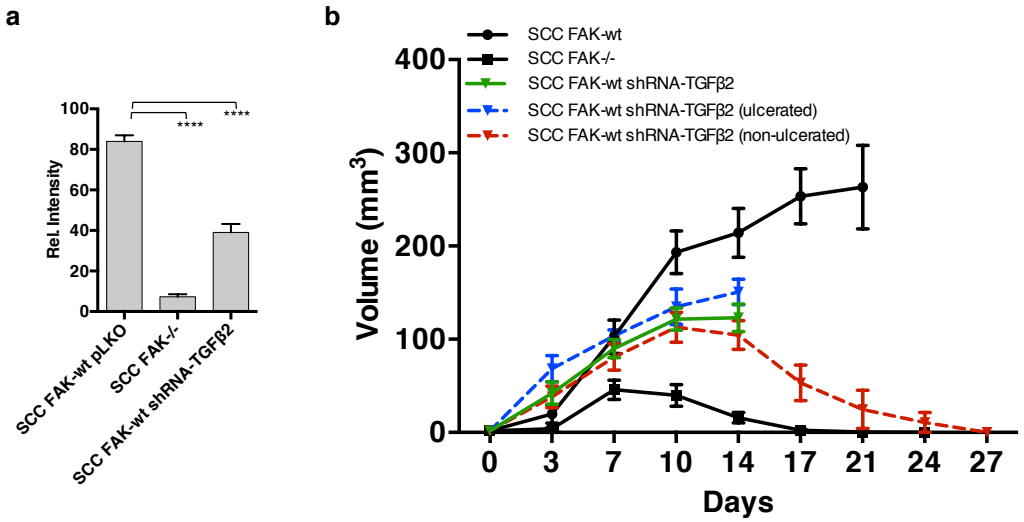

Figure 8.4 | FAK regulates transcription of TGFβ2 that is required for Treg expansion and tumour growth. a qRT-PCR analysis of TGFβ2 gene expression knockdown in SCC cells. **b** SCC FAK-wt shRNA-TGFβ2 tumour growth in FVB/N mice. *Green solid line* indicates the mean growth of all SCC FAK-wt shRNA-TGFβ2 tumours until signs of ulceration were observed. Tumour growth was determined by the implantation of 1 x 10^6 SCC FAK-wt or SCC FAK-/- cells in to both flanks of FVB/N mice by bilateral subcutaneous injection. Tumour diameter was measured twice weekly and tumour volume was determined by $4/3\pi r^3$. Statistical significance was calculated by one-way Anova with Tukey's multiple comparisons. *Bar height* = mean, *Error bars* = s.e.m. P-value = Not significant >0.05, * <0.05, ** <0.01, *** <0.001, **** <0.0001.

SCC FAK-wt shRNA-CCL5 cells were generated from two independent shRNAs and knockdown validated using qRT-PCR (**Figure 8.5a**). Clones were chosen with reduced expression levels similar to that of SCC FAK-/- cells (SCC FAK-wt shRNA-CCL5 1 and 2). 1 x 10^6 of both CCL5 shRNA-expressing cells (SCC FAK-wt shRNA-CCL5 1 and 2) were implanted in to the flanks of FVB/N mice (n=3) by bilateral subcutaneous injection, alongside SCC FAK-wt pLKO vector only controls and SCC FAK-/- cells for comparison and tumour growth was measured twice weekly. SCC FAK-wt pLKO and SCC FAK-/- tumours grew as expected (**Figure 8.5b**). Both SCC FAK-wt shRNA-CCL5 1 and 2 tumours grew in a manner akin to SCC FAK-/- cells (**Figure 8.5b**); tumours grew until day 7, at which point tumour growth stalled, until complete tumour regression a day 27 (SCC FAK-wt shRNA-CCL5 1) and day 23 (SCC FAK-wt shRNA-CCL5 2).

These data show that SCC FAK-wt tumour growth is dependant on TGFβ2 and CCL5 expression. Therefore I next wanted to determine whether knockdown of either TGFβ2 or CCL5 was associated with a loss in intra-tumoural Tregs by FACS

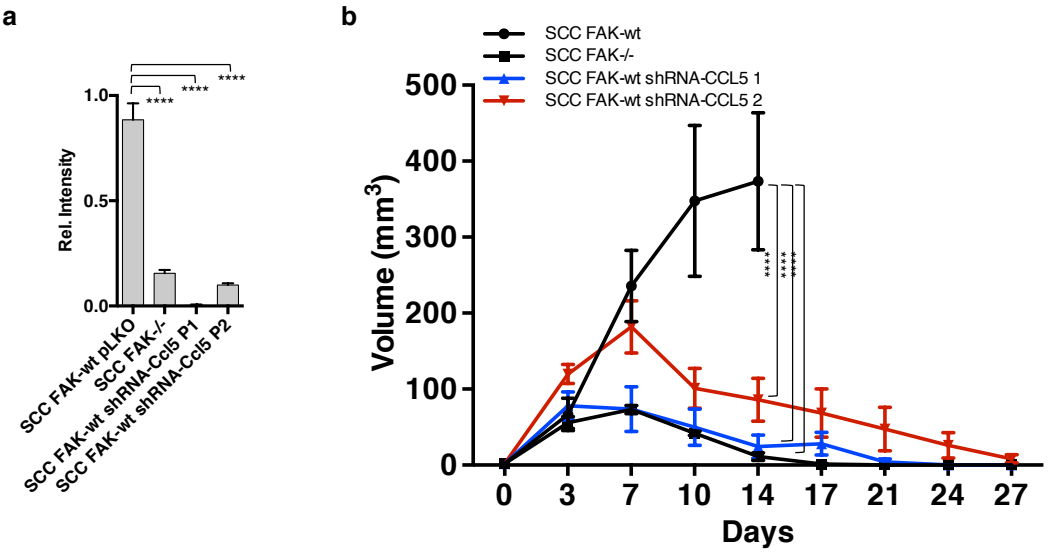

Figure 8.5 | FAK regulates transcription of CCL5 required for Treg recruitment, retention and tumour growth. a qRT-PCR analysis of CCL5 gene expression knockdown in SCC cells. **b** SCC FAK-wt shRNA-CCL5 tumour growth in FVB/N mice. Tumour growth was determined by the implantation of 1 x 10^6 SCC FAK-wt or SCC FAK-/- cells in to both flanks of FVB/N mice by subcutaneous injection. Tumour diameter was measured twice weekly and tumour volume was determined by $4/3\pi r^{3.}$ Statistical significance was calculated by one-way Anova with Tukey's multiple comparisons. *Bar height* = mean, *Error bars* = s.e.m. P-value = Not significant >0.05, * <0.05, ** <0.01, *** <0.001, **** <0.0001

.

analysis. SCC FAK-wt shRNA TGFβ2 and SCC FAK-wt CCL5 1 cells, and SCC FAK-wt and SCC FAK-/- controls, were implanted in to both flanks of FVB/N mice by bilateral subcutaneous injection. Tumours were disaggregated and stained with Stain 4 (**Table 7.1**) Samples were then analysed by FACS as described in **Figure 7.6**.

Comparison between SCC FAK-wt pLKO, SCC FAK-/- and SCC FAK-wt shRNA-CCL5 tumours showed a statically significant decrease between the SCC FAK-/- and SCC FAK-wt shRNA-CCL5, and the SCC FAK-wt tumour (p value = <0.01 and <0.05 respectively; **Figure 8.6a**).

FACS analysis of TGFβ2 shRNA-expressing SCC FAK-wt cells showed a significant decrease in Tregs between SCC FAK-wt shRNA-TGFβ2 and SCC FAK-/- tumours, compared to SCC FAK-wt tumours (p value = <0.0001; **Figure 8.6b**). From this data I concluded that TGFβ2 and CCL5 were required for SCC FAK-wt tumour survival and this was associated with an increase in intra-tumoural Tregs.

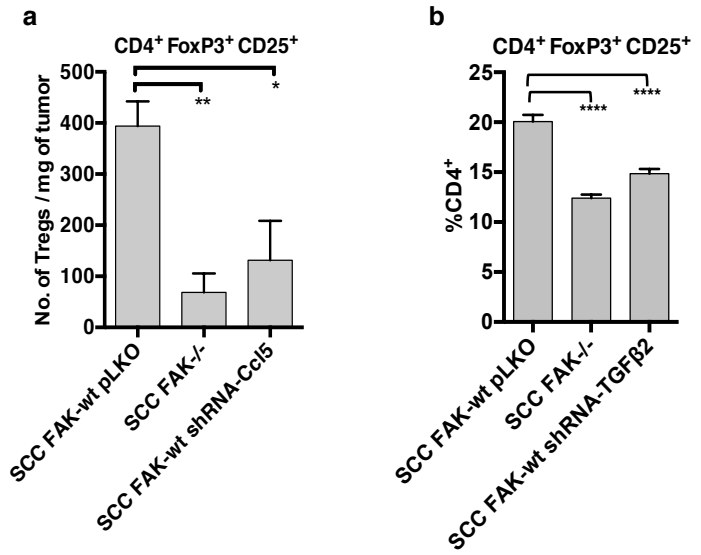

Figure 8.6 | TGFβ2 and CCL5 are required for Treg expansion and tumour growth in SCC FAK-wt tumours. a FACS analysis of the absolute number of Tregs / mg of tumour in SCC FAK-wt CCL5-shRNA tumours. **b** FACS analysis of intra-tumoural SCC FAK-wt TGFβ2-shRNA Tregs and a percentage of $CD4^+$ cell. Tumours were taken 7 days post implantation, disaggregated and stained for FACS with Stain 4 (**Table 7.1**). FACS analysis was gated as described in **Figure 7.6**. Statistical significance was calculated by one-way Anova with Tukey's multiple comparisons. *Bar height* = mean, *Error bars* = s.e.m. P-value = Not significant >0.05, * <0.05, ** <0.01, *** <0.001, **** <0.0001.
.

Conclusion

We have identified a novel paracrine-signalling axis between FAK expressing SCC tumour cells and intra-tumoural Tregs. Chemokines and cytokines regulated by FAK, including TGFβ2 and CCL5, are associated with an increase in intra-tumoural Tregs and sustained SCC FAK-wt tumour growth. Further, I show that transcription of TGFβ2 and CCL5 is dependent on FAK kinase activity, suggesting that they may be modulated by FAK kinase inhibitors to result in a similar outcome. Clinically these observations are important, as they suggest that FAK kinase inhibition may alter the chemokine and cytokine profile being secreted by tumour cells, with a resultant impact on the composition of the tumour immune infiltrate. Further work will focus on whether these phenotypes could be replicated by treatment of a FAK kinase inhibitor.

The regulation of chemokines and cytokines by FAK kinase activity was identified using Affymetrix GeneChip Mouse Genome 430 2.0 microarrays and targeted

chemokine and cytokine qRT-PCR arrays. Steady-state transcriptomic approaches such as these give excellent coverage of transcripts (30000 targets in the GeneChip Mouse genome arrays) and include some alternative probes for select targets, thus allowing for the identification of some non-specific amplification. However, steady-state transcriptomic approaches suffer from a static view of transcription, and thus give no detail into transcriptional kinetics and downstream processing (i.e. the rate of transcription vs. the rate of transcript turnover, the rate of translation, and whether the rates of transcription and translation change over time). Other genetic tools, such as gene reporter constructs, would allow for more dynamic analysis of the transcription of a select number of chemokines and cytokines, and could be utilized to determine whether the rate of transcription of these factors modulate over time.

Further proteomic approaches are also required to determine whether the levels of functional chemokines and cytokines are produced in a FAK kinase-dependent manner. This offers a challenge as the secretion of chemokines and cytokines by tumour cells in culture can often be minimal, and thus can be difficult to detect above the high levels of background found when culturing cells in FBS. Our SCC model strictly requires FBS to be maintained in culture for periods longer than 24 hours, making analysis into chemokine and cytokine secretion difficult. Determination of chemokine and cytokine levels can be achieved however following the treatment of cultured cells with Ionomycin, which activates chemokine and cytokine production, and Brefeldin A, which blocks chemokine and cytokine secretion thus causing their intracellular retention. Treatment with these compounds allow for the quantification of chemokine and cytokine proteins without the inherent high levels of background following secretion into FBS containing media.

This transcriptomic approach however, identified a subset of genes upregulated in SCC FAK-wt cells, known to be involved in Treg biology, including TGFβ2 and CCL5 (**2.1.2.2** and **2.1.3.2**). Although SCC FAK-kd cells were omitted from the initial transcriptomic data set, qRT-PCR data supports the array results and identifies the dependence of FAK kinase activity in the upregulation of TGFβ2 and CCL5. SCC FAK-kd cells display an intermediate phenotype in this regard, potentially due to the small amount of residual FAK kinase activity seen in these kinase deficient

cells in 2D culture conditions, but which is absent in cells grown in 3D culture conditions and most importantly, is insufficient to induce SCC FAK-kd tumour tolerance *in vivo* (see [276]). Although a true kinase dead FAK mutant or *in vitro* 3D culture conditions would help in part to answer this question, the immune-mediated clearance of SCC FAK-kd cells highlights the necessary requirement for full FAK-kinase activity.

Subsequent stable RNAi knockdown of CCL5 and TGFβ2 shows that both these factors are required for FAK-expressing tumour tolerance compared to vector-only transfected SCC FAK-wt pLKO cells. SCC FAK-wt pLKO cells are transfected with the vector-backbone (pLKO) in which both CCL5 and TGFβ2 shRNAs are expressed. These controls were used in lieu of the more commonly used scrambled RNAi controls, as off-target scrambled RNAi mediated depletion of other chemokines and cytokines were observed after the transfection of scrambled RNAi control (data not shown). A vector-only control is effectively a sham-transfection which allows you to determine whether changes observed in experimental parameters, in this case tumour tolerance, are due to the exposure of cells to the transfection agent, retrovirus or other aspects of the transfection protocol (**4.1.15** and **4.2.11**) without any RNAi-mediated effects. A scrambled control also validates these effects, but also determines the probability that any changes in experimental parameters are due to the RNAi-mediated knockdown of a specific target, and not due to off-target depletion by non-targeting RNAi. Although the vector-only controls did not exhibit any observed changes in phenotype, they are not sufficient in determining the specificity of either the CCL5 or TGFβ2 shRNA for their respective targets. The induction of tumour clearance after the RNAi mediated-knockdown of either CCL5 or TGFβ2 could be due to off-target depletion of other non-specific targets. A scrambled control would, in part, help to clarify this. Although the use of multiple shRNAs for both CCL5 and TGFβ2 knockdown reduces the possibility SCC FAK-wt tumour clearance was mediated by off-target effects, it should still be taken into consideration that loss of tumour tolerance could be due to non-target effects of CCL5 or TGFβ2 shRNAs, and a different scrambled control should used used, one which does not effect other chemokines and cytokines to clarify this further.

Knockdown of TGFβ2 resulted in a split phenotype, with some tumours undergoing premature ulceration and others continuing to complete regression. The pleiotropic effects of TGFβ on tumour growth are well characterised. TGFβ signalling has cytostatic effects on epithelial, endothelial and immune cells, specifically T cells, and is critically important in the maintenance of tissue homeostasis and the prevention of hyperproliferative disorders such as cancer[405,406]. TGFβ acts to induce the expression of cyclin-dependant kinase inhibitors *CDKN2B*[407], *CDKN1A*[408] and p27/Kip1[409], resulting in the arrest of G1 to S phase transition[410], and also by the repression of the proliferation-inducing transcription factor c-Myc[411]. The loss of controlled proliferation by TGFβ has been observed in a number of different human cancers due to mutations in various components of the TGFβ signalling pathway. Loss of function or truncating mutations in *Smad2* and *Smad4* as well as *TGFβRI* and *TGFβRII* have been detected in colorectal, pancreatic, gastric and prostate cancers[406,412-419]. Futhermore, TGFβ is well recognized to enhance the proliferation of CAFs, mediated indirectly by the secretion of TGFβ-induced connective tissue growth factor (CTGF), which stimulates fibroblast proliferation and ECM generation[406,420]. This increase in ECM generation, specifically the deposition of collagen I and II fibrils, promotes cellular adhesions, and thus increase mechanical forces within the tumour, enhancing the mechanosensory conversion of fibroblasts to differentiated myofibroblasts[421,422]. Therefore inhibiting the cytostatic functions of TGFβ by RNAi may act a pro-tumorigenic and enhance the proliferation of both tumour cells and pro-tumorigenic stromal populations. To counter these pro-tumorigenic functions, and as stated previously (**2.2.1.2** and **2.2.1.3**) TGFβ acts to suppress of $CD8^+$ T cell proliferation and acts to differentiae $CD4^+$ T cells into immunosuppressive Tregs. It is therefore not unsurprising that the RNAi-mediated knockdown of TGFβ2 results in a split phenotype. However, considering that a reduction in Tregs was observed after TGFβ2 knockdown, and that neither SCC FAK-wt pLKO or SCC FAK-wt tumours are seen to regress, I concluded that TGFβ2 was in fact crucial to the survival of SCC FAK-wt cell, despite the pleotropic phenotype observed.

9 FAK kinase inhibitor VS-4718 shows preclinical potential as an immunotherapy.

9.1 Introduction

Small molecule FAK kinase inhibitors are currently being tested in a number of clinical trails, and it will be imperative to identify their potential utility and prioritise combinations for further testing. FAK is upregulated in a number of cancers including breast[423,424], pancreatic[425], colorectal[426], melanoma[427] and squamous cell carcinoma[264] where FAK inhibition has been shown to prevent cell motility, invasion, cancer progression and survival[264]. I wanted to investigate whether treatment with FAK kinase inhibitor VS-4718, which is currently in clinical development, recapitulated our previous results that highlighted the immunomodulatory effects of FAK.

9.2 Aims

- To determine how treatment with a FAK inhibitor compares with our genetic model
- To investigate the response to FAK inhibition in multiple syngeneic cancer models
- To assess the relationship between PD-L1/2 expression and response to FAK inhibitor monotherapy

9.3 Results

9.3.1 FAK kinase inhibitor VS-4718 induced SCC FAK-wt tumour regression associated with a reduction in intra-tumoural Tregs.

To complement our data establishing a kinase-defective mutation in FAK (SCC FAK-kd) driving immune mediated tumour clearance, studies were preformed with FAK inhibitor VS-4718, which is currently in clinical development (**Figure 9.1**).

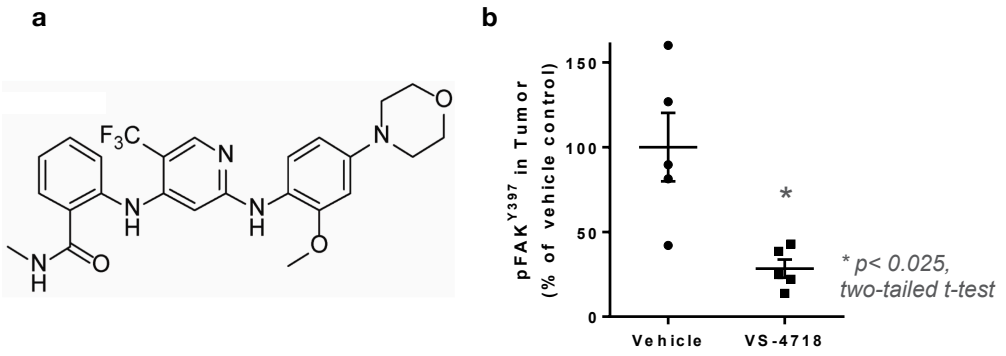

Figure 9.1 Analysis of FAK pY397 phosphorylation in tumors following treatment with VS-4718. a Structure of VS-4718. Figure taken from *Merlin Deficiency Predicts FAK Inhibitor Sensitivity: A Synthetic Lethal Relationship.* Shapiro *et al.* Sci Transl Med, 2014. **b** Phosphorylation of FAK on Y397 was measured in protein lysates isolated from tumors following treatment with VS-4718 using ELISA. Tumors were removed within 30 minutes of treatment. N = 5. *Figure courtesy of Jen Ring, Verastem*

FVB/N mice (n=5) were treated with 75mg/kg VS-4718 for 24 hours prior to bilateral subcutaneous injection of 1 x 10^6 SCC FAK-wt and SCC FAK-/- cells in both flanks, and twice daily thereafter. VS-4718 treated SCC FAK-wt and SCC FAK-/- tumours grew in manor akin to the SCC FAK-/- vehicle treated control (**Figure 9.2**); a significant delay in tumour growth was seen until day 10 (compared to SCC FAK-wt vehicle treated control; p value = <0.0001) where growth stalled, resulting in tumour clearance by day 24. Moreover, following cessation of VS-4718 treatment, no tumour regrowth was observed (data not shown). Although SCC FAK-/- tumour growth and subsequent clearance was largely unaffected by VS-4718 treatment, implying that anti-tumour effects of VS-4718 treatment were due to FAK inhibition in tumour cells, a growth delay was observed between both drug treated

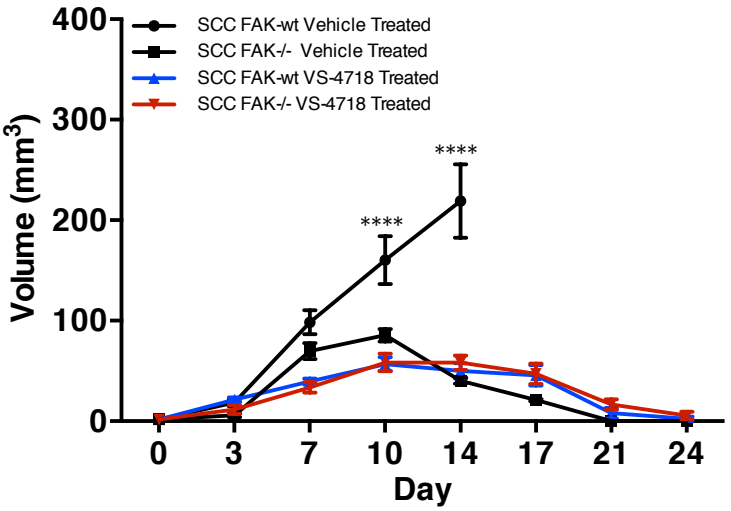

Figure 9.2 | The FAK kinase inhibitor VS-4718 leads clearance of SCC FAK-wt tumours. SCC FAK-wt and SCC FAK-/- tumour growth in animals treated with either vehicle or with 75 mg/kg VS-4718, BID by oral gavage. Treatment started 24 hours pre-tumour cell inoculation and continued for the duration of the experiment. 1 x 10^6 SCC FAK-wt or SCC FAK-/- cells were implanted by bilateral subcutaneous injection into each flank of FVB/N mice. Tumour diameter was measured twice weekly and tumour volume was calculated using the formula $4/3\pi r^3$. Statistical significance determined by matched, two-way Anova with Tukey's multiple comparisons Data are represented as mean ± s.e.m. P-value = Not significant >0.05, * <0.05, ** <0.01, *** <0.001, **** <0.0001.

tumours and the SCC FAK-/- vehicle controls at day 7 (**Figure 9.2**). Although this did not reach significance, it may be a consequence of targeting FAK in the stromal compartments prior to an established anti-tumour immune response, or alternatively it may represent a small off-target effect of VS-4718.

To determine whether the mechanism of action of VS-4718 complimented our previous results, FVB/N mice were treated with 75mg/kg VS-4718 for 24 hours prior to bilateral subcutaneous injection of 1 x 10^6 SCC FAK-wt and SCC FAK-/- cells in both flanks, and twice daily thereafter. Tumours were removed, disaggregated and stained with Stain 2 (**Table 6.3**) and Stain 4 (**Table 7.1**). Samples were analysed as described in **Figure 6.5** and **Figure 7.1** respectively. Regression of VS-4718 treated tumours was not attributed to decreased cell viability, shown by Cell viability marker eFluor® 506 conjugated fixable viability dye (**Figure 9.3**). In both SCC FAK-wt tumours, treatment with VS-4718 increased cell viability, but this increase did not reach significance (p value = >0.05; **Figure 9.3**).

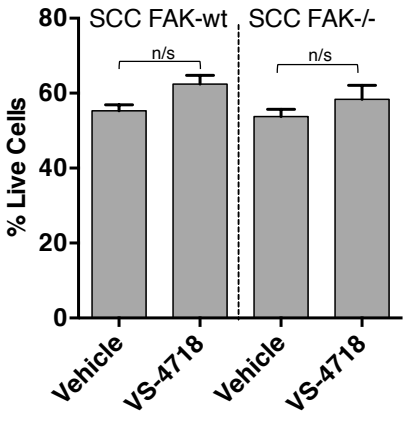

Figure 9.3 | FAK kinase inhibitor VS-4718 did not effect tumour viability in early SCC FAK-wt and SCC FAK-/- tumours. FVB/N mice treated with either vehicle or with 75 mg/kg VS-4718, B.I.D by oral gavage. Treatment started 24 hours before cell inoculation and continued for the duration of the experiment. 1.0 x 10^6 SCC FAK-wt and SCC FAK-/- cells were implanted into both flanks of FVB/N mice by bilateral subcutaneous injection. Tumours were disaggregated at day 7, stained with fixable viability dye eFluor® 506 and analyzed by FACS (n = 5). Statistical significance was determined by one-way Anova with Tukey's multiple comparisons. Data are represented as mean ± s.e.m. P-value = Not significant >0.05, * <0.05, ** <0.01, *** <0.001, **** <0.0001
.

Regarding T-cells, a statistically significant increase in $CD8^+$ T-cells was evident in SCC FAK-wt VS-4718-treated tumours (mean ± s.e.m. = FAK-wt vehicle, 3.94% ± 0.20; FAK-wt VS-4718 = 7.32% ± 0.65; FAK-/- vehicle = 6.34% ± 0.56; FAK-/- VS-4718 = 3.20% ± 0.85; **Figure 9.4a**), but no change was observed in effector $CD8^+$ T-cells (mean ± s.e.m. = FAK-wt vehicle = 43.25% ± 2.11; FAK-wt VS-4718 = 44.93% ± 1.69; FAK-/- vehicle = 40.66% ± 5.04; FAK-/- VS-4718 = 40.68% ± 3.19; **Figure 9.4b**). Decreases were observed in total $CD4^+$ T-cells between SCC FAK-wt VS-4718 treated tumours (mean ± s.e.m. = FAK-wt vehicle, 15.47% ± 0.53; FAK-wt VS-4718, 23% ± 0.74; FAK-/- vehicle, 21.62% ± 2.07; FAK-/- VS-4718, 21.87% ± 1.73; **Figure 9.4c**) and effector $CD4^+$ T-cells (mean ± s.e.m. = FAK-wt vehicle = 52.37% ± 1.58; FAK-wt VS-4718 = 74.03% ± 1.46; FAK-/- vehicle= 65.37% ± 4.53; FAK-/- VS-4718 = 61.54% ± 4.16; **Figure 9.4d**).

Crucially, there was a significant reduction in $CD4^+CD25^+FoxP3^+$ Treg cells in VS-4718-treated SCC FAK-wt tumours (mean ± s.e.m. = FAK-wt vehicle, 24.71% ± 0.50; FAK-wt VS-4718, 13.64% ± 2.32; p value = <0.0001; **Figure 9.5**), which was similar to that observed in vehicle (mean ± s.e.m. = 14.17% ± 0.59; p value = <0.001) and VS-4718-treated SCC FAK-/- tumours (mean ± s.e.m. = 14.56% ± 0.90;

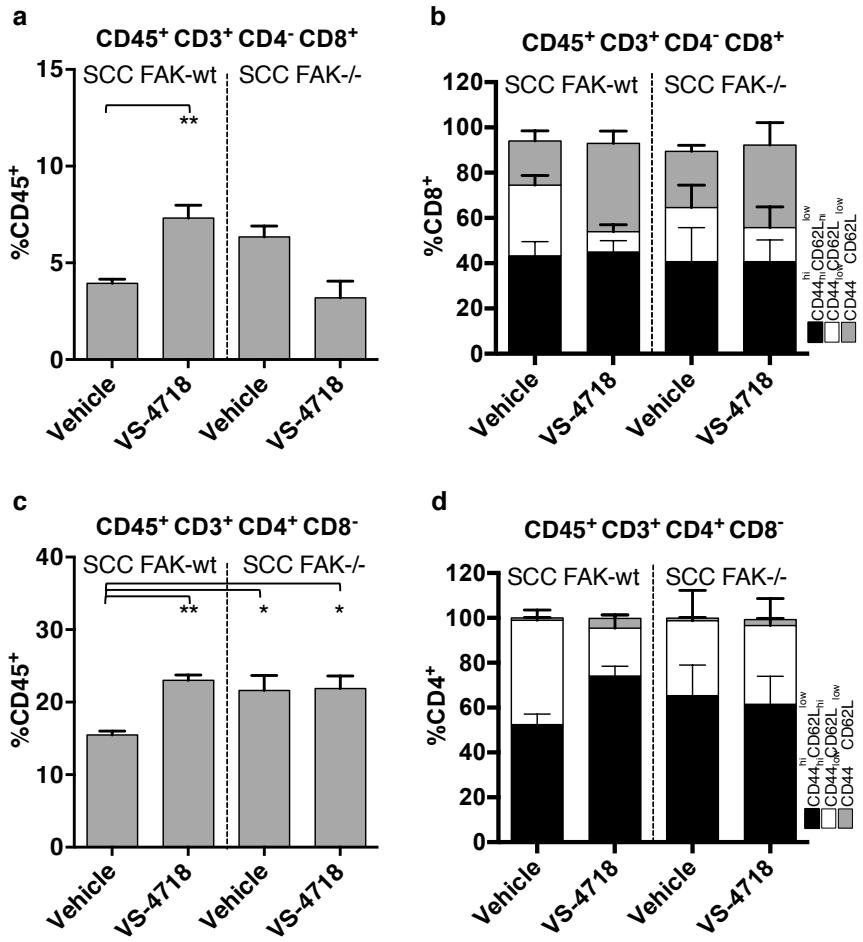

Figure 9.4 | VS-4718 treatment modulates intra-tumoural T-cell populations. **a** FACS analysis of tumor infiltrating $CD8^+$ T-cells from vehicle or VS-4718 treated tumours. **b** FACS sub categorization of tumor infiltrating $CD8^+$ T-cells $CD44^{hi}$ $CD62L^{lo}$ (*black bar)*, $CD44^{hi}$ $CD62L^{hi}$ (*white bar*) and $CD44^{lo}$ $CD62L^{lo}$ (*grey bar)*. **c** FACS analysis of tumor infiltrating $CD4^+$ T-cells from vehicle or VS-4718 treated tumors. **d** FACS sub categorization of tumor infiltrating $CD4^+$ T-cells $CD44^{hi}$ $CD62L^{lo}$ (*black bar)*, $CD44^{hi}$ $CD62L^{hi}$ (*white bar*) and $CD44^{lo}$ $CD62L^{lo}$ (*grey bar)*1.0×10^6 SCC FAK-wt and SCC FAK-/- cells were implanted into both flanks of FVB/N mice by bilateral subcutaneous injection. Tumours were disaggregated at day 7, and stained with Stain 2 (**Table 5.3**). FACS analysis was gated as described in **Figure 5.5**. Data are represented as mean ± s.e.m. P-value = Not significant >0.05, * <0.05, ** <0.01, *** <0.001, **** <0.0001.

p value = <0.001; **Figure 9.5**). Thus, VS-4718 promoted robust anti-tumour activity, by decreasing levels of intra-tumoural Tregs.

I have shown that $CD8^+$ T-cells were responsible for the immune mediated clearance of SCC FAK-/- tumours (**Figure 4.9b**). Thus, if the anti-tumour effects of VS-4718 were indeed mediated through the immune response, I hypothesised that $CD8^+$ T-cells were required for the clearance of SCC FAK-wt tumours treated with VS-4718. To test this hypothesis, FVB/N mice were treated with a combination of

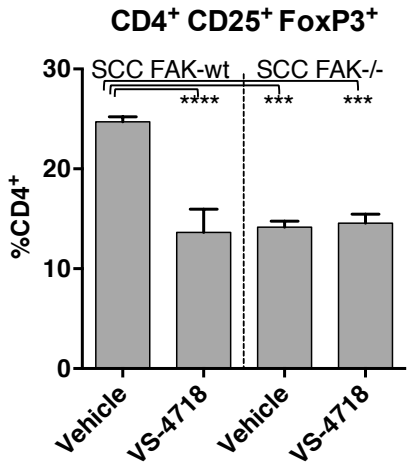

Figure 9.5 | VS-4718 treatment reduces reduces Tregs in SCC FAK-wt tumours. FACS analysis of intra-tumoural Tregs expressed as a percentage of tumour infiltrating $CD4^+$ T-cells. 1.0 x 10^6 SCC FAK-wt and SCC FAK-/- cells were implanted into both flanks of FVB/N mice by bilateral subcutaneous injection. Tumours were disaggregated at day 7, and stained with Stain 4 (**Table 7.1**). FACS analysis was gated as described in **Figure 7.6**. Statistical significance was determined by one-way Anova with Tukey's multiple comparisons. Data are represented as mean ± s.e.m. P-value = Not significant >0.05, * <0.05, ** <0.01, *** <0.001, **** <0.0001.

VS-4718 and CD8 depleting antibodies, as described in **Figure 9.6**. Animals treated with CD8 depleting antibodies or isotype control in combination with vehicle grew as expected; SCC FAK-wt $CD8^+$ depletion with vehicle treatment (**Figure 9.7** *solid red line*) showed a significant increase in tumour growth compared to the control treated tumours (SCC FAK-wt isotype and vehicle treated; **Figure 9.7** *solid black line*). In mice treated with VS-4718 in combination with isotype control, SCC FAK-wt tumours were cleared by day 21 (**Figure 9.7** *dashed black line*), as shown previously with VS-4718 treatment alone (**Figure 9.2)**. However in animals treated with both VS-4718 and CD8 depleting antibody (**Figure 9.7** *dashed red line*), tumours grew in a manner similar to VS-4718 in combination with isotype control until day 10, at which point tumour growth significantly increased until day 21 at which point animals had to sacrificed due to signs of ulceration. The final tumour volume reached a similar size to SCC FAK-wt $CD8^+$ depletion with vehicle treated tumours. I concluded that VS-4718 required $CD8^+$ T-cells to clear SCC FAK-wt tumours.

To determine if VS-4718 showed similar anti-tumour effects in a clinically relevant situation, 1 x 10^6 SCC FAK-wt or SCC FAK-/- cell were implanted into both flanks

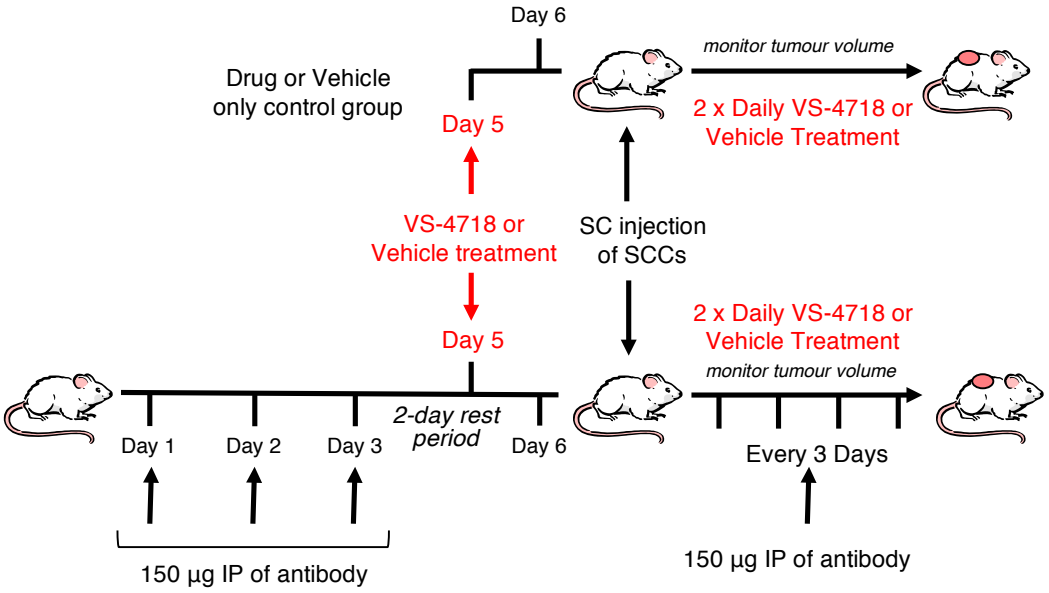

Figure 9.6 | Schematic describing treatment regime for combined antibody-mediated T-cell depletion and VS-4718 treatment. FVB/N mice were treated daily for 3 consecutive days with 150 µg of $CD8^+$ depleting antibody or isotype control antibody by IP injection. Antibody treatment then ceased for 2 days. VS-4718 treatment began 24 hours before tumour cell inoculation. Mice were treated with 75 mg/kg VS-4718 or vehicle control BID by oral gavage. 1 x 10^6 SCC FAK-wt or SCC FAK-/- cells were implanted by bilateral subcutaneous injection into each flank at day 6. Tumour diameter was measured twice weekly and tumour volume calculated using the formula $4/3\pi r^3$. T-cell depletion was maintained by 150 µg IP injection of antibody every 3 days, and VS-4718 BID treatment continued until the end of the experiment. *SC = bilateral subcutaneous injection; IP = intraperitoneal*

.

of FVB/N (n = 5) by bilateral subcutaneous injection. At day 5, mice were treated with 75mg/kg of VS-4718 or vehicle twice daily, when a palpable tumour of approximately 50 mm^3 was present (**Figure 9.8**). SCC FAK-wt tumours treated with VS-4718 grew until day 10, at which point tumour growth slowed and subsequent complete regression was observed by day 21. Vehicle treated SCC FAK-wt tumours grew as expected and SCC FAK-/- tumour growth remained unaffected by VS-4718 treatment. Thus, VS-4718 appeared to have the same anti-tumour activity against pre-established FAK expressing tumours as shown with mice pre-treated with VS-4718 prior to tumour cell implantation.

From these data, I concluded that the effects of VS-4718 treatment correlated with modulation of FAK expression and FAK kinase activity in tumour cells alone; both VS-4718 treatment and SCC FAK-kd tumours underwent immune-mediated regression by $CD8^+$ T-cells, which was associated with a decrease in intra-tumoural

Tregs. Thus the anti-tumour effects of VS-4718 are likely due to the tumour-specific inhibition of FAK.

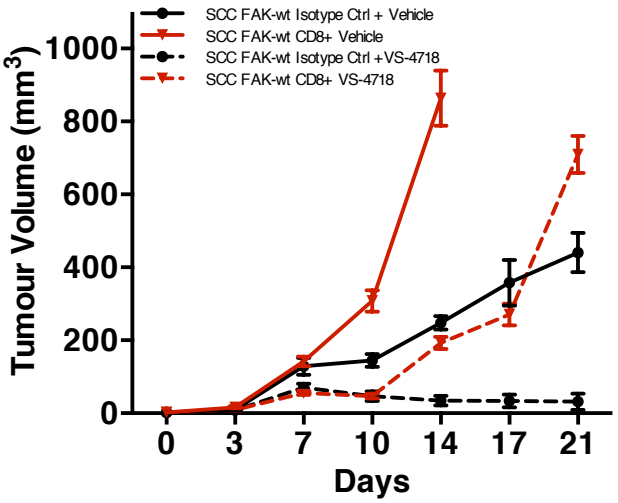

Figure 9.7 | VS-4718 induced SCC FAK-wt regression is dependent on CD8$^+$ T-cells. Tumour growth of SCC FAK-wt treated with either CD8 depleting antibodies or isotype control, in combination with VS-4718 or vehicle treatment. FVB/N animals were treated as described in **Figure 9.6** (n = 5). Tumour diameter was measured twice weekly and tumour volume calculated using the formula $4/3\pi r^3$. Data are represented as mean ± s.e.m.

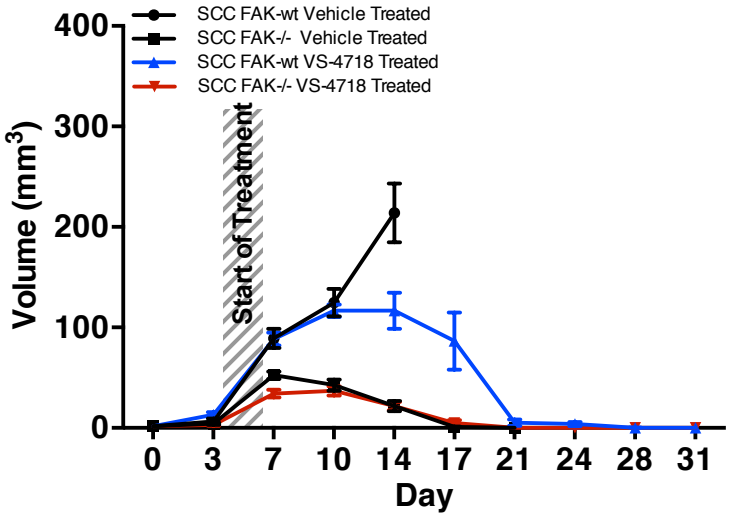

Figure 9.8 | VS-4718 treatment results in regression of established SCC FAK-wt tumours. SCC FAK-wt and SCC FAK-/- tumour growth in FVB/N mice (n = 5) treated with either vehicle or VS-4718. Treatment started 5 days post-inoculation with 1 x 10^6 tumour cells and continued for the duration of the experiment. Tumour diameter was measured twice weekly and tumour volume calculated using the formula $4/3\pi r^3$. Data are represented as mean ± s.e.m.

9.3.2 VS-4718 treatment of a panel of syngeneic mouse models of cancer

Thus far, the work described has focussed on a single model system. Therefore, it was important to investigate the broad relevance of these findings across multiple syngeneic models of cancer harbouring different genetic driver mutations, different tissues of origin, and different mouse strains of origin. Therefore, so I set out to investigate the effects of VS-4718 on a number of syngeneic mouse models of cancer. A panel of different syngeneic cancer models were selected covering a number of different host-strains, cancer types, genetic drivers and pathological grades (**Table 9.1;** Mel31[428], Panc043, Panc047 and Panc117 were generously donated by the Samson Lab, The Beatson Institute for Cancer Research, Glasgow; Met01 were generously donated by Bin-Zhi Qian, Centre for Reproductive Health, University of Edinburgh, Edinburgh). These included breast, skin and pancreatic cancer models, from BALB/c, FVB/N and c57BL/6 mouse strains, and a number of genetic drivers including MMTV-PyMT (mouse mammary tumour virus LTR driven polyoma middle T antigen), CDK4 and KPC (KrasLSL.G12D/+; p53R172H/+; PdxCretg/+). I included the parental heterogeneous SCC population (SCC 7.1) from which our SCC model was derived, and an additional independently derived heterogenous SCC cell model, SCC 6.2 (**Table 9.1**). For each model, mice (n = 3) were treated with 75 mg/kg VS-4718 for 24 hours prior to bilateral subcutaneous injection of 1 x 10^6 cells in both flanks, and twice daily thereafter. Tumour diameter was measured twice weekly and tumour volume calculated using the formula $4/3\pi r^3$.

All tumour models were observed to respond to VS-4718, albeit to varying extents. Models were grouped into those in which a significant growth delay was observed between VS-4718 treated and vehicle treated controls (moderate response; **Figure 9.9**) and those in which VS-4718 resulted in disease stabilization or tumour regression (high response; **Figure 9.10**).

Cell Line	4T1	Met01	Mel31	Panc043	Panc047	Panc117	SCC 7.1	SCC 6.2	SCC FAK-wt
Cancer Location	Breast	Breast	Skin	Pancreatic	Pancreatic	Pancreatic	Skin	Skin	Skin
Pathological Classification	Mammory Gland Carcinoma	Adenoma	Melanoma	Ductal Adenocarcinoma	Ductal Adenocarcinoma	Ductal Adenocarcinoma	Squamous Cell Carcinoma	Squamous Cell Carcinoma	Squamous Cell Carcinoma
Oncogenic Driver	MMTV-PyMT	MMTV-PyMT	HGF-CDK4(R24C)	KPC	KPC	KPC	Ha-ras	Ha-ras	Ha-ras
Chemical							*	*	*
Backgound mouse strain	Balb/c	FVB/N	c57Bl/6	c57Bl/6	c57Bl/6	c57Bl/6	FVB/N	FVB/N	FVB/N
Further Notes	Highly aggressive and spontaneous metastasis seen			Independently derived cell lines from same model			Parental population for SCC FAK-wt	Independently derived SCC model	SCC FAK-/- clone re-expressing WT FAK

Table 9.1 | Syngeneic mouse models of cancer treated with VS-4718. Comparison of syngeneic cell models, comparing cancer location, pathological classification, oncogenic driver, and derived mouse genetic background. *MMTV-PyMT = mouse mammary tumour virus LTR driven polyma middle T antigen); KPC = KrasLSL.G12D/+; p53R172H/+; PdxCretg/+*

Five models showed a moderate response to VS-4718 treatment (**Figure 9.9a-e**). Panc041, Panc043, and Panc117 tumours grew until day 7, where growth stalled, resulting in a statistically significant growth delay by day 14 (p value = <0.0001; **Figure 9.9a-c**). Tumours continued to grow until day 17, at which point animals had to be sacrificed due to the onset of ulceration. Control-treated animals showed signs of ulceration by day 14, and had to be sacrificed in accordance with home office guidelines. VS-4718 treated Mel31 tumour growth stalled at day 7, resulting in a significant growth delay by day 14 (p value = <0.001; **Figure 9.9d**). Both VS-4718 and control treated tumours continued to grow until day 17, and a significant growth delay observed in VS-4718 treated tumours (p value = <0.0001), but by day 17 tumours showed signs of ulceration and animals were sacrificed. Finally, 4T1 tumour growth was complicated by the highly metastatic nature of this model. VS-4718 treated 4T1 tumours showed a significant growth delay by day 10 compared to vehicle treated control (p value = <0.001; **Figure 9.9e**), but animals became increasing ill and showed signs of advanced metastatic disease by days 14 and 10 respectively, and therefore mice had to be sacrificed in accordance with home-office guidelines. Following sacrifice, multi-organ metastasis was observed in both cohorts of mice.

SCC 7.1 and Met01 tumours responded better to VS-4718 treatment (**Figure 9.10**). VS-4718 treated SCC 7.1 tumours grew until day 7, at which point tumour growth stalled and regressed until day 24 (**Figure 9.10a**). At this point some SCC 7.1 tumours appeared to rebound while still receiving VS-4718, and grew rapidly thereafter even in the presence of VS-4718. Analysis of individual tumour growth determined that most tumours regressed by day 18, but two tumours (from different mice) escaped tumour regression at day 24 (**Figure 9.10b**). Tumour growth increased in both tumours until day 38, at which point animals were sacrificed and tumours were removed, so that cell lines could be derived from them (**Figure 9.10b**). VS-4718 treated Met01 tumour growth stalled at day 7, after which tumour growth stabilized (**Figure 9.10c**). Tumour growth did not regress after 28 days but continued to remain stable.

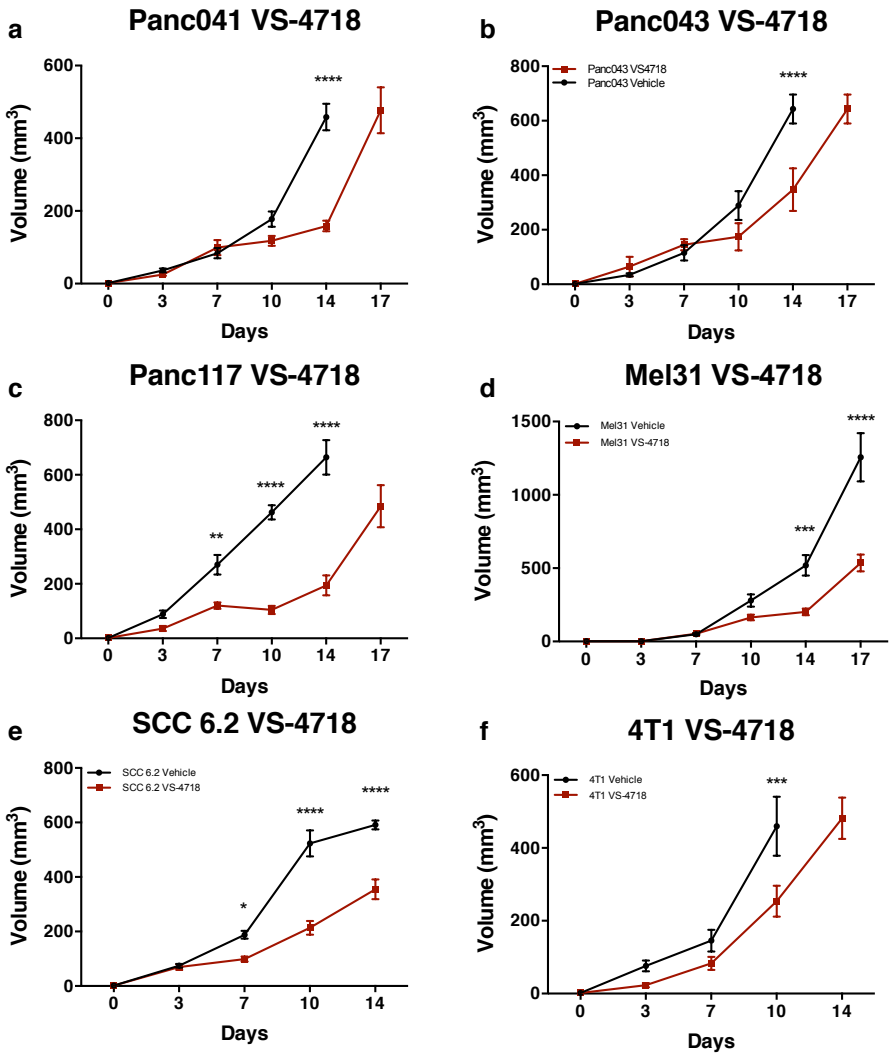

Figure 9.9 | Syngeneic mouse models with moderate response to VS-4718. 1 x 10^6 cells were implanted into both flanks of mice (n = 5) by bilateral subcutaneous injection. **a** Panc041, **b** Panc047, **c** Panc117 and **d** Mel31 cells were implanted into c57Bl/6 mice. **e** SCC 6.2 cells were implanted into FVB/N mice and **f** 4t1 cells were implanted in BALB/c mice (**Table 9.1**). Mice were treated with either vehicle or with 75 mg/kg VS-4718, BID by oral gavage. Treatment started 24 hours before cell inoculation and continued for the duration of the experiment. Tumour diameter was measured twice weekly and tumour volume calculated using the formula $4/3\pi r^3$. Statistical significance was determined by matched, two-way Anova with Tukey's multiple. Data are represented as mean ± s.e.m. P-value = Not significant >0.05, * <0.05, ** <0.01, *** <0.001, **** <0.0001.

A number of preliminary conclusions can be drawn from these data. Firstly, all syngeneic cell models responded to VS-4718 treatment, albeit to different extents. Despite this variation, all responses were observed to result in a significant growth delay. Secondly, the point at which VS-4781 treated tumours deviated from their controls, was consistently 7 days post-implantation, correlating with the average time thought to be required to mount an adaptive immune response (**2.1**). And finally, with regards to the parental SCC 7.1 model, although this most tumours regressed in this model, this model also contained cells with the capacity to escape clearance suggesting potential mechanisms of resistance. These observations led us to consider the possibility that additional mechanisms of immune evasion, independent of those regulated by FAK, may influence tumour response to FAK inhibitor monotherapy. Such potential mechanisms include tumour cell surface expression of co-inhibitory ligands belonging to the so called 'immune checkpoint' pathways.

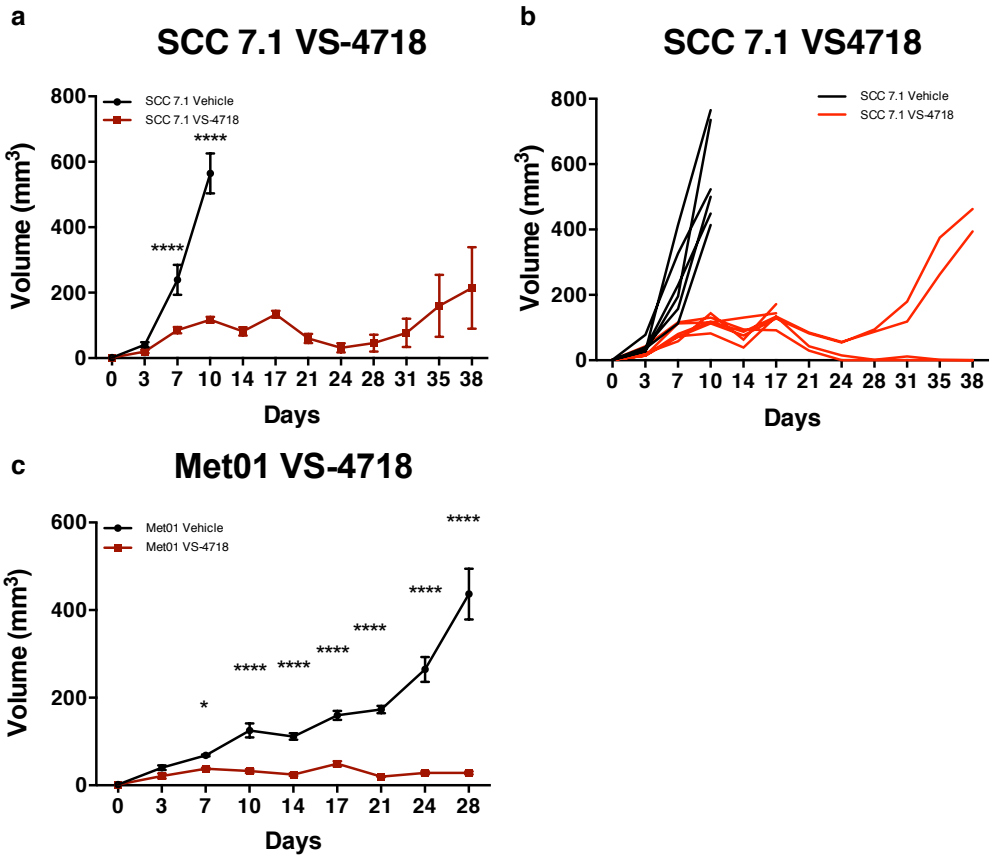

Figure 9.10 | SCC 7.1 and Met01 models exhibit a good response to VS-4718. **a** Average Tumour growth of SCC 7.1 cells and **b** the growth of each individual tumour. **c** Tumour growth of Met01 cells. 1 x 10^6 cells were implanted into both flanks of FVB/N mice (n = 5) by bilateral subcutaneous injection (**Table 9.1**). Mice were treated with either vehicle or with 75 mg/kg VS-4718, BID by oral gavage. Treatment started 24 hours before cell inoculation and continued for the duration of the experiment. Tumour diameter was measured twice weekly and tumour volume calculated using the formula $4/3\pi r^3$. Statistical significance was determined by matched, two-way Anova with Tukey's multiple comparisons. Data are represented as mean ± s.e.m. P-value = Not significant >0.05, * <0.05, ** <0.01, *** <0.001, **** <0.0001.

9.3.3 PD-L1/PD-L2 and CD80 expression correlated with response to VS-4718 treatment.

Tumour cells may regulate the adaptive immune response through a number of mechanisms. These include tumour cell expression of PD-1 ligands PDL-1 and PD-L2, which after engagement with T-cell expressed PD-1, induce T-cell anergy and exhaustion (**2.4**). A second mechanism is through the upregulation of co-stimulatory molecules such as CD80, which can induce T-cell activation and lead to increased Tregs or T-cell anergy exhaustion (**2.4**). Therefore, I set out to determine whether any of our syngeneic tumour models expressed PD-L1, PD-L2 or CD80, and whether levels of expression correlated with response to VS-4718. 1 x 10^6 cultered-4T1, Met01, Mel31, Panc041, Panc043, Panc117, SCC 6.1, SCC FAK-wt and SCC 7.1 cells were stained with PD-L1, PD-L2 and CD80 fluorescently labelled antibodies and analysed by FACS (**Figure 9.11**). 4T1, Met01, Mel31, Panc041, Panc043, Panc117 and SCC 6.1 all expressed PD-L1 and PD-L2. SCC FAK-wt and

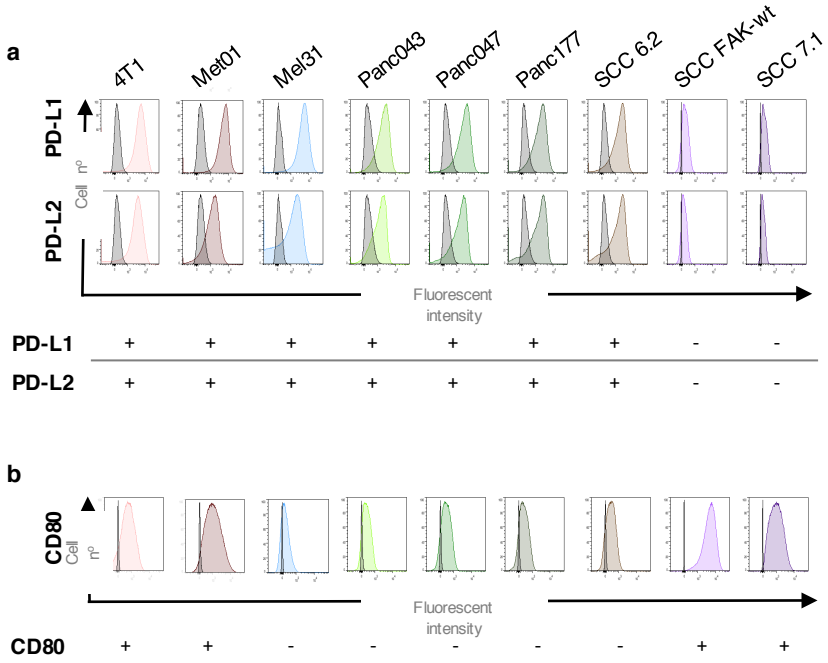

Figure 9.11 | Levels of PD-L1, PD-L2 and CD80 expression on a panel of syngeneic mouse tumour cell lines. FACS analysis of a panel of cell lines from syngeneic models of breast cancer, melanoma, pancreatic cancer and SCC (see **Table 9.1**). Each FACS blot representative of 5 x 10^5 cells. *Grey populations* = negative

SCC 7.1 did not express PD-L1 or PD-L2 (**Figure 9.11a**). 4T1, Met01, SCC FAK-wt and SCC 7.1 were found to express CD80, whereas Mel31, Panc041, Panc043, Panc117 and SCC 6.1 did not (**Figure 9.11b**).

Both SCC FAK-wt and SCC 7.1 cells showed the greatest response to VS-4718 treatment, and were the only models to show complete tumour regression following treatment. Both SCC FAK-wt and SCC 7.1 cells expressed CD80 and did not express PD-L1 and PD-L2. Met01 tumours showed a good response to VS-4718 treatment, and were found to express CD80. Met01 also expressed PD-L1 and PD-L2, which may explain why tumour regression was not seen in this model. Mel31, Panc041, Panc043, Panc117 and SCC 6.1 all responded modestly to VS-4718 treatment, and were all negative for CD80 and positive for PD-L1 and PD-L2. This small dataset highlighted a potential link between CD80, PD-L1 and PD-L2 expression and response to VS-4718. However, a much larger data set is required to make any definitive conclusions.

9.4 Conclusion

Here I have shown that the small molecule FAK kinase inhibitor VS-4718 shows preclinical potential as an anti-cancer immunotherapy agent. VS-4718 treatment of SCC FAK-wt tumours resulted in tumour clearance associated with a reduction in intra-tumoural Tregs. Across a panel of syngeneic tumour models VS-4718 treatment resulted in a significant growth delay in all cases, with a tentative correlation between increased CD80 expression and response to monotherapy. Further work is required to determine whether immune-modulation is a general phenomenon in these models when treated with a FAK kinase inhibitor, or when FAK expression in cancer cells is down regulated, especially in models that continue to grow in the presence of FAK inhibitor treatment. These models may represent good candidates for testing combination therapies, such anti-PD-1 or anti-CTLA-4, with the aim of unlocking the potential anti-tumour activity of FAK kinase inhibitors.

VS-4718 was administered twice-daily (BID) by oral gavage as per the protocol submitted by the manufacturer, Verastem. Although details regarding the work undertaken to set up the clinical protocol for VS-4718 are protected under licence, Phase I clinical trials with VS-4718 are currently being undertaken (ClinicalTrials.gov Identifier**:** NCT02651727), with the clinical protocol for these stating oral administration of VS-4718 BID. The timings of drug dosage are typically determined by the pharmacodynamics of the therapeutic in question, and consider the biological half-life of the drug ($t_{1/2}$). $t_{1/2}$ refers to the time taken for a substance to lose half its its pharmacologic and biologic activity, typically associated with the renal clearance of the drug, and may be measured as the time taken for blood plasma concentrations of a therapeutic to halve if biological activity is not possible to determine. Substances with shorter half-lives require more frequent dosage, or are administered at an increased dosage if well tolerated. Although the BID dosing schedule in both humans and mice alludes to the short half-life of VS-4718 *in vivo*, this raises the question as to the rationale behind the differences in administration route between clinical patients and mouse models.

Enteral administration protocols such as oral gavage, therapeutics admixed into food stuffs or water, or by nasogastric gavage have the benefits of being economical, convenient, reliable and relatively safe[429,430] compared to other routes such as intraperitoneal (IP)[431] or intravenous (IV)[432] administration. Furthermore, the Home Office procedural standards surrounding experiments with animals and their welfare, regards the severity of oral gavage to be less than other administration routes due to animals becoming accustomed to the procedure over time, not seen in IP or IV administrations[433,434]. Although admixing drugs into food stuffs or water is by far the least invasive/stressful enteral admiration route[435], it suffers from the lack of accurate and consistent dosage. Cohorts of caged mice will eat varying amounts of food, requiring food to be weight before and after administrations, but also mice within each cohort will ingest significantly different levels of food[436]. This depends of factors such as social and physical dominance within caged cohorts, and with effects on appetite by therapeutic agents or by the onset/implantation of tumours, factors that will will vary between each treated mouse and across different genetic backgrounds[429]. Therefore, even though the voluntary oral consumption of VS-4718

in mice would reflect more accurately the clinical protocol in humans, oral gavage allows the drug to be administered with the same dosing schedule as with humans, but in a more reliable, effective and controlled manner.

Oral administration in this way also allows for the evaluation of possible pharmacologically inactivation following gastric ingestion of VS-4718. Although in majority of cases, metabolism of therapeutics occurs in the liver by oxidation, reduction, hydrolysis, hydration, conjugation, condensation, or isomerization, in some cases metabolism/inactivation can occur in the stomach, rendering them inert[437]. In consideration of this and other factors involved in pharmacodynamics, and to validate the effective delivery of VS-4718 to the tumour, collaborators at Verastem undertook an *in vivo* FAK pY397 Eliza (**Figure 9.1**). Crucially, the inhibition of FAK pY397 as shown here, indicates that the route of administration, dosing schedule and pharmacodynamics of VS-4781 in our mouse studies results in effective inhibition of FAK kinase activity.

The mouse models of cancer used in this chapter only include subcutaneously implanted models. This raises the question as to whether a more diverse range of mouse models should have been used to address the clinical potential of FAK activity inhibition with VS-4718. Transgenic mouse model allow tumours to develop in a more clinically relevant setting, but which take significantly longer than implantation models. The extended time frame however, subjects the tumour to a number of significant developmental changes within the tumour itself and within the tumour microenvironment, the most pertinent in this case being the development of T-cell exhaustion and anergy[143,144]. This decrease in the effective cytotoxic activity of $CD8^+$ T-cells could reduce the clinical efficacy of VS-4718, but invites the possibility of combinations of VS-4718 and checkpoint inhibitors targeting PD-1 such as nivolumab or pembrolizumab, discussed in further detail below (**10**). Therefor the treatment of transgenic models with VS-4718 may give further insight into the potentially clinical efficacy of FAK kinase inhibition.

As metastatic disease is the primary cause of death in cancer patients, and as FAK has been a target previously for the reduction of metastatic progression, it may been appropriate to determine the roles of FAK within a metastatic mouse model. Previous

work focused on the roles of FAK in cell migration and adhesion collectively concluded that FAK inhibition reduces metastatic development and progression[4,265,302,438-447]. None of these studies consider changes in the immune compartment to contribute to metastasis but focus on FAK as an adhesion molecule and regulator of cell migration. The work presented here regarding FAK kinase activity modulating the tumour microenvironment, highlights the need to re-address the role of FAK in the metastatic cascade as a number of immune compartments modulated by FAK activity contribute to metastatic progression[31,54,55,73]. Use of metastatic mouse models will help not only to address these points but to also in part, help to consider the multifaceted potential activity of FAK inhibition in clinical setting, to not only modulate the tumour immune response but to also inhibit metastasis.

CD80 is a high affinity ligand for the receptor CTLA-4 which is constitutively expressed on Tregs, and ligand-receptor interaction has been shown to enhance Treg suppressive capacity[448]. Profiling of CD80 expression on the surface of our syngeneic panel of cell lines revealed high surface expression on the SCC FAK-wt, SCC 7.1, Met01, and 4T1 cell lines. Thus, three of the four models that respond robustly to VS-4718 treatment express high surface levels of CD80. While small sample numbers preclude the conclusion that high CD80 surface expression may represent a biomarker for sensitivity to FAK kinase inhibitor monotherapy, it is tempting to speculate that CD80 expression may drive increased Treg dependence rendering these tumours more susceptible to FAK inhibition.

One potential issue with the DMBA/TPA chemically induced model was with the restriction of neoantigens by the isolation of SCC FAK-/- clone by single cell cloning (see **5.4**). This would have generated an atypically immunogenic SCC FAK-wt cell line, which in turn would increase the immunomodulation, and consequently the efficacy of VS-4718 treatment. The good response observed with the treatment of SCC 7.1 with VS-4718 indicates that the clone selected is indicative of the heterogeneous population. Regarding the escape of a small number of tumours, one potential hypothesis is that these tumours are capable of evading the immune

modulation of VS-4718 treatment, and this could present new information regarding the resistance to VS-4718, and these findings should be investigated further.

10 Discussion and Concluding Remarks

Using an SCC tumour cell model in which FAK has been genetically deleted (SCC FAK-/-), I have shown that loss of FAK results in complete SCC tumour regression when grown in immune-competent mice (the FVB/N strain from which the cell model was derived). Re-expression of a kinase-defective mutant into SCC FAK-/- cells was not sufficient to rescue tumour growth, implying that FAK-dependent immune escape required FAK catalytic activity. Treatment with the FAK kinase inhibitor VS-4718, which is currently in Phase 1 clinical trials, resulted in complete regression of SCC FAK-wt tumours irrespective of whether treatment was initiated prior to tumour cell inoculation, or after tumours had reached approximately 50 mm^3. $CD8^+$ T-cell depletion was sufficient to rescue both SCC FAK-/- tumour growth, and VS-4718 mediated SCC FAK-wt clearance. Thus, for the first time I show that loss of FAK expression or catalytic activity is sufficient to release the anti-tumour effects of antigen-primed $CD8^+$ T-cells and drive tumour regression. This response is suppressed in SCC FAK-wt tumours as a consequence of FAK-dependent recruitment of immuno-suppressive Tregs into the tumour niche, the requirement for these cells being confirmed by both anti-$CD25^+$ and anti-$CD4^+$ T-cell depletion. Mechanistically, we identify a new role for FAK in the transcriptional regulation of chemokines and cytokines in SCC cells, and show that FAK-driven expression of both CCL5 and TGFβ2 is required for elevated intra-tumoural Treg levels and sustained SCC FAK-wt tumour growth. Furthermore, analysis of chemokine receptor expression on intra-tumoural Tregs revealed a paracrine signalling axis between FAK-expressing SCC cells and intra-tumoural Tregs based on chemokine ligand-receptor interaction, that likely plays a role in driving Treg recruitment and retention in the tumour bed. Our data implies that FAK may contribute to the development of malignancy in vivo by increasing the recruitment and retention of intra-tumoural Tregs, leading to a change in the balance between $CD8^+$ T-cells and Tregs resulting in tumour tolerance. This proposed mechanism is summarized in **Figure 9.1**.

The secretion of chemokines and cytokines into the tumour environment represents an important mode of communication between cell types, and drives recruitment of immune cells into tumours[19,44,52]. Identification that FAK expression results in the transcriptional upregulation of a number of these molecules, suggests that FAK may play a role in governing this type of communication between tumour cells and tumour infiltrating immune cells. Indeed our observation that both FAK-dependent expression of CCL5 and TGFβ2 was required for elevated intra-tumoural Tregs, and that CCL5 represents part of a paracrine signalling axis between tumour cells and Tregs, supports this notion and implies a critical role for FAK-dependent chemokine regulation in the development and progression of SCC tumours. In our model, a clear outcome of this signalling was to alter the $CD8^+$ T-cell to Treg ratio within the tumour, a parameter that is a prognostic indicator in ovarian[449], breast[450], pancreatic[182,451], colorectal[452], oesophageal and gastric cancers[453]. Furthermore, inhibition of FAK kinase activity through expression of a kinase-deficient FAK protein (FAK-kd) resulted in reduced CCL5 and TGFβ2 expression that was associated with a reduction in Tregs and SCC tumour regression. Similar observations were made following VS-4718 treatment. Thus, FAK regulates the tumour immune environment through promoting expression of chemokines and cytokines that favour tumour tolerance. FAK has been reported to regulate secreted factors in other cell models, including IL-6[454], VEGF[455] and TGFβ[398], suggesting that our observations are not unique to our tumour cell model.

The SCC cell model used in this study was derived using the DMBA / TPA model of skin chemical carcinogenesis, and FAK expression has been identified to increase with malignant progression in this model. Furthermore, deletion of FAK in this model prevents benign papilloma formation and progression to malignant carcinoma[456], implying that FAK is required to support tumour development. In support of our findings, genetic ablation of $CD4^+$ T-cells has been shown to reduce the number of tumours formed after DMBA/TPA treatment, while ablation of $CD8^+$ T-cells resulted in enhanced tumour formation[457]. Thus, it is possible that at least one outcome of elevated FAK expression in this model is to modulate the tumour immune environment and promote tumour growth and progression. FAK has also been reported to be required for tumour development and progression in a number of

other pre-clinical mouse models of cancer, including breast, prostate, and colon cancer[279,458-462] and it will be interesting to identify whether targeting FAK in these models, or transplantable cell lines derived from similar models, also results in underlying immune-modulation.

I have demonstrated that treatment of a number of syngeneic mouse models covering breast, pancreatic, melanoma, and skin cancer with VS-4718 either results in a growth delay, disease stabilisation, or disease regression. The effects of FAK inhibition in these models does not become apparent until 7 days post tumour cell implantation and treatment initiation, a timeline that would correlate with the development of an adaptive immune response. It is perhaps not surprising that the SCC 7.1 tumours exhibited a similar sensitivity to VS-4718 when compared with the SCC FAK-wt tumours, given that the SCC FAK-wt cells are essentially a subclone from this parental heterogeneous population. However, the rebound of some SCC 7.1 tumours following an extended period of disease stabilisation while on VS-4718 was surprising, and suggests either the development of intrinsic tumour cell resistance or the emergence of environmental changes that negate the anti-tumour properties of VS-4718 treatment. This characteristic was not observed when using the SCC FAK-wt tumours. Further investigation is warranted in order to understand the mechanistic basis of this resistance.

Comparison of VS-4718 sensitivity between the SCC 7.1 and SCC 6.2 tumours also provides further interesting insights. Both cell types were derived from late-stage carcinomas albeit from different mice. Both have a mesenchymal morphology, and both were derived using DMBA/TPA treatment and thus likely have a similar mutagenic burden. Therefore it seems reasonable to hypothesise that high mutagenic burden as a consequence of exposure to carcinogens does not dictate sensitivity to VS-4718. While it is difficult to stratify such conclusions from small sample numbers, this theory is supported by our observations when using the Met01 model. This transplantable cell line was derived from the MMTV-PyMT model of breast cancer, and when treated with VS-4718 shows durable disease stabilization. This oncogene driven model is likely to have a very low mutagenic burden, yet responds robustly to VS-4718 treatment. Interestingly, studies by the Rudensky Lab have

shown that in the MMTV-PyMT *FoxP3*^{DTR} knockin mouse, Treg ablation following treatment with diphtheria toxin (DT) results in tumour regression and a reduction in metastatic progression[393]. Combination of Treg ablation with the immune checkpoint inhibitors anti-PD-1 and anti-CTLA-4 did not increase therapeutic efficacy over that of Treg ablation alone[393], suggesting that this model is highly dependent on the immuno-suppressive capabilities of Tregs to support tumour growth and progression. These observations parallel with those observed using our SCC FAK-wt tumour model, and suggest that the observed Met01 response to VS-4718 may be due to FAK-dependent regulation of intra-tumoural Treg levels. Further work will be required to determine if this is indeed the case.

A number of models tested exhibited a growth delay (but not disease stabilisation or regression) when treated with VS-4718, suggesting that other mechanisms of immune-suppression, independent of FAK, are likely involved in supporting tumour growth. For example, the three cell models derived form the KPC Kras P53 model of pancreatic cancer[463], namely the Panc043, Panc047, and Panc117, all showed sensitivity to VS-4718 that manifested at day 7 but was overcome only a few days later. Profiling of surface ligand expression on these cells revealed that all expressed high levels of PD-L1 and PD-L2, but little to no CD80. Thus, it is tempting to speculate that engagement of the PD-1 pathway may circumvent the anti-tumour activity of VS-4718 in these models by helping to overcome the impact of modulating intra-tumoural Tregs, and that combination of these two therapies may prove efficacious in this instance. In support of this hypothesis targeting intra-tumoural Tregs with a p110δ inhibitor was reported to result in a small survival benefit in mice from the KPC pancreatic model[464]. However, targeting Tregs alone was not sufficient to gain long-term tumour control and drive tumour regression. Similar observations have been reported for strategies targeting the CXCR4 axis[463], and tumour infiltrating macrophages[87]. However, when these strategies were combined with anti-PD-1 treatment, tumour control and regression was observed[87]. FAK kinase inhibitors have been reported to block CAF recruitment into tumours by virtue of FAK's role in regulating their migration[302], with similar observations reported for macrophage recruitment following FAK inhibitor treatment. Thus, the immuno-modulatory outcome of treatment with FAK kinase inhibitors may extend

beyond that identified here to encompass multiple immune and stromal cell types that contribute to promoting tumour growth through suppressing $CD8^+$ T-cell activity. Therefore FAK inhibitors may represent a therapeutic strategy for broad targeting of tumour promoting immune and stromal cell types, providing rational for their testing in combination with immune-checkpoint inhibitors including anti-PD1.

Treatment of human tumours with immune-checkpoint therapies has proven highly efficacious in some tumour types. For example, a clinical study combining agents targeting cytotoxic-T-Lymphocyte-associated Antigen-4 (CTLA-4), which is thought to influence Treg function[104,169,170,465-467], and Programmed Death Receptor-1 (PD-1), which blocks signals that inhibit T-cell function[147,468,469], has reported impressive responses in patients with advanced melanoma, with 53% of patients having an objective response resulting in greater than 80% reduction in tumour burden[232,470](**2.3**). However, this combination of checkpoint blockade antibodies was also reported to elicit substantial side-effects (clinical grade 3-4) in greater than 50% of patients, highlighting the need to find alternative combinations with improved tolerability profiles (**2.3**). A number of FAK inhibitors are in early Phase I / II clinical trials, and initial reports on one of these, GSK2256098 (Clinical trial identifier: NCT01938443), suggests a favorable tolerability profile (clinical toxicity grades 1-2) with some activity as a monotherapy[471]. No autoimmune side effects were reported. Alternative methods for targeting immune populations, including anti-CD25 monoclonal antibodies[472], and anti-CSF1-receptor antagonists[473], are in clinical trials. However, this approach of targeting immune populations directly is hampered by immune-based toxicity due to the homeostatic roles of their target populations[148,149,469,470,474,475]. It is interesting to consider why FAK kinase inhibitors do not appear to exhibit immune-related toxicity given the role I have established for FAK in controlling Treg levels. It is possible that the role I have identified is limited to a minority of tumour models, or alternatively that the immune-modulatory function of FAK is specific to malignant cancer cells. Since finishing the work for my PhD, my colleagues in the Frame Laboratory have identified that the immuno-modulatory function of FAK in the SCC tumour model is dependent of FAK nuclear translocation, and that this only occurs in malignant cancer cells. These recent findings support the conclusion that FAKs immuno-modulatory function is specific

to cancer cells, and that in normal cells FAK does not translocate to the nucleus and excerpt regulatory control over chemokine and cytokine expression. Such observations may underlie the lack of autoimmune side effects in clinic when treating with FAK kinase inhibitors.

Taken collectively our data suggest that targeting the pleiotropic cellular functions of FAK, both nuclear and adhesion-related, using small molecule inhibitors may have a broad impact on the immunosuppressive tumour microenvironment, differentiating these agents from many of the therapeutic approaches currently being tested in the clinic which target single immune cell populations. Our findings provide good rationale for pre-clinical and clinical testing of FAK kinase inhibitors alongside agents that stimulate CD8+ T-cell activity, such as the checkpoint blockade therapies that target CTLA-4 and PD-1[104], and have prompted a clinical trial combining VS-6063 (A FAK kinase inhibitor closely related to VS-4718 which has shown better efficacy in humans; Verastem) and anti-PD-1 therapy as part of the CRUK Combination Alliance.

11 Future Work

Future work will focus on investigating the immuno-modulatory effects of FAK in multiple models of cancer, including those in **Table 9.1**. This will include both inhibiting FAK kinase activity (FAKi) with VS-4718 and the genetic deletion of FAK, using clustered regularly interspaced short palindromic repeats (CRISPR)/ Cas technology. This will include phenotyping T-cells, Tregs, macrophages, MDSCs and CAFs using FACS analysis. The key objectives here will be to identify the underlying immune changes that result from FAK deletion and VS-4718 treatment. Furthermore, SCC cells will be derived from c57BL/6 K14CreER $FAK^{flox/flox}$ mice by the two-stage DMBA/TPA chemical carcinogenesis protocol, and this work is currently underway. By re-deriving the SCC model onto a c58BL/6 background, will allow access to a number of c57BL/6 transgenic mouse models that will help investigate the immuno-modulatory roles of FAK. These include mice harboring human diphtheria toxin receptor (DTR) expressed under a variety of leukocytes-specific promoters, in which the chronic administration of diphtheria toxin (DT) leads to conditional, targeted cell ablation. The aim will be to use the DTR/DT system to deplete immune populations such as Tregs with greater specificity than using antibody-mediated depletion.

These results will help guide further work into the translational aspects of the FAKi/anti-PD-1 Combinations Alliance clinical trial, which is proposed to start within the next year in Edinburgh and four other centers across the UK. Together with Dr Stefan Symeonides (Edinburgh Cancer Center), further work will investigate pre-clinical dosing and scheduling studies in order to interrogate and optimize the commination of VS-4718 and anti-PD-1 inhibitors. Other inhibitors of co-inhibitory receptors, such as anti-CTLA4 treatment in multiple syngeneic mouse models of cancer will also be assessed. Utilization of c57BL/6 PD-1 knockout mice for work involving pancreatic and melanoma models initially (generated on c57BL/6 backgrounds) and further work will focus on the re-derived c57BL/6 SCC model. Associated with this, markers of T-cell exhaustion will be investigated across our panel of cancer models to determine to what extent $CD8^+$ T-cells are exhausted, how

this contributes to tumour tolerance and investigate whether FAKi modulates these factors. This includes further characterization of exhausted T-cells identified in SCC FAK-wt tumours. This will be done using FACS analysis of PD-1, LAG-3 and Tim-3 alongside secreted chemokine and cytokine arrays and functional studies.

One potential caveat with the proposal for the clinical trial is how will the success of FAKi/anti-PD-1 therapy in modulating immune populations be determined. Access to tissue will be very limited and will be either frozen or embedded in paraffin blocks for histology, making FACS analysis not plausible. By identifying and characterizing the cell populations most frequently altered by FAKi, these may in turn, be used to predict rational choices as biomarkers of response. Histology could be used as a clinical read out, specifically fluorescent histology using fluorophore-conjugated antibodies that has been optimized in the lab previously, which will allow us to identify a number of cell populations and their activation statuses simultaneously. Collaborators on this trial (Prof. Christian Ottensmeier, Faculty of Medicine, University of Southampton) will be using RNA sequencing to determine and quantify leukocyte-specific gene signatures present within tissue samples, and I hope that our histology approach will complement these analyses.

VS-4718 treatment of the cell models in **Table 9.1** raised several questions that require further investigation. Firstly, long-term analysis of Met01 tumour growth with VS-4718 treatment is required to determine the outcome of VS-4718 treatment in this model. Furthermore to understand whether VS-4718's control of the Met01 tumour growth is immune mediated, and if 'rebound' or resistance can occur upon prolonged drug treatment, further work will include immune phenotyping Met01 tumours, comparing tumours at both early and later time points. This would also include T-cell depletion studies. Secondly, I have derived cells from SCC 7.1 tumours that appear to 'rebound' following VS-4718 treatment. Further characterization of these cells will identify whether re-occurrence of tumour growth was as a consequence of acquired resistance to VS-4718 treatment or whether other mechanisms within the tumour microenvironment, independent of FAK, were responsible. These mechanisms could include the upregulation of PD-1 and other co-inhibitory molecules, and through FACS analysis this hypothesis will be tested.

Finally, further investigation will take place into chemokine and cytokine regulation, using our unique forward phase protein arrays, currently under development and generated using our Aushon BioSystems' 2470 array printing platform. Current commercially available arrays typically include only a select few chemokines and cytokines, may only be used to analyze one sample per array and do not contain controls for the validation of analyte binding. The Aushon BioSystems' 2470 array printing platform has the capacity to generate forward phase protein microarrays that cover a much more extensive range of chemokines, cytokines and growth factors and that contain dilution series of each printed anybody for the validation and quantification of analyte binding. Using this microarray-printing platform in combination with a ArrayIt Innoscan 710 high-resolution microarray scanner, miniaturization of current available arrays occurs to such an extent that the levels of chemokines, cytokines and growth factors can be determined in multiple samples on each array simultaneously. When completed, these arrays will be able to monitor the status of chemokines and cytokine for both lab-based studies, with the ultimate goal of utilizing this technology within the clinical trial.

12 References

1 Stewart, B. W., Wild, C., International Agency for Research on Cancer & World Health Organization. *World cancer report 2014*. (International Agency for Research on Cancer, WHO Press, 2014).

2 Hanahan, D. & Weinberg, R. A. The hallmarks of cancer. *Cell* **100**, 57-70 (2000).

3 Hanahan, D. & Weinberg, R. A. Hallmarks of cancer: the next generation. *Cell* **144**, 646-674, doi:10.1016/j.cell.2011.02.013 (2011).

4 Albini, A. Tumor microenvironment, a dangerous society leading to cancer metastasis. From mechanisms to therapy and prevention. *Cancer Metastasis Rev* **27**, 3-4, doi:10.1007/s10555-007-9102-y (2008).

5 Albini, A. & Sporn, M. B. The tumour microenvironment as a target for chemoprevention. *Nature reviews. Cancer* **7**, 139-147, doi:10.1038/nrc2067 (2007).

6 McClinton, S., Miller, I. D. & Eremin, O. An immunohistochemical characterisation of the inflammatory cell infiltrate in benign and malignant prostatic disease. *Br J Cancer* **61**, 400-403 (1990).

7 Dvorak, A. M., Mihm, M. C., Jr., Osage, J. E. & Dvorak, H. F. Melanoma. An ultrastructural study of the host inflammatory and vascular responses. *J Invest Dermatol* **75**, 388-393 (1980).

8 Dvorak, A. M. *et al.* Bullous pemphigoid, an ultrastructural study of the inflammatory response: eosinophil, basophil and mast cell granule changes in multiple biopsies from one patient. *J Invest Dermatol* **78**, 91-101 (1982).

9 Dvorak, H. F., Dickersin, G. R., Dvorak, A. M., Manseau, E. J. & Pyne, K. Human breast carcinoma: fibrin deposits and desmoplasia. Inflammatory cell type and distribution. Microvasculature and infarction. *J Natl Cancer Inst* **67**, 335-345 (1981).

10 Dvorak, H. F. Tumors: Wounds That Do Not Heal. *New England Journal of Medicine* **315**, 1650-1659, doi:doi:10.1056/NEJM198612253152606 (1986).

11 Liotta, L. A. & Kohn, E. C. The microenvironment of the tumour-host interface. *Nature* **411**, 375-379, doi:10.1038/35077241 (2001).

12 Wernert, N. The multiple roles of tumour stroma. *Virchows Arch* **430**, 433-443 (1997).

13 Hanahan, D. & Coussens, L. M. Accessories to the crime: functions of cells recruited to the tumor microenvironment. *Cancer Cell* **21**, 309-322, doi:10.1016/j.ccr.2012.02.022 (2012).

14 Murphy, K., Travers, P., Walport, M. & Janeway, C. *Janeway's immunobiology*. 7th edn, (Garland Science, 2008).

15 de Visser, K. E., Eichten, A. & Coussens, L. M. Paradoxical roles of the immune system during cancer development. *Nature reviews. Cancer* **6**, 24-37, doi:10.1038/nrc1782 (2006).

16 Buckley, C. D., Gilroy, D. W., Serhan, C. N., Stockinger, B. & Tak, P. P. The resolution of inflammation. *Nat Rev Immunol* **13**, 59-66, doi:10.1038/nri3362 (2013).

17 Wallace, J. L. Nitric oxide as a regulator of inflammatory processes. *Mem I Oswaldo Cruz* **100**, 5-9 (2005).

18 Gilroy, D. W., Lawrence, T., Perretti, M. & Rossi, A. G. Inflammatory resolution: new opportunities for drug discovery. *Nat Rev Drug Discov* **3**, 401-416, doi:10.1038/nrd1383 (2004).

19 Balkwill, F. & Mantovani, A. Inflammation and cancer: back to Virchow? *Lancet* **357**, 539-545, doi:10.1016/S0140-6736(00)04046-0 (2001).

20 de Martel, C. *et al.* Global burden of cancers attributable to infections in 2008: a review and synthetic analysis. *Lancet Oncol* **13**, 607-615, doi:10.1016/S1470-2045(12)70137-7 (2012).

21 Salama, N. R., Hartung, M. L. & Muller, A. Life in the human stomach: persistence strategies of the bacterial pathogen Helicobacter pylori. *Nat Rev Microbiol* **11**, 385-399, doi:10.1038/nrmicro3016 (2013).

22 Castle, P. E. *et al.* An association of cervical inflammation with high-grade cervical neoplasia in women infected with oncogenic human papillomavirus (HPV). *Cancer Epidemiol Biomarkers Prev* **10**, 1021-1027 (2001).

23 Rothenberg, S. M. & Ellisen, L. W. The molecular pathogenesis of head and neck squamous cell carcinoma. *J Clin Invest* **122**, 1951-1957 (2012).

24 Arzumanyan, A., Reis, H. M. & Feitelson, M. A. Pathogenic mechanisms in HBV- and HCV-associated hepatocellular carcinoma. *Nature reviews. Cancer* **13**, 123-135, doi:10.1038/nrc3449 (2013).

25 Dyson, J. K. & Rutter, M. D. Colorectal cancer in inflammatory bowel disease: what is the real magnitude of the risk? *World J Gastroenterol* **18**, 3839-3848, doi:10.3748/wjg.v18.i29.3839 (2012).

26 Pinho, A. V., Chantrill, L. & Rooman, I. Chronic pancreatitis: a path to pancreatic cancer. *Cancer Lett* **345**, 203-209, doi:10.1016/j.canlet.2013.08.015 (2014).

27 Jayson, G. C., Kohn, E. C., Kitchener, H. C. & Ledermann, J. A. Ovarian cancer. *Lancet* **384**, 1376-1388, doi:10.1016/S0140-6736(13)62146-7 (2014).

28 Giraldo, N. A., Becht, E., Vano, Y., Sautes-Fridman, C. & Fridman, W. H. The immune response in cancer: from immunology to pathology to immunotherapy. *Virchows Arch*, doi:10.1007/s00428-015-1787-7 (2015).

29 Chia, W. K., Ali, R. & Toh, H. C. Aspirin as adjuvant therapy for colorectal cancer--reinterpreting paradigms. *Nat Rev Clin Oncol* **9**, 561-570, doi:10.1038/nrclinonc.2012.137 (2012).

30 Basha, R. *et al.* Therapeutic applications of NSAIDS in cancer: special emphasis on tolfenamic acid. *Front Biosci (Schol Ed)* **3**, 797-805 (2011).

31 Qian, B. Z. & Pollard, J. W. Macrophage diversity enhances tumor progression and metastasis. *Cell* **141**, 39-51, doi:10.1016/j.cell.2010.03.014 (2010).

32 Mantovani, A. & Sica, A. Macrophages, innate immunity and cancer: balance, tolerance, and diversity. *Current opinion in immunology* **22**, 231-237, doi:10.1016/j.coi.2010.01.009 (2010).

33 Mittal, D., Gubin, M. M., Schreiber, R. D. & Smyth, M. J. New insights into cancer immunoediting and its three component phases--elimination, equilibrium and escape. *Current opinion in immunology* **27**, 16-25, doi:10.1016/j.coi.2014.01.004 (2014).

34 Grivennikov, S. I., Greten, F. R. & Karin, M. Immunity, inflammation, and cancer. *Cell* **140**, 883-899, doi:10.1016/j.cell.2010.01.025 (2010).

35 Ruffell, B. *et al.* Leukocyte composition of human breast cancer. *Proceedings of the National Academy of Sciences of the United States of America* **109**, 2796-2801, doi:10.1073/pnas.1104303108 (2012).

36 Mestas, J. & Hughes, C. C. Of mice and not men: differences between mouse and human immunology. *Journal of immunology* **172**, 2731-2738 (2004).

37 Biswas, S. K. & Mantovani, A. Macrophage plasticity and interaction with lymphocyte subsets: cancer as a paradigm. *Nat Immunol* **11**, 889-896, doi:10.1038/ni.1937 (2010).

38 Ostuni, R., Kratochvill, F., Murray, P. J. & Natoli, G. Macrophages and cancer: from mechanisms to therapeutic implications. *Trends Immunol* **36**, 229-239, doi:10.1016/j.it.2015.02.004 (2015).

39 Lawrence, T. & Natoli, G. Transcriptional regulation of macrophage polarization: enabling diversity with identity. *Nat Rev Immunol* **11**, 750-761, doi:10.1038/nri3088 (2011).

40 Ostuni, R. & Natoli, G. Transcriptional control of macrophage diversity and specialization. *European journal of immunology* **41**, 2486-2490, doi:10.1002/eji.201141706 (2011).

41 Martinez, F. O., Helming, L. & Gordon, S. Alternative activation of macrophages: an immunologic functional perspective. *Annu Rev Immunol* **27**, 451-483, doi:10.1146/annurev.immunol.021908.132532 (2009).

42 Steidl, C. *et al.* Tumor-associated macrophages and survival in classic Hodgkin's lymphoma. *The New England journal of medicine* **362**, 875-885, doi:10.1056/NEJMoa0905680 (2010).

43 Bingle, L., Brown, N. J. & Lewis, C. E. The role of tumour-associated macrophages in tumour progression: implications for new anticancer therapies. *J Pathol* **196**, 254-265, doi:10.1002/path.1027 (2002).

44 Balkwill, F., Charles, K. A. & Mantovani, A. Smoldering and polarized inflammation in the initiation and promotion of malignant disease. *Cancer Cell* **7**, 211-217, doi:10.1016/j.ccr.2005.02.013 (2005).

45 Porta, C. *et al.* Tolerance and M2 (alternative) macrophage polarization are related processes orchestrated by p50 nuclear factor kappaB. *Proceedings of the National Academy of Sciences of the United States of America* **106**, 14978-14983, doi:10.1073/pnas.0809784106 (2009).

46 Yu, H., Kortylewski, M. & Pardoll, D. Crosstalk between cancer and immune cells: role of STAT3 in the tumour microenvironment. *Nat Rev Immunol* **7**, 41-51, doi:10.1038/nri1995 (2007).

47 Karin, M. & Greten, F. R. NF-kappaB: linking inflammation and immunity to cancer development and progression. *Nat Rev Immunol* **5**, 749-759, doi:10.1038/nri1703 (2005).

48 Greten, F. R. *et al.* IKKbeta links inflammation and tumorigenesis in a mouse model of colitis-associated cancer. *Cell* **118**, 285-296, doi:10.1016/j.cell.2004.07.013 (2004).

49 Pang, B. *et al.* Lipid peroxidation dominates the chemistry of DNA adduct formation in a mouse model of inflammation. *Carcinogenesis* **28**, 1807-1813, doi:10.1093/carcin/bgm037 (2007).

50 Meira, L. B. *et al.* DNA damage induced by chronic inflammation contributes to colon carcinogenesis in mice. *J Clin Invest* **118**, 2516-2525, doi:10.1172/JCI35073 (2008).

51 Filler, R. B., Roberts, S. J. & Girardi, M. Cutaneous two-stage chemical carcinogenesis. *CSH Protoc* **2007**, pdb prot4837, doi:10.1101/pdb.prot4837 (2007).

52 Balkwill, F. Tumour necrosis factor and cancer. *Nature reviews. Cancer* **9**, 361-371, doi:10.1038/nrc2628 (2009).

53 Gordon, S. Alternative activation of macrophages. *Nat Rev Immunol* **3**, 23-35, doi:10.1038/nri978 (2003).

54 Pollard, J. W. Trophic macrophages in development and disease. *Nat Rev Immunol* **9**, 259-270, doi:10.1038/nri2528 (2009).

55 Pollard, J. W. Tumour-educated macrophages promote tumour progression and metastasis. *Nature reviews. Cancer* **4**, 71-78, doi:10.1038/nrc1256 (2004).

56 Saccani, A. *et al.* p50 nuclear factor-kappaB overexpression in tumor-associated macrophages inhibits M1 inflammatory responses and antitumor resistance. *Cancer research* **66**, 11432-11440, doi:10.1158/0008-5472.CAN-06-1867 (2006).

57 Lewis, C. E. & Pollard, J. W. Distinct role of macrophages in different tumor microenvironments. *Cancer research* **66**, 605-612, doi:10.1158/0008-5472.CAN-05-4005 (2006).

58 Lin, E. Y. *et al.* Progression to malignancy in the polyoma middle T oncoprotein mouse breast cancer model provides a reliable model for human diseases. *Am J Pathol* **163**, 2113-2126, doi:10.1016/S0002-9440(10)63568-7 (2003).

59 Lin, E. Y. *et al.* Macrophages regulate the angiogenic switch in a mouse model of breast cancer. *Cancer research* **66**, 11238-11246, doi:10.1158/0008-5472.CAN-06-1278 (2006).

60 Zumsteg, A. & Christofori, G. Corrupt policemen: inflammatory cells promote tumor angiogenesis. *Curr Opin Oncol* **21**, 60-70, doi:10.1097/CCO.0b013e32831bed7e (2009).

61 Lin, E. Y., Nguyen, A. V., Russell, R. G. & Pollard, J. W. Colony-stimulating factor 1 promotes progression of mammary tumors to malignancy. *The Journal of experimental medicine* **193**, 727-740 (2001).

62 Lin, E. Y. & Pollard, J. W. Tumor-associated macrophages press the angiogenic switch in breast cancer. *Cancer research* **67**, 5064-5066, doi:10.1158/0008-5472.CAN-07-0912 (2007).

63 Leek, R. D. & Harris, A. L. Tumor-associated macrophages in breast cancer. *J Mammary Gland Biol Neoplasia* **7**, 177-189 (2002).

64 De Palma, M. *et al.* Tumor-targeted interferon-alpha delivery by Tie2-expressing monocytes inhibits tumor growth and metastasis. *Cancer Cell* **14**, 299-311, doi:10.1016/j.ccr.2008.09.004 (2008).

65 De Palma, M. *et al.* Tie2 identifies a hematopoietic lineage of proangiogenic monocytes required for tumor vessel formation and a mesenchymal population of pericyte progenitors. *Cancer Cell* **8**, 211-226, doi:10.1016/j.ccr.2005.08.002 (2005).

66 Ojalvo, L. S., King, W., Cox, D. & Pollard, J. W. High-density gene expression analysis of tumor-associated macrophages from mouse mammary tumors. *Am J Pathol* **174**, 1048-1064, doi:10.2353/ajpath.2009.080676 (2009).

67 Pucci, F. *et al.* A distinguishing gene signature shared by tumor-infiltrating Tie2-expressing monocytes, blood "resident" monocytes, and embryonic macrophages suggests common functions and developmental relationships. *Blood* **114**, 901-914, doi:10.1182/blood-2009-01-200931 (2009).

68 Fantin, A. *et al.* Tissue macrophages act as cellular chaperones for vascular anastomosis downstream of VEGF-mediated endothelial tip cell induction. *Blood* **116**, 829-840, doi:10.1182/blood-2009-12-257832 (2010).

69 Mazzieri, R. *et al.* Targeting the ANG2/TIE2 axis inhibits tumor growth and metastasis by impairing angiogenesis and disabling rebounds of proangiogenic myeloid cells. *Cancer Cell* **19**, 512-526, doi:10.1016/j.ccr.2011.02.005 (2011).

70 Condeelis, J. & Pollard, J. W. Macrophages: obligate partners for tumor cell migration, invasion, and metastasis. *Cell* **124**, 263-266, doi:10.1016/j.cell.2006.01.007 (2006).

71 Wyckoff, J. *et al.* A paracrine loop between tumor cells and macrophages is required for tumor cell migration in mammary tumors. *Cancer research* **64**, 7022-7029, doi:10.1158/0008-5472.CAN-04-1449 (2004).

72 Wyckoff, J. B. *et al.* Direct visualization of macrophage-assisted tumor cell intravasation in mammary tumors. *Cancer research* **67**, 2649-2656, doi:10.1158/0008-5472.CAN-06-1823 (2007).

73 Qian, B. Z. *et al.* CCL2 recruits inflammatory monocytes to facilitate breast-tumour metastasis. *Nature* **475**, 222-225, doi:10.1038/nature10138 (2011).

74 Qian, J. *et al.* Aberrant methylation of GTPase regulator associated with the focal adhesion kinase (GRAF) promoter is an adverse prognostic factor in myelodysplastic syndrome. *Eur J Haematol* **85**, 174-176, doi:10.1111/j.1600-0609.2010.01453.x (2010).

75 Bonapace, L. *et al.* Cessation of CCL2 inhibition accelerates breast cancer metastasis by promoting angiogenesis. *Nature* **515**, 130-133, doi:10.1038/nature13862 (2014).

76 Cortez-Retamozo, V. *et al.* Origins of tumor-associated macrophages and neutrophils. *Proceedings of the National Academy of Sciences of the United States of America* **109**, 2491-2496, doi:10.1073/pnas.1113744109 (2012).

77 Wiktor-Jedrzejczak, W. W., Ahmed, A., Szczylik, C. & Skelly, R. R. Hematological characterization of congenital osteopetrosis in op/op mouse. Possible mechanism for abnormal macrophage differentiation. *The Journal of experimental medicine* **156**, 1516-1527 (1982).

78 Fogg, D. K. *et al.* A clonogenic bone marrow progenitor specific for macrophages and dendritic cells. *Science* **311**, 83-87, doi:10.1126/science.1117729 (2006).

79 Valledor, A. F., Borras, F. E., Cullell-Young, M. & Celada, A. Transcription factors that regulate monocyte/macrophage differentiation. *J Leukoc Biol* **63**, 405-417 (1998).

80 Richards, D. M., Hettinger, J. & Feuerer, M. Monocytes and macrophages in cancer: development and functions. *Cancer Microenviron* **6**, 179-191, doi:10.1007/s12307-012-0123-x (2013).

81 Houthuijzen, J. M. *et al.* Lysophospholipids secreted by splenic macrophages induce chemotherapy resistance via interference with the DNA damage response. *Nat Commun* **5**, 5275, doi:10.1038/ncomms6275 (2014).

82 De Palma, M. & Lewis, C. E. Macrophage regulation of tumor responses to anticancer therapies. *Cancer Cell* **23**, 277-286, doi:10.1016/j.ccr.2013.02.013 (2013).

83 Mantovani, A., Polentarutti, N., Luini, W., Peri, G. & Spreafico, F. Role of host defense merchanisms in the antitumor activity of adriamycin and daunomycin in mice. *J Natl Cancer Inst* **63**, 61-66 (1979).

84 Kodumudi, K. N. *et al.* A novel chemoimmunomodulating property of docetaxel: suppression of myeloid-derived suppressor cells in tumor bearers.

Clin Cancer Res **16**, 4583-4594, doi:10.1158/1078-0432.CCR-10-0733 (2010).

85 Germano, G. *et al.* Role of macrophage targeting in the antitumor activity of trabectedin. *Cancer Cell* **23**, 249-262, doi:10.1016/j.ccr.2013.01.008 (2013).

86 Bruchard, M. *et al.* Chemotherapy-triggered cathepsin B release in myeloid-derived suppressor cells activates the Nlrp3 inflammasome and promotes tumor growth. *Nat Med* **19**, 57-64, doi:10.1038/nm.2999 (2013).

87 DeNardo, D. G. *et al.* Leukocyte complexity predicts breast cancer survival and functionally regulates response to chemotherapy. *Cancer Discov* **1**, 54-67, doi:10.1158/2159-8274.CD-10-0028 (2011).

88 Shree, T. *et al.* Macrophages and cathepsin proteases blunt chemotherapeutic response in breast cancer. *Genes & development* **25**, 2465-2479, doi:10.1101/gad.180331.111 (2011).

89 Milas, L., Wike, J., Hunter, N., Volpe, J. & Basic, I. Macrophage content of murine sarcomas and carcinomas: associations with tumor growth parameters and tumor radiocurability. *Cancer research* **47**, 1069-1075 (1987).

90 Xu, J. *et al.* CSF1R signaling blockade stanches tumor-infiltrating myeloid cells and improves the efficacy of radiotherapy in prostate cancer. *Cancer research* **73**, 2782-2794, doi:10.1158/0008-5472.CAN-12-3981 (2013).

91 Ahn, G. O. *et al.* Inhibition of Mac-1 (CD11b/CD18) enhances tumor response to radiation by reducing myeloid cell recruitment. *Proceedings of the National Academy of Sciences of the United States of America* **107**, 8363-8368, doi:10.1073/pnas.0911378107 (2010).

92 Hughes, R. *et al.* Perivascular M2 Macrophages Stimulate Tumor Relapse after Chemotherapy. *Cancer research* **75**, 3479-3491, doi:10.1158/0008-5472.CAN-14-3587 (2015).

93 Jiang, Y., Li, Y. & Zhu, B. T-cell exhaustion in the tumor microenvironment. *Cell Death Dis* **6**, e1792, doi:10.1038/cddis.2015.162 (2015).

94 Okkenhaug, K., Bilancio, A., Emery, J. L. & Vanhaesebroeck, B. Phosphoinositide 3-kinase in T cell activation and survival. *Biochem Soc Trans* **32**, 332-335, doi:10.1042/ (2004).

95 Wherry, E. J. & Ahmed, R. Memory CD8 T-cell differentiation during viral infection. *J Virol* **78**, 5535-5545, doi:10.1128/JVI.78.11.5535-5545.2004 (2004).

96 Kaech, S. M., Wherry, E. J. & Ahmed, R. Effector and memory T-cell differentiation: implications for vaccine development. *Nat Rev Immunol* **2**, 251-262, doi:10.1038/nri778 (2002).

97 Kaech, S. M. & Ahmed, R. Memory CD8+ T cell differentiation: initial antigen encounter triggers a developmental program in naive cells. *Nat Immunol* **2**, 415-422, doi:10.1038/87720 (2001).

98 Schluns, K. S. & Lefrancois, L. Cytokine control of memory T-cell development and survival. *Nat Rev Immunol* **3**, 269-279, doi:10.1038/nri1052 (2003).

99 Blankenstein, T., Coulie, P. G., Gilboa, E. & Jaffee, E. M. The determinants of tumour immunogenicity. *Nature reviews. Cancer* **12**, 307-313, doi:10.1038/nrc3246 (2012).

100 Willimsky, G. *et al.* Immunogenicity of premalignant lesions is the primary cause of general cytotoxic T lymphocyte unresponsiveness. *The Journal of experimental medicine* **205**, 1687-1700, doi:10.1084/jem.20072016 (2008).

101 Huppa, J. B. & Davis, M. M. T-cell-antigen recognition and the immunological synapse. *Nat Rev Immunol* **3**, 973-983, doi:10.1038/nri1245 (2003).

102 Banchereau, J. & Steinman, R. M. Dendritic cells and the control of immunity. *Nature* **392**, 245-252, doi:10.1038/32588 (1998).

103 Hivroz, C., Chemin, K., Tourret, M. & Bohineust, A. Crosstalk between T Lymphocytes and Dendritic Cells. **32**, 139-155, doi:10.1615/CritRevImmunol.v32.i2.30 (2012).

104 Pardoll, D. M. The blockade of immune checkpoints in cancer immunotherapy. *Nat Rev Cancer* **12**, 252-264, doi:10.1038/nrc3239 (2012).

105 Linard, B. *et al.* A ras-mutated peptide targeted by CTL infiltrating a human melanoma lesion. *Journal of immunology* **168**, 4802-4808 (2002).

106 Sharkey, M. S., Lizee, G., Gonzales, M. I., Patel, S. & Topalian, S. L. CD4(+) T-cell recognition of mutated B-RAF in melanoma patients harboring the V599E mutation. *Cancer research* **64**, 1595-1599 (2004).

107 Wolfel, T. *et al.* A p16INK4a-insensitive CDK4 mutant targeted by cytolytic T lymphocytes in a human melanoma. *Science* **269**, 1281-1284 (1995).

108 Gjertsen, M. K., Bjorheim, J., Saeterdal, I., Myklebust, J. & Gaudernack, G. Cytotoxic CD4+ and CD8+ T lymphocytes, generated by mutant p21-ras (12Val) peptide vaccination of a patient, recognize 12Val-dependent nested epitopes present within the vaccine peptide and kill autologous tumour cells carrying this mutation. *International journal of cancer. Journal international du cancer* **72**, 784-790 (1997).

109 Bosch, G. J., Joosten, A. M., Kessler, J. H., Melief, C. J. & Leeksma, O. C. Recognition of BCR-ABL positive leukemic blasts by human CD4+ T cells elicited by primary in vitro immunization with a BCR-ABL breakpoint peptide. *Blood* **88**, 3522-3527 (1996).

110 Makita, M. *et al.* Leukemia-associated fusion proteins, dek-can and bcr-abl, represent immunogenic HLA-DR-restricted epitopes recognized by fusion peptide-specific CD4+ T lymphocytes. *Leukemia* **16**, 2400-2407, doi:10.1038/sj.leu.2402742 (2002).

111 Yotnda, P. *et al.* Cytotoxic T cell response against the chimeric p210 BCR-ABL protein in patients with chronic myelogenous leukemia. *J Clin Invest* **101**, 2290-2296, doi:10.1172/JCI488 (1998).

112 Kim, P. S. & Ahmed, R. Features of responding T cells in cancer and chronic infection. *Current opinion in immunology* **22**, 223-230, doi:10.1016/j.coi.2010.02.005 (2010).

113 Qi, Q. & August, A. Keeping the (kinase) party going: SLP-76 and ITK dance to the beat. *Sci STKE* **2007**, pe39, doi:10.1126/stke.3962007pe39 (2007).

114 Milstein, O. *et al.* CTLs respond with activation and granule secretion when serving as targets for T-cell recognition. *Blood* **117**, 1042-1052, doi:10.1182/blood-2010-05-283770 (2011).

115 Chaudhry, A. & Rudensky, A. Y. Control of inflammation by integration of environmental cues by regulatory T cells. *J Clin Invest* **123**, 939-944, doi:10.1172/JCI57175 (2013).

116 Szabo, S. J. *et al.* Distinct effects of T-bet in TH1 lineage commitment and IFN-gamma production in CD4 and CD8 T cells. *Science* **295**, 338-342, doi:10.1126/science.1065543 (2002).

117 Kim, H. J. & Cantor, H. CD4 T-cell subsets and tumor immunity: the helpful and the not-so-helpful. *Cancer Immunol Res* **2**, 91-98, doi:10.1158/2326-6066.CIR-13-0216 (2014).

118 Hoyler, T. *et al.* The transcription factor GATA-3 controls cell fate and maintenance of type 2 innate lymphoid cells. *Immunity* **37**, 634-648, doi:10.1016/j.immuni.2012.06.020 (2012).

119 Tepper, R. I., Coffman, R. L. & Leder, P. An eosinophil-dependent mechanism for the antitumor effect of interleukin-4. *Science* **257**, 548-551 (1992).

120 Tepper, R. I., Pattengale, P. K. & Leder, P. Murine interleukin-4 displays potent anti-tumor activity in vivo. *Cell* **57**, 503-512 (1989).

121 Tatsumi, T. *et al.* Disease-associated bias in T helper type 1 (Th1)/Th2 CD4(+) T cell responses against MAGE-6 in HLA-DRB10401(+) patients with renal cell carcinoma or melanoma. *The Journal of experimental medicine* **196**, 619-628 (2002).

122 Bettelli, E. *et al.* Reciprocal developmental pathways for the generation of pathogenic effector TH17 and regulatory T cells. *Nature* **441**, 235-238, doi:10.1038/nature04753 (2006).

123 Lee, Y. *et al.* Induction and molecular signature of pathogenic TH17 cells. *Nat Immunol* **13**, 991-999, doi:10.1038/ni.2416 (2012).

124 Miyahara, Y. *et al.* Generation and regulation of human CD4+ IL-17-producing T cells in ovarian cancer. *Proceedings of the National Academy of Sciences of the United States of America* **105**, 15505-15510, doi:10.1073/pnas.0710686105 (2008).

125 Zhang, B. *et al.* The prevalence of Th17 cells in patients with gastric cancer. *Biochem Biophys Res Commun* **374**, 533-537, doi:10.1016/j.bbrc.2008.07.060 (2008).

126 Sfanos, K. S. *et al.* Phenotypic analysis of prostate-infiltrating lymphocytes reveals TH17 and Treg skewing. *Clin Cancer Res* **14**, 3254-3261, doi:10.1158/1078-0432.CCR-07-5164 (2008).

127 Kryczek, I. *et al.* Cutting edge: Th17 and regulatory T cell dynamics and the regulation by IL-2 in the tumor microenvironment. *Journal of immunology* **178**, 6730-6733 (2007).

128 Langowski, J. L. *et al.* IL-23 promotes tumour incidence and growth. *Nature* **442**, 461-465, doi:10.1038/nature04808 (2006).

129 Numasaki, M. *et al.* IL-17 enhances the net angiogenic activity and in vivo growth of human non-small cell lung cancer in SCID mice through promoting CXCR-2-dependent angiogenesis. *Journal of immunology* **175**, 6177-6189 (2005).

130 Tartour, E. *et al.* Interleukin 17, a T-cell-derived cytokine, promotes tumorigenicity of human cervical tumors in nude mice. *Cancer research* **59**, 3698-3704 (1999).

131 Muranski, P. *et al.* Th17 cells are long lived and retain a stem cell-like molecular signature. *Immunity* **35**, 972-985, doi:10.1016/j.immuni.2011.09.019 (2011).

132 Muranski, P. & Restifo, N. P. Essentials of Th17 cell commitment and plasticity. *Blood* **121**, 2402-2414, doi:10.1182/blood-2012-09-378653 (2013).

133 Hinterberger, M. *et al.* Autonomous role of medullary thymic epithelial cells in central CD4(+) T cell tolerance. *Nat Immunol* **11**, 512-519, doi:10.1038/ni.1874 (2010).

134 Pacholczyk, R., Ignatowicz, H., Kraj, P. & Ignatowicz, L. Origin and T cell receptor diversity of Foxp3+CD4+CD25+ T cells. *Immunity* **25**, 249-259, doi:10.1016/j.immuni.2006.05.016 (2006).

135 Burchill, M. A. *et al.* Linked T cell receptor and cytokine signaling govern the development of the regulatory T cell repertoire. *Immunity* **28**, 112-121, doi:10.1016/j.immuni.2007.11.022 (2008).

136 Lio, C. W. & Hsieh, C. S. A two-step process for thymic regulatory T cell development. *Immunity* **28**, 100-111, doi:10.1016/j.immuni.2007.11.021 (2008).

137 Tan, M. C. *et al.* Disruption of CCR5-dependent homing of regulatory T cells inhibits tumor growth in a murine model of pancreatic cancer. *Journal of immunology* **182**, 1746-1755 (2009).

138 Chang, L. Y. *et al.* Tumor-derived chemokine CCL5 enhances TGF-beta-mediated killing of CD8(+) T cells in colon cancer by T-regulatory cells. *Cancer research* **72**, 1092-1102, doi:10.1158/0008-5472.CAN-11-2493 (2012).

139 Josefowicz, S. Z., Lu, L. F. & Rudensky, A. Y. Regulatory T cells: mechanisms of differentiation and function. *Annu Rev Immunol* **30**, 531-564, doi:10.1146/annurev.immunol.25.022106.141623 (2012).

140 Shevach, E. M. & Thornton, A. M. tTregs, pTregs, and iTregs: similarities and differences. *Immunological reviews* **259**, 88-102, doi:10.1111/imr.12160 (2014).

141 Pot, C., Apetoh, L. & Kuchroo, V. K. Type 1 regulatory T cells (Tr1) in autoimmunity. *Semin Immunol* **23**, 202-208, doi:10.1016/j.smim.2011.07.005 (2011).

142 Boon, T., Cerottini, J. C., Van den Eynde, B., van der Bruggen, P. & Van Pel, A. Tumor antigens recognized by T lymphocytes. *Annu Rev Immunol* **12**, 337-365, doi:10.1146/annurev.iy.12.040194.002005 (1994).

143 Chappert, P. & Schwartz, R. H. Induction of T cell anergy: integration of environmental cues and infectious tolerance. *Current opinion in immunology* **22**, 552-559, doi:10.1016/j.coi.2010.08.005 (2010).

144 Xing, Y. & Hogquist, K. A. T-cell tolerance: central and peripheral. *Cold Spring Harb Perspect Biol* **4**, doi:10.1101/cshperspect.a006957 (2012).

145 Powell, J. D. & Delgoffe, G. M. The mammalian target of rapamycin: linking T cell differentiation, function, and metabolism. *Immunity* **33**, 301-311, doi:10.1016/j.immuni.2010.09.002 (2010).

146 Zheng, Y., Delgoffe, G. M., Meyer, C. F., Chan, W. & Powell, J. D. Anergic T cells are metabolically anergic. *Journal of immunology* **183**, 6095-6101, doi:10.4049/jimmunol.0803510 (2009).

147 Keir, M. E., Butte, M. J., Freeman, G. J. & Sharpe, A. H. PD-1 and its ligands in tolerance and immunity. *Annu Rev Immunol* **26**, 677-704, doi:10.1146/annurev.immunol.26.021607.090331 (2008).

148 Nishimura, H., Nose, M., Hiai, H., Minato, N. & Honjo, T. Development of lupus-like autoimmune diseases by disruption of the PD-1 gene encoding an ITIM motif-carrying immunoreceptor. *Immunity* **11**, 141-151 (1999).

149 Nishimura, H. *et al.* Autoimmune dilated cardiomyopathy in PD-1 receptor-deficient mice. *Science* **291**, 319-322, doi:10.1126/science.291.5502.319 (2001).

150 Guleria, I. *et al.* A critical role for the programmed death ligand 1 in fetomaternal tolerance. *The Journal of experimental medicine* **202**, 231-237, doi:10.1084/jem.20050019 (2005).

151 Anderson, M. S. & Bluestone, J. A. The NOD mouse: a model of immune dysregulation. *Annu Rev Immunol* **23**, 447-485, doi:10.1146/annurev.immunol.23.021704.115643 (2005).

152 Delovitch, T. L. & Singh, B. The nonobese diabetic mouse as a model of autoimmune diabetes: immune dysregulation gets the NOD. *Immunity* **7**, 727-738 (1997).

153 Salama, A. D. *et al.* Critical role of the programmed death-1 (PD-1) pathway in regulation of experimental autoimmune encephalomyelitis. *The Journal of experimental medicine* **198**, 71-78, doi:10.1084/jem.20022119 (2003).

154 Wherry, E. J. T cell exhaustion. *Nat Immunol* **12**, 492-499 (2011).

155 Blackburn, S. D. *et al.* Coregulation of CD8+ T cell exhaustion by multiple inhibitory receptors during chronic viral infection. *Nat Immunol* **10**, 29-37, doi:10.1038/ni.1679 (2009).

156 Grosso, J. F. *et al.* Functionally distinct LAG-3 and PD-1 subsets on activated and chronically stimulated CD8 T cells. *Journal of immunology* **182**, 6659-6669, doi:10.4049/jimmunol.0804211 (2009).

157 Tivol, E. A. *et al.* Loss of CTLA-4 leads to massive lymphoproliferation and fatal multiorgan tissue destruction, revealing a critical negative regulatory role of CTLA-4. *Immunity* **3**, 541-547 (1995).

158 Dolcetti, L. *et al.* Hierarchy of immunosuppressive strength among myeloid-derived suppressor cell subsets is determined by GM-CSF. *European journal of immunology* **40**, 22-35, doi:10.1002/eji.200939903 (2010).

159 Youn, J. I., Nagaraj, S., Collazo, M. & Gabrilovich, D. I. Subsets of myeloid-derived suppressor cells in tumor-bearing mice. *Journal of immunology* **181**, 5791-5802 (2008).

160 Movahedi, K. *et al.* Identification of discrete tumor-induced myeloid-derived suppressor cell subpopulations with distinct T cell-suppressive activity. *Blood* **111**, 4233-4244, doi:10.1182/blood-2007-07-099226 (2008).

161 Mandruzzato, S. *et al.* IL4Ralpha+ myeloid-derived suppressor cell expansion in cancer patients. *Journal of immunology* **182**, 6562-6568, doi:10.4049/jimmunol.0803831 (2009).

162 Khattri, R., Cox, T., Yasayko, S. A. & Ramsdell, F. An essential role for Scurfin in CD4+CD25+ T regulatory cells. *Nat Immunol* **4**, 337-342, doi:10.1038/ni909 (2003).

163 Fontenot, J. D., Gavin, M. A. & Rudensky, A. Y. Foxp3 programs the development and function of CD4+CD25+ regulatory T cells. *Nat Immunol* **4**, 330-336, doi:10.1038/ni904 (2003).

164 Lin, W. *et al.* Regulatory T cell development in the absence of functional Foxp3. *Nat Immunol* **8**, 359-368, doi:10.1038/ni1445 (2007).

165 Wan, Y. Y. & Flavell, R. A. Regulatory T-cell functions are subverted and converted owing to attenuated Foxp3 expression. *Nature* **445**, 766-770, doi:10.1038/nature05479 (2007).

166 Gavin, M. A. *et al.* Foxp3-dependent programme of regulatory T-cell differentiation. *Nature* **445**, 771-775, doi:10.1038/nature05543 (2007).

167 Schmidt, A., Oberle, N. & Krammer, P. H. Molecular mechanisms of treg-mediated T cell suppression. *Frontiers in immunology* **3**, 51, doi:10.3389/fimmu.2012.00051 (2012).

168 Pandiyan, P., Zheng, L. X., Ishihara, S., Reed, J. & Lenardo, M. J. CD4(+) CD25(+) Foxp3(+) regulatory T cells induce cytokine deprivation -mediated apoptosis of effector CD4(+) T cells. *Nature Immunology* **8**, 1353-1362, doi:10.1038/ni1536 (2007).

169 Friedline, R. H. *et al.* CD4+ regulatory T cells require CTLA-4 for the maintenance of systemic tolerance. *The Journal of experimental medicine* **206**, 421-434, doi:10.1084/jem.20081811 (2009).

170 Wing, K. *et al.* CTLA-4 control over Foxp3+ regulatory T cell function. *Science* **322**, 271-275, doi:10.1126/science.1160062 (2008).

171 Kim, J. M., Rasmussen, J. P. & Rudensky, A. Y. Regulatory T cells prevent catastrophic autoimmunity throughout the lifespan of mice. *Nat Immunol* **8**, 191-197, doi:10.1038/ni1428 (2007).

172 Qureshi, O. S. *et al.* Trans-endocytosis of CD80 and CD86: a molecular basis for the cell-extrinsic function of CTLA-4. *Science* **332**, 600-603, doi:10.1126/science.1202947 (2011).

173 Fallarino, F. *et al.* Modulation of tryptophan catabolism by regulatory T cells. *Nat Immunol* **4**, 1206-1212, doi:10.1038/ni1003 (2003).

174 Fallarino, F. *et al.* T cell apoptosis by kynurenines. *Adv Exp Med Biol* **527**, 183-190 (2003).

175 Borsellino, G. *et al.* Expression of ectonucleotidase CD39 by Foxp3+ Treg cells: hydrolysis of extracellular ATP and immune suppression. *Blood* **110**, 1225-1232, doi:10.1182/blood-2006-12-064527 (2007).

176 Kobie, J. J. *et al.* T regulatory and primed uncommitted CD4 T cells express CD73, which suppresses effector CD4 T cells by converting 5'-adenosine monophosphate to adenosine. *Journal of immunology* **177**, 6780-6786 (2006).

177 Ernst, P. B., Garrison, J. C. & Thompson, L. F. Much ado about adenosine: adenosine synthesis and function in regulatory T cell biology. *Journal of immunology* **185**, 1993-1998, doi:10.4049/jimmunol.1000108 (2010).

178 Ormandy, L. A. *et al.* Increased populations of regulatory T cells in peripheral blood of patients with hepatocellular carcinoma. *Cancer research* **65**, 2457-2464, doi:10.1158/0008-5472.CAN-04-3232 (2005).

179 Wolf, A. M. *et al.* Increase of regulatory T cells in the peripheral blood of cancer patients. *Clin Cancer Res* **9**, 606-612 (2003).

180 Schaefer, C. *et al.* Characteristics of CD4+CD25+ regulatory T cells in the peripheral circulation of patients with head and neck cancer. *Br J Cancer* **92**, 913-920, doi:10.1038/sj.bjc.6602407 (2005).

181 Liyanage, U. K. *et al.* Prevalence of regulatory T cells is increased in peripheral blood and tumor microenvironment of patients with pancreas or breast adenocarcinoma. *Journal of immunology* **169**, 2756-2761 (2002).

182 Hiraoka, N., Onozato, K., Kosuge, T. & Hirohashi, S. Prevalence of FOXP3+ regulatory T cells increases during the progression of pancreatic ductal

adenocarcinoma and its premalignant lesions. *Clin Cancer Res* **12**, 5423-5434, doi:10.1158/1078-0432.CCR-06-0369 (2006).

183 Sasada, T., Kimura, M., Yoshida, Y., Kanai, M. & Takabayashi, A. CD4+CD25+ regulatory T cells in patients with gastrointestinal malignancies: possible involvement of regulatory T cells in disease progression. *Cancer* **98**, 1089-1099, doi:10.1002/cncr.11618 (2003).

184 Curiel, T. J. *et al.* Specific recruitment of regulatory T cells in ovarian carcinoma fosters immune privilege and predicts reduced survival. *Nat Med* **10**, 942-949, doi:10.1038/nm1093 (2004).

185 Sato, E. *et al.* Intraepithelial CD8+ tumor-infiltrating lymphocytes and a high CD8+/regulatory T cell ratio are associated with favorable prognosis in ovarian cancer. *Proceedings of the National Academy of Sciences of the United States of America* **102**, 18538-18543, doi:10.1073/pnas.0509182102 (2005).

186 Bates, G. J. *et al.* Quantification of regulatory T cells enables the identification of high-risk breast cancer patients and those at risk of late relapse. *J Clin Oncol* **24**, 5373-5380, doi:10.1200/JCO.2006.05.9584 (2006).

187 Carmeliet, P. & Jain, R. K. Molecular mechanisms and clinical applications of angiogenesis. *Nature* **473**, 298-307, doi:10.1038/nature10144 (2011).

188 Carmeliet, P. & Jain, R. K. Angiogenesis in cancer and other diseases. *Nature* **407**, 249-257, doi:10.1038/35025220 (2000).

189 Carmeliet, P. & Jain, R. K. Principles and mechanisms of vessel normalization for cancer and other angiogenic diseases. *Nat Rev Drug Discov* **10**, 417-427, doi:10.1038/nrd3455 (2011).

190 Chi, A. S., Sorensen, A. G., Jain, R. K. & Batchelor, T. T. Angiogenesis as a therapeutic target in malignant gliomas. *Oncologist* **14**, 621-636, doi:10.1634/theoncologist.2008-0272 (2009).

191 Crawford, Y. *et al.* PDGF-C mediates the angiogenic and tumorigenic properties of fibroblasts associated with tumors refractory to anti-VEGF treatment. *Cancer Cell* **15**, 21-34, doi:10.1016/j.ccr.2008.12.004 (2009).

192 Folkman, J. Tumor angiogenesis: therapeutic implications. *The New England journal of medicine* **285**, 1182-1186, doi:10.1056/nejm197111182852108 (1971).

193 Hanahan, D. & Folkman, J. Patterns and emerging mechanisms of the angiogenic switch during tumorigenesis. *Cell* **86**, 353-364 (1996).

194 Bergers, G., Javaherian, K., Lo, K. M., Folkman, J. & Hanahan, D. Effects of angiogenesis inhibitors on multistage carcinogenesis in mice. *Science* **284**, 808-812 (1999).

195 Nagy, J. A., Chang, S. H., Shih, S. C., Dvorak, A. M. & Dvorak, H. F. Heterogeneity of the tumor vasculature. *Semin Thromb Hemost* **36**, 321-331, doi:10.1055/s-0030-1253454 (2010).

196 Jain, R. K. Normalization of tumor vasculature: an emerging concept in antiangiogenic therapy. *Science* **307**, 58-62, doi:10.1126/science.1104819 (2005).

197 Baluk, P., Hashizume, H. & McDonald, D. M. Cellular abnormalities of blood vessels as targets in cancer. *Curr Opin Genet Dev* **15**, 102-111, doi:10.1016/j.gde.2004.12.005 (2005).

198 Gerber, H. P. & Ferrara, N. Pharmacology and pharmacodynamics of bevacizumab as monotherapy or in combination with cytotoxic therapy in preclinical studies. *Cancer research* **65**, 671-680 (2005).

199 Johnson, D. H. *et al.* Randomized phase II trial comparing bevacizumab plus carboplatin and paclitaxel with carboplatin and paclitaxel alone in previously untreated locally advanced or metastatic non-small-cell lung cancer. *J Clin Oncol* **22**, 2184-2191, doi:10.1200/JCO.2004.11.022 (2004).

200 Yang, J. C. *et al.* A randomized trial of bevacizumab, an anti-vascular endothelial growth factor antibody, for metastatic renal cancer. *The New England journal of medicine* **349**, 427-434, doi:10.1056/NEJMoa021491 (2003).

201 Ferrara, N., Hillan, K. J. & Novotny, W. Bevacizumab (Avastin), a humanized anti-VEGF monoclonal antibody for cancer therapy. *Biochem Biophys Res Commun* **333**, 328-335, doi:10.1016/j.bbrc.2005.05.132 (2005).

202 Patel, A. S. *et al.* TIE2-expressing monocytes/macrophages regulate revascularization of the ischemic limb. *EMBO Mol Med* **5**, 858-869, doi:10.1002/emmm.201302752 (2013).

203 Ohlund, D., Elyada, E. & Tuveson, D. Fibroblast heterogeneity in the cancer wound. *The Journal of experimental medicine* **211**, 1503-1523, doi:10.1084/jem.20140692 (2014).

204 Bissell, M. J. & Hines, W. C. Why don't we get more cancer? A proposed role of the microenvironment in restraining cancer progression. *Nat Med* **17**, 320-329, doi:10.1038/nm.2328 (2011).

205 Naba, A. *et al.* The matrisome: in silico definition and in vivo characterization by proteomics of normal and tumor extracellular matrices. *Mol Cell Proteomics* **11**, M111 014647, doi:10.1074/mcp.M111.014647 (2012).

206 Dolberg, D. S. & Bissell, M. J. Inability of Rous sarcoma virus to cause sarcomas in the avian embryo. *Nature* **309**, 552-556 (1984).

207 Stoker, A. W., Hatier, C. & Bissell, M. J. The embryonic environment strongly attenuates v-src oncogenesis in mesenchymal and epithelial tissues, but not in endothelia. *The Journal of cell biology* **111**, 217-228 (1990).

208 Paszek, M. J. *et al.* Tensional homeostasis and the malignant phenotype. *Cancer Cell* **8**, 241-254, doi:10.1016/j.ccr.2005.08.010 (2005).

209 Chun, T. H. *et al.* A pericellular collagenase directs the 3-dimensional development of white adipose tissue. *Cell* **125**, 577-591, doi:10.1016/j.cell.2006.02.050 (2006).

210 Cirri, P. & Chiarugi, P. Cancer associated fibroblasts: the dark side of the coin. *Am J Cancer Res* **1**, 482-497 (2011).

211 Santhanam, A. N., Baker, A. R., Hegamyer, G., Kirschmann, D. A. & Colburn, N. H. Pdcd4 repression of lysyl oxidase inhibits hypoxia-induced breast cancer cell invasion. *Oncogene* **29**, 3921-3932, doi:10.1038/onc.2010.158 (2010).

212 Juin, A. *et al.* Physiological type I collagen organization induces the formation of a novel class of linear invadosomes. *Mol Biol Cell* **23**, 297-309, doi:10.1091/mbc.E11-07-0594 (2012).

213 Barker, H. E., Cox, T. R. & Erler, J. T. The rationale for targeting the LOX family in cancer. *Nature reviews. Cancer* **12**, 540-552, doi:10.1038/nrc3319 (2012).

214 Cox, T. R. *et al.* The hypoxic cancer secretome induces pre-metastatic bone lesions through lysyl oxidase. *Nature* **522**, 106-110, doi:10.1038/nature14492 (2015).

215 Linder, S. Invadosomes at a glance. *J Cell Sci* **122**, 3009-3013, doi:10.1242/jcs.032631 (2009).

216 Plow, E. F., Haas, T. A., Zhang, L., Loftus, J. & Smith, J. W. Ligand binding to integrins. *J Biol Chem* **275**, 21785-21788, doi:10.1074/jbc.R000003200 (2000).

217 Pankov, R. & Yamada, K. M. Fibronectin at a glance. *J Cell Sci* **115**, 3861-3863 (2002).

218 Chen, S. H. *et al.* Up-regulation of fibronectin and tissue transglutaminase promotes cell invasion involving increased association with integrin and MMP expression in A431 cells. *Anticancer Res* **30**, 4177-4186 (2010).

219 Mitra, A. K. *et al.* Ligand-independent activation of c-Met by fibronectin and alpha(5)beta(1)-integrin regulates ovarian cancer invasion and metastasis. *Oncogene* **30**, 1566-1576, doi:10.1038/onc.2010.532 (2011).

220 Kobayashi, N. *et al.* Hyaluronan deficiency in tumor stroma impairs macrophage trafficking and tumor neovascularization. *Cancer research* **70**, 7073-7083, doi:10.1158/0008-5472.CAN-09-4687 (2010).

221 Zeisberg, M., Strutz, F. & Muller, G. A. Role of fibroblast activation in inducing interstitial fibrosis. *J Nephrol* **13 Suppl 3**, S111-120 (2000).

222 Eyden, B. The myofibroblast: a study of normal, reactive and neoplastic tissues, with an emphasis on ultrastructure. Part 1--normal and reactive cells. *J Submicrosc Cytol Pathol* **37**, 109-204 (2005).

223 Eyden, B. The myofibroblast: a study of normal, reactive and neoplastic tissues, with an emphasis on ultrastructure. part 2 - tumours and tumour-like lesions. *J Submicrosc Cytol Pathol* **37**, 231-296 (2005).

224 Dumont, N. *et al.* Breast fibroblasts modulate early dissemination, tumorigenesis, and metastasis through alteration of extracellular matrix characteristics. *Neoplasia* **15**, 249-262 (2013).

225 Quail, D. F. & Joyce, J. A. Microenvironmental regulation of tumor progression and metastasis. *Nat Med* **19**, 1423-1437, doi:10.1038/nm.3394 (2013).

226 Franco, O. E., Shaw, A. K., Strand, D. W. & Hayward, S. W. Cancer associated fibroblasts in cancer pathogenesis. *Semin Cell Dev Biol* **21**, 33-39, doi:10.1016/j.semcdb.2009.10.010 (2010).

227 Orimo, A. *et al.* Cancer-associated myofibroblasts possess various factors to promote endometrial tumor progression. *Clin Cancer Res* **7**, 3097-3105 (2001).

228 Erez, N., Truitt, M., Olson, P., Arron, S. T. & Hanahan, D. Cancer-Associated Fibroblasts Are Activated in Incipient Neoplasia to Orchestrate Tumor-Promoting Inflammation in an NF-kappaB-Dependent Manner. *Cancer Cell* **17**, 135-147, doi:10.1016/j.ccr.2009.12.041 (2010).

229 Fang, L., Lonsdorf, A. S. & Hwang, S. T. Immunotherapy for advanced melanoma. *J Invest Dermatol* **128**, 2596-2605, doi:10.1038/jid.2008.101 (2008).

230 Sharma, P., Wagner, K., Wolchok, J. D. & Allison, J. P. Novel cancer immunotherapy agents with survival benefit: recent successes and next steps. *Nature reviews. Cancer* **11**, 805-812, doi:10.1038/nrc3153 (2011).

231 Wolchok, J. D. & Saenger, Y. The mechanism of anti-CTLA-4 activity and the negative regulation of T-cell activation. *Oncologist* **13 Suppl 4**, 2-9, doi:10.1634/theoncologist.13-S4-2 (2008).

232 Wolchok, J. D. *et al.* Nivolumab plus ipilimumab in advanced melanoma. *The New England journal of medicine* **369**, 122-133, doi:10.1056/NEJMoa1302369 (2013).

233 Li, B. *et al.* Anti-programmed death-1 synergizes with granulocyte macrophage colony-stimulating factor--secreting tumor cell immunotherapy providing therapeutic benefit to mice with established tumors. *Clin Cancer Res* **15**, 1623-1634, doi:10.1158/1078-0432.CCR-08-1825 (2009).

234 van Elsas, A., Hurwitz, A. A. & Allison, J. P. Combination immunotherapy of B16 melanoma using anti-cytotoxic T lymphocyte-associated antigen 4 (CTLA-4) and granulocyte/macrophage colony-stimulating factor (GM-CSF)-producing vaccines induces rejection of subcutaneous and metastatic tumors accompanied by autoimmune depigmentation. *The Journal of experimental medicine* **190**, 355-366 (1999).

235 Kalluri, R. & Zeisberg, M. Fibroblasts in cancer. *Nature reviews. Cancer* **6**, 392-401, doi:10.1038/nrc1877 (2006).

236 Marsh, T., Pietras, K. & McAllister, S. S. Fibroblasts as architects of cancer pathogenesis. *Biochim Biophys Acta* **1832**, 1070-1078, doi:10.1016/j.bbadis.2012.10.013 (2013).

237 Elmore, S. Apoptosis: A Review of Programmed Cell Death. *Toxicologic pathology* **35**, 495-516, doi:10.1080/01926230701320337 (2007).

238 Pang, B. *et al.* Direct antigen presentation and gap junction mediated cross-presentation during apoptosis. *Journal of immunology* **183**, 1083-1090, doi:10.4049/jimmunol.0900861 (2009).

239 Ma, Y. *et al.* Anticancer chemotherapy-induced intratumoral recruitment and differentiation of antigen-presenting cells. *Immunity* **38**, 729-741, doi:10.1016/j.immuni.2013.03.003 (2013).

240 Tesniere, A. *et al.* Molecular characteristics of immunogenic cancer cell death. *Cell Death Differ* **15**, 3-12, doi:10.1038/sj.cdd.4402269 (2008).

241 Zitvogel, L., Tesniere, A. & Kroemer, G. Cancer despite immunosurveillance: immunoselection and immunosubversion. *Nat Rev Immunol* **6**, 715-727, doi:10.1038/nri1936 (2006).

242 Gabrilovich, D. I., Ostrand-Rosenberg, S. & Bronte, V. Coordinated regulation of myeloid cells by tumours. *Nat Rev Immunol* **12**, 253-268, doi:10.1038/nri3175 (2012).

243 Trapani, J. A. The dual adverse effects of TGF-beta secretion on tumor progression. *Cancer Cell* **8**, 349-350, doi:10.1016/j.ccr.2005.10.018 (2005).

244 Frame, M. C., Patel, H., Serrels, B., Lietha, D. & Eck, M. J. The FERM domain: organizing the structure and function of FAK. *Nat Rev Mol Cell Biol* **11**, 802-814, doi:10.1038/nrm2996 (2010).

245 McLean, G. W. *et al.* Specific deletion of focal adhesion kinase suppresses tumor formation and blocks malignant progression. *Genes Dev* **18**, 2998-3003, doi:10.1101/gad.316304 (2004).

246 Serrels, B., Sandilands, E. & Frame, M. C. Signaling of the direction-sensing FAK/RACK1/PDE4D5 complex to the small GTPase Rap1. *Small GTPases* **2**, 54-61, doi:10.4161/sgtp.2.1.15137 (2011).

247 Serrels, B. *et al.* A complex between FAK, RACK1, and PDE4D5 controls spreading initiation and cancer cell polarity. *Current biology : CB* **20**, 1086-1092, doi:10.1016/j.cub.2010.04.042 (2010).

248 Serrels, B. *et al.* Focal adhesion kinase controls actin assembly via a FERM-mediated interaction with the Arp2/3 complex. *Nat Cell Biol* **9**, 1046-1056, doi:10.1038/ncb1626 (2007).

249 Canel, M. *et al.* Quantitative in vivo imaging of the effects of inhibiting integrin signaling via Src and FAK on cancer cell movement: effects on E-cadherin dynamics. *Cancer research* **70**, 9413-9422, doi:10.1158/0008-5472.CAN-10-1454 (2010).

250 Mitra, S. K. & Schlaepfer, D. D. Integrin-regulated FAK-Src signaling in normal and cancer cells. *Curr Opin Cell Biol* **18**, 516-523, doi:10.1016/j.ceb.2006.08.011 (2006).

251 Schlaepfer, D. D. & Mitra, S. K. Multiple connections link FAK to cell motility and invasion. *Curr Opin Genet Dev* **14**, 92-101, doi:10.1016/j.gde.2003.12.002 (2004).

252 Zhao, J. H., Reiske, H. & Guan, J. L. Regulation of the cell cycle by focal adhesion kinase. *J Cell Biol* **143**, 1997-2008 (1998).

253 Westhoff, M. A., Serrels, B., Fincham, V. J., Frame, M. C. & Carragher, N. O. SRC-mediated phosphorylation of focal adhesion kinase couples actin and adhesion dynamics to survival signaling. *Mol Cell Biol* **24**, 8113-8133, doi:10.1128/MCB.24.18.8113-8133.2004 (2004).

254 Serrels, A. *et al.* The role of focal adhesion kinase catalytic activity on the proliferation and migration of squamous cell carcinoma cells. *Int J Cancer* **131**, 287-297, doi:10.1002/ijc.26351 (2012).

255 Cance, W. G. *et al.* Immunohistochemical analyses of focal adhesion kinase expression in benign and malignant human breast and colon tissues: correlation with preinvasive and invasive phenotypes. *Clin Cancer Res* **6**, 2417-2423 (2000).

256 Owens, L. V. *et al.* Overexpression of the focal adhesion kinase (p125FAK) in invasive human tumors. *Cancer Res* **55**, 2752-2755 (1995).

257 Pylayeva, Y. *et al.* Ras- and PI3K-dependent breast tumorigenesis in mice and humans requires focal adhesion kinase signaling. *J Clin Invest* **119**, 252-266, doi:10.1172/JCI37160 (2009).

258 Tremblay, L. *et al.* Focal adhesion kinase (pp125FAK) expression, activation and association with paxillin and p50CSK in human metastatic prostate carcinoma. *Int J Cancer* **68**, 164-171 (1996).

259 Kornberg, L. J. Focal adhesion kinase expression in oral cancers. *Head Neck* **20**, 634-639 (1998).

260 Rodrigo, J. P. *et al.* Focal adhesion kinase and E-cadherin as markers for nodal metastasis in laryngeal cancer. *Arch Otolaryngol Head Neck Surg* **133**, 145-150, doi:10.1001/archotol.133.2.145 (2007).

261 Agochiya, M. *et al.* Increased dosage and amplification of the focal adhesion kinase gene in human cancer cells. *Oncogene* **18**, 5646-5653, doi:10.1038/sj.onc.1202957 (1999).

262 Lu, P., Weaver, V. M. & Werb, Z. The extracellular matrix: a dynamic niche in cancer progression. *The Journal of cell biology* **196**, 395-406, doi:10.1083/jcb.201102147 (2012).

263 Schaller, M. D. Cellular functions of FAK kinases: insight into molecular mechanisms and novel functions. *J Cell Sci* **123**, 1007-1013, doi:10.1242/jcs.045112 (2010).

264 McLean, G. W. *et al.* The role of focal-adhesion kinase in cancer - a new therapeutic opportunity. *Nature reviews. Cancer* **5**, 505-515, doi:10.1038/nrc1647 (2005).

265 Sulzmaier, F. J., Jean, C. & Schlaepfer, D. D. FAK in cancer: mechanistic findings and clinical applications. *Nature reviews. Cancer* **14**, 598-610, doi:10.1038/nrc3792 (2014).

266 Ilic, D. *et al.* Reduced cell motility and enhanced focal adhesion contact formation in cells from FAK-deficient mice. *Nature* **377**, 539-544, doi:10.1038/377539a0 (1995).

267 Yu, H. G. *et al.* p190RhoGEF (Rgnef) promotes colon carcinoma tumor progression via interaction with focal adhesion kinase. *Cancer research* **71**, 360-370, doi:10.1158/0008-5472.CAN-10-2894 (2011).

268 Lawson, C. *et al.* FAK promotes recruitment of talin to nascent adhesions to control cell motility. *The Journal of cell biology* **196**, 223-232, doi:10.1083/jcb.201108078 (2012).

269 Barbero, S. *et al.* Caspase-8 association with the focal adhesion complex promotes tumor cell migration and metastasis. *Cancer research* **69**, 3755-3763, doi:10.1158/0008-5472.CAN-08-3937 (2009).

270 Tomar, A. & Schlaepfer, D. D. Focal adhesion kinase: switching between GAPs and GEFs in the regulation of cell motility. *Curr Opin Cell Biol* **21**, 676-683, doi:10.1016/j.ceb.2009.05.006 (2009).

271 Cicchini, C. *et al.* TGFbeta-induced EMT requires focal adhesion kinase (FAK) signaling. *Exp Cell Res* **314**, 143-152, doi:10.1016/j.yexcr.2007.09.005 (2008).

272 Li, X. Y. *et al.* Snail1 controls epithelial-mesenchymal lineage commitment in focal adhesion kinase-null embryonic cells. *The Journal of cell biology* **195**, 729-738, doi:10.1083/jcb.201105103 (2011).

273 Canel, M., Serrels, A., Frame, M. C. & Brunton, V. G. E-cadherin-integrin crosstalk in cancer invasion and metastasis. *J Cell Sci* **126**, 393-401, doi:10.1242/jcs.100115 (2013).

274 Zhao, J. & Guan, J. L. Signal transduction by focal adhesion kinase in cancer. *Cancer Metastasis Rev* **28**, 35-49, doi:10.1007/s10555-008-9165-4 (2009).

275 Lane, D., Goncharenko-Khaider, N., Rancourt, C. & Piche, A. Ovarian cancer ascites protects from TRAIL-induced cell death through alphavbeta5 integrin-mediated focal adhesion kinase and Akt activation. *Oncogene* **29**, 3519-3531, doi:10.1038/onc.2010.107 (2010).

276 Serrels, A. *et al.* The role of focal adhesion kinase catalytic activity on the proliferation and migration of squamous cell carcinoma cells. *International journal of cancer. Journal international du cancer* **131**, 287-297, doi:10.1002/ijc.26351 (2012).

277 Zhao, J. H., Reiske, H. & Guan, J. L. Regulation of the cell cycle by focal adhesion kinase. *The Journal of cell biology* **143**, 1997-2008 (1998).

278 Nagy, T. *et al.* Mammary epithelial-specific deletion of the focal adhesion kinase gene leads to severe lobulo-alveolar hypoplasia and secretory

immaturity of the murine mammary gland. *J Biol Chem* **282**, 31766-31776, doi:10.1074/jbc.M705403200 (2007).

279 Provenzano, P. P., Inman, D. R., Eliceiri, K. W., Beggs, H. E. & Keely, P. J. Mammary epithelial-specific disruption of focal adhesion kinase retards tumor formation and metastasis in a transgenic mouse model of human breast cancer. *Am J Pathol* **173**, 1551-1565, doi:10.2353/ajpath.2008.080308 (2008).

280 Ravenhall, C., Guida, E., Harris, T., Koutsoubos, V. & Stewart, A. The importance of ERK activity in the regulation of cyclin D1 levels and DNA synthesis in human cultured airway smooth muscle. *Br J Pharmacol* **131**, 17-28, doi:10.1038/sj.bjp.0703454 (2000).

281 Wang, X., Urvalek, A. M., Liu, J. & Zhao, J. Activation of KLF8 transcription by focal adhesion kinase in human ovarian epithelial and cancer cells. *J Biol Chem* **283**, 13934-13942, doi:10.1074/jbc.M709300200 (2008).

282 Ossovskaya, V., Lim, S. T., Ota, N., Schlaepfer, D. D. & Ilic, D. FAK nuclear export signal sequences. *FEBS Lett* **582**, 2402-2406, doi:10.1016/j.febslet.2008.06.004 (2008).

283 Lim, S. T. *et al.* Nuclear FAK promotes cell proliferation and survival through FERM-enhanced p53 degradation. *Mol Cell* **29**, 9-22, doi:10.1016/j.molcel.2007.11.031 (2008).

284 Lim, S. T. *et al.* Nuclear-localized focal adhesion kinase regulates inflammatory VCAM-1 expression. *The Journal of cell biology* **197**, 907-919, doi:10.1083/jcb.201109067 (2012).

285 Hall, J. E., Fu, W. & Schaller, M. D. Focal adhesion kinase: exploring Fak structure to gain insight into function. *Int Rev Cell Mol Biol* **288**, 185-225, doi:10.1016/B978-0-12-386041-5.00005-4 (2011).

286 Mitra, S. K., Hanson, D. A. & Schlaepfer, D. D. Focal adhesion kinase: in command and control of cell motility. *Nat Rev Mol Cell Biol* **6**, 56-68, doi:10.1038/nrm1549 (2005).

287 Astier, A. *et al.* The related adhesion focal tyrosine kinase differentially phosphorylates p130Cas and the Cas-like protein, p105HEF1. *J Biol Chem* **272**, 19719-19724 (1997).

288 Avraham, S. & Avraham, H. Characterization of the novel focal adhesion kinase RAFTK in hematopoietic cells. *Leuk Lymphoma* **27**, 247-256, doi:10.3109/10428199709059681 (1997).

289 Ganju, R. K. *et al.* RAFTK, a novel member of the focal adhesion kinase family, is phosphorylated and associates with signaling molecules upon activation of mature T lymphocytes. *The Journal of experimental medicine* **185**, 1055-1063 (1997).

290 Hatch, W. C., Ganju, R. K., Hiregowdara, D., Avraham, S. & Groopman, J. E. The related adhesion focal tyrosine kinase (RAFTK) is tyrosine phosphorylated and participates in colony-stimulating factor-1/macrophage

colony-stimulating factor signaling in monocyte-macrophages. *Blood* **91**, 3967-3973 (1998).

291 Ostergaard, H. L. & Lysechko, T. L. Focal adhesion kinase-related protein tyrosine kinase Pyk2 in T-cell activation and function. *Immunol Res* **31**, 267-282, doi:10.1385/IR:31:3:267 (2005).

292 Zheng, C. *et al.* Differential regulation of Pyk2 and focal adhesion kinase (FAK). The C-terminal domain of FAK confers response to cell adhesion. *J Biol Chem* **273**, 2384-2389 (1998).

293 Choi, C. H., Webb, B. A., Chimenti, M. S., Jacobson, M. P. & Barber, D. L. pH sensing by FAK-His58 regulates focal adhesion remodeling. *The Journal of cell biology* **202**, 849-859, doi:10.1083/jcb.201302131 (2013).

294 Corsi, J. M., Rouer, E., Girault, J. A. & Enslen, H. Organization and post-transcriptional processing of focal adhesion kinase gene. *BMC Genomics* **7**, 198, doi:10.1186/1471-2164-7-198 (2006).

295 Chandel, N. S., Trzyna, W. C., McClintock, D. S. & Schumacker, P. T. Role of oxidants in NF-kappa B activation and TNF-alpha gene transcription induced by hypoxia and endotoxin. *Journal of immunology* **165**, 1013-1021 (2000).

296 Renard, P. *et al.* Effects of antioxidant enzyme modulations on interleukin-1-induced nuclear factor kappa B activation. *Biochemical pharmacology* **53**, 149-160 (1997).

297 Kume, A., Nishiura, H., Suda, J. & Suda, T. Focal adhesion kinase upregulated by granulocyte-macrophage colony-stimulating factor but not by interleukin-3 in differentiating myeloid cells. *Blood* **89**, 3434-3442 (1997).

298 Abshire, M. Y., Thomas, K. S., Owen, K. A. & Bouton, A. H. Macrophage motility requires distinct alpha5beta1/FAK and alpha4beta1/paxillin signaling events. *J Leukoc Biol* **89**, 251-257, doi:10.1189/jlb.0710395 (2011).

299 Owen, K. A. *et al.* Regulation of lamellipodial persistence, adhesion turnover, and motility in macrophages by focal adhesion kinase. *The Journal of cell biology* **179**, 1275-1287, doi:10.1083/jcb.200708093 (2007).

300 Walsh, C. *et al.* Oral delivery of PND-1186 FAK inhibitor decreases tumor growth and spontaneous breast to lung metastasis in pre-clinical models. *Cancer Biol Ther* **9**, 778-790 (2010).

301 Wendt, M. K. & Schiemann, W. P. Therapeutic targeting of the focal adhesion complex prevents oncogenic TGF-beta signaling and metastasis. *Breast Cancer Res* **11**, R68, doi:10.1186/bcr2360 (2009).

302 Stokes, J. B. *et al.* Inhibition of focal adhesion kinase by PF-562,271 inhibits the growth and metastasis of pancreatic cancer concomitant with altering the tumor microenvironment. *Mol Cancer Ther* **10**, 2135-2145, doi:10.1158/1535-7163.MCT-11-0261 (2011).

303 Kasorn, A. *et al.* Focal adhesion kinase regulates pathogen-killing capability and life span of neutrophils via mediating both adhesion-dependent and -

independent cellular signals. *Journal of immunology* **183**, 1032-1043, doi:10.4049/jimmunol.0802984 (2009).

304 Batista, S. *et al.* Haematopoietic focal adhesion kinase deficiency alters haematopoietic homeostasis to drive tumour metastasis. *Nat Commun* **5**, 5054, doi:10.1038/ncomms6054 (2014).

305 Recher, C. *et al.* Expression of focal adhesion kinase in acute myeloid leukemia is associated with enhanced blast migration, increased cellularity, and poor prognosis. *Cancer research* **64**, 3191-3197 (2004).

306 Chapman, N. M., Connolly, S. F., Reinl, E. L. & Houtman, J. C. Focal adhesion kinase negatively regulates Lck function downstream of the T cell antigen receptor. *Journal of immunology* **191**, 6208-6221, doi:10.4049/jimmunol.1301587 (2013).

307 Wiemer, A. J. *et al.* The focal adhesion kinase inhibitor PF-562,271 impairs primary CD4+ T cell activation. *Biochemical pharmacology* **86**, 770-781, doi:10.1016/j.bcp.2013.07.024 (2013).

308 Katagiri, T., Takahashi, T., Sasaki, T., Nakamura, S. & Hattori, S. Protein-tyrosine kinase Pyk2 is involved in interleukin-2 production by Jurkat T cells via its tyrosine 402. *J Biol Chem* **275**, 19645-19652, doi:10.1074/jbc.M909828199 (2000).

309 Beinke, S. *et al.* Proline-rich tyrosine kinase-2 is critical for CD8 T-cell short-lived effector fate. *Proceedings of the National Academy of Sciences of the United States of America* **107**, 16234-16239, doi:10.1073/pnas.1011556107 (2010).

310 Judokusumo, E., Tabdanov, E., Kumari, S., Dustin, M. L. & Kam, L. C. Mechanosensing in T lymphocyte activation. *Biophys J* **102**, L5-7, doi:10.1016/j.bpj.2011.12.011 (2012).

311 Schultze, A. & Fiedler, W. Therapeutic potential and limitations of new FAK inhibitors in the treatment of cancer. *Expert Opin Investig Drugs* **19**, 777-788, doi:10.1517/13543784.2010.489548 (2010).

312 Bagi, C. M. *et al.* Sunitinib and PF-562,271 (FAK/Pyk2 inhibitor) effectively block growth and recovery of human hepatocellular carcinoma in a rat xenograft model. *Cancer Biol Ther* **8**, 856-865 (2009).

313 Halder, J. *et al.* Therapeutic efficacy of a novel focal adhesion kinase inhibitor TAE226 in ovarian carcinoma. *Cancer research* **67**, 10976-10983, doi:10.1158/0008-5472.CAN-07-2667 (2007).

314 Jean, C. *et al.* Inhibition of endothelial FAK activity prevents tumor metastasis by enhancing barrier function. *The Journal of cell biology* **204**, 247-263, doi:10.1083/jcb.201307067 (2014).

315 Tavora, B. *et al.* Endothelial FAK is required for tumour angiogenesis. *EMBO Mol Med* **2**, 516-528, doi:10.1002/emmm.201000106 (2010).

316 Schmidt, T. T. *et al.* Conditional deletion of FAK in mice endothelium disrupts lung vascular barrier function due to destabilization of RhoA and

Rac1 activities. *Am J Physiol Lung Cell Mol Physiol* **305**, L291-300, doi:10.1152/ajplung.00094.2013 (2013).

317 Shen, T. L. *et al.* Conditional knockout of focal adhesion kinase in endothelial cells reveals its role in angiogenesis and vascular development in late embryogenesis. *The Journal of cell biology* **169**, 941-952, doi:10.1083/jcb.200411155 (2005).

318 Zhao, X., Peng, X., Sun, S., Park, A. Y. & Guan, J. L. Role of kinase-independent and -dependent functions of FAK in endothelial cell survival and barrier function during embryonic development. *The Journal of cell biology* **189**, 955-965, doi:10.1083/jcb.200912094 (2010).

319 Dave, J. M., Kang, H., Abbey, C. A., Maxwell, S. A. & Bayless, K. J. Proteomic profiling of endothelial invasion revealed receptor for activated C kinase 1 (RACK1) complexed with vimentin to regulate focal adhesion kinase (FAK). *J Biol Chem* **288**, 30720-30733, doi:10.1074/jbc.M113.512467 (2013).

320 Angelucci, A. & Bologna, M. Targeting vascular cell migration as a strategy for blocking angiogenesis: the central role of focal adhesion protein tyrosine kinase family. *Curr Pharm Des* **13**, 2129-2145 (2007).

321 Chen, X. L. *et al.* VEGF-induced vascular permeability is mediated by FAK. *Dev Cell* **22**, 146-157, doi:10.1016/j.devcel.2011.11.002 (2012).

322 Le Boeuf, F., Houle, F. & Huot, J. Regulation of vascular endothelial growth factor receptor 2-mediated phosphorylation of focal adhesion kinase by heat shock protein 90 and Src kinase activities. *J Biol Chem* **279**, 39175-39185, doi:10.1074/jbc.M405493200 (2004).

323 Hiratsuka, S. *et al.* Endothelial focal adhesion kinase mediates cancer cell homing to discrete regions of the lungs via E-selectin up-regulation. *Proceedings of the National Academy of Sciences of the United States of America* **108**, 3725-3730, doi:10.1073/pnas.1100446108 (2011).

324 Barker, H. E., Bird, D., Lang, G. & Erler, J. T. Tumor-secreted LOXL2 activates fibroblasts through FAK signaling. *Mol Cancer Res* **11**, 1425-1436, doi:10.1158/1541-7786.MCR-13-0033-T (2013).

325 Greenberg, R. S. *et al.* FAK-dependent regulation of myofibroblast differentiation. *FASEB J* **20**, 1006-1008, doi:10.1096/fj.05-4838fje (2006).

326 Quintanilla, M., Brown, K., Ramsden, M. & Balmain, A. Carcinogen-specific mutation and amplification of Ha-ras during mouse skin carcinogenesis. *Nature* **322**, 78-80, doi:10.1038/322078a0 (1986).

327 Frisch, S. M., Vuori, K., Ruoslahti, E. & Chan-Hui, P. Y. Control of adhesion-dependent cell survival by focal adhesion kinase. *The Journal of cell biology* **134**, 793-799 (1996).

328 de Hoon, M. J., Imoto, S., Nolan, J. & Miyano, S. Open source clustering software. *Bioinformatics* **20**, 1453-1454, doi:10.1093/bioinformatics/bth078 (2004).

329 Saldanha, A. J. Java Treeview--extensible visualization of microarray data. *Bioinformatics* **20**, 3246-3248, doi:10.1093/bioinformatics/bth349 (2004).

330 Chen, J., Bardes, E. E., Aronow, B. J. & Jegga, A. G. ToppGene Suite for gene list enrichment analysis and candidate gene prioritization. *Nucleic acids research* **37**, W305-311, doi:10.1093/nar/gkp427 (2009).

331 Alexander, S. P. *et al.* The Concise Guide to PHARMACOLOGY 2013/14: G protein-coupled receptors. *Br J Pharmacol* **170**, 1459-1581, doi:10.1111/bph.12445 (2013).

332 Pawson, A. J. *et al.* The IUPHAR/BPS Guide to PHARMACOLOGY: an expert-driven knowledgebase of drug targets and their ligands. *Nucleic acids research* **42**, D1098-1106, doi:10.1093/nar/gkt1143 (2014).

333 Bachelerie, F. *et al.* International Union of Basic and Clinical Pharmacology. [corrected]. LXXXIX. Update on the extended family of chemokine receptors and introducing a new nomenclature for atypical chemokine receptors. *Pharmacological reviews* **66**, 1-79, doi:10.1124/pr.113.007724 (2014).

334 Shannon, P. *et al.* Cytoscape: a software environment for integrated models of biomolecular interaction networks. *Genome research* **13**, 2498-2504, doi:10.1101/gr.1239303 (2003).

335 Chow, S.-C. Sample size calculations for clinical trials

Wiley Interdisciplinary Reviews: Computational Statistics Volume 3, Issue 5. *Wiley Interdisciplinary Reviews: Computational Statistics* **3**, 414-427 (2011). <http://onlinelibrary.wiley.com/doi/10.1002/wics.155/abstract>.

336 Hennings, H. *et al.* FVB/N mice: an inbred strain sensitive to the chemical induction of squamous cell carcinomas in the skin. *Carcinogenesis* **14**, 2353-2358 (1993).

337 Castagna, M. *et al.* Direct activation of calcium-activated, phospholipid-dependent protein kinase by tumor-promoting phorbol esters. *J Biol Chem* **257**, 7847-7851 (1982).

338 Lee, W. Y., Lockniskar, M. F. & Fischer, S. M. Interleukin-1 alpha mediates phorbol ester-induced inflammation and epidermal hyperplasia. *FASEB J* **8**, 1081-1087 (1994).

339 McLean, G. W. *et al.* Specific deletion of focal adhesion kinase suppresses tumor formation and blocks malignant progression. *Genes & development* **18**, 2998-3003, doi:10.1101/gad.316304 (2004).

340 Sieg, D. J., Hauck, C. R. & Schlaepfer, D. D. Required role of focal adhesion kinase (FAK) for integrin-stimulated cell migration. *J Cell Sci* **112 (Pt 16)**, 2677-2691 (1999).

341 Schorpp, M., Hofmann, M., Dear, T. N. & Boehm, T. Characterization of mouse and human nude genes. *Immunogenetics* **46**, 509-515 (1997).

342 Siddiqui, W. A., Ahad, A. & Ahsan, H. The mystery of BCL2 family: Bcl-2 proteins and apoptosis: an update. *Arch Toxicol* **89**, 289-317, doi:10.1007/s00204-014-1448-7 (2015).

343 Adams, J. M. & Cory, S. The Bcl-2 apoptotic switch in cancer development and therapy. *Oncogene* **26**, 1324-1337, doi:10.1038/sj.onc.1210220 (2007).

344 Sonoda, Y. *et al.* Anti-apoptotic role of focal adhesion kinase (FAK). Induction of inhibitor-of-apoptosis proteins and apoptosis suppression by the overexpression of FAK in a human leukemic cell line, HL-60. *J Biol Chem* **275**, 16309-16315 (2000).

345 Sakurai, S. *et al.* Mutated focal adhesion kinase induces apoptosis in a human glioma cell line, T98G. *Biochem Biophys Res Commun* **293**, 174-181, doi:10.1016/S0006-291X(02)00192-4 (2002).

346 Solana, R. *et al.* Effect of phorbol ester TPA on macrophage metabolic activity. *Methods Find Exp Clin Pharmacol* **6**, 67-71 (1984).

347 McGranahan, N. *et al.* Clonal neoantigens elicit T cell immunoreactivity and sensitivity to immune checkpoint blockade. *Science* **351**, 1463-1469, doi:10.1126/science.aaf1490 (2016).

348 Vremec, D., Pooley, J., Hochrein, H., Wu, L. & Shortman, K. CD4 and CD8 expression by dendritic cell subtypes in mouse thymus and spleen. *Journal of immunology* **164**, 2978-2986 (2000).

349 Wang, B. *et al.* Multiple paths for activation of naive CD8+ T cells: CD4-independent help. *J Immunol* **167**, 1283-1289 (2001).

350 Bevan, M. J. Helping the CD8(+) T-cell response. *Nat Rev Immunol* **4**, 595-602, doi:10.1038/nri1413 (2004).

351 Norment, A. M., Salter, R. D., Parham, P., Engelhard, V. H. & Littman, D. R. Cell-cell adhesion mediated by CD8 and MHC class I molecules. *Nature* **336**, 79-81, doi:10.1038/336079a0 (1988).

352 Koretzky, G. A. Multiple roles of CD4 and CD8 in T cell activation. *Journal of immunology* **185**, 2643-2644, doi:10.4049/jimmunol.1090076 (2010).

353 Watkins, S. K., Zhu, Z., Watkins, K. E. & Hurwitz, A. A. Isolation of immune cells from primary tumors. *J Vis Exp*, e3952, doi:10.3791/3952 (2012).

354 Freshney, R. I. *Culture of animal cells : a manual of basic technique and specialized applications*. 6th edn, (Wiley-Blackwell, 2010).

355 Cerra, R., Zarbo, R. J. & Crissman, J. D. Dissociation of cells from solid tumors. *Methods Cell Biol* **33**, 1-12 (1990).

356 Kanitakis, J., Karayannopoulou, G., Roux, A. & Euvrard, S. Histopathologic Features Predictive of Aggressiveness of Post-transplant Cutaneous Squamous-cell Carcinomas. *Anticancer Res* **35**, 2305-2308 (2015).

357 Jewell, R. *et al.* The clinicopathological and gene expression patterns associated with ulceration of primary melanoma. *Pigment Cell Melanoma Res* **28**, 94-104, doi:10.1111/pcmr.12315 (2015).

358 San Mateo, L. R., Toffer, K. L., Orndorff, P. E. & Kawula, T. H. Immune cells are required for cutaneous ulceration in a swine model of chancroid. *Infect Immun* **67**, 4963-4967 (1999).

359 Cruse, J. M. *et al.* Facilitation of immune function, healing of pressure ulcers, and nutritional status in spinal cord injury patients. *Exp Mol Pathol* **68**, 38-54, doi:10.1006/exmp.1999.2292 (2000).

360 Lee, H. J., Kim, M. K., Wee, W. R. & Oh, J. Y. Interplay of Immune Cells in Mooren Ulcer. *Cornea* **34**, 1164-1167, doi:10.1097/ICO.0000000000000471 (2015).

361 Umemura, N. *et al.* Tumor-infiltrating myeloid-derived suppressor cells are pleiotropic-inflamed monocytes/macrophages that bear M1- and M2-type characteristics. *J Leukoc Biol* **83**, 1136-1144, doi:10.1189/jlb.0907611 (2008).

362 Hengel, R. L. *et al.* Cutting edge: L-selectin (CD62L) expression distinguishes small resting memory CD4+ T cells that preferentially respond to recall antigen. *Journal of immunology* **170**, 28-32 (2003).

363 Ponta, H., Sherman, L. & Herrlich, P. A. CD44: from adhesion molecules to signalling regulators. *Nat Rev Mol Cell Biol* **4**, 33-45, doi:10.1038/nrm1004 (2003).

364 Beyer, M. & Schultze, J. L. Regulatory T cells in cancer. *Blood* **108**, 804-811, doi:10.1182/blood-2006-02-002774 (2006).

365 Biragyn, A. & Longo, D. L. Neoplastic "Black Ops": cancer's subversive tactics in overcoming host defenses. *Seminars in cancer biology* **22**, 50-59, doi:10.1016/j.semcancer.2012.01.005 (2012).

366 Marigo, I., Dolcetti, L., Serafini, P., Zanovello, P. & Bronte, V. Tumor-induced tolerance and immune suppression by myeloid derived suppressor cells. *Immunological reviews* **222**, 162-179, doi:10.1111/j.1600-065X.2008.00602.x (2008).

367 Serrels, A. *et al.* Real-time study of E-cadherin and membrane dynamics in living animals: implications for disease modeling and drug development. *Cancer research* **69**, 2714-2719, doi:10.1158/0008-5472.CAN-08-4308 (2009).

368 Brunton, V. G. & Frame, M. C. Src and focal adhesion kinase as therapeutic targets in cancer. *Curr Opin Pharmacol* **8**, 427-432, doi:10.1016/j.coph.2008.06.012 (2008).

369 Plaza-Menacho, I. *et al.* Focal adhesion kinase (FAK) binds RET kinase via its FERM domain, priming a direct and reciprocal RET-FAK transactivation mechanism. *J Biol Chem* **286**, 17292-17302, doi:10.1074/jbc.M110.168500 (2011).

370 Golubovskaya, V. M. Focal adhesion kinase as a cancer therapy target. *Anticancer Agents Med Chem* **10**, 735-741 (2010).

371 Hao, H. *et al.* Focal adhesion kinase as potential target for cancer therapy (Review). *Oncol Rep* **22**, 973-979 (2009).

372 Golubovskaya, V. M., Kweh, F. A. & Cance, W. G. Focal adhesion kinase and cancer. *Histol Histopathol* **24**, 503-510 (2009).

373 Lim, S. T., Mikolon, D., Stupack, D. G. & Schlaepfer, D. D. FERM control of FAK function: implications for cancer therapy. *Cell Cycle* **7**, 2306-2314 (2008).

374 Genin, M., Clement, F., Fattaccioli, A., Raes, M. & Michiels, C. M1 and M2 macrophages derived from THP-1 cells differentially modulate the response of cancer cells to etoposide. *BMC Cancer* **15**, 577, doi:10.1186/s12885-015-1546-9 (2015).

375 Ikeda, H., Old, L. J. & Schreiber, R. D. The roles of IFN gamma in protection against tumor development and cancer immunoediting. *Cytokine Growth Factor Rev* **13**, 95-109 (2002).

376 Li, S. N. *et al.* IL-21 modulates release of proinflammatory cytokines in LPS-stimulated macrophages through distinct signaling pathways. *Mediators Inflamm* **2013**, 548073, doi:10.1155/2013/548073 (2013).

377 Li, Y., Bleakley, M. & Yee, C. IL-21 influences the frequency, phenotype, and affinity of the antigen-specific CD8 T cell response. *Journal of immunology* **175**, 2261-2269 (2005).

378 Pardon, E. *et al.* A general protocol for the generation of Nanobodies for structural biology. *Nat Protoc* **9**, 674-693, doi:10.1038/nprot.2014.039 (2014).

379 Le Jeune, C. & Thomas, X. Potential for bispecific T-cell engagers: role of blinatumomab in acute lymphoblastic leukemia. *Drug Des Devel Ther* **10**, 757-765, doi:10.2147/DDDT.S83848 (2016).

380 Smits, N. C. & Sentman, C. L. Bispecific T-Cell Engagers (BiTEs) as Treatment of B-Cell Lymphoma. *J Clin Oncol* **34**, 1131-1133, doi:10.1200/JCO.2015.64.9970 (2016).

381 Schmohl, J. U., Gleason, M. K., Dougherty, P. R., Miller, J. S. & Vallera, D. A. Heterodimeric Bispecific Single Chain Variable Fragments (scFv) Killer Engagers (BiKEs) Enhance NK-cell Activity Against CD133+ Colorectal Cancer Cells. *Target Oncol*, doi:10.1007/s11523-015-0391-8 (2015).

382 Wu, M. R. *et al.* B7H6-Specific Bispecific T Cell Engagers Lead to Tumor Elimination and Host Antitumor Immunity. *Journal of immunology* **194**, 5305-5311, doi:10.4049/jimmunol.1402517 (2015).

383 Huehls, A. M., Coupet, T. A. & Sentman, C. L. Bispecific T-cell engagers for cancer immunotherapy. *Immunol Cell Biol* **93**, 290-296, doi:10.1038/icb.2014.93 (2015).

384 Steeland, S., Vandenbroucke, R. E. & Libert, C. Nanobodies as therapeutics: big opportunities for small antibodies. *Drug Discov Today*, doi:10.1016/j.drudis.2016.04.003 (2016).

385 Ivanov, A. A., Khuri, F. R. & Fu, H. Targeting protein-protein interactions as an anticancer strategy. *Trends Pharmacol Sci* **34**, 393-400, doi:10.1016/j.tips.2013.04.007 (2013).

386 Fry, D. C. & Vassilev, L. T. Targeting protein-protein interactions for cancer therapy. *J Mol Med (Berl)* **83**, 955-963, doi:10.1007/s00109-005-0705-x (2005).

387 Oliveira, S., Heukers, R., Sornkom, J., Kok, R. J. & van Bergen En Henegouwen, P. M. Targeting tumors with nanobodies for cancer imaging and therapy. *J Control Release* **172**, 607-617, doi:10.1016/j.jconrel.2013.08.298 (2013).

388 Golubeva, Y., Salcedo, R., Mueller, C., Liotta, L. A. & Espina, V. Laser capture microdissection for protein and NanoString RNA analysis. *Methods Mol Biol* **931**, 213-257, doi:10.1007/978-1-62703-056-4_12 (2013).

389 Stricker, T. P. *et al.* Validation of a prognostic multi-gene signature in high-risk neuroblastoma using the high throughput digital NanoString nCounter system. *Mol Oncol* **8**, 669-678, doi:10.1016/j.molonc.2014.01.010 (2014).

390 Zelenay, S. *et al.* Foxp3+ CD25- CD4 T cells constitute a reservoir of committed regulatory cells that regain CD25 expression upon homeostatic expansion. *Proceedings of the National Academy of Sciences of the United States of America* **102**, 4091-4096, doi:10.1073/pnas.0408679102 (2005).

391 Herndler-Brandstetter, D. *et al.* Non-regulatory CD8+CD45RO+CD25+ T-lymphocytes may compensate for the loss of antigen-inexperienced CD8+CD45RA+ T-cells in old age. *Biol Chem* **389**, 561-568 (2008).

392 Churlaud, G. *et al.* Human and Mouse CD8(+)CD25(+)FOXP3(+) Regulatory T Cells at Steady State and during Interleukin-2 Therapy. *Frontiers in immunology* **6**, 171, doi:10.3389/fimmu.2015.00171 (2015).

393 Bos, P. D., Plitas, G., Rudra, D., Lee, S. Y. & Rudensky, A. Y. Transient regulatory T cell ablation deters oncogene-driven breast cancer and enhances radiotherapy. *The Journal of experimental medicine* **210**, 2435-2466, doi:10.1084/jem.20130762 (2013).

394 Camirand, G. *et al.* CD45 ligation expands Tregs by promoting interactions with DCs. *J Clin Invest* **124**, 4603-4613, doi:10.1172/JCI74087 (2014).

395 Goldstein, J. D. *et al.* Role of cytokines in thymus- versus peripherally derived-regulatory T cell differentiation and function. *Frontiers in immunology* **4**, 155, doi:10.3389/fimmu.2013.00155 (2013).

396 Ondondo, B., Jones, E., Godkin, A. & Gallimore, A. Home sweet home: the tumor microenvironment as a haven for regulatory T cells. *Frontiers in immunology* **4**, 197, doi:10.3389/fimmu.2013.00197 (2013).

397 Hong, S. *et al.* The role of focal adhesion kinase in the TGF-beta-induced myofibroblast transdifferentiation of human Tenon's fibroblasts. *Korean J Ophthalmol* **26**, 45-48, doi:10.3341/kjo.2012.26.1.45 (2012).

398 Chen, R. *et al.* Focal adhesion kinase (FAK) siRNA inhibits human hypertrophic scar by suppressing integrin alpha, TGF-beta and alpha-SMA. *Cell Biol Int* **38**, 803-808, doi:10.1002/cbin.10265 (2014).

399 Forster, R. *et al.* CCR7 coordinates the primary immune response by establishing functional microenvironments in secondary lymphoid organs. *Cell* **99**, 23-33 (1999).

400 Ma, Q. *et al.* Impaired B-lymphopoiesis, myelopoiesis, and derailed cerebellar neuron migration in CXCR4- and SDF-1-deficient mice. *Proceedings of the National Academy of Sciences of the United States of America* **95**, 9448-9453 (1998).

401 Lee, J. H., Kang, S. G. & Kim, C. H. FoxP3+ T cells undergo conventional first switch to lymphoid tissue homing receptors in thymus but accelerated second switch to nonlymphoid tissue homing receptors in secondary lymphoid tissues. *Journal of immunology* **178**, 301-311 (2007).

402 Zheng, S. G., Wang, J. H., Gray, J. D., Soucier, H. & Horwitz, D. A. Natural and induced CD4+CD25+ cells educate CD4+CD25- cells to develop suppressive activity: the role of IL-2, TGF-beta, and IL-10. *Journal of immunology* **172**, 5213-5221 (2004).

403 Andrieux, G., Le Borgne, M. & Theret, N. An integrative modeling framework reveals plasticity of TGF-beta signaling. *BMC Syst Biol* **8**, 30, doi:10.1186/1752-0509-8-30 (2014).

404 Principe, D. R. *et al.* TGF-beta: duality of function between tumor prevention and carcinogenesis. *J Natl Cancer Inst* **106**, djt369, doi:10.1093/jnci/djt369 (2014).

405 Siegel, P. M. & Massague, J. Cytostatic and apoptotic actions of TGF-beta in homeostasis and cancer. *Nature reviews. Cancer* **3**, 807-821, doi:10.1038/nrc1208 (2003).

406 Papageorgis, P. & Stylianopoulos, T. Role of TGFbeta in regulation of the tumor microenvironment and drug delivery (review). *Int J Oncol* **46**, 933-943, doi:10.3892/ijo.2015.2816 (2015).

407 Hannon, G. J. & Beach, D. p15INK4B is a potential effector of TGF-beta-induced cell cycle arrest. *Nature* **371**, 257-261, doi:10.1038/371257a0 (1994).

408 Datto, M. B. *et al.* Transforming growth factor beta induces the cyclin-dependent kinase inhibitor p21 through a p53-independent mechanism. *Proceedings of the National Academy of Sciences of the United States of America* **92**, 5545-5549 (1995).

409 Polyak, K. *et al.* p27Kip1, a cyclin-Cdk inhibitor, links transforming growth factor-beta and contact inhibition to cell cycle arrest. *Genes & development* **8**, 9-22 (1994).

410 Laiho, M., DeCaprio, J. A., Ludlow, J. W., Livingston, D. M. & Massague, J. Growth inhibition by TGF-beta linked to suppression of retinoblastoma protein phosphorylation. *Cell* **62**, 175-185 (1990).

411 Pietenpol, J. A. *et al.* TGF-beta 1 inhibition of c-myc transcription and growth in keratinocytes is abrogated by viral transforming proteins with pRB binding domains. *Cell* **61**, 777-785 (1990).

412 Eppert, K. *et al.* MADR2 maps to 18q21 and encodes a TGFbeta-regulated MAD-related protein that is functionally mutated in colorectal carcinoma. *Cell* **86**, 543-552 (1996).

413 Hahn, S. A. *et al.* Homozygous deletion map at 18q21.1 in pancreatic cancer. *Cancer research* **56**, 490-494 (1996).

414 Thiagalingam, S. *et al.* Evaluation of candidate tumour suppressor genes on chromosome 18 in colorectal cancers. *Nat Genet* **13**, 343-346, doi:10.1038/ng0796-343 (1996).

415 Kim, S. K. *et al.* DPC4, a candidate tumor suppressor gene, is altered infrequently in head and neck squamous cell carcinoma. *Cancer research* **56**, 2519-2521 (1996).

416 Schutte, M. *et al.* DPC4 gene in various tumor types. *Cancer research* **56**, 2527-2530 (1996).

417 Markowitz, S. *et al.* Inactivation of the type II TGF-beta receptor in colon cancer cells with microsatellite instability. *Science* **268**, 1336-1338 (1995).

418 Chen, R. H., Ebner, R. & Derynck, R. Inactivation of the type II receptor reveals two receptor pathways for the diverse TGF-beta activities. *Science* **260**, 1335-1338 (1993).

419 Kim, I. Y. *et al.* Genetic change in transforming growth factor beta (TGF-beta) receptor type I gene correlates with insensitivity to TGF-beta 1 in human prostate cancer cells. *Cancer research* **56**, 44-48 (1996).

420 Grotendorst, G. R. Connective tissue growth factor: a mediator of TGF-beta action on fibroblasts. *Cytokine Growth Factor Rev* **8**, 171-179 (1997).

421 Tomasek, J. J., Gabbiani, G., Hinz, B., Chaponnier, C. & Brown, R. A. Myofibroblasts and mechano-regulation of connective tissue remodelling. *Nat Rev Mol Cell Biol* **3**, 349-363, doi:10.1038/nrm809 (2002).

422 Karagiannis, G. S. *et al.* Cancer-associated fibroblasts drive the progression of metastasis through both paracrine and mechanical pressure on cancer tissue. *Mol Cancer Res* **10**, 1403-1418, doi:10.1158/1541-7786.MCR-12-0307 (2012).

423 Cance, W. G. *et al.* Immunohistochemical analyses of focal adhesion kinase expression in benign and malignant human breast and colon tissues: correlation with preinvasive and invasive phenotypes. *Clin Cancer Res* **6**, 2417-2423 (2000).

424 Oktay, M. H., Oktay, K., Hamele-Bena, D., Buyuk, A. & Koss, L. G. Focal adhesion kinase as a marker of malignant phenotype in breast and cervical carcinomas. *Hum Pathol* **34**, 240-245, doi:10.1053/hupa.2003.40 (2003).

425 Zhang, J., He, D. H., Zajac-Kaye, M. & Hochwald, S. N. A small molecule FAK kinase inhibitor, GSK2256098, inhibits growth and survival of

pancreatic ductal adenocarcinoma cells. *Cell Cycle* **13**, 3143-3149, doi:10.4161/15384101.2014.949550 (2014).

426 Lark, A. L. *et al.* Overexpression of focal adhesion kinase in primary colorectal carcinomas and colorectal liver metastases: immunohistochemistry and real-time PCR analyses. *Clin Cancer Res* **9**, 215-222 (2003).

427 Hess, A. R. & Hendrix, M. J. Focal adhesion kinase signaling and the aggressive melanoma phenotype. *Cell Cycle* **5**, 478-480 (2006).

428 Bald, T. *et al.* Ultraviolet-radiation-induced inflammation promotes angiotropism and metastasis in melanoma. *Nature* **507**, 109-113 (2014).

429 Turner, P. V., Brabb, T., Pekow, C. & Vasbinder, M. A. Administration of substances to laboratory animals: routes of administration and factors to consider. *J Am Assoc Lab Anim Sci* **50**, 600-613 (2011).

430 Brown, A. P., Dinger, N. & Levine, B. S. Stress produced by gavage administration in the rat. *Contemp Top Lab Anim Sci* **39**, 17-21 (2000).

431 Vachon, P., Faubert, S., Blais, D., Comtois, A. & Bienvenu, J. G. A pathophysiological study of abdominal organs following intraperitoneal injections of chloral hydrate in rats: comparison between two anaesthesia protocols. *Lab Anim-Uk* **34**, 84-90, doi:Doi 10.1258/002367700780578082 (2000).

432 Vachon, P. Self-mutilation in rabbits following intramuscular ketamine-xylazine-acepromazine injections. *Can Vet J* **40**, 581-582 (1999).

433 Alban, L. *et al.* The welfare impact of increased gavaging doses in rats. *Anim Welfare* **10**, 303-314 (2001).

434 Bonnichsen, M., Dragsted, N. & Hansen, A. K. The welfare impact of gavaging laboratory rats. *Anim Welfare* **14**, 223-227 (2005).

435 Morton, D. B. *et al.* Refining procedures for the administration of substances. *Lab Anim-Uk* **35**, 1-41, doi:Doi 10.1258/0023677011911345 (2001).

436 Turner, P. V., Pekow, C., Vasbinder, M. A. & Brabb, T. Administration of Substances to Laboratory Animals: Equipment Considerations, Vehicle Selection, and Solute Preparation. *J Am Assoc Lab Anim* **50**, 614-627 (2011).

437 Guengerich, F. P. Common and uncommon cytochrome P450 reactions related to metabolism and chemical toxicity. *Chem Res Toxicol* **14**, 611-650, doi:10.1021/tx0002583 (2001).

438 Abdel-Ghany, M., Cheng, H. C., Elble, R. C. & Pauli, B. U. Focal adhesion kinase activated by beta(4) integrin ligation to mCLCA1 mediates early metastatic growth. *J Biol Chem* **277**, 34391-34400, doi:10.1074/jbc.M205307200 (2002).

439 Albasri, A., Fadhil, W., Scholefield, J. H., Durrant, L. G. & Ilyas, M. Nuclear expression of phosphorylated focal adhesion kinase is associated with poor prognosis in human colorectal cancer. *Anticancer Res* **34**, 3969-3974 (2014).

440 Albini, A., Mirisola, V. & Pfeffer, U. Metastasis signatures: genes regulating tumor-microenvironment interactions predict metastatic behavior. *Cancer Metastasis Rev* **27**, 75-83, doi:10.1007/s10555-007-9111-x (2008).

441 Brenner, W. *et al.* Migration of renal carcinoma cells is dependent on protein kinase Cdelta via beta1 integrin and focal adhesion kinase. *Int J Oncol* **32**, 1125-1131 (2008).

442 Rodrigo, J. P. *et al.* Focal adhesion kinase and E-cadherin as markers for nodal metastasis in laryngeal cancer. *Arch Otolaryngol Head Neck Surg* **133**, 145-150, doi:10.1001/archotol.133.2.145 (2007).

443 Schlaepfer, D. D., Mitra, S. K. & Ilic, D. Control of motile and invasive cell phenotypes by focal adhesion kinase. *Biochim Biophys Acta* **1692**, 77-102, doi:10.1016/j.bbamcr.2004.04.008 (2004).

444 Shanthi, E. *et al.* Focal adhesion kinase inhibitors in the treatment of metastatic cancer: a patent review. *Expert Opin Ther Pat* **24**, 1077-1100, doi:10.1517/13543776.2014.948845 (2014).

445 van Nimwegen, M. J. & van de Water, B. Focal adhesion kinase: a potential target in cancer therapy. *Biochemical pharmacology* **73**, 597-609, doi:10.1016/j.bcp.2006.08.011 (2007).

446 van Nimwegen, M. J., Verkoeijen, S., van Buren, L., Burg, D. & van de Water, B. Requirement for focal adhesion kinase in the early phase of mammary adenocarcinoma lung metastasis formation. *Cancer research* **65**, 4698-4706, doi:10.1158/0008-5472.CAN-04-4126 (2005).

447 Ward, K. K. *et al.* Inhibition of focal adhesion kinase (FAK) activity prevents anchorage-independent ovarian carcinoma cell growth and tumor progression. *Clin Exp Metastasis* **30**, 579-594, doi:10.1007/s10585-012-9562-5 (2013).

448 Zheng, Y. *et al.* CD86 and CD80 differentially modulate the suppressive function of human regulatory T cells. *Journal of immunology* **172**, 2778-2784 (2004).

449 Preston, C. C. *et al.* The ratios of CD8+ T cells to CD4+CD25+ FOXP3+ and FOXP3- T cells correlate with poor clinical outcome in human serous ovarian cancer. *PLoS One* **8**, e80063, doi:10.1371/journal.pone.0080063 (2013).

450 Kim, S. *et al.* Zonal difference and prognostic significance of foxp3 regulatory T cell infiltration in breast cancer. *J Breast Cancer* **17**, 8-17, doi:10.4048/jbc.2014.17.1.8 (2014).

451 Liyanage, U. K. *et al.* Increased prevalence of regulatory T cells (Treg) is induced by pancreas adenocarcinoma. *J Immunother* **29**, 416-424, doi:10.1097/01.cji.0000205644.43735.4e (2006).

452 Somasundaram, R. *et al.* Inhibition of cytolytic T lymphocyte proliferation by autologous CD4+/CD25+ regulatory T cells in a colorectal carcinoma patient is mediated by transforming growth factor-beta. *Cancer research* **62**, 5267-5272 (2002).

453 Ichihara, F. *et al.* Increased populations of regulatory T cells in peripheral blood and tumor-infiltrating lymphocytes in patients with gastric and esophageal cancers. *Clin Cancer Res* **9**, 4404-4408 (2003).

454 Schlaepfer, D. D. *et al.* Tumor necrosis factor-alpha stimulates focal adhesion kinase activity required for mitogen-activated kinase-associated interleukin 6 expression. *J Biol Chem* **282**, 17450-17459, doi:10.1074/jbc.M610672200 (2007).

455 Sheta, E. A., Harding, M. A., Conaway, M. R. & Theodorescu, D. Focal adhesion kinase, Rap1, and transcriptional induction of vascular endothelial growth factor. *J Natl Cancer Inst* **92**, 1065-1073 (2000).

456 McLean, G. W. *et al.* Decreased focal adhesion kinase suppresses papilloma formation during experimental mouse skin carcinogenesis. *Cancer research* **61**, 8385-8389 (2001).

457 Yusuf, N. *et al.* Antagonistic roles of CD4+ and CD8+ T-cells in 7,12-dimethylbenz(a)anthracene cutaneous carcinogenesis. *Cancer research* **68**, 3924-3930, doi:10.1158/0008-5472.CAN-07-3059 (2008).

458 Ashton, G. H. *et al.* Focal adhesion kinase is required for intestinal regeneration and tumorigenesis downstream of Wnt/c-Myc signaling. *Dev Cell* **19**, 259-269, doi:10.1016/j.devcel.2010.07.015 (2010).

459 Lahlou, H. *et al.* Mammary epithelial-specific disruption of the focal adhesion kinase blocks mammary tumor progression. *Proceedings of the National Academy of Sciences of the United States of America* **104**, 20302-20307, doi:10.1073/pnas.0710091104 (2007).

460 Slack-Davis, J. K., Hershey, E. D., Theodorescu, D., Frierson, H. F. & Parsons, J. T. Differential requirement for focal adhesion kinase signaling in cancer progression in the transgenic adenocarcinoma of mouse prostate model. *Mol Cancer Ther* **8**, 2470-2477, doi:10.1158/1535-7163.MCT-09-0262 (2009).

461 Luo, M. *et al.* Mammary epithelial-specific ablation of the focal adhesion kinase suppresses mammary tumorigenesis by affecting mammary cancer stem/progenitor cells. *Cancer research* **69**, 466-474, doi:10.1158/0008-5472.CAN-08-3078 (2009).

462 Pylayeva, Y. *et al.* Ras- and PI3K-dependent breast tumorigenesis in mice and humans requires focal adhesion kinase signaling. *J Clin Invest* **119**, 252-266, doi:10.1172/JCI37160 (2009).

463 Feig, C. *et al.* Targeting CXCL12 from FAP-expressing carcinoma-associated fibroblasts synergizes with anti-PD-L1 immunotherapy in pancreatic cancer. *Proceedings of the National Academy of Sciences of the United States of America* **110**, 20212-20217, doi:10.1073/pnas.1320318110 (2013).

464 Ali, K. *et al.* Inactivation of PI(3)K p110delta breaks regulatory T-cell-mediated immune tolerance to cancer. *Nature* **510**, 407-411, doi:10.1038/nature13444 (2014).

465 Simpson, T. R. *et al.* Fc-dependent depletion of tumor-infiltrating regulatory T cells co-defines the efficacy of anti-CTLA-4 therapy against melanoma. *The Journal of experimental medicine* **210**, 1695-1710, doi:10.1084/jem.20130579 (2013).

466 Peggs, K. S., Quezada, S. A., Chambers, C. A., Korman, A. J. & Allison, J. P. Blockade of CTLA-4 on both effector and regulatory T cell compartments contributes to the antitumor activity of anti-CTLA-4 antibodies. *The Journal of experimental medicine* **206**, 1717-1725, doi:10.1084/jem.20082492 (2009).

467 Quezada, S. A., Peggs, K. S., Curran, M. A. & Allison, J. P. CTLA4 blockade and GM-CSF combination immunotherapy alters the intratumor balance of effector and regulatory T cells. *J Clin Invest* **116**, 1935-1945, doi:10.1172/JCI27745 (2006).

468 Wang, W. *et al.* PD1 blockade reverses the suppression of melanoma antigen-specific CTL by CD4+ CD25(Hi) regulatory T cells. *International immunology* **21**, 1065-1077, doi:10.1093/intimm/dxp072 (2009).

469 Fife, B. T. & Pauken, K. E. The role of the PD-1 pathway in autoimmunity and peripheral tolerance. *Annals of the New York Academy of Sciences* **1217**, 45-59, doi:10.1111/j.1749-6632.2010.05919.x (2011).

470 Larkin, J. *et al.* Combined Nivolumab and Ipilimumab or Monotherapy in Untreated Melanoma. *The New England journal of medicine* **373**, 23-34, doi:10.1056/NEJMoa1504030 (2015).

471 Arkenau, H. T. *et al.* A phase Ib dose-escalation study of GSK2256098 (FAKi) plus trametinib (MEKi) in patients with selected advanced solid tumors. *Journal of Clinical Oncology* **33** (2015).

472 Rech, A. J. & Vonderheide, R. H. Clinical use of anti-CD25 antibody daclizumab to enhance immune responses to tumor antigen vaccination by targeting regulatory T cells. *Annals of the New York Academy of Sciences* **1174**, 99-106, doi:10.1111/j.1749-6632.2009.04939.x (2009).

473 Zhu, Y. *et al.* CSF1/CSF1R blockade reprograms tumor-infiltrating macrophages and improves response to T-cell checkpoint immunotherapy in pancreatic cancer models. *Cancer research* **74**, 5057-5069, doi:10.1158/0008-5472.CAN-13-3723 (2014).

474 Curran, M. A., Montalvo, W., Yagita, H. & Allison, J. P. PD-1 and CTLA-4 combination blockade expands infiltrating T cells and reduces regulatory T and myeloid cells within B16 melanoma tumors. *Proceedings of the National Academy of Sciences of the United States of America* **107**, 4275-4280, doi:10.1073/pnas.0915174107 (2010).

475 Brahmer, J. R. *et al.* Safety and activity of anti-PD-L1 antibody in patients with advanced cancer. *The New England journal of medicine* **366**, 2455-2465, doi:10.1056/NEJMoa1200694 (2012).

Article

Cell

Nuclear FAK Controls Chemokine Transcription, Tregs, and Evasion of Anti-tumor Immunity

Graphical Abstract

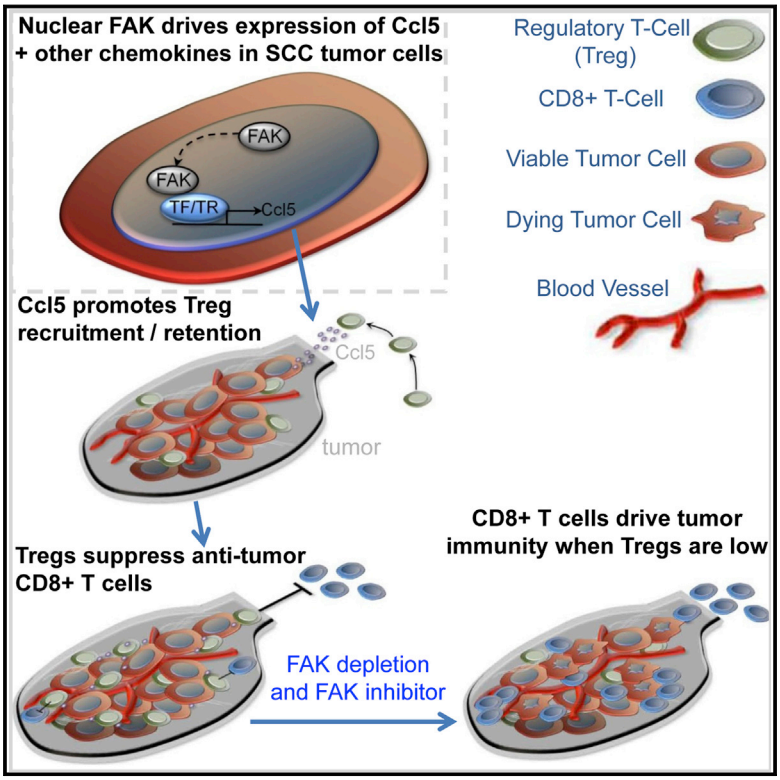

Highlights

- Depletion or kinase inhibition of FAK can cause squamous cell carcinoma regression
- FAK promotes tumor evasion by inducing an immuno-suppressive microenvironment
- Nuclear FAK promotes transcription of chemokines that drive recruitment of Tregs
- FAK-induced Tregs inhibit cytotoxic CD8+ T cells, allowing tumor tolerance and growth

Authors

Alan Serrels, Tom Lund, Bryan Serrels, ..., Stephen M. Anderton, Robert J.B. Nibbs, Margaret C. Frame

Correspondence

a.serrels@ed.ac.uk (A.S.),
m.frame@ed.ac.uk (M.C.F.)

In Brief

Nuclear focal adhesion kinase (FAK) regulates transcription of chemokines that drive recruitment of tumor-associated regulatory T cells (Tregs), thereby creating a tumor suppressive microenvironment by inhibiting cytotoxic CD8+ T cell activity.

Accession Numbers

GSE71662

Serrels et al., 2015, Cell *163*, 160–173
September 24, 2015 ©2015 The Authors
http://dx.doi.org/10.1016/j.cell.2015.09.001

Cell

Article

Nuclear FAK Controls Chemokine Transcription, Tregs, and Evasion of Anti-tumor Immunity

Alan Serrels,[1,7,*] Tom Lund,[1,7] Bryan Serrels,[1] Adam Byron,[1] Rhoanne C. McPherson,[2] Alexander von Kriegsheim,[1] Laura Gómez-Cuadrado,[1] Marta Canel,[1] Morwenna Muir,[1] Jennifer E. Ring,[3] Eleni Maniati,[4] Andrew H. Sims,[1] Jonathan A. Pachter,[3] Valerie G. Brunton,[1] Nick Gilbert,[5] Stephen M. Anderton,[2] Robert J.B. Nibbs,[6] and Margaret C. Frame[1,*]

[1]Edinburgh Cancer Research UK Centre, Institute of Genetics and Molecular Medicine, University of Edinburgh, Edinburgh EH4 2XR, UK
[2]MRC Centre for Inflammation Research, The Queens Medical Research Institute, University of Edinburgh, Edinburgh EH16 4TJ, UK
[3]Verastem Inc., 117 Kendrick Street, Suite 500, Needham, MA 02494, USA
[4]Queen Mary, University of London, Centre for Cancer and Inflammation, Charterhouse Square, London EC1M 6BQ, UK
[5]MRC Human Genetics Unit, Institute of Genetics and Molecular Medicine, University of Edinburgh, Edinburgh EH4 2XU, UK
[6]Institute of Infection, Immunity, and Inflammation, University of Glasgow, Glasgow G12 8TA, UK
[7]Co-first author
*Correspondence: a.serrels@ed.ac.uk (A.S.), m.frame@ed.ac.uk (M.C.F.)
http://dx.doi.org/10.1016/j.cell.2015.09.001

SUMMARY

Focal adhesion kinase (FAK) promotes anti-tumor immune evasion. Specifically, the kinase activity of nuclear-targeted FAK in squamous cell carcinoma (SCC) cells drives exhaustion of $CD8^+$ T cells and recruitment of regulatory T cells (Tregs) in the tumor microenvironment by regulating chemokine/cytokine and ligand-receptor networks, including via transcription of Ccl5, which is crucial. These changes inhibit antigen-primed cytotoxic $CD8^+$ T cell activity, permitting growth of FAK-expressing tumors. Mechanistically, nuclear FAK is associated with chromatin and exists in complex with transcription factors and their upstream regulators that control Ccl5 expression. Furthermore, FAK's immuno-modulatory nuclear activities may be specific to cancerous squamous epithelial cells, as normal keratinocytes do not have nuclear FAK. Finally, we show that a small-molecule FAK kinase inhibitor, VS-4718, which is currently in clinical development, also drives depletion of Tregs and promotes a $CD8^+$ T cell-mediated anti-tumor response. Therefore, FAK inhibitors may trigger immune-mediated tumor regression, providing previously unrecognized therapeutic opportunities.

INTRODUCTION

First described more than a decade ago (Onizuka et al., 1999; Shimizu et al., 1999), regulatory T cells (Tregs) have become recognized as a core component of the immuno-suppressive armory utilized by many tumors to keep the anti-tumor activity of antigen-primed $CD8^+$ T cells at bay. Increased Treg numbers has been associated with poorer survival in ovarian (Curiel et al., 2004), gastrointestinal (Sasada et al., 2003), and esophageal (Kono et al., 2006) cancer. Indeed, the ratio of $CD8^+$ T cells/Tregs correlates with poor prognosis, shifting the balance from anti-tumor immunity toward tumor tolerance (Quezada et al., 2006; Sato et al., 2005; Shah et al., 2011). Through secreting a range of chemokines and cytokines, cancer cells can promote the recruitment of Tregs into tumors and can also facilitate their peripheral expansion and retention (Darrasse-Jèze and Podsypanina, 2013; Ondondo et al., 2013). Thus, Tregs can act as a barrier to effective immune-based therapy aimed at activation of a $CD8^+$ T cell anti-tumor immune response. However, the specific signals within tumor cells that stimulate elevated intra-tumoral Tregs, giving rise to tumor tolerance, remain elusive.

FAK is a tyrosine kinase that regulates diverse cellular functions, including adhesion, migration, invasion, polarity, proliferation, and survival (Frame et al., 2010). Using targeted gene deletion in mouse skin, we have previously shown a requirement for *fak* in tumor initiation and progression to malignant disease (McLean et al., 2004). FAK is also required for mammary tumor progression, intestinal tumorigenesis, and the androgen-independent formation of neuroendocrine carcinoma in a mouse model of prostate cancer (Ashton et al., 2010; Lahlou et al., 2007; Luo et al., 2009a; Provenzano et al., 2008; Pylayeva et al., 2009; Slack-Davis et al., 2009). Expression of FAK is elevated in a number of tumor types (reviewed in McLean et al., 2005), and FAK inhibitors are being developed as potential cancer therapeutics (Roberts et al., 2008; Shapiro et al., 2014). Many of FAK's functions in cancer are via its role in signaling downstream of integrins and growth factor receptors at the plasma membrane. FAK also contains putative nuclear localization sequences (NLS) within the F2 lobe of its FERM domain and can localize to the nucleus upon receipt of cellular stress, where it binds to p53 (Lim et al., 2008). However, the extent of FAK's nuclear functions remains largely unknown. Here, we report a function for nuclear FAK in regulating transcription of inflammatory cytokines and chemokines, in turn promoting an immuno-suppressive, pro-tumorigenic microenvironment. This is mediated

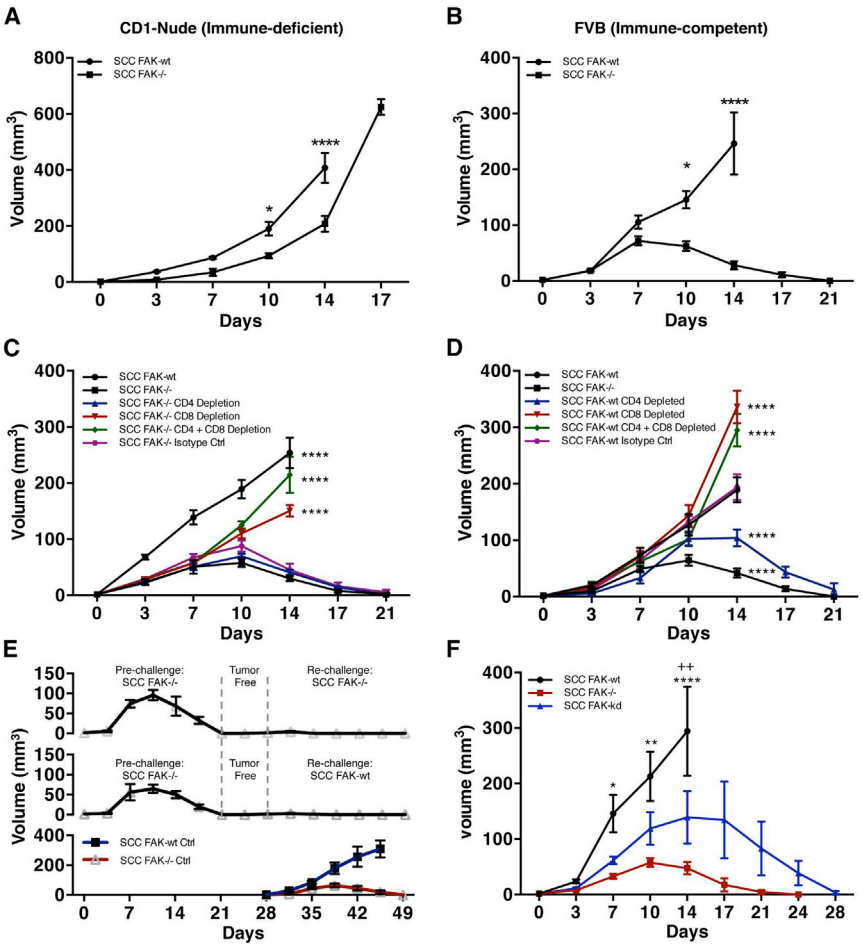

Figure 1. Loss of FAK or FAK Kinase Activity Results in CD8$^+$ T Cell-Dependent SCC Tumor Clearance

(A and B) SCC FAK-WT and SCC *FAK*$^{-/-}$ subcutaneous tumor growth in immune-deficient CD-1 nude mice (A) and immune-competent FVB mice (B).

(C and D) SCC *FAK*$^{-/-}$ (C) and SCC FAK-WT (D) tumor growth in FVB mice treated with T-cell-depleting antibodies.

(E) Secondary tumor re-challenge with SCC *FAK*$^{-/-}$ (top) and SCC FAK-WT (middle) cells following a pre-challenge with SCC *FAK*$^{-/-}$ cells and a 7-day tumor-free period. Subcutaneous growth of SCC FAK-WT and SCC *FAK*$^{-/-}$ tumors injected at day 28 without pre-challenge (bottom).

(F) Tumor growth in FVB mice following subcutaneous injection of SCC FAK-WT, SCC *FAK*$^{-/-}$, and SCC FAK-KD cells.

*p < 0.05, **p or $^{++}$p < 0.01, ****p < 0.0001; Sidak-corrected two-way ANOVA (A and B) or Tukey-corrected two-way ANOVA (C, versus SCC *FAK*$^{-/-}$; D, versus SCC FAK-WT; F, *, versus SCC *FAK*$^{-/-}$ and $^+$, versus SCC FAK-KD). Data are represented as mean ± SEM; n = 5–6 tumors.

by recruitment and expansion of Tregs via FAK-regulated chemokine/cytokine networks, and we have found an important role for Ccl5 and TGFβ2. Therefore, FAK controls the tumor environment, and suppressing FAK activity, including via a clinically relevant FAK inhibitor, may be therapeutically beneficial by triggering immune-mediated tumor regression.

RESULTS

FAK-Deficient SCC Tumors Undergo Regression in an Immune-Competent Host

We used a syngeneic model of SCC in which the *fak* gene had been deleted by Cre-lox recombination (McLean et al., 2004; Serrels et al., 2012) and mutant tumor cell lines generated. We monitored tumor growth following injection of 1 × 10^6 FAK-deficient cells (*FAK*$^{-/-}$) or FAK-deficient cells that re-expressed wild-type FAK (FAK-WT) at comparable levels to endogenous FAK in both CD-1 nude and FVB (syngeneic) host mouse strains. In CD-1 nude mice, SCC *FAK*$^{-/-}$ tumor growth was characterized by a modest growth delay (Figure 1A) as reported previously (Serrels et al., 2012). By contrast, in FVB mice, SCC *FAK*$^{-/-}$ tumor growth was characterized by an initial period of growth in the first 7 days followed by complete regression by day 21 (Figure 1B). Thus, FAK expression is required for the survival and growth of SCC tumors in FVB mice with a functional adaptive immune system.

SCC *FAK*$^{-/-}$ Tumor Regression Is Dependent on CD8$^+$ T Cells

To characterize the role of adaptive immunity in *FAK*$^{-/-}$ SCC tumor regression, we used antibody-mediated T cell depletion in animals bearing *FAK*$^{-/-}$ tumors (Figures 1C and S1). Depletion of CD4$^+$ T cells had no effect on tumor growth. In contrast, depletion of CD8$^+$ T cells, either alone or in combination with CD4$^+$ T cells, restored SCC *FAK*$^{-/-}$ tumor growth. This implies that cytotoxic CD8$^+$ T cells were responsible for regression of *FAK*$^{-/-}$ tumors (Figure 1C) but does not exclude an accessory role for CD4$^+$ T cells. T cell depletion in mice bearing SCC FAK-WT tumors (Figure 1D) revealed that: (1) depletion of CD8$^+$ T cells, either alone or in combination with CD4$^+$ T cells, caused a significant increase in tumor growth when compared to isotype-treated controls at day 14, and (2) depletion of CD4$^+$ T cells alone caused regression of FAK-WT SCC tumors by day 21. This implied that FAK-expressing tumors were also under negative pressure from the immune system and that cells from the CD4$^+$ T cell compartment play a role in protecting FAK-WT tumors from immune-mediated regression (reason discussed later; Figure 3).

Next, we re-challenged mice with 1 × 10^6 SCC FAK-WT cells after regression of primary *FAK*$^{-/-}$ SCC tumors, following 7 days of tumor-free survival after the tumors had regressed (Figure 1E, top and middle graphs). Neither FAK-deficient nor FAK-expressing SCC cells were able to grow after the mice had been pre-challenged with SCC *FAK*$^{-/-}$ cells. As controls, SCC FAK-WT and *FAK*$^{-/-}$ cells were injected at day 28 into mice with no pre-challenge, and these grew as expected (Figure 1E, bottom).

This implies that, following *FAK*$^{-/-}$ SCC tumor regression, host mice remain immunized against further tumor challenge because immunological memory had been established. It is possible that either broad immunization against SCCs may have occurred or, more likely, that the *FAK*$^{-/-}$ and FAK-WT SCCs shared common antigen(s) that are expressed irrespective of FAK status. We conclude that FAK enables SCC cancer cells to suppress an adaptive immune response rather than to circumvent it through evading recognition per se. SCC *FAK*$^{-/-}$ cells in which a FAK kinase-deficient mutant was re-expressed (SCC FAK-KD) initially grew and then regressed with kinetics that were only modestly delayed when compared to *FAK*$^{-/-}$ cells, indicating that immune suppression depends on FAK kinase activity (Figure 1F).

We next investigated the nature of the T cell response within tumors derived from all three SCC cell lines using FACS analysis on disaggregated tumor tissue taken at day 7. We did not observe a significant change in the percentage of total CD4$^+$ T cells (Figures 2A and S2 and Table S2) or the percentage of CD4$^+$ T cells that expressed the activation marker CD69 (Figure 2B). In contrast, we did observe a significant increase in the proportion of effector CD4$^+$CD44^{hi}CD62L^{low} T cells in SCC *FAK*$^{-/-}$ and FAK-KD tumors when compared to FAK-WT tumors (Figures 2C and S2 and Table S2). Analysis of tumor-infiltrating CD8$^+$ T cells revealed a significant increase in SCC *FAK*$^{-/-}$ and SCC FAK-KD tumors when compared to SCC FAK-WT tumors (Figures 2D and S2 and Table S2), indicative of a heightened cytotoxic anti-tumor immune response. Staining with the activation marker CD69 identified the presence of CD8$^+$CD69$^+$ T cells in all tumors (Figure 2E). Further analysis revealed an increase in percentage of effector CD8$^+$CD44^{hi}CD62L^{low} T cells in SCC *FAK*$^{-/-}$ and SCC FAK-KD tumors when compared to SCC FAK-WT tumors (Figures 2F and S2 and Table S2), especially when effector CD8$^+$ T cell numbers were normalized to account for the observed changes in total CD8$^+$ T cells and presented as a "fold change" (Figure 2G). However, while SCC *FAK*$^{-/-}$ and SCC FAK-KD tumors had increased effector CD8$^+$ T cells, there were activated CD8$^+$ T cells present in all of the SCC tumors, raising the question of why SCC FAK-WT tumors do not succumb to the cytotoxic CD8$^+$ T cell response.

It is now established that not only the quantity of tumor-infiltrating CD8$^+$ T cells is important, but also their "quality." Tumor-induced T cell exhaustion has been reported in a number of tumor types, including melanoma (Fourcade et al., 2010) and ovarian cancer (Matsuzaki et al., 2010), and is characterized by expression of co-inhibitory surface receptors, including programmed death receptor 1 (PD-1), lymphocyte-activation gene 3 (LAG-3), and T cell immunoglobulin mucin-3 (Tim-3), either alone or in combination (Fourcade et al., 2010; Sakuishi et al., 2010; Wherry, 2011). Analysis of these markers on antigen-primed CD8$^+$CD44^{hi} T cells infiltrating SCC FAK-WT, *FAK*$^{-/-}$, and FAK-KD tumors revealed increased surface expression of PD-1, LAG-3, and Tim-3 in CD8$^+$CD44^{hi} T cells present in SCC FAK-WT tumors (Figures 2H–2J). Together, our data imply that antigen-primed CD8$^+$CD44^{hi} T cells infiltrating SCC FAK-WT tumors exhibit a heightened state of exhaustion indicative of a dysfunctional T cell response. Linked to their exhausted state, there was also evidence of decreased proliferation of CD8$^+$ T cells isolated from SCC FAK-WT tumors (judged by Ki-67 staining in Figure 2K).

Histological staining of tumor sections taken at day 7 revealed that: (1) CD8$^+$ T cells are present throughout all tumors, and (2) while CD8$^+$ T cells infiltrating SCC FAK-WT tumors appear predominantly as individual cells, CD8$^+$ T cells infiltrating SCC *FAK*$^{-/-}$ and FAK-KD tumors are clustered (Figure 2L). Thus, the ability of SCC FAK-WT tumors to evade the anti-tumor immune response is not due to limited CD8$^+$ T cell penetration into these tumors.

FAK Expression Drives Establishment of an Immuno-Suppressive Environment

Macrophages, myeloid-derived suppressor cells (MDSC), and Tregs with intrinsic immuno-suppressive capabilities can promote tumor development by inhibiting cytotoxic CD8$^+$ T cell activity in mouse and humans (Beyer and Schultze, 2006; Biragyn and Longo, 2012; Marigo et al., 2008). Flow cytometric analysis revealed no differences in macrophage or MDSC populations that correlated with tumor regression (Figures 3A, 3B, S3, and S4 and Table S2), although this does not rule out an accessory role for these cells in eventual tumor clearance. However, we did find a significantly greater number of CD4$^+$FoxP3$^+$CD25$^+$ Tregs in SCC FAK-WT tumors (Figures 3C and S4 and Table S2) when compared with *FAK*$^{-/-}$ and FAK-KD tumors (Figure 3C). Tregs have been associated with the development of CD8$^+$ T cell exhaustion (Sakuishi et al., 2013) and may therefore be linked to the CD8$^+$ T cell exhaustion that we observed in SCC FAK-WT tumors (Figures 2H–2J). We next calculated the ratio of CD8$^+$ T cells to Tregs (Figure 3D), as this has been reported to correlate with poor prognosis in a number of tumor types (Sato et al., 2005; Shah et al., 2011). We found a substantially lower CD8$^+$ T cell to Treg ratio in SCC FAK-WT tumors when compared to SCC *FAK*$^{-/-}$ and SCC FAK-KD tumors, which correlated with outcome in terms of tumor tolerance versus immune-mediated tumor regression.

Tregs Protect FAK-WT Tumors from Immune-Mediated Regression

We next examined SCC FAK-WT tumor growth in animals treated with an anti-CD25 antibody to deplete Tregs (Figure 3E). Depletion of CD25$^+$ cells led to regression of SCC FAK-WT tumors. Therefore, FAK-dependent Tregs are required for the growth of FAK-WT-expressing tumors by creating an immuno-suppressive environment that impairs cytotoxic CD8$^+$ T cell activity. This role of CD4$^+$ Tregs is the likely reason for effects of the CD4-depleting antibody in promoting regression of SCC FAK-WT tumors (Figure 1D). We note that high Treg levels have been reported in a number of solid tumor types (Beyer and Schultze, 2006) and that elevated Tregs are linked to poor clinical outcome (Beyer and Schultze, 2006; Sato et al., 2005).

We demonstrated that Tregs derived from SCC FAK-WT tumors expressed the transcription factor (TF) Helios (Figure S5A), indicative of thymic origin (Thornton et al., 2010). Thus, we hypothesized that FAK may drive the recruitment and expansion of the intra-tumoral Tregs by influencing the availability of secreted factors.

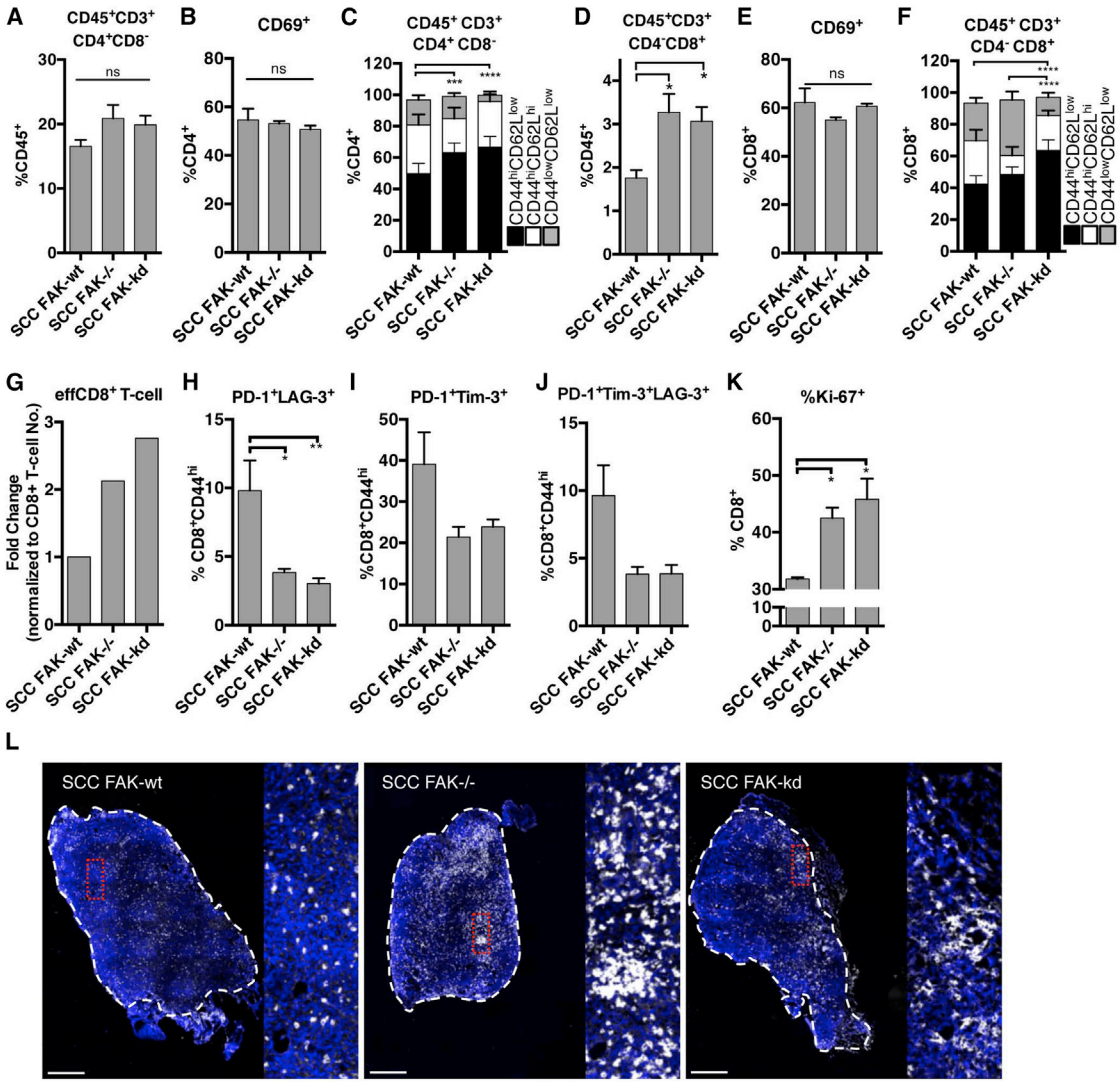

Figure 2. FAK-Depleted Tumors Exhibit a Heightened CD8$^+$ T Cell Response

(A) FACS quantification of total intra-tumoral CD4$^+$ T cells.

(B) FACS quantification of CD69$^+$ cells as a percentage of CD4$^+$ T cells.

(C) FACS quantification of CD4$^+$CD44^{hi}CD62L^{low}, CD4$^+$CD44^{hi}CD62L^{hi}, CD4$^+$CD44^{low}CD62L^{low} T cell subpopulations.

(D) FACS quantification of total intra-tumoral CD8$^+$ T cells.

(E) FACS quantification of CD69$^+$ cells as a percentage of CD8$^+$ T cells.

(F) Quantification of CD8$^+$CD44^{hi}CD62L^{low}, CD8$^+$CD44^{hi}CD62L^{hi}, CD8$^+$CD44^{low}CD62L^{low} T cell subpopulations.

(G) Changes in effector (CD8$^+$CD44^{hi}CD62L^{low}) CD8$^+$ T cells normalized to total CD8$^+$ T cell proportions.

(H) FACS quantification of PD-1$^+$LAG-3$^+$ T cells as a percentage of CD8$^+$CD44^{hi} tumor-infiltrating T cells. n = 6 tumors.

(I) FACS quantification of PD-1$^+$Tim-3$^+$ T cells as a percentage of CD8$^+$CD44^{hi} tumor-infiltrating T cells. n = 3 tumors.

(J) FACS quantification of PD-1$^+$Tim-3$^+$LAG-3$^+$ T cells as a percentage of CD8$^+$CD44^{hi} tumor-infiltrating T cells. n = 3 tumors.

(K) FACS quantification of Ki-67$^+$ cells as a percentage of tumor-infiltrating CD8$^+$ T cells. n = 3 tumors.

(L) Representative histological staining of CD8 in frozen sections from SCC FAK-WT, SCC *FAK*$^{-/-}$, and SCC FAK-KD tumors. Dashed white lines demark tumor boundary.

Scale bars, 500 μm. *p < 0.05, **p < 0.01, ***p < 0.001, ****p < 0.0001; ns, not significant; Tukey-corrected one-way ANOVA (C and F, CD44^{hi}CD62L^{low} only). Data are represented as mean ± SEM; n = 5 tumors unless stated.

FAK Regulates the Transcription of Chemokines and Cytokines to Control Tregs

To address how FAK activity in SCC cancer cells promotes elevated intra-tumoral Tregs, we next analyzed global transcriptional profiles of SCC FAK-WT and SCC *FAK*$^{-/-}$ cells using Affymetrix GeneChip microarrays (Figure 4A). FAK expression resulted in the upregulation of 498 genes and the downregulation of 598 genes (p < 0.01). The upregulated transcript set in SCC

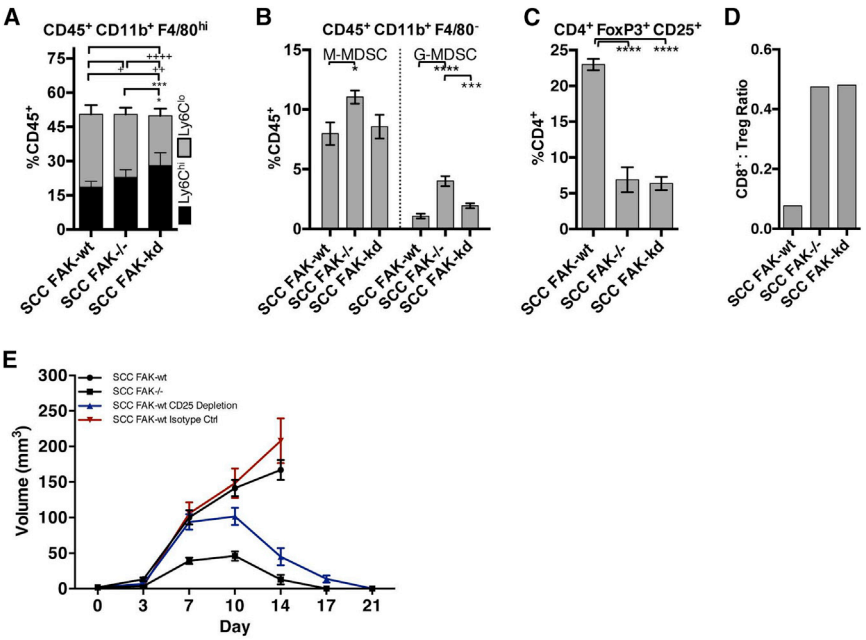

Figure 3. FAK Regulates the Immuno-Suppressive Microenvironment

(A) FACS quantification of Ly6C^{hi} and Ly6C^{low} macrophage populations expressed as a percentage of tumor-infiltrating CD45$^+$ leukocytes.

(B) FACS quantification of Ly6C^{hi}Gr1^{low} (M-MDSC) and Ly6C^{int}Gr1^{hi} (G-MDSC) populations expressed as a percentage of tumor-infiltrating CD45$^+$ leukocytes.

(C) Quantification of CD4$^+$CD25$^+$FoxP3$^+$ Tregs expressed as a percentage of tumor-infiltrating CD4$^+$ T cells.

(D) CD8$^+$ T cell-to-Treg ratio calculated using mean values from Figures 2D and 3C.

(E) SCC FAK-WT tumor growth in FVB mice treated with anti-CD25 depleting antibody.

n = 6 tumors. * or $^+$p < 0.05, $^{++}$p < 0.01, ***p < 0.001, **** or $^{++++}$p < 0.0001; Tukey-corrected one-way ANOVA (A, *, Ly6C^{hi}; $^+$, Ly6C^{low}). Data are represented as mean ± SEM; n = 5 tumors unless stated.

FAK-WT cells was associated with a number of processes, including cell migration, receptor binding, secretion, wounding, and ovulation (Figure 4B, top). Analysis of this gene set revealed the chemokine ligand group of genes to be significantly overrepresented (Figure 4B, bottom), which is interesting given that a number of these chemokines and cytokines mediate both Treg recruitment to tumors and induction of peripheral Tregs within tumors (Goldstein et al., 2013; Ondondo et al., 2013).

To establish which chemokines and cytokines were regulated by FAK and to address whether the FAK-dependent transcriptional profile was linked to chemokine receptor expression on tumor-infiltrating Tregs, we performed quantitative (q)RT-PCR array analysis. Comparison of chemokine/cytokine transcript levels between SCC FAK-WT and SCC *FAK*$^{-/-}$ cells revealed a subset of ligands increased >2-fold in SCC FAK-WT cells (Figure 4C). Several of these (*Ccl1*, *Ccl5*, *Ccl7*, *Cxcl10*) have roles in Treg recruitment (Ondondo et al., 2013) (green arrowheads, Figure 4C), while one (*Tgfb2*) has a reported role in peripheral induction and expansion of Tregs (Goldstein et al., 2013) (red arrowhead, Figure 4C). To complement this, comparison of Tregs isolated from the thymus of normal FVB mice with those isolated directly from SCC FAK-WT tumors revealed a chemokine receptor switch (Figure 4D). We found increased expression of the cognate receptors for five of the six chemokine ligands upregulated in SCC FAK-WT cells (Figure 4C). These receptor changes may represent a switch from lymphoid homing receptors, including Ccr7 and Cxcr4, toward expression of memory/effector-type chemokine receptors, including Ccr2, Ccr5, Ccr8, and Cxcr6, involved in recruitment to non-lymphoid tissues and sites of inflammation. Network analysis of the relationship between FAK-dependent chemokine ligand expression in SCC cells and tumor-infiltrating Treg chemokine receptor expression revealed the existence of a FAK-dependent paracrine signaling axis between cancer cells and intra-tumoral Tregs based on chemokine ligand-receptor interactions (Figure 4E). Furthermore, (q)RT-PCR analysis of *Ccl5*, *Cxcl10*, and *Tgfb2* demonstrated that their expression was dependent on FAK kinase activity (Figure 4F). We note that disruption of the Ccl5/Ccr5 axis in a model of pancreatic adenocarcinoma results in reduced intra-tumoral Tregs and slows tumor growth (Tan et al., 2009), implying that FAK-dependent regulation of this paracrine signaling axis may be more generally important. Thus, FAK activity regulates the expression of a subset of chemokines that can specifically mediate crosstalk between tumor cells and tumor-infiltrating Tregs. This likely has importance in recruitment and retention of CD4$^+$FoxP3$^+$CD25$^+$ Tregs into SCC FAK-WT tumors.

Nuclear FAK Regulates the Transcription of Ccl5 and TGFβ2 to Increase Tregs

The finding that the Tregs enriched in SCC FAK-WT tumors were likely recruited into SCC FAK-WT tumors led us to consider a potential role for Ccl5 that has been implicated in the recruitment and expansion of CD4$^+$FoxP3$^+$CD25$^+$ Tregs (Tan et al., 2009), via the paracrine signaling axis that we identified. We found that efficient knockdown of *Ccl5* using two independent shRNA hairpins (P1 and P2, Figure 5A) resulted in SCC FAK-WT shRNA-Ccl5 tumor regression by days 21–27 (Figure 5B). We measured the absolute number of Tregs in SCC FAK-WT shRNA-Ccl5 tumors at day 7 and found that there was a substantial reduction in both Ccl5-depleted tumors when compared with empty vector control SCC FAK-WT pLKO tumors (Figure 5C).

Expanding on these findings, shRNA-mediated knockdown of *Tgfb2* expression in SCC FAK-WT cells also influenced tumor growth (Figures S5B and S5C). Partial knockdown of TGFβ2 had complex effects, which resulted in one of two outcomes. One group (Figure S5C, dashed blue line), grew more rapidly and ulcerated, leading to removal from study at day 14. In the

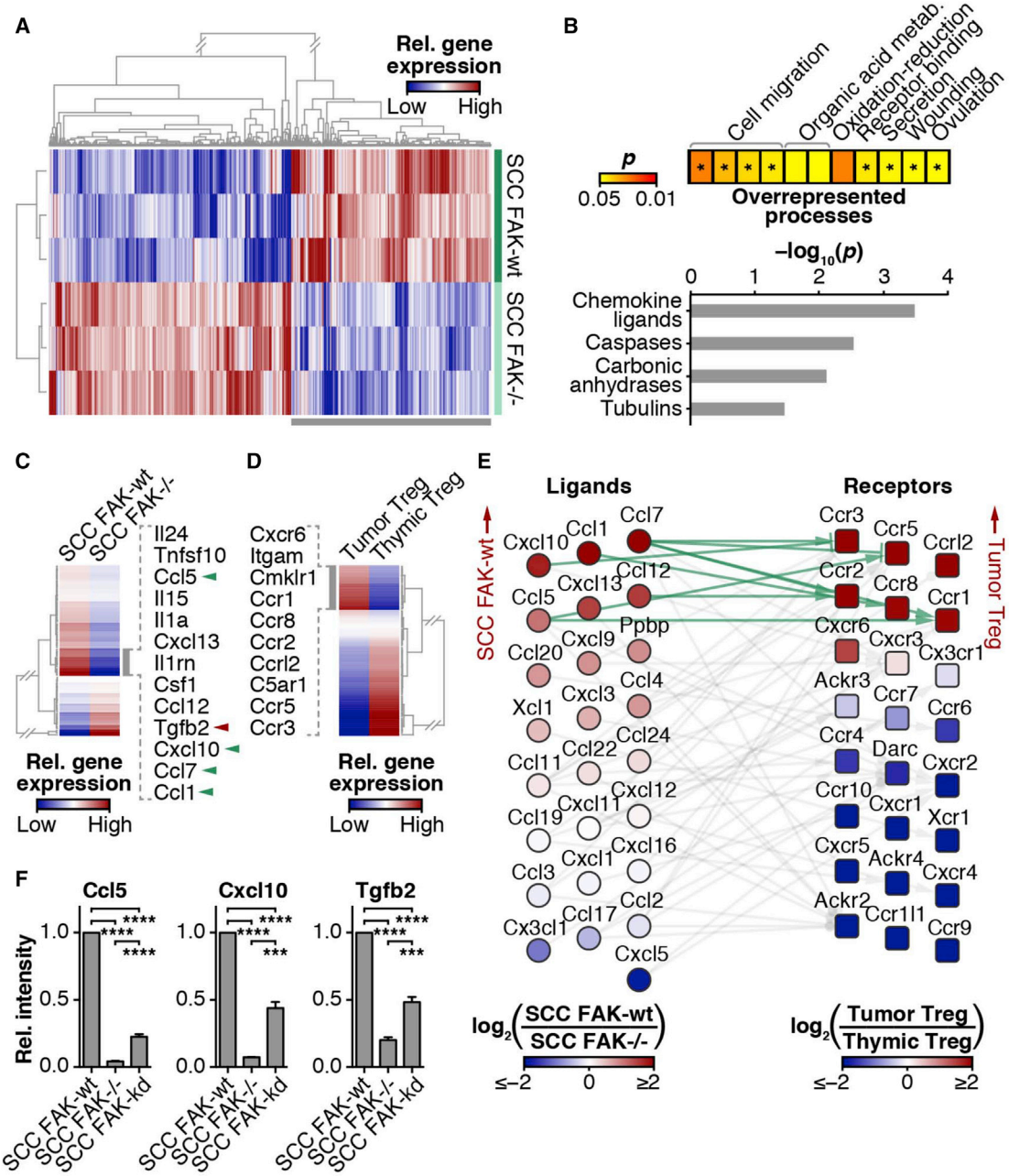

Figure 4. FAK Regulates Transcription of Cytokines Implicated in Treg Recruitment and Expansion

(A) Transcriptomic profiling of SCC FAK-WT and SCC *FAK*$^{-/-}$ cells.

(B) Functional enrichment analysis of genes upregulated in SCC FAK-WT cells (bottom gray bar in A). Overrepresented biological processes are displayed as a heatmap (log_{10}-transformed color scale) (top); asterisks indicate presence of cytokine-related genes. Overrepresented gene families are displayed as a bar chart (bottom). $p < 0.05$; Benjamini–Hochberg-corrected hypergeometric tests.

(C) qRT-PCR array analysis of cytokine and chemokine expression in SCC FAK-WT and SCC *FAK*$^{-/-}$ cells. Gray bar indicates cluster of genes upregulated in SCC FAK-WT cells; cytokine and chemokine gene names are listed. Green arrowheads indicate reported roles in Treg recruitment; red arrowhead indicates reported role in peripheral Treg induction.

(D) qRT-PCR array analysis of chemokine and receptor expression in tumor- and thymus-derived Tregs. Gray bar indicates cluster of genes upregulated in tumor-derived Tregs; receptor gene names are listed.

(E) Interaction network analysis of chemokine ligand gene expression detected in SCC cells (circles, left) and corresponding receptor gene expression detected in Tregs (squares, right). Genes are ordered vertically by fold change. Light gray lines connect receptor-ligand pairs; green lines indicate pairs upregulated at least 2-fold in SCC FAK-WT cells and tumor-derived Tregs.

(F) qRT-PCR analysis of selected cytokine and chemokine gene expression in SCC cells. ***$p < 0.001$, ****$p < 0.0001$; Tukey-corrected one-way ANOVA. Data are represented as mean ± SEM.

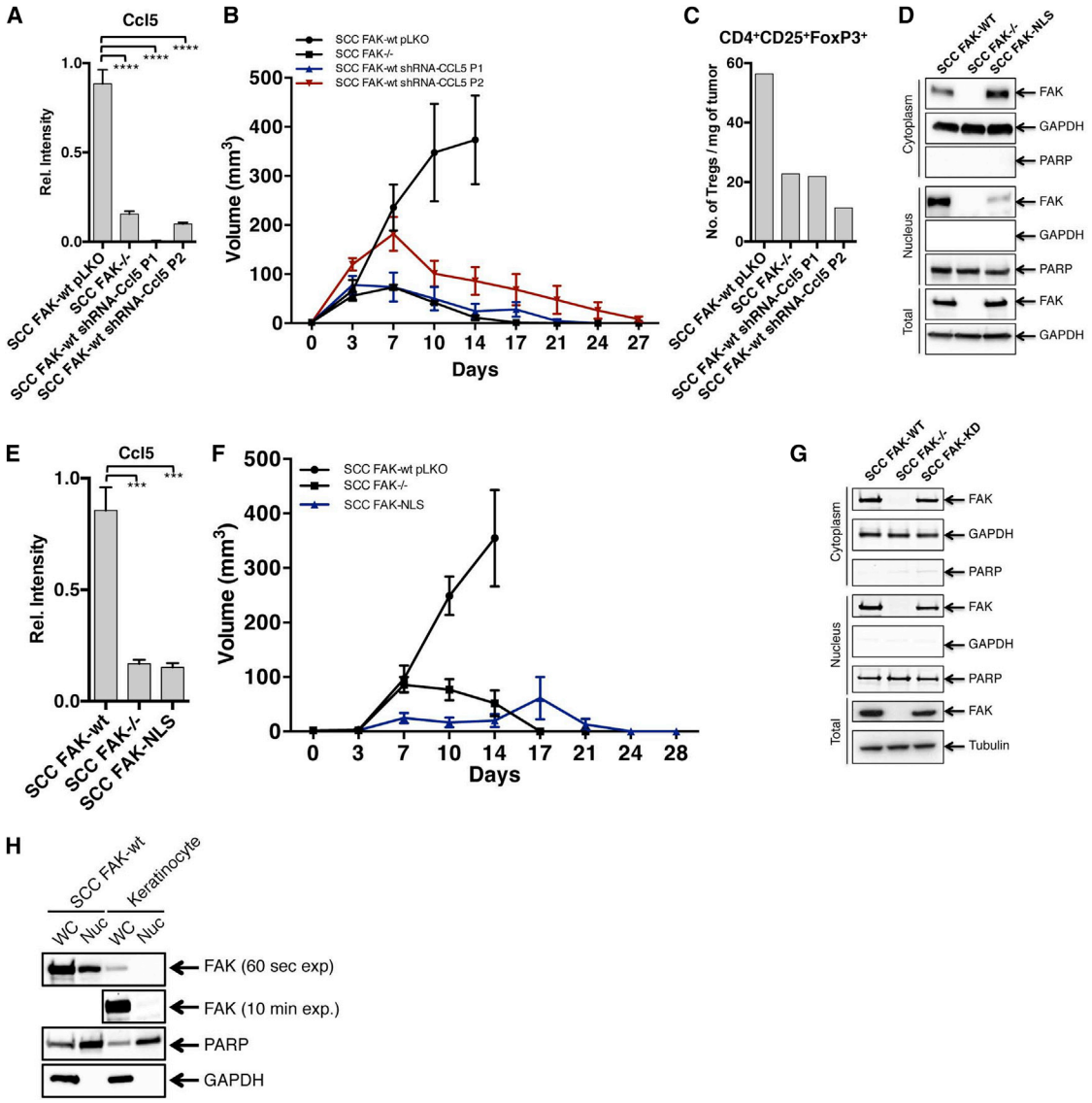

Figure 5. Nuclear FAK Regulates Transcription of Ccl5, which Is Required for Treg Recruitment and Tumor Growth

(A) qRT-PCR analysis of *Ccl5* gene expression knockdown in SCC FAK-WT cells stably expressing two independent shRNA constructs targeting Ccl5 (P1 and P2).

(B) SCC FAK-WT shRNA-Ccl5 tumor growth in FVB mice. n = 6 tumors.

(C) FACS quantitation of tumor-infiltrating Treg numbers from SCC FAK-WT shRNA-Ccl5 tumors. Data represent a single value from six pooled tumors.

(D) Western blotting of cytoplasmic, nuclear, and total protein fractions from SCC FAK-WT, SCC *FAK*$^{-/-}$, and SCC FAK-NLS cells.

(E) qRT-PCR analysis of *Ccl5* gene expression in SCC FAK-NLS cells.

(F) Tumor growth of SCC FAK-NLS cells in FVB mice.

(G) Western blotting of cytoplasmic, nuclear, and total protein fractions from SCC FAK-WT, SCC *FAK*$^{-/-}$, and SCC FAK-KD cells.

(H) Western blotting of whole-cell (WC) and nuclear (Nuc) protein fractions from SCC FAK-WT cells and primary skin keratinocytes. 60 s exposure time is shown for all samples; additional 10 min exposure time is shown for FAK in keratinocyte samples. GAPDH, cytoplasmic; PARP, nuclear.

***p < 0.001, ****p < 0.0001; Tukey-corrected one-way ANOVA. Data are represented as mean ± SEM unless stated.

other group that did not display such frank ulceration, we observed tumor regression by day 27 (Figure S5C, dashed red line). Analysis of Treg levels in SCC FAK-WT shRNA-TGFβ2 tumors at day 7 (regardless of initial growth characteristics) revealed that TGFβ2 knockdown was also associated with a reduction in CD4^{+}FoxP3^{+}CD25^{+} Tregs (Figure S5D). Therefore, while the effects of reducing TGFβ2 expression are more complicated than for Ccl5, FAK-dependent TGFβ2 expression does contribute to elevated CD4^{+}FoxP3^{+}CD25^{+} Tregs in SCC FAK-WT tumors; and in the subset of mice bearing tumors that were able to complete the study, TGFβ2 knockdown also caused tumor regression.

Our findings that FAK regulated the transcription of cytokines and chemokines (including Ccl5 and TGFβ2) that were associated with elevated intra-tumoral Tregs and tumor tolerance led us to consider a possible role for nuclear FAK in regulating the transcription of these genes. Based on previous reports (Lim et al., 2008), which identified putative NLSs within the FERM domain of FAK, we constructed an optimally nuclear targeting-impaired mutant FAK by replacing two arginines (positions 177 and 178) and four lysines (positions 190, 191, 216, and 218) with alanines (termed FAK-NLS). Western blotting of cytoplasmic and nuclear fractions confirmed that the FAK-NLS mutant was indeed defective in nuclear localization (Figure 5D). Subsequent (q)RT-PCR analysis of *Ccl5* and *Tgfb2* expression in SCC cells expressing only FAK-NLS revealed that FAK nuclear localization was required for transcription of these genes (Figures 5E and S5E, respectively). Thus, nuclear FAK drives the transcription of Ccl5 and TGFβ2, which are required for recruitment and expansion of immuno-suppressive Tregs into SCC tumors, altering the balance between $CD8^+$ T cells and Tregs in favor of tumor tolerance. In support of this, growth of SCC FAK-NLS tumor cells was similar to that of SCC $FAK^{-/-}$, with ultimate tumor regression (Figure 5F). This confirmed that it was nuclear FAK that afforded protection from the anti-tumor immune response. Western blotting of cytoplasmic and nuclear fractions from SCC FAK-KD showed that the kinase-deficient mutant was able to localize to the nucleus, so we conclude that the immune modulatory effects of FAK are dependent on FAK kinase activity in the nucleus (Figure 5G).

We next examined nuclear FAK levels in primary skin keratinocytes, the normal cellular counterparts of the SCC cells used here, and did not find detectable nuclear FAK (Figure 5H). Thus, abundant nuclear localization, and therefore the capacity to exert regulatory control over chemokine and cytokine expression, is likely a feature of oncogenic transformation in skin keratinocytes. This suggests that the nuclear functions of FAK that we have identified—namely, regulating transcription of chemokine/cytokine networks—may be associated with the cancerous state when FAK is highly expressed.

Nuclear FAK Interacts with a Network of Ccl5 Transcriptional Regulators

Having established an important role for the nuclear FAK-dependent transcription of Ccl5 in mediating recruitment and expansion of intra-tumoral Tregs, we wanted to determine how nuclear FAK could exert control over Ccl5 transcription. Using sucrose gradients, we fractionated the nuclei of SCC FAK-WT cells and demonstrated that nuclear FAK was present in the chromatin-containing fraction (Figure 6A). Transcriptional regulation of *Ccl5* is mediated predominantly through six short regulatory elements contained within a region of the *Ccl5* promoter spanning ~300 base pairs (Fessele et al., 2002). These regulatory elements contain binding sites for a number of TFs, including AP-1, C/EBP, IRF-1, NF-κB, and TATA box-binding protein (TBP), which is part of the transcription factor IID complex (TFIID). Using FAK immunoprecipitation and quantitative label-free mass spectrometry, we identified FAK binding partners in purified nuclear extracts and contextualized these by mapping onto a network of proteins associated with predicted Ccl5 TFs (constructed in silico; Figure 6B). This integrative approach identified a subset of Ccl5 TFs and regulators of these that interact with FAK in SCC cell nuclei (Figures 6C, S6 and Table S1). Interaction network analysis of this protein subset revealed nuclear FAK binding partners with roles in multiple transcriptional pathways, including regulators of AP-1, C/EBP, IRF-1/-7, NF-κB/Rel, and TFIID. Thus, we identified nuclear FAK binding partners that can interact, directly or indirectly, with five of the six main regulatory elements reported to control transcription of Ccl5 in multiple cell types (Fessele et al., 2002). Given that our interaction network was somewhat dominated by proteins associated with the TFIID pathway, including three TBP-associated factors (TAFs) (Figures 6C and S6), we used co-immunoprecipitation to confirm the interaction of nuclear FAK with one of these, TAF9, a core component of the TFIID complex (D'Alessio et al., 2009) (Figure 6D). Our data show that FAK binds to core components of the transcriptional machinery, many of which are known to be located on the promoter of genes undergoing active transcription and that are known or predicted to regulate Ccl5. Therefore, in SCC cells, nuclear FAK associates with chromatin and is physically linked to a network of TFs and their regulators known to modulate Ccl5 expression.

Small-Molecule FAK Kinase Inhibitor Promotes Immune-Mediated Tumor Clearance

Therapeutic targeting of FAK kinase activity using small-molecule inhibitors will inhibit FAK signaling not only in tumor cells, but also potentially in multiple host cell types. To complement expression of the FAK-KD mutant protein in the cancer cells and investigate whether a FAK inhibitor could induce immune-mediated regression of SCC tumors, we used the FAK/Pyk2 kinase inhibitor VS-4718 (Shapiro et al., 2014), which is currently in clinical development. Mice were treated with VS-4718 at 75 mg/kg for 24 hr prior to injection of 1×10^6 FAK-WT or $FAK^{-/-}$ SCC tumor cells and twice daily thereafter. This resulted in VS-4718-induced regression of SCC FAK-WT tumors by day 24 (Figure 7A). Following cessation of VS-4718 treatment, no tumor regrowth was observed (data not shown). SCC $FAK^{-/-}$ tumor growth and clearance was not greatly affected by VS-4718 treatment, suggesting that the anti-tumor effects of VS-4718 can be explained by FAK inhibition in tumor cells. Activity of VS-4718 was confirmed using an ELISA to measure FAK autophosphorylation on tyrosine-397 in tumor lysates from mice treated with 75 mg/kg VS-4718 (Figure S7). Regression of VS-4718-treated SCC tumors was not accompanied by loss of cell viability at day 7, as measured by FACS using a viability stain following tumor disaggregation (Figure 7B). There was a significant but small increase in leukocytes in VS-4718-treated SCC FAK-WT tumors (Figure 7C) and a significant increase in total $CD4^+$ T cells (Figures 7D and S2 and Table S2) and effector $CD4^+CD44^{hi}CD62L^{low}$ T cells (Figures 7E and S2 and Table S2). A significant increase in $CD8^+$ T cells was also evident in SCC FAK-WT VS-4718-treated tumors (Figures 7F and S2 and Table S2), although there was no change in effector $CD8^+CD44^{hi}CD62L^{low}$ T cells (Figures 7G and S2 and Table S2). Crucially, there was a significant reduction in $CD4^+CD25^+FoxP3^+$ Treg cells in VS-4718-treated SCC FAK-WT tumors, which was similar to that observed in vehicle and

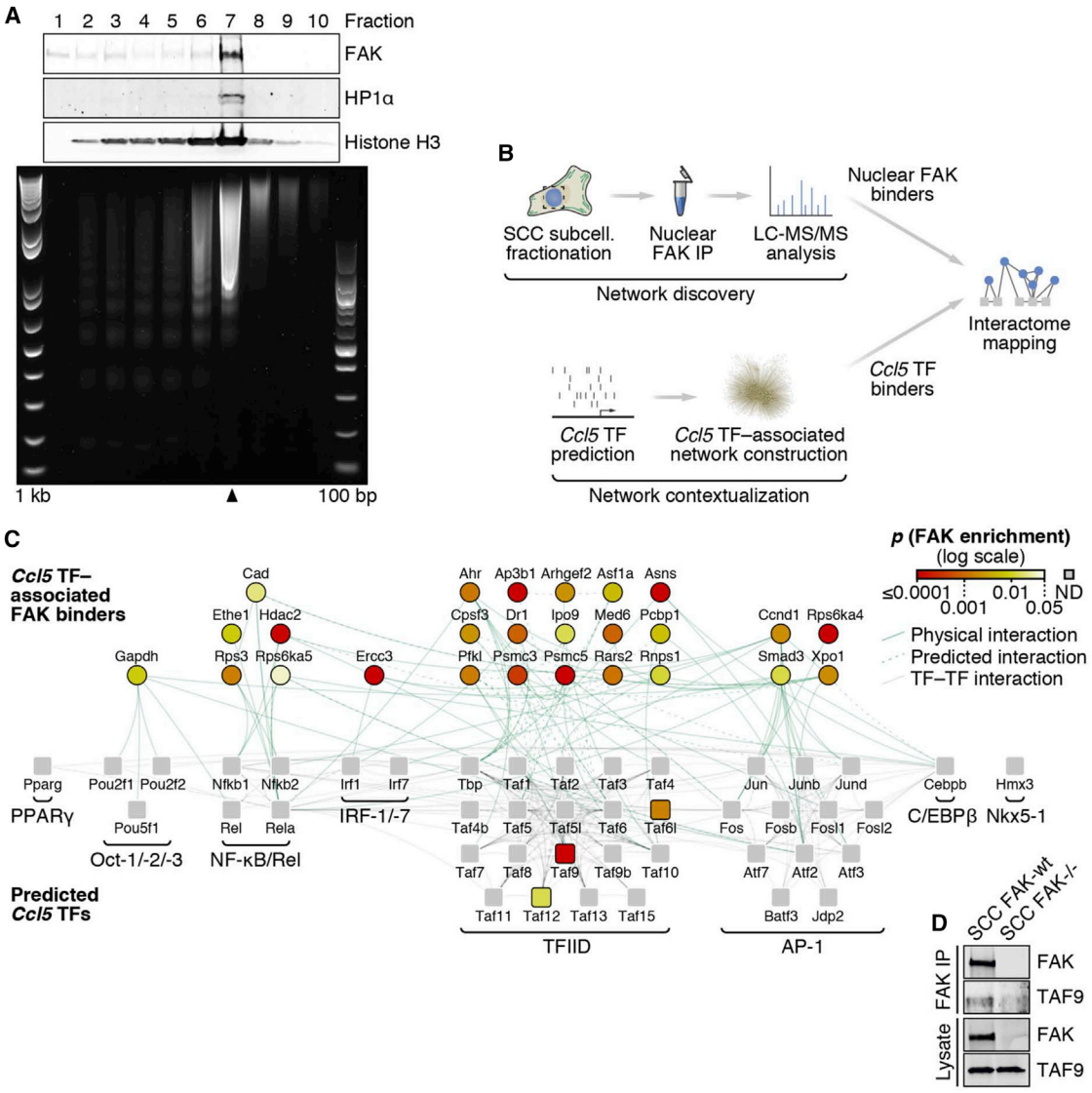

Figure 6. Nuclear FAK Interacts with Regulators of Ccl5 Transcription

(A) Sucrose fractionation of soluble chromatin prepared from SCC FAK-WT cell nuclei. Protein preparations recovered from each fraction were analyzed by western blotting (top). DNA recovered from each fraction was analyzed by agarose gel electrophoresis (bottom, 1 kilobase [kb] and 100 base pair [bp] ladders shown). Fraction 7 (black arrowhead) represents the chromatin-containing fraction.

(B) Schematic detailing the workflow used for proteomic analysis of the nuclear FAK interactome in the context of *Ccl5* transcription factors (TFs).

(C) Interaction network analysis of proteins that bind FAK in the nucleus of SCC cells. Predicted *Ccl5* TFs (squares, bottom) and respective TF binders (circles, top) enriched by at least 4-fold in nuclear FAK immunoprecipitations (SCC FAK-WT over SCC *FAK*$^{-/-}$ controls; $p < 0.05$) are shown (stringent network). *Ccl5* TFs not detected (ND) are shown as gray squares. TF complexes or groups are indicated; proteins are labeled with gene names for clarity. TF binders are aligned above TF groups with which there are the greatest number of reported interactions. For full network, see Figure S6; for protein interaction list, see Table S1.

(D) Isolation of the TFIID component TAF9 by FAK immunoprecipitation (IP) from SCC FAK-WT cell nuclear extracts.

VS-4718-treated SCC *FAK*$^{-/-}$ tumors (Figures 7H and S4 and Table S2).

Thus, VS-4718 promoted robust anti-tumor activity, with similar immune cell changes to that observed upon FAK deletion or expression of a kinase-deficient form of FAK. Furthermore, anti-tumor efficacy of VS-4718 was also dependent on CD8$^+$ T cells, and SCC FAK-WT tumors treated with VS-4718 on a CD8$^+$ T cell-depleted background exhibited a growth delay but did not undergo tumor regression (Figure 7I). We conclude that the FAK kinase inhibitor targets mechanisms of immune suppression and may therefore represent a form of effective "immuno-modulatory" therapy that reduces Tregs in the tumor environment. Importantly, the FAK kinase inhibitor does not affect the cytotoxic function of antigen-primed CD8$^+$ T cells. We also found that VS-4718 treatment that was initiated 5 days post-inoculation of 1 × 10^6 SCC FAK-WT cells, when these had

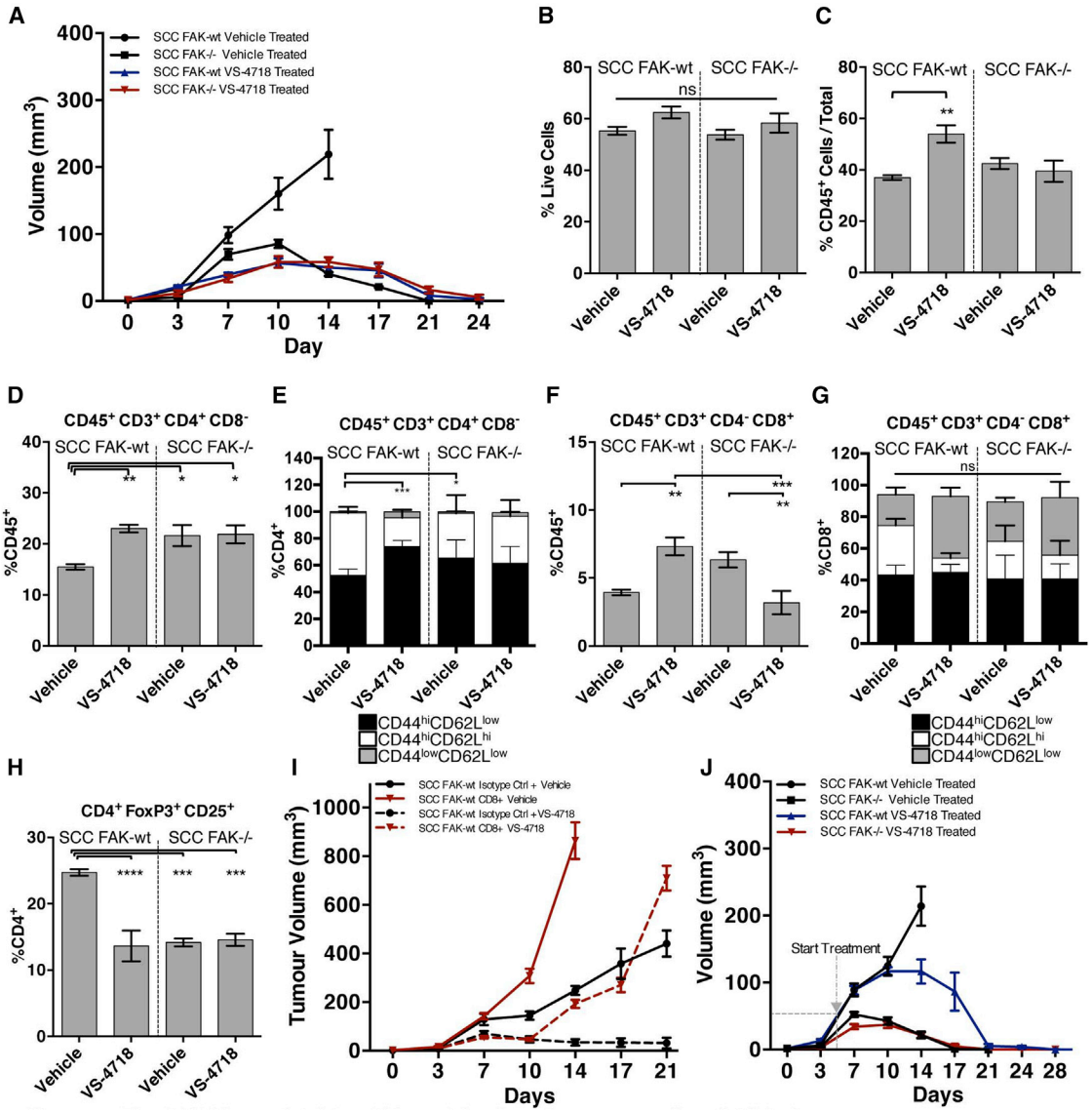

Figure 7. The FAK Kinase Inhibitor VS-4718 Leads to Immune-Mediated SCC Clearance

(A) SCC FAK-WT and SCC *FAK*$^{-/-}$ tumor growth in FVB mice treated with either vehicle or VS-4718. Treatment started 24 hr pre-tumor cell inoculation and continued for the duration of the experiment.

(B) FACS analysis of cell viability from disaggregated tumors treated with either vehicle or VS-4718.

(C) FACS analysis of vehicle- or VS-4718-treated tumor-infiltrating leukocytes expressed as a percentage of viable CD45$^+$ cells relative to the total number of single cells.

(D) FACS analysis of tumor-infiltrating CD4$^+$ T cells from vehicle- or VS-4718-treated tumors.

(E) FACS sub-categorization of tumor-infiltrating CD4$^+$ T cells into CD45$^+$CD3$^+$CD4$^+$CD8$^-$CD44^{hi}CD62L^{low}, CD45$^+$CD3$^+$CD4$^+$CD8$^-$CD44^{hi}CD62L^{hi}, and CD45$^+$CD3$^+$CD4$^+$CD8$^-$CD44^{low}CD62L^{low} populations.

(F) FACS analysis of tumor-infiltrating CD8$^+$ T cells from vehicle- or VS-4718-treated tumors.

(G) FACS sub-categorization of tumor-infiltrating CD8$^+$ T cells into CD45$^+$CD3$^+$CD4$^-$CD8$^+$CD44^{hi}CD62L^{low}, CD45$^+$CD3$^+$CD4$^-$CD8$^+$CD44^{hi}CD62L^{hi}, and CD45$^+$CD3$^+$CD4$^-$CD8$^+$CD44^{low}CD62L^{low} populations.

(H) FACS analysis of tumor-infiltrating CD4$^+$CD25$^+$FoxP3$^+$ Tregs expressed as a percentage of tumor-infiltrating CD4$^+$ T cells.

(I) SCC FAK-WT tumor growth in FVB mice treated with either vehicle or VS-4718 and either isotype control or CD8-depleting antibodies.

(J) SCC FAK-WT and SCC *FAK*$^{-/-}$ tumor growth in FVB mice treated with either vehicle or VS-4718. Treatment started 5 days post-tumor cell inoculation (gray dashed line) and continued for the duration of the experiment.

*p < 0.05, **p < 0.01, ***p < 0.001, ****p < 0.0001; ns, not significant; Tukey-corrected one-way ANOVA (E and G, CD44^{hi}CD62L^{low} only). Data are represented as mean ± SEM; n = 6 tumors.

already formed palpable tumors of ~50 mm^3, led to complete tumor regression (Figure 7J).

DISCUSSION

We show that nuclear FAK in SCC cancer cells drives the transcription of chemokines and cytokines, including Ccl5 and TGFβ2, which promote the formation of an immuno-suppressive, pro-tumorigenic microenvironment. This is dependent on FAK kinase activity, and expression of a catalytically inactive mutant FAK protein (FAK-KD) or treatment with a small-molecule inhibitor causes tumor regression. This is effective even when tumors are already established, raising the exciting possibility that targeting of FAK kinase activity may have immune-mediated anti-tumor efficacy in patients. We established that nuclear FAK is associated with chromatin and interacts with a number of TFs and transcriptional regulators, including components of the TFIID complex, that are linked to regulation of Ccl5 expression. Our data imply that FAK interacts with core transcriptional machinery to influence gene transcription and promote tumor immune escape.

Historically, FAK has been recognized as an adhesion-related non-receptor protein tyrosine kinase that clusters at focal adhesion (FA) structures and regulates cancer-associated processes, including adhesion, migration, invasion, survival, and proliferation (reviewed in Frame et al., 2010). FAK was also found to translocate to the nucleus (Lim et al., 2008; Luo et al., 2009b), leading to the idea of nuclear functions for FAK within the nucleus. Our data show that, at least in cancer cells, FAK regulates inflammatory transcriptional programs associated with generation and maintenance of a pro-tumorigenic and immuno-suppressive microenvironment. FAK associates with chromatin, and in the context of Ccl5 expression, it interacts with a number of TFs, and regulators of TFs, that bind regulatory elements in the Ccl5 promoter (Fessele et al., 2002). Our data imply that FAK exists in complexes with a number of TAF proteins, including TAF9 and TAF12, key components of the core promoter complex TFIID that serves to initiate transcription by driving recruitment of chromatin remodeling complexes, coactivators, and RNA polymerase II to the promoter (D'Alessio et al., 2009). Therefore, FAK interacts with components of the core transcriptional machinery in order to drive transcription of chemokines and cytokines that contribute to recruitment of Tregs into the tumor environment, promoting immunological tolerance and permitting tumor growth.

Recently, nuclear accumulation of active FAK (phosphorylated on Tyr-397) within tumor cells of patients with colorectal cancer was reported to correlate with poor prognosis (Albasri et al., 2014), highlighting the need to understand the nature of FAK's role within the nucleus. Studies using endothelial cells, muscle cells, and fibroblasts have previously reported low steady-state levels of nuclear FAK that are substantially increased in response to cellular stress (Lim, 2013; Lim et al., 2008; Luo et al., 2009b). Our work implies that oncogenic stress is another route to inducing high levels of nuclear FAK and that this, in turn, can influence transcriptional programs, such as the chemokine and cytokine networks that control the tumor microenvironment.

A number of therapeutic strategies targeting components of the immuno-suppressive tumor microenvironment are currently being tested, with the aim of restoring anti-tumor immunity by releasing the break on $CD8^+$ T cell cytotoxic activity. In pre-clinical models of cancer, targeting Tregs (Ali et al., 2014; Bos et al., 2013) has shown anti-tumor efficacy, either alone or when used in combination with agents that enhance $CD8^+$ T cell activation. A clinical study combining agents targeting cytotoxic-T-lymphocyte-associated antigen 4 (CTLA-4), which is thought to influence Treg function (Peggs et al., 2009; Quezada et al., 2006; Simpson et al., 2013; Wing et al., 2008), and PD-1, which blocks signals that inhibit T cell function, has reported impressive responses in patients with advanced melanoma (Wolchok et al., 2013). However, this combination of checkpoint blockade antibodies elicits substantial side effects in >50% of patients, highlighting the need to find alternative combinations with improved tolerability. We have shown that targeting FAK kinase activity has the potential to modulate intra-tumoral Treg levels, resulting in robust $CD8^+$ T cell anti-tumor immunity, while others have reported previously that FAK kinase inhibitors block monocyte/macrophage and cancer-associated fibroblast recruitment into tumors by virtue of FAK's role in regulating their migration (Stokes et al., 2011). Taken together, these findings suggest that targeting the pleiotropic cellular functions of FAK may have a broad impact on the immuno-suppressive tumor microenvironment, differentiating these agents from many therapeutic approaches that target single immune cell populations.

Targeting a molecular pathway that is upregulated in cancer cells may provide tumor specificity and help to overcome some of the potential issues with severe autoimmunity when modulating immune cell populations. FAK inhibitors, such as VS-4718, are in clinical development. VS-4718 is currently in a phase I dose escalation clinical trial in patients with solid tumors (www.clinicaltrials.gov NCT01849744). Our findings provide good rationale for pre-clinical and clinical testing of FAK kinase inhibitors alongside agents that stimulate $CD8^+$ T cell activity, such as the checkpoint blockade therapies that target PD-1 and CTLA-4, which are both in clinical development (Pardoll, 2012).

EXPERIMENTAL PROCEDURES

Experiments involving animals were carried out in accordance with the UKCCCR guidelines by approved protocol (HO PL 60/4248). Brief experimental procedures are listed here. For details, please see the Supplemental Experimental Procedures.

Generation of FAK Nuclear Localization Mutant

Mutations were introduced into FAK-WT at R177A, R178A, K190A, K191A, K216A, and K218A using PCR-based site-directed mutagenesis.

Cell Lines

Isolation and generation of the FAK SCC cell model is described in Serrels et al. (2012). Keratinocyte cultures were prepared as detailed in McLean et al. (2004).

Western Blot Analysis

To prepare whole-cell lysates, cells were washed in cold PBS and lysed in RIPA buffer. Cytoplasmic and nuclear extracts were prepared as described in Lim et al. (2008). Lysates were resolved by gel electrophoresis, transferred to nitrocellulose, and probed with respective antibodies.

Subcutaneous Tumor Growth

Cells were injected into both flanks of either CD-1 nude mice or FVB mice and tumor growth measured twice-weekly. Animals were sacrificed when tumors reached maximum allowed size or when signs of ulceration were evident. For treatment with VS-4718, drug was prepared in 0.5% carboxymethyl cellulose + 0.1% Tween 80 and mice treated at 75 mg/kg BID by gavage. No signs of toxicity were observed.

Tumor Growth following Re-Challenge

SCC *FAK*$^{-/-}$ cells were injected into the left flank of FVB mice. Following tumor regression, mice were left for 7 days before being challenged with SCC FAK-WT or *FAK*$^{-/-}$ cells injected into the right flank. Tumor growth was measured twice-weekly. Control groups were injected into both flanks at day 28 using mice that had not been pre-challenged with SCC *FAK*$^{-/-}$ cells.

CD4$^+$, CD8$^+$, and CD25$^+$ T Cell Depletion

T cell depletion was achieved following IP injection of 150 μg of depleting antibody into female age-matched FVB mice for 3 consecutive days and was maintained by further IP injection at 3 day intervals until the study was terminated. SCC FAK-WT or *FAK*$^{-/-}$ cells were injected into both flanks 6 days after initial antibody treatment and tumor growth measured. The extent of T cell depletion was determined at the end of the study using FACS (Figure S1).

FACS Analysis of Immune Cell Populations

Tumors established following injection of SCC cells into both flanks of an FVB mouse were removed at day 7. Tumor tissue was processed to obtain single cell suspension for staining and subsequent FACS analysis (antibodies listed in Table S2).

Gene Expression Profiling

RNA was analyzed using the GeneChip Mouse Genome 430 2.0 Array. Normalized data for differentially expressed genes were median centered and clustered using Cluster 3.0 and Java TreeView. Functional enrichment analysis was performed using ToppGene.

Quantitative RT^2-PCR Array Analysis of Cytokine, Chemokine, and Chemokine Receptor Expression

RNA prepared from SCC cells was analyzed using the mouse cytokine and chemokine RT^2 Profiler PCR Array and that from isolated Tregs was analyzed using the mouse chemokine and receptor array. Relative gene expression ($2^{-\Delta Ct}$) values were log transformed, median centered, and subjected to hierarchical clustering as for microarray analysis. An interactome of chemokine ligands and receptors was constructed using the IUPHAR/BPS Guide to Pharmacology database and curated from the literature, onto which expression data for detected genes were mapped and visualized using Cytoscape. Expression of selected cytokine and chemokine genes was assessed by standard quantitative RT-PCR.

shRNA-Mediated TGFβ2 and Ccl5 Knockdown

Cells were subject to two rounds of lentiviral infection prior to selection with puromycin. shRNA constructs used were part of the pLKO lentiviral TRC library.

Preparation and Fractionation of Nuclei and Chromatin

Nuclei were prepared as described (Gilbert et al., 2003) but with a reduced concentration (0.05%) of NP-40 in nuclei buffer B. Soluble chromatin was prepared as described (Gilbert et al., 2004) and fractionated on a sucrose step gradient to separate soluble and chromatin-associated nuclear proteins. DNA was recovered from fractions and subjected to agarose gel electrophoresis. Protein was purified using TCA precipitation. Samples were analyzed by SDS-PAGE and blotted using anti FAK, HP1α, and histone H3 antibodies.

Proteomic Analysis of Nuclear FAK Protein Complexes

FAK nuclear protein complexes were subjected to on-bead proteolytic digestion, desalting, and liquid chromatography-tandem mass spectrometry, as described (Turriziani et al., 2014). For interaction network analysis, Ccl5 transcription factors were extracted from the DECODE database and used to seed a network of 1,000 transcription factor-related proteins using the GeneMANIA plugin in Cytoscape. Proteins specifically isolated in nuclear FAK protein complexes were mapped onto the interactome, and those with physical or predicted direct or indirect interactions with Ccl5 transcription factors were analyzed using the NetworkAnalyzer plugin in Cytoscape.

CD8 T Cell Fluorescent Immunohistochemistry

Tumors were removed 7 days post-implantation and frozen by submersing in liquid nitrogen. Tumor sections were cut, processed and stained. They were imaged using an Olympus FV1000 confocal microscope.

ACCESSION NUMBERS

The microarray data discussed in this manuscript has been deposited in NCBI's Gene Expression Omnibus and is accessible through GEO series accession number GEO: GSE71662.

SUPPLEMENTAL INFORMATION

Supplemental Information includes Supplemental Experimental Procedures, seven figures, and two tables and can be found with this article online at http://dx.doi.org/10.1016/j.cell.2015.09.001.

AUTHOR CONTRIBUTIONS

A.S. and M.C.F. devised and oversaw the project. A.S., T.L., B.S., A.B., S.M.A., R.J.B.N., and M.C.F. designed the experiments with contributions from E.M., J.A.P., V.G.B., and N.G. A.S., T.L., B.S., A.B., R.C.M., and A.v.K. performed experiments with contributions from L.G.-C., M.C., M.M., and J.E.R. A.S., T.L., B.S., A.B., R.C.M., A.v.K., and A.H.S. analyzed the data. A.B. and A.H.S. performed bioinformatic analysis. A.S. and M.C.F. wrote the manuscript with contributions from T.L., B.S., and A.B.; all authors commented on and approved the final version. We consider that A.S. and T.L. made equal contributions and that B.S. and A.B. made equal contributions.

ACKNOWLEDGMENTS

This work was supported by Cancer Research UK (Grant no. C157/A15703 to M.C.F.), European Research Council (Grant no. 29440 Cancer Innovation to M.C.F.) and Medical Research Council (Grant no. G1100084 to S.M.A.). We thank Frederic Li Mow Chee for help with transcriptomic analysis, Amaya García-Muñoz for help with mass spectrometry, Elisabeth Freyer for help with FACS, and Arkadiusz Welman for help with manuscript preparation. J.E.R. and J.A.P. are employees of Verastem Inc.

Received: March 6, 2015
Revised: July 17, 2015
Accepted: August 27, 2015
Published: September 24, 2015

REFERENCES

Albasri, A., Fadhil, W., Scholefield, J.H., Durrant, L.G., and Ilyas, M. (2014). Nuclear expression of phosphorylated focal adhesion kinase is associated with poor prognosis in human colorectal cancer. Anticancer Res. *34*, 3969–3974.

Ali, K., Soond, D.R., Piñeiro, R., Hagemann, T., Pearce, W., Lim, E.L., Bouabe, H., Scudamore, C.L., Hancox, T., Maecker, H., et al. (2014). Inactivation of PI(3)K p110δ breaks regulatory T-cell-mediated immune tolerance to cancer. Nature *510*, 407–411.

Ashton, G.H., Morton, J.P., Myant, K., Phesse, T.J., Ridgway, R.A., Marsh, V., Wilkins, J.A., Athineos, D., Muncan, V., Kemp, R., et al. (2010). Focal adhesion kinase is required for intestinal regeneration and tumorigenesis downstream of Wnt/c-Myc signaling. Dev. Cell *19*, 259–269.

Beyer, M., and Schultze, J.L. (2006). Regulatory T cells in cancer. Blood *108*, 804–811.

Biragyn, A., and Longo, D.L. (2012). Neoplastic "Black Ops": cancer's subversive tactics in overcoming host defenses. Semin. Cancer Biol. *22*, 50–59.

Bos, P.D., Plitas, G., Rudra, D., Lee, S.Y., and Rudensky, A.Y. (2013). Transient regulatory T cell ablation deters oncogene-driven breast cancer and enhances radiotherapy. J. Exp. Med. *210*, 2435–2466.

Curiel, T.J., Coukos, G., Zou, L., Alvarez, X., Cheng, P., Mottram, P., Evdemon-Hogan, M., Conejo-Garcia, J.R., Zhang, L., Burow, M., et al. (2004). Specific recruitment of regulatory T cells in ovarian carcinoma fosters immune privilege and predicts reduced survival. Nat. Med. *10*, 942–949.

D'Alessio, J.A., Wright, K.J., and Tjian, R. (2009). Shifting players and paradigms in cell-specific transcription. Mol. Cell *36*, 924–931.

Darrasse-Jèze, G., and Podsypanina, K. (2013). How numbers, nature, and immune status of foxp3(+) regulatory T-cells shape the early immunological events in tumor development. Front. Immunol. *4*, 292.

Fessele, S., Maier, H., Zischek, C., Nelson, P.J., and Werner, T. (2002). Regulatory context is a crucial part of gene function. Trends Genet. *18*, 60–63.

Fourcade, J., Sun, Z., Benallaoua, M., Guillaume, P., Luescher, I.F., Sander, C., Kirkwood, J.M., Kuchroo, V., and Zarour, H.M. (2010). Upregulation of Tim-3 and PD-1 expression is associated with tumor antigen-specific CD8+ T cell dysfunction in melanoma patients. J. Exp. Med. *207*, 2175–2186.

Frame, M.C., Patel, H., Serrels, B., Lietha, D., and Eck, M.J. (2010). The FERM domain: organizing the structure and function of FAK. Nat. Rev. Mol. Cell Biol. *11*, 802–814.

Gilbert, N., Boyle, S., Sutherland, H., de Las Heras, J., Allan, J., Jenuwein, T., and Bickmore, W.A. (2003). Formation of facultative heterochromatin in the absence of HP1. EMBO J. *22*, 5540–5550.

Gilbert, N., Boyle, S., Fiegler, H., Woodfine, K., Carter, N.P., and Bickmore, W.A. (2004). Chromatin architecture of the human genome: gene-rich domains are enriched in open chromatin fibers. Cell *118*, 555–566.

Goldstein, J.D., Pérol, L., Zaragoza, B., Baeyens, A., Marodon, G., and Piaggio, E. (2013). Role of cytokines in thymus- versus peripherally derived-regulatory T cell differentiation and function. Front. Immunol. *4*, 155.

Kono, K., Kawaida, H., Takahashi, A., Sugai, H., Mimura, K., Miyagawa, N., Omata, H., and Fujii, H. (2006). CD4(+)CD25high regulatory T cells increase with tumor stage in patients with gastric and esophageal cancers. Cancer Immunol. Immunother. *55*, 1064–1071.

Lahlou, H., Sanguin-Gendreau, V., Zuo, D., Cardiff, R.D., McLean, G.W., Frame, M.C., and Muller, W.J. (2007). Mammary epithelial-specific disruption of the focal adhesion kinase blocks mammary tumor progression. Proc. Natl. Acad. Sci. USA *104*, 20302–20307.

Lim, S.T. (2013). Nuclear FAK: a new mode of gene regulation from cellular adhesions. Mol. Cells *36*, 1–6.

Lim, S.T., Chen, X.L., Lim, Y., Hanson, D.A., Vo, T.T., Howerton, K., Larocque, N., Fisher, S.J., Schlaepfer, D.D., and Ilic, D. (2008). Nuclear FAK promotes cell proliferation and survival through FERM-enhanced p53 degradation. Mol. Cell *29*, 9–22.

Luo, M., Fan, H., Nagy, T., Wei, H., Wang, C., Liu, S., Wicha, M.S., and Guan, J.L. (2009a). Mammary epithelial-specific ablation of the focal adhesion kinase suppresses mammary tumorigenesis by affecting mammary cancer stem/progenitor cells. Cancer Res. *69*, 466–474.

Luo, S.W., Zhang, C., Zhang, B., Kim, C.H., Qiu, Y.Z., Du, Q.S., Mei, L., and Xiong, W.C. (2009b). Regulation of heterochromatin remodelling and myogenin expression during muscle differentiation by FAK interaction with MBD2. EMBO J. *28*, 2568–2582.

Marigo, I., Dolcetti, L., Serafini, P., Zanovello, P., and Bronte, V. (2008). Tumor-induced tolerance and immune suppression by myeloid derived suppressor cells. Immunol. Rev. *222*, 162–179.

Matsuzaki, J., Gnjatic, S., Mhawech-Fauceglia, P., Beck, A., Miller, A., Tsuji, T., Eppolito, C., Qian, F., Lele, S., Shrikant, P., et al. (2010). Tumor-infiltrating NY-ESO-1-specific CD8+ T cells are negatively regulated by LAG-3 and PD-1 in human ovarian cancer. Proc. Natl. Acad. Sci. USA *107*, 7875–7880.

McLean, G.W., Komiyama, N.H., Serrels, B., Asano, H., Reynolds, L., Conti, F., Hodivala-Dilke, K., Metzger, D., Chambon, P., Grant, S.G., and Frame, M.C. (2004). Specific deletion of focal adhesion kinase suppresses tumor formation and blocks malignant progression. Genes Dev. *18*, 2998–3003.

McLean, G.W., Carragher, N.O., Avizienyte, E., Evans, J., Brunton, V.G., and Frame, M.C. (2005). The role of focal-adhesion kinase in cancer - a new therapeutic opportunity. Nat. Rev. Cancer *5*, 505–515.

Ondondo, B., Jones, E., Godkin, A., and Gallimore, A. (2013). Home sweet home: the tumor microenvironment as a haven for regulatory T cells. Front. Immunol. *4*, 197.

Onizuka, S., Tawara, I., Shimizu, J., Sakaguchi, S., Fujita, T., and Nakayama, E. (1999). Tumor rejection by in vivo administration of anti-CD25 (interleukin-2 receptor alpha) monoclonal antibody. Cancer Res. *59*, 3128–3133.

Pardoll, D.M. (2012). The blockade of immune checkpoints in cancer immunotherapy. Nat. Rev. Cancer *12*, 252–264.

Peggs, K.S., Quezada, S.A., Chambers, C.A., Korman, A.J., and Allison, J.P. (2009). Blockade of CTLA-4 on both effector and regulatory T cell compartments contributes to the antitumor activity of anti-CTLA-4 antibodies. J. Exp. Med. *206*, 1717–1725.

Provenzano, P.P., Inman, D.R., Eliceiri, K.W., Beggs, H.E., and Keely, P.J. (2008). Mammary epithelial-specific disruption of focal adhesion kinase retards tumor formation and metastasis in a transgenic mouse model of human breast cancer. Am. J. Pathol. *173*, 1551–1565.

Pylayeva, Y., Gillen, K.M., Gerald, W., Beggs, H.E., Reichardt, L.F., and Giancotti, F.G. (2009). Ras- and PI3K-dependent breast tumorigenesis in mice and humans requires focal adhesion kinase signaling. J. Clin. Invest. *119*, 252–266.

Quezada, S.A., Peggs, K.S., Curran, M.A., and Allison, J.P. (2006). CTLA4 blockade and GM-CSF combination immunotherapy alters the intratumor balance of effector and regulatory T cells. J. Clin. Invest. *116*, 1935–1945.

Roberts, W.G., Ung, E., Whalen, P., Cooper, B., Hulford, C., Autry, C., Richter, D., Emerson, E., Lin, J., Kath, J., et al. (2008). Antitumor activity and pharmacology of a selective focal adhesion kinase inhibitor, PF-562,271. Cancer Res. *68*, 1935–1944.

Sakuishi, K., Apetoh, L., Sullivan, J.M., Blazar, B.R., Kuchroo, V.K., and Anderson, A.C. (2010). Targeting Tim-3 and PD-1 pathways to reverse T cell exhaustion and restore anti-tumor immunity. J. Exp. Med. *207*, 2187–2194.

Sakuishi, K., Ngiow, S.F., Sullivan, J.M., Teng, M.W., Kuchroo, V.K., Smyth, M.J., and Anderson, A.C. (2013). TIM3(+)FOXP3(+) regulatory T cells are tissue-specific promoters of T-cell dysfunction in cancer. OncoImmunology *2*, e23849.

Sasada, T., Kimura, M., Yoshida, Y., Kanai, M., and Takabayashi, A. (2003). CD4+CD25+ regulatory T cells in patients with gastrointestinal malignancies: possible involvement of regulatory T cells in disease progression. Cancer *98*, 1089–1099.

Sato, E., Olson, S.H., Ahn, J., Bundy, B., Nishikawa, H., Qian, F., Jungbluth, A.A., Frosina, D., Gnjatic, S., Ambrosone, C., et al. (2005). Intraepithelial CD8+ tumor-infiltrating lymphocytes and a high CD8+/regulatory T cell ratio are associated with favorable prognosis in ovarian cancer. Proc. Natl. Acad. Sci. USA *102*, 18538–18543.

Serrels, A., McLeod, K., Canel, M., Kinnaird, A., Graham, K., Frame, M.C., and Brunton, V.G. (2012). The role of focal adhesion kinase catalytic activity on the proliferation and migration of squamous cell carcinoma cells. Int. J. Cancer *131*, 287–297.

Shah, W., Yan, X., Jing, L., Zhou, Y., Chen, H., and Wang, Y. (2011). A reversed CD4/CD8 ratio of tumor-infiltrating lymphocytes and a high percentage of CD4(+)FOXP3(+) regulatory T cells are significantly associated with clinical outcome in squamous cell carcinoma of the cervix. Cell. Mol. Immunol. *8*, 59–66.

Shapiro, I.M., Kolev, V.N., Vidal, C.M., Kadariya, Y., Ring, J.E., Wright, Q., Weaver, D.T., Menges, C., Padval, M., McClatchey, A.I., et al. (2014). Merlin deficiency predicts FAK inhibitor sensitivity: a synthetic lethal relationship. Sci. Transl. Med. *6*, 237ra68.

Shimizu, J., Yamazaki, S., and Sakaguchi, S. (1999). Induction of tumor immunity by removing CD25+CD4+ T cells: a common basis between tumor immunity and autoimmunity. J. Immunol. *163*, 5211–5218.

Simpson, T.R., Li, F., Montalvo-Ortiz, W., Sepulveda, M.A., Bergerhoff, K., Arce, F., Roddie, C., Henry, J.Y., Yagita, H., Wolchok, J.D., et al. (2013). Fc-dependent depletion of tumor-infiltrating regulatory T cells co-defines the efficacy of anti-CTLA-4 therapy against melanoma. J. Exp. Med. *210*, 1695–1710.

Slack-Davis, J.K., Hershey, E.D., Theodorescu, D., Frierson, H.F., and Parsons, J.T. (2009). Differential requirement for focal adhesion kinase signaling in cancer progression in the transgenic adenocarcinoma of mouse prostate model. Mol. Cancer Ther. *8*, 2470–2477.

Stokes, J.B., Adair, S.J., Slack-Davis, J.K., Walters, D.M., Tilghman, R.W., Hershey, E.D., Lowrey, B., Thomas, K.S., Bouton, A.H., Hwang, R.F., et al. (2011). Inhibition of focal adhesion kinase by PF-562,271 inhibits the growth and metastasis of pancreatic cancer concomitant with altering the tumor microenvironment. Mol. Cancer Ther. *10*, 2135–2145.

Tan, M.C., Goedegebuure, P.S., Belt, B.A., Flaherty, B., Sankpal, N., Gillanders, W.E., Eberlein, T.J., Hsieh, C.S., and Linehan, D.C. (2009). Disruption of CCR5-dependent homing of regulatory T cells inhibits tumor growth in a murine model of pancreatic cancer. J. Immunol. *182*, 1746–1755.

Thornton, A.M., Korty, P.E., Tran, D.Q., Wohlfert, E.A., Murray, P.E., Belkaid, Y., and Shevach, E.M. (2010). Expression of Helios, an Ikaros transcription factor family member, differentiates thymic-derived from peripherally induced Foxp3+ T regulatory cells. J. Immunol. *184*, 3433–3441.

Turriziani, B., Garcia-Munoz, A., Pilkington, R., Raso, C., Kolch, W., and von Kriegsheim, A. (2014). On-beads digestion in conjunction with data-dependent mass spectrometry: a shortcut to quantitative and dynamic interaction proteomics. Biology (Basel) *3*, 320–332.

Wherry, E.J. (2011). T cell exhaustion. Nat. Immunol. *12*, 492–499.

Wing, K., Onishi, Y., Prieto-Martin, P., Yamaguchi, T., Miyara, M., Fehervari, Z., Nomura, T., and Sakaguchi, S. (2008). CTLA-4 control over Foxp3+ regulatory T cell function. Science *322*, 271–275.

Wolchok, J.D., Kluger, H., Callahan, M.K., Postow, M.A., Rizvi, N.A., Lesokhin, A.M., Segal, N.H., Ariyan, C.E., Gordon, R.A., Reed, K., et al. (2013). Nivolumab plus ipilimumab in advanced melanoma. N. Engl. J. Med. *369*, 122–133.

Cell

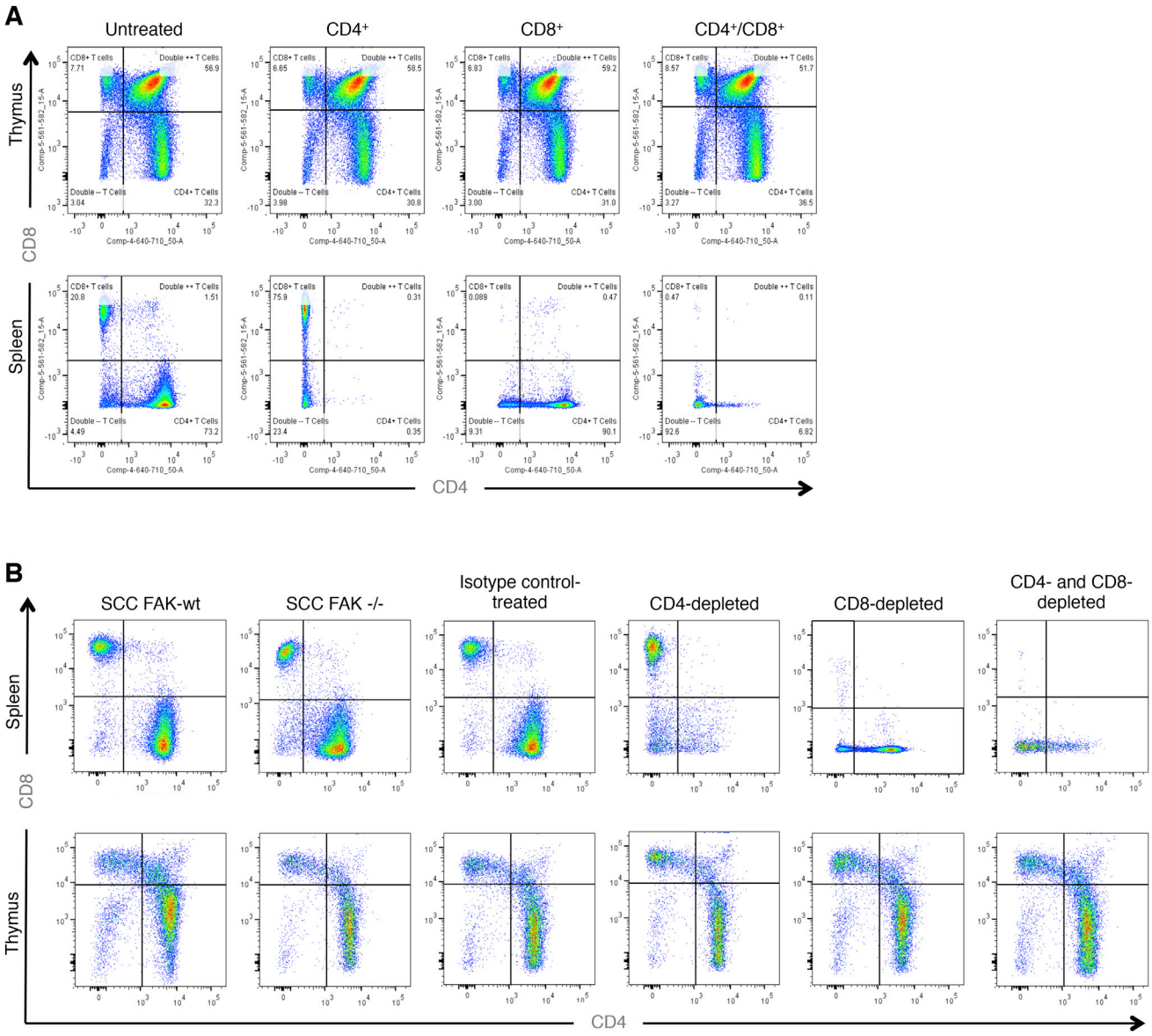

Figure S1. T Cell FACS Analysis Post Antibody-Mediated T Cell Depletion, Related to Figure 1

(A) FACS analysis of spleen and thymus tissue from non-tumor-bearing animals 6 days after commencing antibody treatment. (B) FACS analysis of T cell populations from spleen and thymus tissue from tumor-bearing animals at the end of T cell depletion studies in Figures 1C and 1D.

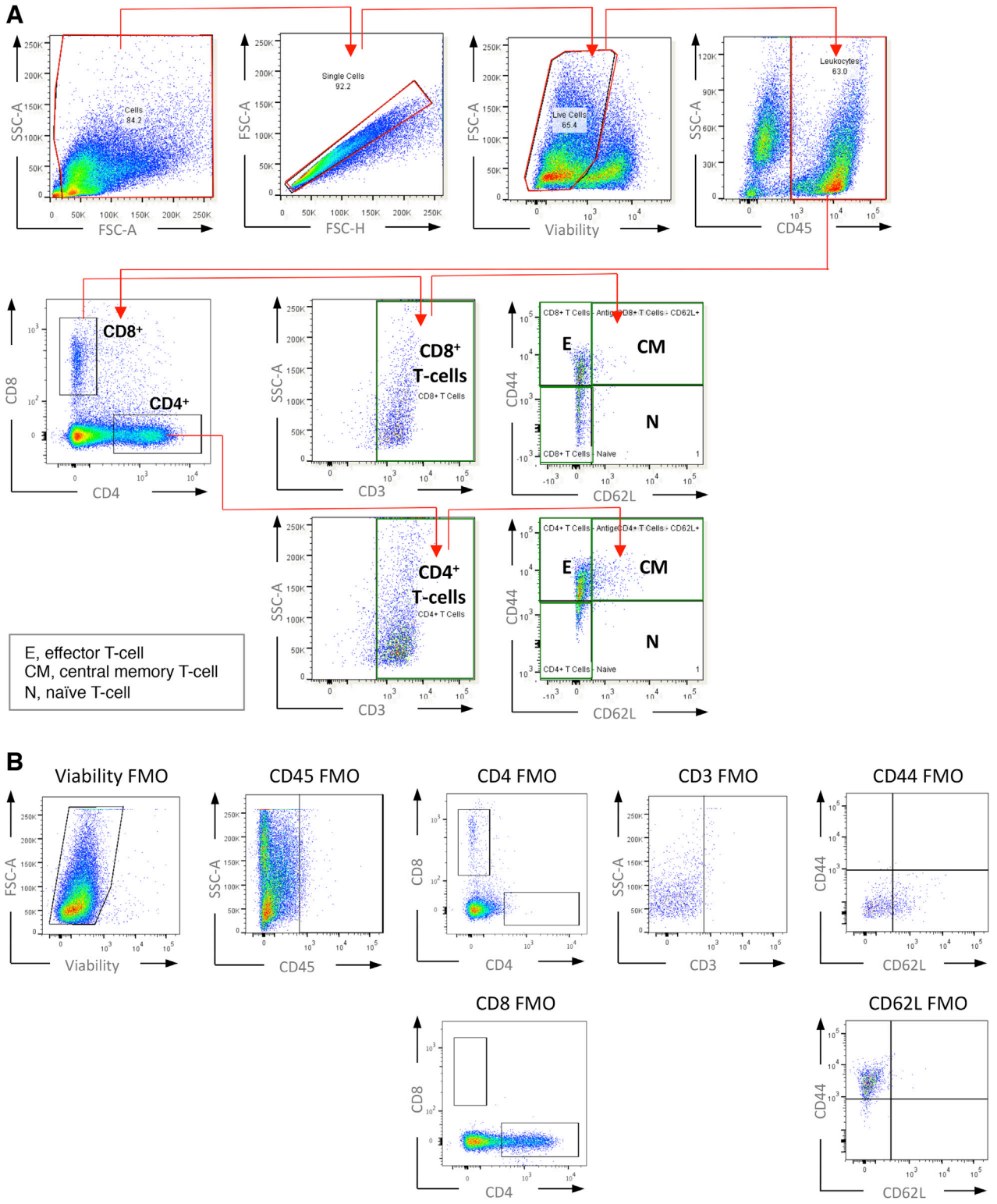

Figure S2. T Cell FACS Gating Strategy, Related to Figures 2 and 7

(A) FACS gating strategy applied for identification of T cell sub-populations. E = effector, CM = central memory, and N = naive. (B) FMO (full antibody set minus one) control samples used to determine correct gating for T cell sub-population identification.

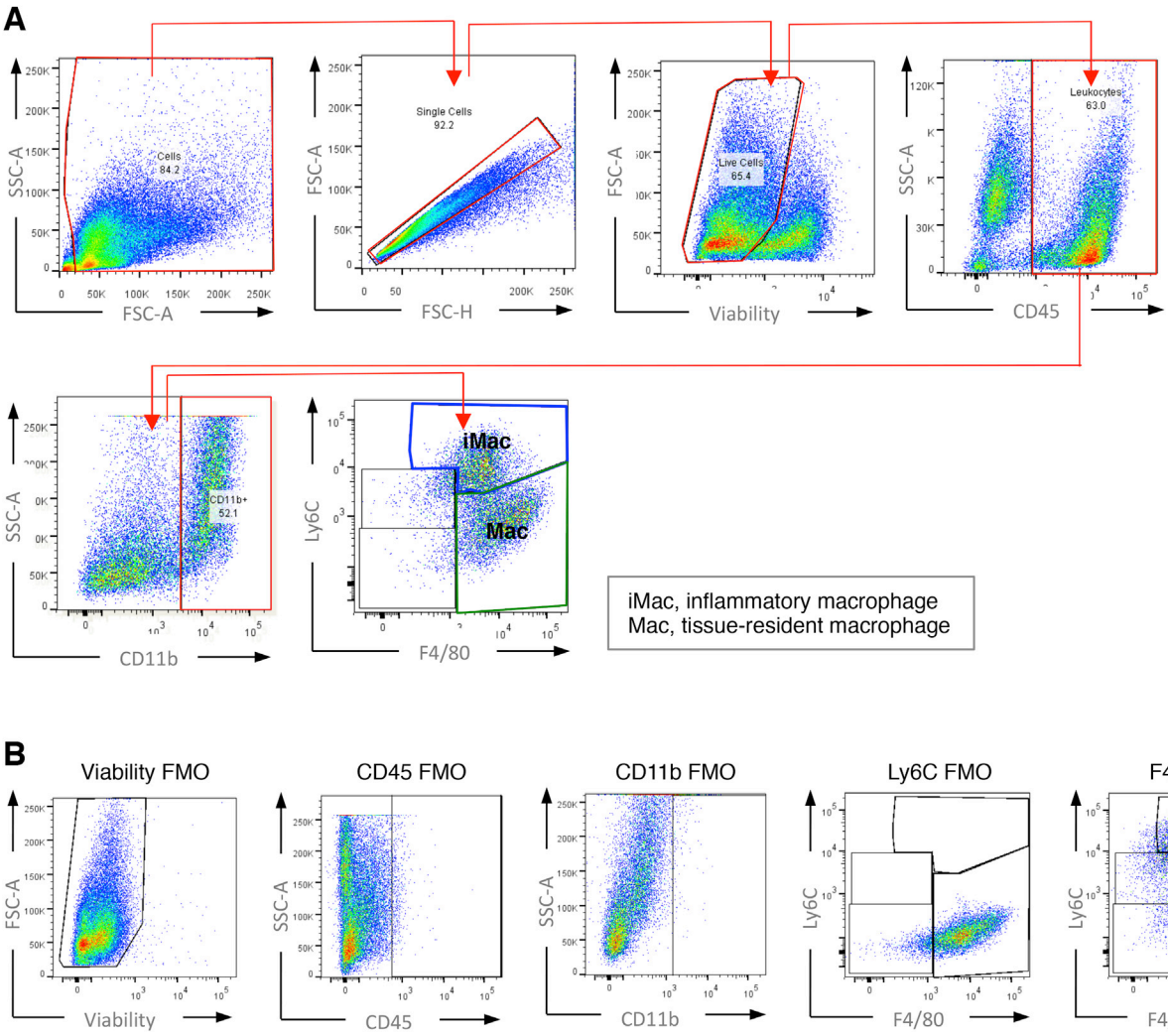

Figure S3. Macrophage FACS Gating Strategy, Related to Figure 3

(A) FACS gating strategy applied for identification of macrophage sub-populations. (B) FMO control samples used to determine correct gating for macrophage sub-population identification.

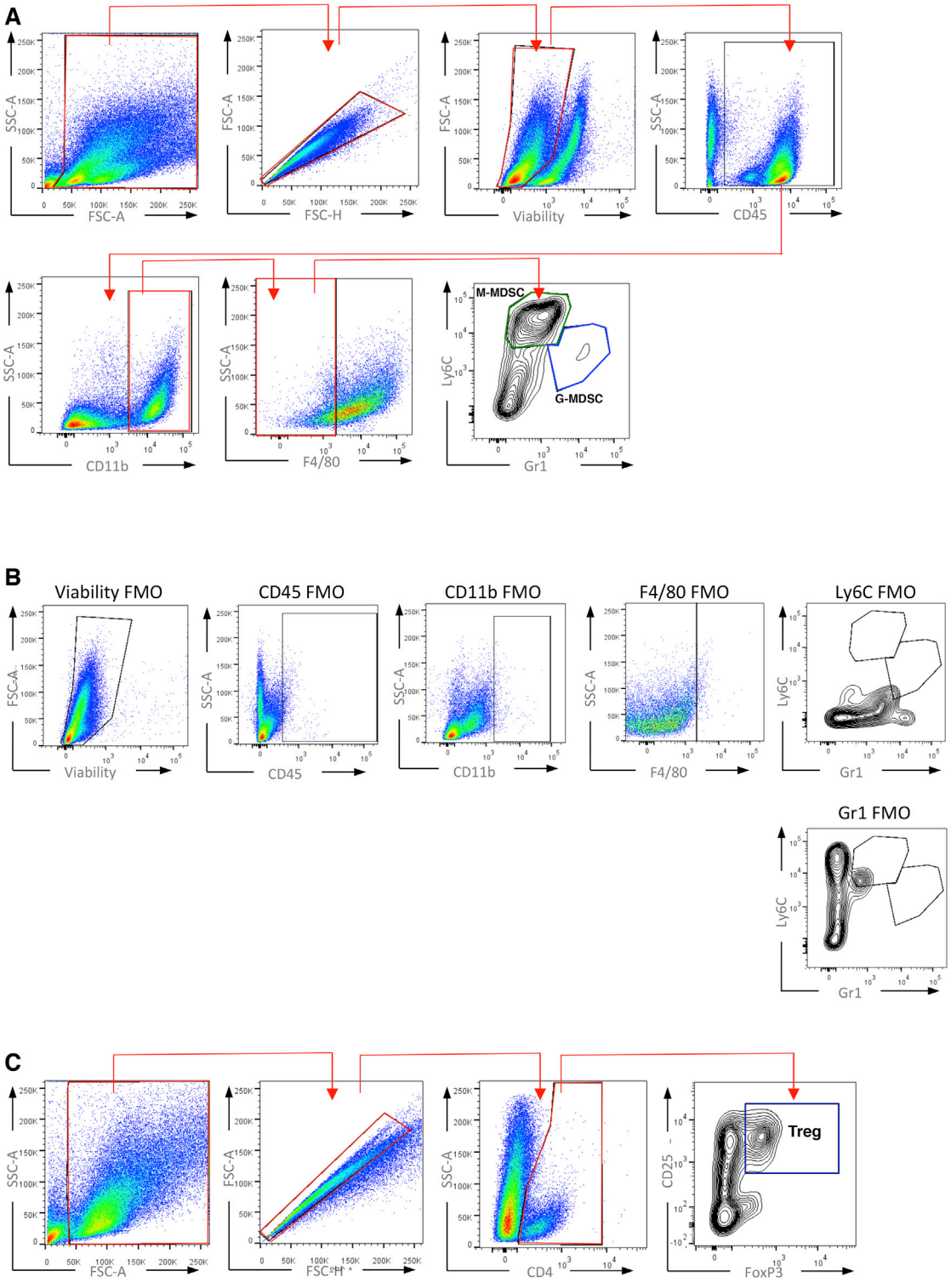

Figure S4. MDSC and Treg FACS Gating Strategy, Related to Figures 3 and 7

(A) FACS gating strategy applied for identification of MDSC sub-populations. M-MDSC – Monocytic Myeloid Derived Suppressor Cell; G-MDSC – Granulocytic Myeloid Derived Suppressor Cell. (B) FMO control samples used to determine correct gating for MDSC sub-population identification. (C) FACS gating strategy applied for identification of regulatory T cells (Treg).

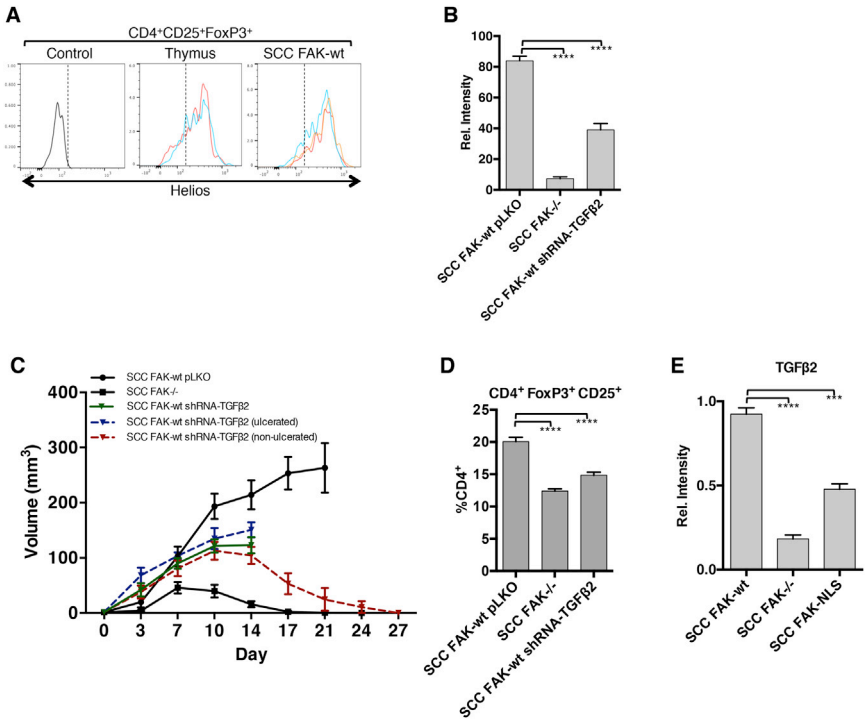

Figure S5. Tregs Infiltrating SCC FAK-WT Tumors Express the Thymic Marker Helios; Nuclear FAK Regulates Transcription of TGFβ2, which Contributes to Treg Expansion and Tumor Growth, Related to Figures 3 and 5

(A) FACS analysis of Helios expression in $CD4^+CD25^+FOXP3^+$ SCC FAK-WT tumor-infiltrating Tregs and Tregs isolated from the thymus of tumor-bearing mice. Control represents background signal from a sample stained with CD4, CD25, and FoxP3 conjugated antibodies but not Helios. Representative replicates are shown in different colors for thymus and SCC FAK-WT samples. (B) qRT-PCR analysis of *Tgfb2* gene expression knockdown in SCC cells. ****$p < 0.0001$ (Tukey-corrected one-way ANOVA). (C) SCC FAK-WT shRNA-TGFβ2 tumor growth in FVB mice. Blue dashed line indicates growth of SCC FAK-WT shRNA-TGFβ2 tumors that had to be sacrificed due to ulceration at day 14. Red dashed line indicates growth of SCC FAK-WT shRNA-TGFβ2 tumors that showed no ulceration. Green solid line indicates the mean growth of all SCC FAK-WT shRNA-TGFβ2 tumors up until cohort numbers were reduced due to ulceration. n = 6 tumors / group. (D) FACS analysis of SCC FAK-WT shRNA-TGFβ2 tumor infiltrating Tregs. ****$p < 0.0001$ (Tukey-corrected one-way ANOVA) (E) qRT-PCR analysis of *Tgfb2* gene expression in SCC FAK-NLS mutant cells. ***$p < 0.001$, ****$p < 0.0001$ (Tukey-corrected one-way ANOVA). Data are represented as mean ± SEM.

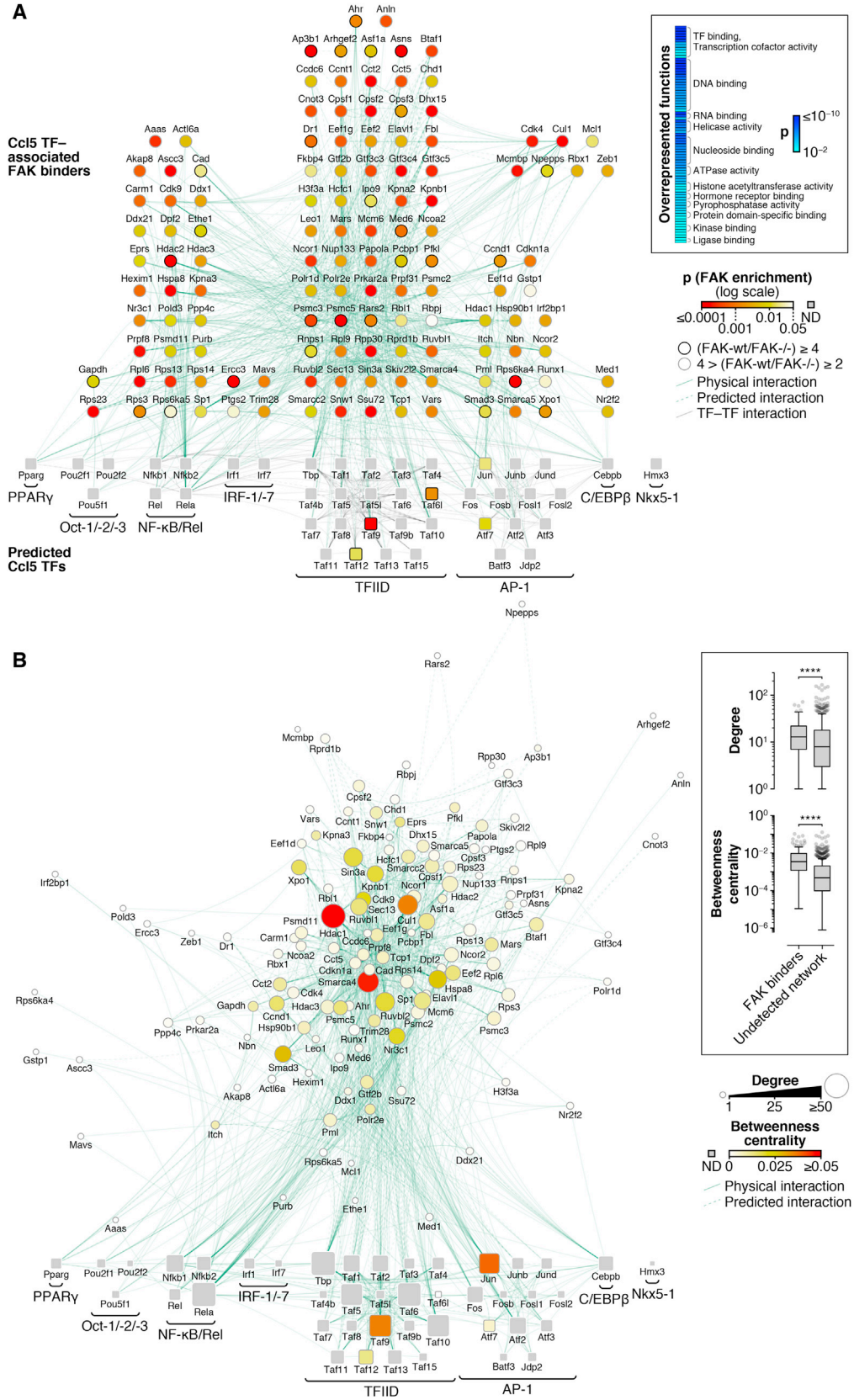

(legend on next page)

Figure S6. Nuclear FAK Interactome in the Context of Ccl5 Transcription Factors, Related to Figure 6 and Table S1

(A) Interaction network analysis of proteins that bind FAK in the nucleus of SCC cells. Predicted Ccl5 transcription factors (TFs) (squares; bottom) and respective TF binders (circles; top) enriched by at least two-fold in nuclear FAK immunoprecipitations (SCC FAK-WT over SCC *FAK*$^{-/-}$ controls; $p < 0.05$) are shown. Ccl5 TFs not detected (ND) are shown as gray squares. TF complexes or groups are indicated; proteins are labeled with gene names for clarity. TF binders are aligned above TF groups with which there are the greatest number of reported interactions. Overrepresented molecular functions determined by functional enrichment analysis are displayed as a heat map (log_{10}-transformed color scale) (inset). Displayed terms satisfy $p < 0.01$ (Benjamini–Hochberg-corrected hypergeometric test) with > 5 proteins assigned per term. (B) Topological analysis of Ccl5 TF–associated proteins identified in the nuclear FAK interactome. Ccl5 TF binders were clustered using the yFiles Organic algorithm implemented in Cytoscape. Topological parameters were computed using NetworkAnalyzer, excluding self-interactions. Protein node size is proportional to the number of interaction partners in the network (degree); node color indicates betweenness centrality (normalized number of shortest paths between proteins; a measure of the control a protein exerts over the interactions of other proteins in the network). Box-and-whisker plots (inset) show the distributions of degree and betweenness centrality for Ccl5 TF–associated proteins that bind nuclear FAK compared to those that were not enriched in nuclear FAK immunoprecipitations, indicating that FAK binders tend to have more interactions and be more central in the interaction network than undetected Ccl5 TF–associated proteins. Plots display the median (line), interquartile range (box) and 1.5 × interquartile range (whiskers) (n = 169 and 761 Ccl5 TF–associated proteins detected and not detected, respectively, with degree $\geq$ 1 based on physical or predicted interactions). ****$p < 0.0001$ (two-tailed Mann–Whitney test).

See also Table S1.

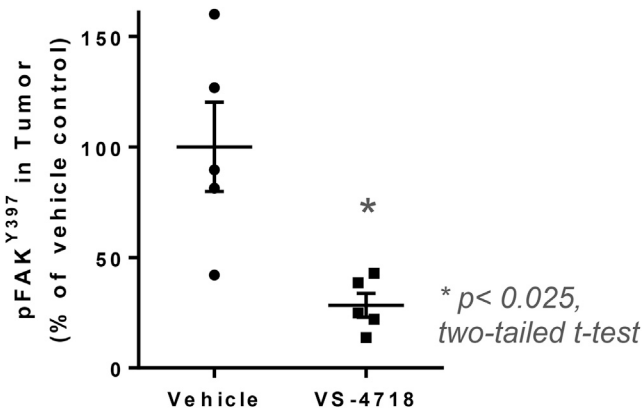

Figure S7. Analysis of FAK pY397 Phosphorylation in Tumors following Treatment with VS-4718, Related to Figure 7

Phosphorylation of FAK on Y397 was measured in protein lysates isolated from tumors following treatment with VS-4718 using ELISA. Tumors were removed within 30 min of treatment. n = 5. Data are represented as mean ± SEM.